République Algérienne Démocratique Et Populaire
Ministère De L'enseignement Supérieur Et De La Recherche Scientifique
Université 20 Août 1955 Skikda

Faculté De Technologie
Département De Génie Des Procédés

Réf : D012125009D

Laboratoire de domiciliation : Laboratoire de Physico-Chimie des Surfaces et des Interfaces (LRPCSI)

THÈSE

EN VUE DE L'OBTENTION DU DIPLOME DE DOCTORAT EN 3ème CYCLE_LMD

Domaine : Science et technologie **Filière :** Génie des procédés

Spécialité : Catalyse

Présentée par

ABDENNOURI Amdjed

Intitulée

Valorisation des algues et déchets industriels pour production des biocarburants via catalyse hétérogène

Soutenu le : 27/02/2025 Devant le jury composé de :

Nom et Prénom	**Grade**	**Etablissement**	**Qualité**
Mme SOBHI Chafia	Professeur	Université de Skikda	Présidente
Mme ZOUAOUI Emna	Professeur	Université de Skikda	Promotrice
Mr BOUHDIBA Abdelaziz	Professeur	Université de Skikda	Examinateur
Mr ALLAL Hamza	MCA	Université de Constantine 3	Examinateur
Mme FERKOUS Hana	MCA	Université de Skikda	Invitée

Année universitaire : 2024-2025

People's Democratic Republic of Algeria
Ministry of Higher Education and Scientific Research
University 20 August 1955 Skikda

Faculty of Technology
Process Engineering Department

Ref : D012125009D

Home laboratory: Laboratoire de Physico-Chimie des Surfaces et des Interfaces (LRPCSI)

THESIS

Thesis submitted in partial fulfillment of the requirements for the degree 3rd CYCLE_LMD Doctorat

Domain: Science and technology **Field:** Process engineering

Specialty: Catalysis

Presented by

ABDENNOURI Amdjed

Entitled

Valorization of algae and industrial waste for the production of biofuels via heterogeneous catalysis

Organized in: ….

In front of a jury composed of :

First & last name	**Grade**	**Establishment**	**Quality**
Mme SOBHI Chafia	Professeur	University of Skikda	President
Mme ZOUAOUI Emna	Professeur	University of Skikda	Thesis Director
Mr BOUHDIBA Abdelaziz	Professeur	University of Skikda	Examiner
Mr ALLAL Hamza	MCA	University of Constantine 3	Examiner
Mme FERKOUS Hana	MCA	University of Skikda	Invited

University year: 2024-2025

One day, in retrospect, the years of
struggle will strike you as the most beautiful.

- Sigmund Freud-

Acknowledgements

It is difficult to begin writing this page, as the number and significance of the individuals who have contributed, in one way or another, to the completion of this work are immense. At the conclusion of this research, I would like to extend my heartfelt gratitude to my thesis advisors. First and foremost, ***Pr. Emna Zouaoui***, for her invaluable support, guidance, and insightful advice, as well as her exemplary human qualities. I am deeply grateful for all she has done for me during all these years. I also wish to thank ***Dr. Hana Ferkous***, for her scientific insight, thoughtful guidance, and constant encouragement have been pivotal throughout this journey.

I am also profoundly grateful to the members of my jury. My sincere thanks to ***Pr. Chafia Sobhi*** from the University of Skikda for honoring me by presiding over the jury. I extend my appreciation to the examiners, ***Pr. Abdelaziz Bouhadiba*** from the University of skikda and ***Dr. Hamza Allal*** from the University of Constantine, for their thoughtful evaluations and for being part of my jury.

This work was conducted in the pedagogical laboratories of the Process Engineering and Petrochemical Departments at the Faculty of Technology. I am deeply thankful to all the engineers from various laboratories for their technical assistance.

I would like to express my gratitude to the engineers in the laboratories of Technology Hall, all with their names, especially ***Noura Abdennouri*** for her assistance to me all these years.

I am deeply and sincerely thankful to the many incredible doctors and professors whose guidance, support, and encouragement have been instrumental in helping me reach this milestone. Among them, I am especially grateful to ***Dr.Amel Delimi***, ***Pr. Benguerba Yacine***, ***Dr, Abir Boublia*** , ***Pr. Ayhan Oral***

I am also grateful to ***Prof. Faycal Djezi***, director of the Surfaces and Interfaces Physics and Chemistry Laboratory, for her kind welcome and support in her laboratory.

I want to express my deepest gratitude to my dear friend ***Amir Hamza***. Without his unwavering support and encouragement, this work would not have been possible. Despite working in different fields, he selflessly extended his time, knowledge, and effort to collaborate with me, demonstrating a remarkable spirit of generosity and friendship. His belief in me never faltered, even in the most challenging moments, and his willingness to stand by my side made all the difference. Amir, your kindness and dedication have left an indelible mark on this journey, and for that, I will forever be grateful.

I extend my heartfelt gratitude to my dear friends ***Seif El Islam Boudagha***, ***Bouzenad Nawal***, ***Nada Hamrouche***. ***Ilyes Othmane,*** and ***Hana Bouchetta*** Your invaluable assistance, wise advice, and constant encouragement have been the guiding light in moments of doubt and difficulty. Your unwavering support and genuine friendship have not only made every challenge more bearable but have also filled this journey with joy, warmth, and meaning. Every shared laughter, every comforting word, and every moment of understanding has left an indelible mark on my heart. Thank you for walking this path with me, for believing in me when I needed it most, and for reminding me that no dream is too big when you have friends like you by your side. I will cherish these memories forever.

I also wish to thank the members of the pedagogical laboratories of the Process Engineering Department and the Technology Hall, as well as all the faculty members of the Process Engineering and Petrochemical Departments, for fostering a collaborative and friendly work environment.

Lastly, I express my deepest gratitude to all my friends ***Amar***, ***Kader***, ***Fateh***, ***Yasser***, ***Khaled***, ***Smail***, ***Ali***.. and colleagues for their support and kindness throughout this journey. Your hospitality, assistance, understanding, encouragement, and empathy have been invaluable to me.

Dedication

To my beloved mother, whose memory is my greatest source of strength and inspiration. This work is a tribute to her endless love, sacrifices, and unwavering belief in me. Though she is no longer here, I feel her guidance in every step I take, and I dedicate this achievement to her with all my heart.

To my dear father, who has always stood by me with prayers, support, and encouragement, helping me pursue my dreams.

To my brother Aboubeker, a constant source of motivation.

To my Sisters, Amina, Selma, Oumaima, Soumaia, and little Wissal

To my Brothers Amine, Hamza.

To all my grandparents, uncles and aunts.

To all my family, who have surrounded me with love and support.

To my friends, who have walked this journey with me, sharing in the challenges and triumphs.

This work is for all of you, with my deepest gratitude and love.

Abstract

This thesis focuses on the urgent global waste problem, especially in developing countries where poor waste management causes environmental and health issues. One solution is waste valorization, which transforms waste into useful products like biodiesel. Biodiesel is made by converting waste oils and fats into fuel, offering both environmental and economic benefits, particularly when renewable materials like waste cooking oil and algae are used. This thesis examines biodiesel production using calcium oxide (CaO) catalysts made from cuttlefish bones and evaluates how well waste cooking oil, spirulina, and chlorella algae perform as feedstocks. Furthermore, it introduces an AI-based technique for improving the analysis of SEM images of CaO catalysts, demonstrating its potential to enhance catalyst characterization and recognition to enhance the experimental protocol to produce effective catalysts. Experimental results show significant improvements in biodiesel production efficiency using the CaO catalyst with several feedstocks alongside the SCWSO AI technique, which presents a high analytical accuracy and facilitates the discovery of catalyst morphology.

Keywords : Biodiesel, Algae, industrial waste, Catalysis, Valorization, Artificial intelligence

Résumé

Cette thèse se concentre sur le problème mondial urgent des déchets, en particulier dans les pays en développement où une mauvaise gestion des déchets entraîne des problèmes environnementaux et sanitaires. L'une des solutions est la valorisation des déchets, qui transforme les déchets en produits utiles tels que le biodiesel. Le biodiesel est obtenu en convertissant les huiles et les graisses usagées en carburant, ce qui présente des avantages environnementaux et économiques, en particulier lorsque des matériaux renouvelables tels que l'huile de cuisson usagée et les algues sont utilisés. Cette thèse examine la production de biodiesel à l'aide de catalyseurs à base d'oxyde de calcium (CaO) fabriqués à partir d'os de seiche et évalue les performances des huiles de cuisson usagées, de la spiruline et de l'algue Chlorella en tant que matières premières. En outre, il introduit une technique basée sur l'IA pour améliorer l'analyse des images SEM des catalyseurs CaO, démontrant son potentiel pour améliorer la caractérisation et la reconnaissance des catalyseurs afin d'améliorer le protocole expérimental pour produire des catalyseurs efficaces. Les résultats expérimentaux montrent des améliorations significatives de l'efficacité de la production de biodiesel en utilisant le catalyseur CaO avec plusieurs matières premières ainsi que la technique d'IA SCWSO, qui présente une grande précision analytique et facilite la découverte de la morphologie du catalyseur.

Mots-clés : Biodiesel, algues, déchets industriels, catalyse, valorisation, intelligence artificielle

ملخص

تركز هذه الأطروحة على المشكلة العالمية الملحة للنفايات، لا سيما في البلدان النامية حيث يؤدي سوء إدارة النفايات إلى مشاكل بيئية وصحية. ويتمثل أحد الحلول في تحويل النفايات إلى طاقة، حيث يتم تحويل النفايات إلى منتجات مفيدة مثل وقود الديزل الحيوي. يتم الحصول على وقود الديزل الحيوي عن طريق تحويل نفايات الزيوت والدهون إلى وقود، وهو ما ينطوي على فوائد بيئية واقتصادية، خاصة عند استخدام مواد متجددة مثل نفايات زيوت الطهي والطحالب. تبحث هذه الأطروحة في إنتاج وقود الديزل الحيوي باستخدام محفزات أكسيد الكالسيوم المصنوعة من عظم الحبار، وتقيّم أداء نفايات زيت الطهي وطحالب السبيرولينا والكلوريلا كمواد وسيطة. بالإضافة إلى ذلك، يقدم هذا البحث تقنية قائمة على الذكاء الاصطناعي لتحسين تحليل صور لمحفزات أكسيد الكالسيوم، مما يدل على قدرتها على تحسين توصيف المحفزات والتعرف عليها من أجل تحسين البروتوكول التجريبي لإنتاج محفزات فعالة. تُظهر النتائج التجريبية تحسينات كبيرة في

مع العديد من المواد الأولية بالإضافة إلى تقنية الذكاء الاصطناعي، التي كفاءة إنتاج وقود الديزل الحيوي باستخدام محفز .تتميز بدقة تحليلية عالية وتسهل اكتشاف مورفولوجيا المحفز

الكلمات المفتاحية: وقود الديزل الحيوي، الطحالب، النفايات الصناعية، الحفز، الاستغلال، الذكاء الاصطناعي

List of figures

Chapter I : Algeria waste and energy challenges

Chapter II : Biodiesel feedstock and production processes and catalysts

Chapter III : Artificial intelligence in biodiesel production

Chapter IV : Materials and methods

Chapter V : Results and discussion

List of tables

Chapter II : Biodiesel feedstock and production processes and catalysts

Chapter III : Artificial intelligence in biodiesel production

Chapter IV : Materials and methods

Chapter V : Results and discussion

List of abbreviations

- **AI:** Artificial Intelligence
- **ANN:** Artificial Neural Network
- **BIAs:** Bio-Inspired Algorithms
- **CDO:** Chornobyl Disaster Optimizer
- **CE:** Circular Economy
- **Chimp:** Chimp Optimization Algorithm
- **CWSO:** Chaotic War Strategy Optimizer
- **DFT:** Density Functional Theory
- **DWSIM:** Open Source Chemical Process Simulator
- **ECTs:** Evolutionary Computation Techniques
- **FSIM:** Feature Similarity Index Measure
- **FT:** Freidman Test
- **GJO:** Golden Jackal Optimization
- **GPR:** Gaussian processes regression
- **GWO:** Grey Wolf Optimizer
- **IGWO:** Improved Grey Wolf Optimizer
- **KNN:** K-nearest neighbors
- **ML:** Machine Learning
- **MLP:** Multi-layer perceptron
- **MSE:** Mean Square Error
- **MWSO:** Modified War Strategy Optimizer
- **NIOAs:** Nature-Inspired Optimization Algorithms
- **nTh:** Number of thresholds
- **OECD:** Organization for Economic Co-operation and Development
- **OPEC:** Organization of the Petroleum Exporting Countries
- **PSNR:** Peak Signal-to-Noise Ratio
- **PV:** Photovoltaic
- **RSA:** Reptile Search Algorithm
- **RSM:** Response Surface Methodology
- **SCA:** Sine Cosine Algorithm
- **SCWSO:** Symmetric Chaotic War Strategy Optimization
- **SEM:** Scanning Electron Microscopy
- **SPSS:** Statistical Package for the Social Sciences
- **SSIM:** Structural Similarity Index Measure
- **Std:** Standard Deviations
- **USD:** United States Dollar
- **WCO:** Waste Cooking Oil
- **WSO:** War Strategy Optimization

Table of contents

Chapter II : Biodiesel feedstock and production processes and catalysts

Chapter III : Artificial intelligence in biodiesel production

Chapter IV : Materials and methods

Chapter V : Results and discussion

General introduction

General Introduction

Our modern societies are currently dealing with multiple obstacles arising from the growth of industries and cities, one of which is the increasing amount of waste generation globally, which is expected to reach 3.4 billion tons by 2050, according to recent studies [1]. This rise in waste is primarily caused by growing cities, a rising population, and economic development, particularly in developing countries where industrial activities are expanding, as mentioned previously. This waste problem is especially serious in developing countries, where a large amount of rubbish is not effectively handled and is frequently discarded without treatment, resulting in negative impacts [2]. Improperly handled waste, such as landfilling and open dumping, creates substantial environmental problems, including greenhouse gas emissions, pollution, and hazards to human health [3].

So, to limit the harsh drawbacks of the waste generation worldwide, different strategies have developed to valorize the huge trash quantities. In definition, Waste valorization is the process of turning waste into useful products like energy, chemicals, or materials, helping to manage waste sustainably. This approach includes technologies such as recycling, composting, and chemical recovery, each suited to different types of waste[4]. The main benefits of waste valorization are reducing pollution and greenhouse gas emissions, saving resources by recovering materials and energy, and boosting the economy through new revenue streams and job creation in recycling and manufacturing. By converting waste into valuable resources, waste valorization plays a vital role in moving towards a circular economy and tackling global environmental and economic challenges [5].

One of this high value added products gotten from waste valorization is biodiesel, this resource is a renewable, biodegradable fuel made from different feedstocks such as natural oils and fats, such as vegetable oils, animal fats, and recycled cooking grease, using a chemical process known as transesterification, which converts the fats into fatty acid methyl esters (FAME)[6], the chemical compounds that make up biodiesel. Biodiesel can be utilized in a variety of ways, including pure or blended with petroleum diesel in varying proportions, making it an adaptable alternative fuel for diesel engines. Biodiesel offers numerous advantages, including fewer greenhouse gas emissions and pollutants such as particulate matter and carbon monoxide, which improve air quality when compared to fossil fuels. It also improves engine lubrication, extends engine life, and reduces reliance on foreign oil, limiting the use of traditional fuels[7]. As highlighted previously, there are many raw materials to use in biodiesel production, vegetable oils, animal fats, waste cooking oils, and algae are all common feedstocks, as are non-edible crops like jatropha and camelina. The kind of feedstock used influences the characteristics and environmental impact of biodiesel, with second-generation sources such as waste oils and algae producing significant greenhouse gas reductions [8].

Another significant factor in biodiesel production is the use of appropriate catalysts during the transesterification process, which turns fats or oils into biodiesel. Catalysts are vital because they accelerate the reaction, boost efficiency, and improve selectivity, resulting in a larger biodiesel yield in a shorter period of time[9]. There are three types of catalysts used: homogeneous (soluble in the reaction mixture), heterogeneous (insoluble and reusable), and enzymatic (biological). Each kind has advantages, and ongoing research has resulted in the creation of new catalysts that greatly speed up, enhance the efficiency, and reduce the environmental impact of biodiesel production.

The evaluation and characterization of developed catalysts for biodiesel production are typically conducted using various techniques such as X-ray diffraction (XRD), Scanning Electron Microscopy (SEM), and Fourier-Transform Infrared Spectroscopy (FT-IR). However, these methods have limitations, including potential errors from inexperienced analysts and difficulties such as noisy images, which can affect the accuracy of the results. To overcome these challenges, new approaches are needed to simplify the analysis and improve accuracy. Integrating Artificial Intelligence (AI) techniques into the catalyst evaluation process can address these issues by enhancing data interpretation, providing more precise predictions, and streamlining the overall analysis in biodiesel production [10].

This thesis aims to address various issues and answer key questions about waste management in Algeria, including the types of waste prevalent in the environment, the current waste situation, and how the impact of waste valorization on energy production in the country will be. Different biodiesel feedstocks will be displayed alongside with the transesterification reaction mechanism, and the catalysts used to enhance reaction efficiency. Additionally, the theoretical section will cover recent AI techniques applied in biodiesel production and catalyst analysis.

The experimental part of the thesis will be divided into two sections. The first section focuses on developing a novel AI technique based on segmentation methods to improve the analysis of SEM images of calcium oxide (CaO) catalysts, demonstrating its superiority over existing segmentation methods. The second section investigates the use of CaO derived from cuttlefish bones as a catalyst for biodiesel production using waste cooking oil and two types of algae—spirulina and chlorella. Experiments will evaluate and compare the effectiveness of these different feedstocks in biodiesel production, providing insights into their performance and efficiency.

The thesis is structured as follows:

A theoretical part contains the following chapters :

Chapter I which examines Algeria's waste management and energy challenges, emphasizing circular economy approaches that aim to minimize environmental and economic impacts of pollution.

- **Chapter II** delves into biodiesel production, detailing the main feedstocks, chemical processes involved in transesterification, and catalyst development.
- **Chapter III** reviews theoretical methods applied in biodiesel production, focusing on techniques that enhance data analysis and prediction from various experiments.

The experimental part is divided into two chapters:

- **Chapter IV** outlines the materials and methods used in the study that aim to develop AI technique which make analysis of SEM images simple alongside with biodiesel production protocol.
- **Chapter V** presents and analyzes the results obtained from these methods.

The thesis concludes with a summary of the key findings and outcomes of the research.

References

[1] Z. Zhang *et al.*, 'Municipal solid waste management challenges in developing regions: A comprehensive review and future perspectives for Asia and Africa', *Science of the Total Environment*, p. 172794, 2024.

[2] S. Khan, R. Anjum, S. T. Raza, N. A. Bazai, and M. Ihtisham, 'Technologies for municipal solid waste management: Current status, challenges, and future perspectives', *Chemosphere*, vol. 288, p. 132403, 2022.

[3] M. M. Maja and S. F. Ayano, 'The Impact of Population Growth on Natural Resources and Farmers' Capacity to Adapt to Climate Change in Low-Income Countries', *Earth Syst Environ*, vol. 5, no. 2, pp. 271–283, Jun. 2021, doi: 10.1007/s41748-021-00209-6.

[4] A. Mohajerani *et al.*, 'Recycling waste rubber tyres in construction materials and associated environmental considerations: A review', *Resources, Conservation and Recycling*, vol. 155, p. 104679, 2020.

[5] P. Pal *et al.*, 'Circular Bioeconomy in Action: Transforming Food Wastes into Renewable Food Resources', *Foods*, vol. 13, no. 18, Art. no. 18, Jan. 2024, doi: 10.3390/foods13183007.

[6] S. M. Farouk, A. M. Tayeb, S. M. S. Abdel-Hamid, and R. M. Osman, 'Recent advances in transesterification for sustainable biodiesel production, challenges, and prospects: a comprehensive review', *Environ Sci Pollut Res*, vol. 31, no. 9, pp. 12722–12747, Feb. 2024, doi: 10.1007/s11356-024-32027-4.

[7] S. Parida, M. Singh, and S. Pradhan, 'Biomass wastes: A potential catalyst source for biodiesel production', *Bioresource Technology Reports*, vol. 18, p. 101081, 2022.

[8] M. A. H. Shaah *et al.*, 'A review on non-edible oil as a potential feedstock for biodiesel: physicochemical properties and production technologies', *RSC advances*, vol. 11, no. 40, pp. 25018–25037, 2021.

[9] M. N. B. Mohiddin *et al.*, 'Evaluation on feedstock, technologies, catalyst and reactor for sustainable biodiesel production: A review', *Journal of Industrial and Engineering Chemistry*, vol. 98, pp. 60–81, 2021.

[10] A. Abdennouri, E. Zouaoui, H. Ferkous, A. Hamza, M. Grimes, and A. Boukabou, 'An improved Symmetric Chaotic War strategy optimization algorithm for efficient Scanning electron microscopy image segmentation: Calcium oxide catalyst case', *Chemometrics and Intelligent Laboratory Systems*, vol. 244, p. 105043, 2024.

Chapter I

Algeria waste and energy challenges

I.1. Introduction

The entire world faces several environmental concerns, including water pollution, soil and air pollution, and climate change caused by greenhouse gas emissions, where Since 1850, the total land and ocean temperature has grown at an average pace of 0.06°C every decade [1]. The most prevalent source of pollution comes from a growth in solid waste amount generated, both in developed and developing nations, which is difficult to regulate owing to its complexity and inadequate disposal. Food, paper, glass, and plastic are among the most common components of municipal solid waste [2]. Urbanization due to the population expansion, which led high demand for energy and supplies all contribute to the rapid development and accumulation of solid waste, especially in developing nations [3].

Various methods of disposal, such as burning and landfilling, have drawbacks, including maintenance, incineration, and open dumping. Recycling is an efficient solution, but it involves more effort and development. On the other side, CO_2 emissions are unavoidable as the world's population grows [4], this gas emissions originate from petroleum, electricity and other industries, which seek to provide the energy required to meet the rising demands of various sectors. it is another concern that needs to be solved rapidly due to its impact on pollution alongside waste.

A circular economy model, which enables the reuse and recycling of waste and materials after their use [5], can help achieve both environmental protection and economic benefits so in summary, applying this type of economic model could be the solution for the current situation of waste and gases come from fossil fuels. One of the most important projects that can be achieved in this scoop is the production of energy from various biomass waste, which leads to multiplying the resources of energy used in different sectors.

This chapter explores the waste and energy situation in Algeria and highlights circular economy models, for a better understanding of the advantages of using this kind of model to limit the harmful consequences of pollution coming from both waste and gas emissions and its impact on the environment, economy, and so on.

I.2. Types of wastes found around the world

By definition, waste is a product or material that is no longer useful for its original purpose. Whereas waste is used as food or a reactant in natural ecosystems, these waste products are usually generated by human activities and are frequently very resilient and take a long time to disintegrate which leads to the problem of its existence in nature for a long time which conduct to the pollution of soil and water [6]. The next subsections present the major type of waste presented in the environment.

I.2.1. Solid waste

As previously stated, waste is defined as a material that no longer has inherent value due to its use, and it can include a variety of elements such as food, diapers, pet waste, paper, wood, yard, and garden waste, textiles with rubber and leather, and other organics, glass, metals, building materials, and plastics. All of these components are solid; hence this form of solid waste consists of two categories. Hazardous waste can be organic or a mixture, such as railway ties and biosolids, and there is hazardous waste that contains non-organic (metal, glass), organic (paper, plastic, food, etc.), and combination trash (tier) [7] . the classification of solid waste is indicated in Fig I. <Q1.

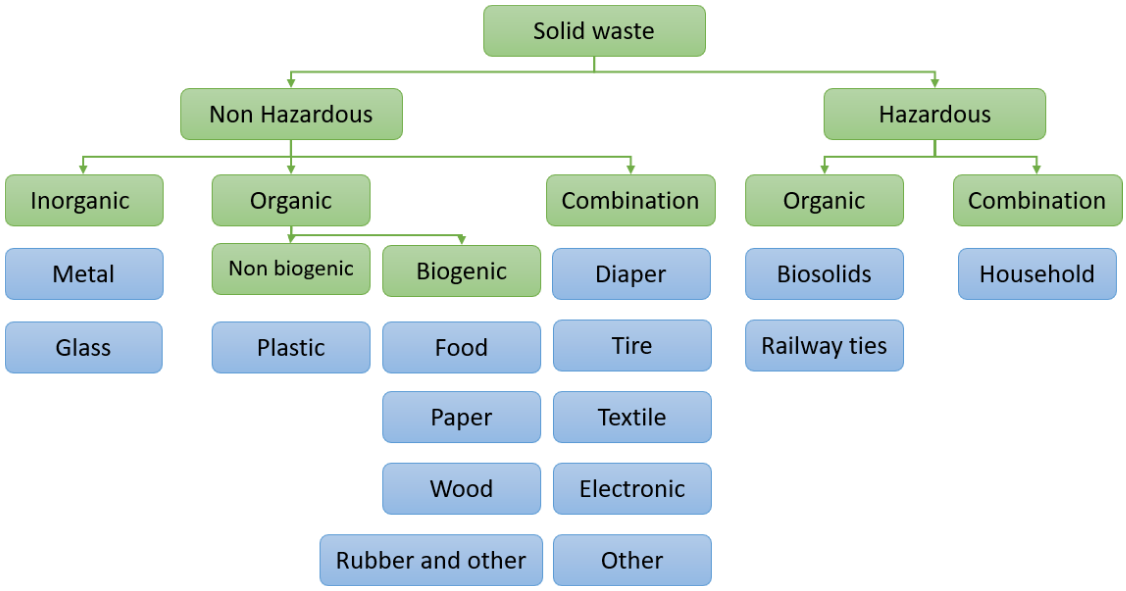

Figure I.1 : Solid waste classification [7].

As shown in Figure 2, the growth of solid waste is acknowledged and increasing, particularly in developed countries Fig I.2(a), due to the large number of industries and activities that generate trash. However, the difficulty is that poor management emerges especially in developing countries as indicated in Fig I.2(b), resulting in less value for this garbage and, as a result, an increasing amount of trash being thrown away.

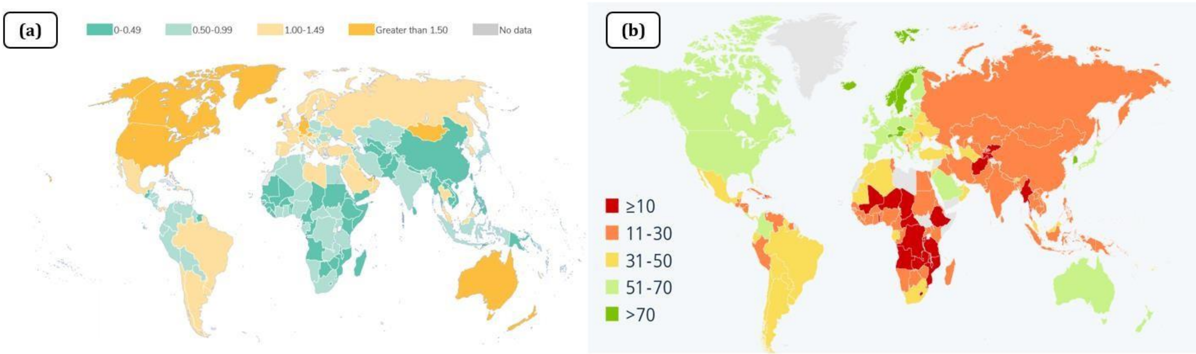

Figure I.2 : Annual municipal solid waste generated per capita (kilograms/capita/day) [8], (b): The global state of waste management [9].

I.2.2. Plastic waste

Nowadays, and because of its diverse chemical composition, plastic has seen a growth in uses in a variety of industries, including engineering, medical, electrical, food packaging, and more as indicated in Fig I.3 where the most plastic generated found in packaging sector. However, managing plastic waste is a highly delicate operation due to the ever-increasing volume of plastic waste collected each time, the difficulty of biodegradation, and the negative impact on both the environment and society [10].

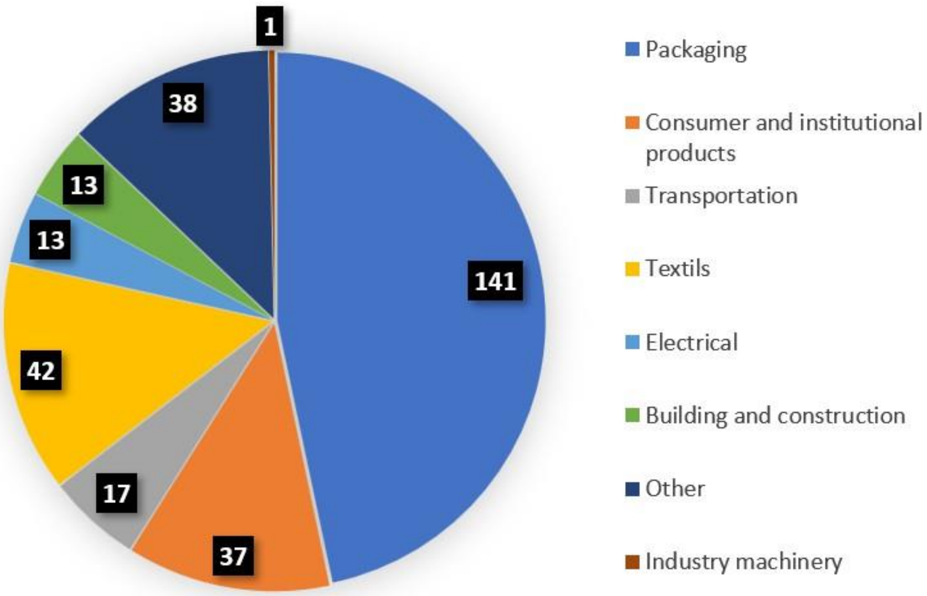

Figure I.3 : Plastic waste generation by sector (million tonnes) [11].

According to the most recent statistics for the year 2023 [12], the entire world produces around 350 million tons of plastic trash every year. Almost a quarter of this waste is mishandled or littered. Approximately 82 million tons. One-quarter of the total, 19 million tons, gets spilled into the environment. 13 million tonnes to terrestrial habitats, with 6 million tonnes going to rivers or coasts. In conclusion. Around 0.5% of plastic waste ends up in the ocean, posing a significant risk to marine life. As mentioned previously, the increase in plastic waste generation was mainly due to the development of industrial sectors to satisfy the requirements of consumers. And this increase is highly noticed in countries with powerful economic potential. where the countries that generate plastic waste as mentioned in Fig I.4 are the United States, EU India, China, and so on.

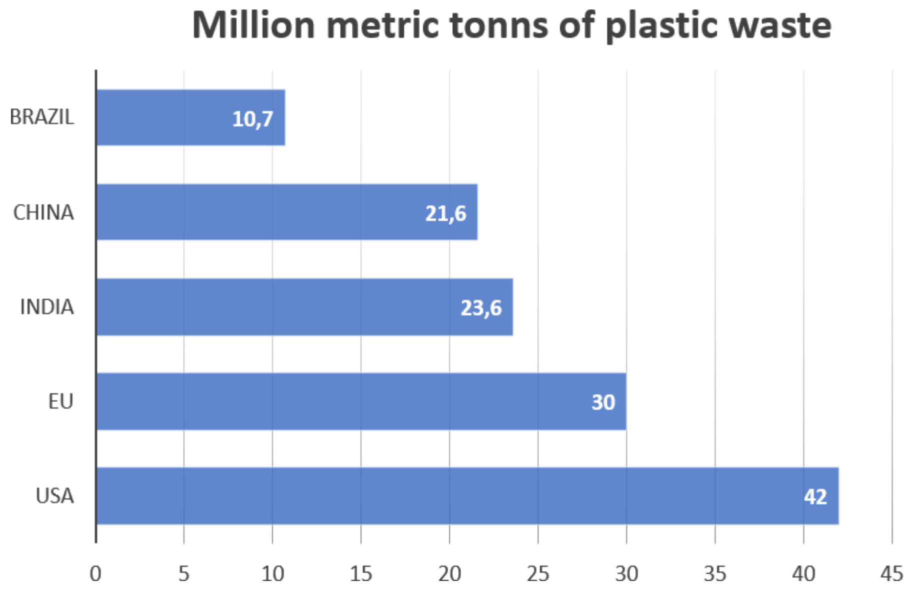

Figure I.4 : Plastic waste generation by country [13].

I.2.3. Agricultural Waste

Recently, agriculture's value contributed rose by 68% between 2000 and 2018, reaching nearly 3.4 trillion USD. Between 2000 and 2018, vegetable oil output increased by 108%, meat production rose by 47%, and crop production increased by 50% [14].

Agricultural wastes are non-product outflows of agricultural product manufacturing and processing that can contain material that could help people but have a lower economic worth than the cost of collection, transportation, and processing for beneficial use [15].

Although agricultural by-products play a crucial role in serving as valuable resources for various industries, their disposal and management present significant challenges, particularly concerning their environmental impact. One of the most pressing concerns is their contribution to climate change through the emission of greenhouse gases.

When agricultural by-products such as crop residues, animal manure, and food waste are improperly managed, they undergo decomposition processes that release significant amounts of methane (CH_4) and nitrous oxide (N_2O) into the atmosphere.

According to the statistical yearbook of food and agriculture organization of 2020 [14], Between 2000 and 2017, greenhouse gas emissions from crops and livestock grew by 16%. Enteric fermentation accounts for approximately 40% of total emissions. Cattle meat production generates 45 times more greenhouse gasses than chicken meat production, and water stress levels are near or above 100% in practically all Near Eastern and North African nations, with Kuwait, the United Arab Emirates, and Saudi Arabia having the highest values.

These gases are potent greenhouse gases, the implications of these emissions on climate change are profound. They contribute to the intensification of global warming, exacerbating issues such as rising temperatures, altered precipitation patterns, and extreme weather events. Moreover, the environmental consequences extend beyond climate change, impacting air quality, soil health, and water resources.

I.3. Major resources of energy around the world

Due to the rapid growth in population in the last, the enhancement of life quality resulted from pressure on the industries sector to increase the number of its products from electricity, food, and cosmetics, and because of the industrial revolution especially in the 19th Century the production of these matters was simplified but need energy, so to satisfy the requirements of populations around the globe. This increase in industry activities requires the use of more energy, as indicated in Fig I.5 the world's consumption of energy has increased rapidly especially in the last 30 years to reach a value of 160.000 TWh in 2022.

Fig I.5 illustrates the different types of energy resources used, which can be categorized into non-renewable and renewable energies. The following section will focus on major resources from these two groups.

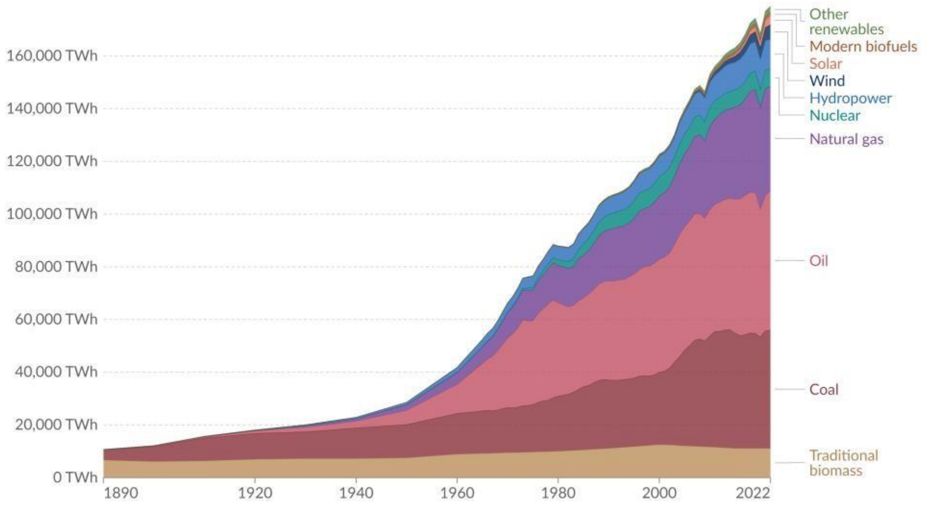

Figure I.5 : World consumption of energy [16].

I.3.1. Non-renewable energies

Non-renewable energies are energy sources the amount of which on earth is finite and that cannot be replaced or regenerated in an appropriate period on a human scale [17]. These energy sources include fossil fuels like coal, oil, and natural gas, as well as nuclear energy. These non-renewable energy sources have formed the foundation of global energy production for decades, but their scarcity, environmental damage, and role in climate change have prompted attempts to shift to cleaner and more sustainable alternatives.

I.3.1.1. Coal

Coal is a combustible black or brownish-black sedimentary rock with a high concentration of carbon and hydrocarbons [18]. It is the most abundant fossil fuel and has traditionally provided a significant amount of energy for power generation and industrial activities. The biggest coal mining locations in the world are China, which will produce 3,942 million tons in 2021 [19], and the United States. Yet, Indonesia, Australia, Russia, South Africa, and Colombia also generate significant amounts of coal [20]. However, it emits more nitrogen oxides, sulfur dioxide, carbon dioxide, heavy metals, and particulate matter per unit of energy than other fuel sources, all of which are considered hazardous pollutants that cause a variety of diseases, including respiratory and cardiovascular disease [20], and contribute significantly to air pollution and climate change.

I.3.1.2. Oil

Crude oil, which is also known as petroleum fossil fuels, is a combination of hydrocarbons that formed millions of years ago. It was created from the remains of animals and plants that lived in a marine environment. These remains were buried under layers of sand, silt, and rock, which were compressed and heated to produce crude oil or petroleum[21]. Crude oil is widely used as a fuel for transportation, heating, and power generation, and its usage has increased significantly over the last three decades as highlighted in Fig I.6. Despite the COVID-19 pandemic causing a decline in crude oil consumption in 2020, so oil is still considered an essential resource in these last years [22].

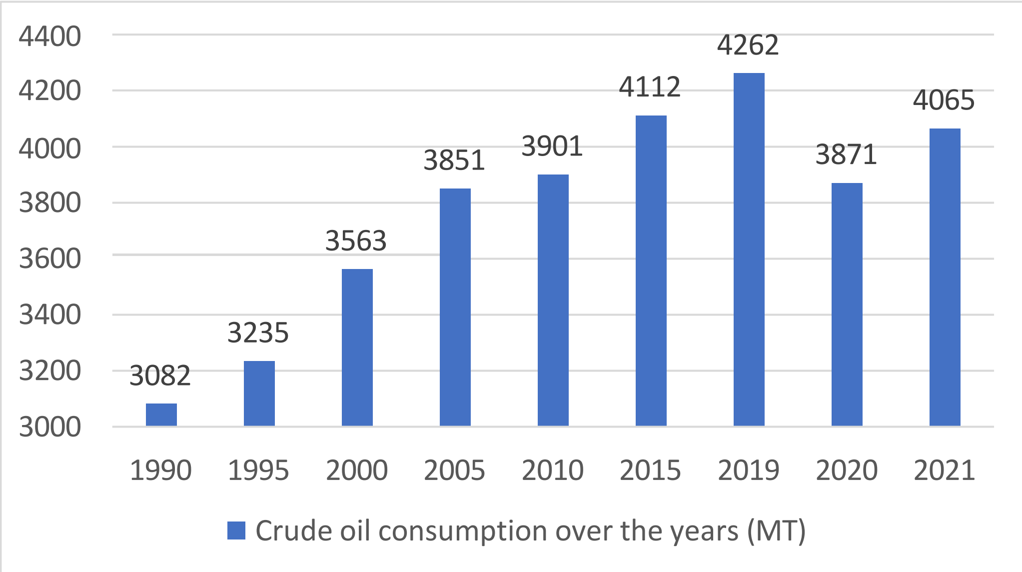

Figure I.6 : Oil consumption in the world with years [22].

As indicated in Fig I.7 which displayed the largest producers of oil in 2023 .The United States, Saudi Arabia, and Russia are the largest producers of crude oil with 20.2, 12.1, and 10.9 million barrels per day, but other key countries like Canada, China, and the Arabian Gulf region also have significant oil deposits [23]. However, the extraction and use of crude oil have significant environmental impacts. For example, oil spills pose a constant threat to millions of miles of coastline, rivers, lakes, and terrestrial ecosystems, particularly in regions with significant oil drilling, refining, and transportation [24]. They also contribute to habitat loss and greenhouse gas emissions.

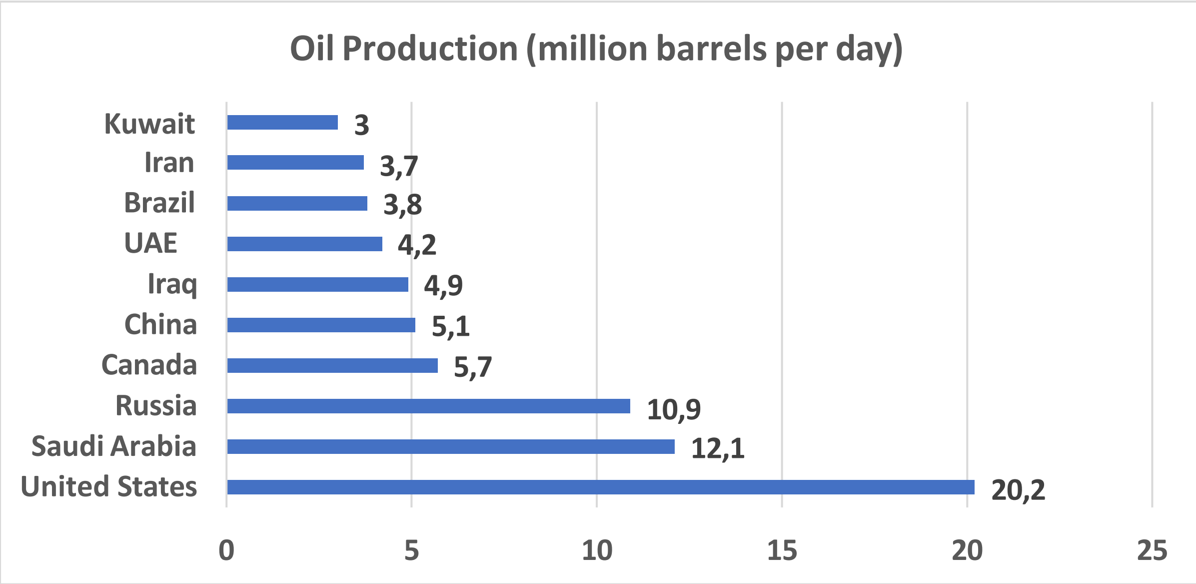

Figure I.7 : Oil majors' producers in the world [23].

I.3.1.3. Natural Gas

Natural gas is a valuable resource consisting mainly of hydrocarbon gases, predominantly methane, found in underground reservoirs or near other fossil fuel sources. It has numerous applications, including its use in the production of paper, glass, bricks, steel, and iron, as well as the manufacturing of fertilizers, petrochemicals, and hydrogen for renewable energy. Moreover, it is also used in medicinal items, heating, fire, and dehumidification. Its uses extend beyond energy generation to a variety of fields [25]. According to the Energy Institute - Statistical Review of World Energy (2023), natural gas production has seen a significant growth of 87% from 21,104.49 TWh in 1995 to 39,413.04 TWh in 2022 [26].

In 2020, the United States was the world's largest natural gas producer with a total output of 914.6 billion cubic meters. Russia was the second-largest producer of natural gas, with a total output of 638.5 billion cubic meters. These two countries are by far the top producers of natural gas. Following them are Iran, China, Qatar, Canada, Australia, Saudi Arabia, Norway, and Algeria, as seen in the Fig I.8 [27].

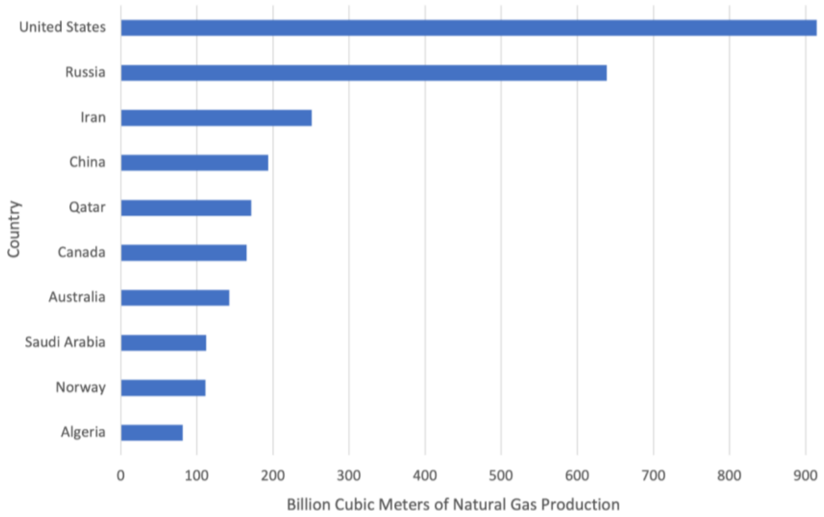

Figure I.8 : Biggest natural gas producers in the world [27].

While natural gas combustion produces fewer emissions than coal and oil, its extraction, particularly through hydraulic fracturing (fracking), poses environmental risks such as water contamination and methane leakage into the environment, leading to soil and water pollution, and more severe issues such as diseases.

I.3.1.4. Nuclear energy

Nuclear energy is produced by nuclear fission. During this process, an atom's nucleus is split to produce energy. Uranium, a naturally occurring radioactive element, nuclear power is one of the most significant sources of energy in the world. It accounts for approximately 11% of global electricity and 21% of OECD nations' electricity, with a total capacity of over 380,000 Mwe [28]. Several countries, including Russia, China, France, the United Kingdom, and the United States, have successfully generated power using nuclear reactors. In the next 25 years, nuclear capacity is expected to increase by approximately 25% [29].

Even though nuclear energy is clean and emissions-free, it is considered non-renewable because uranium is scarce, and nuclear fission produces radioactive waste that must be stored and managed for a long time. The radioactive waste generated from nuclear reactors is highly toxic and can remain radioactive for thousands of years, leading to severe illnesses. This poses a hidden risk and a significant concern for scientists [30].

I.3.2. Renewable energy

Renewable energy refers to energy derived from sources that are naturally renewing but flow-limited. Renewable resources have an almost infinite duration, but there is a finite quantity of energy accessible per unit of time [31]. Some examples of renewable resources include sunlight and wind. Renewable energy is seen as the primary solution to climate change since it produces no emissions, reducing pollution rates. As a result, many governments are investing heavily in various forms of renewable energy and attempting to replace nonrenewable sources with renewable sources as soon as it is economically feasible. The following sections provide basic information on various renewable resources [32].

I.3.2.1. Solar energy

Solar energy is the conversion of sun rays into power, either directly using photovoltaic (PV) or indirectly using concentrated energy or concentrated solar PV [33]. It is estimated that Earth receives energy from the Sun 10,000 times more than the planet's total energy demand [34]. However, despite its recent fast acceptance and ardent backing from both the scientific establishment and energy investors, it still accounts for a modest share of overall energy use [35].

China's solar capabilities are the most developed and used. The country is the world's greatest generator of solar energy, with 430 GW of capacity in April 2023. followed by both the United States and Japan [36].

I.3.2.2. Wind energy

Wind power is the second largest renewable resource after hydropower and one of the fastest-growing electricity sources [37]. It generates electricity and energy by converting the kinetic energy of moving air into electricity. Modern wind turbines use wind to move the rotor blades, converting kinetic energy into rotational energy [38].

Like solar energy, China has taken the initiative and become the first producer of wind energy since its government assisted in the construction of turbines. 329 GW of energy has been generated from wind in China, with the United States coming in second with 132.7 GW and Germany coming in third with 64 GW [39].

Wind as a power source offers several advantages, including easy installation, scalability, and a low carbon impact throughout the project's life cycle [37]. However, wind energy has a number of drawbacks, including variable wind speed, low wind strength, vast wind farms, and restricted energy consumption. It cannot replace fossil fuels, can only handle low power demands, and can be costly and harmful to animals during commissioning. Additionally, noise pollution may be an issue in highly populated places [40].

I.3.2.3. Hydropower

Hydropower is one of the ancient power production methods, and the world's largest power plants generate this kind of power [41]. Despite a high increase in new renewable production technology, hydropower has the second lowest life cycle greenhouse gas (GHG) emissions per 11 kWh of any energy source, behind only wind energy. Hydropower is the world's greatest source of renewable electricity generation, accounting for 15.9% of overall renewable electricity output [42]. In 2022, China reaffirmed its competence in the renewable energy sectors by topping global hydropower production with more than 1300 TWh, followed by Brazil and Canada with 428.06 and 392.51 TWh respectively, all of which are making promising attempts to promote this type of renewable energy [43].

Hydropower is a green, sustainable energy source with several benefits. Dam systems provide power without causing greenhouse gas emissions or air pollution. It can generate energy continuously, close sluice gates when not needed, and store water for later use. They may live for decades and help generate power. A dam's lake serves several purposes, including irrigation [44]. However, it has significant limitations, including expensive construction, equipment, and transmission line costs, as well as longer development times compared to other power plants. Excessive water consumption and global warming have accelerated environmental degradation, particularly in tropical places with fast expansion, soil decomposition, and forest loss. They can also have an impact on the water quality of reservoirs and streams in nearby countries [45].

I.3.2.4. Biomass

Biomass energy is generated by organic resources like wood, agricultural wastes, and organic waste. There are several techniques for producing energy from biomass. The most prevalent approach is direct burning. All biomass may be burnt directly to heat buildings and water, provide industrial process heat, or generate electricity in steam turbines. Pyrolysis, hydrotreating, gasification, and anaerobic digestion are all key methods for producing energy from biomass, whether in the form of heat, biogas, or biofuels [46]. These types of energy sources are promising since they are low-cost resources that provide low-emission energy while also decreasing the amount of trash created, which is an issue in numerous countries.

The United States, China, and Brazil are considered the main countries that produce energy from biomass sources. Brazil is the largest producer of bioethanol from sugar cane, which is used in transportation and is regarded as a successful example of biomass use. China and the United States primarily use wood pellets and waste to generate heating and energy [47].

However, good waste management is critical in developing nations to avoid pollution and illnesses caused by haphazard trash disposal. It has the potential to stimulate economic growth, create jobs, and open up new commercial opportunities. In contrast, affluent countries are turning agricultural supplies like maize into biofuel, boosting demand and necessitating additional acreage for farmers. This contributes to greenhouse gas emissions and food security concerns [48].

I.4. Circular economy

I.4.1. Definition

The European Parliament defines the circular economy as a production and consumption model that prioritizes sharing, leasing, reusing, repairing, refurbishing, and recycling resources and goods to extend their lifespan. This extends the product's life cycle [49].

According to the Environmental Protection Agency (EPA), a circular economy maintains resources and goods in circulation for as long as feasible and tries to eliminate waste via the improved design of materials, products, and systems [50].

A circular economy is a model that aims to reduce the amount of waste generated at the end of a product's life cycle. It is based on three fundamental principles, known as the 3R: Reduce, Recycle, and Reuse. Reduce focuses on developing eco-friendly methods for product extraction and exploitation. This helps extend the product's life cycle and reduces the amount of waste generated. Recycling encourages proper waste management and recycling of the waste generated from the product's life cycle. This waste then can be used in other production lines and get new life cycles. Reuse promotes using a product for multiple life cycles by repairing and responsibly consuming it. This method helps limit the amount of waste generated and encourages responsible consumption. In summary, a circular economy is a sustainable model that aims to reduce waste and promote responsible consumption through the principles of

Reduce, Recycle, and Reuse. not like a classical linear economic model which in a general way led to massive consumption of natural resources and ends up by the end of the life of a product generating a huge amount of waste without proper treatment. Fig I.9 (a) and (b) displayed the differences between linear and circular economy.

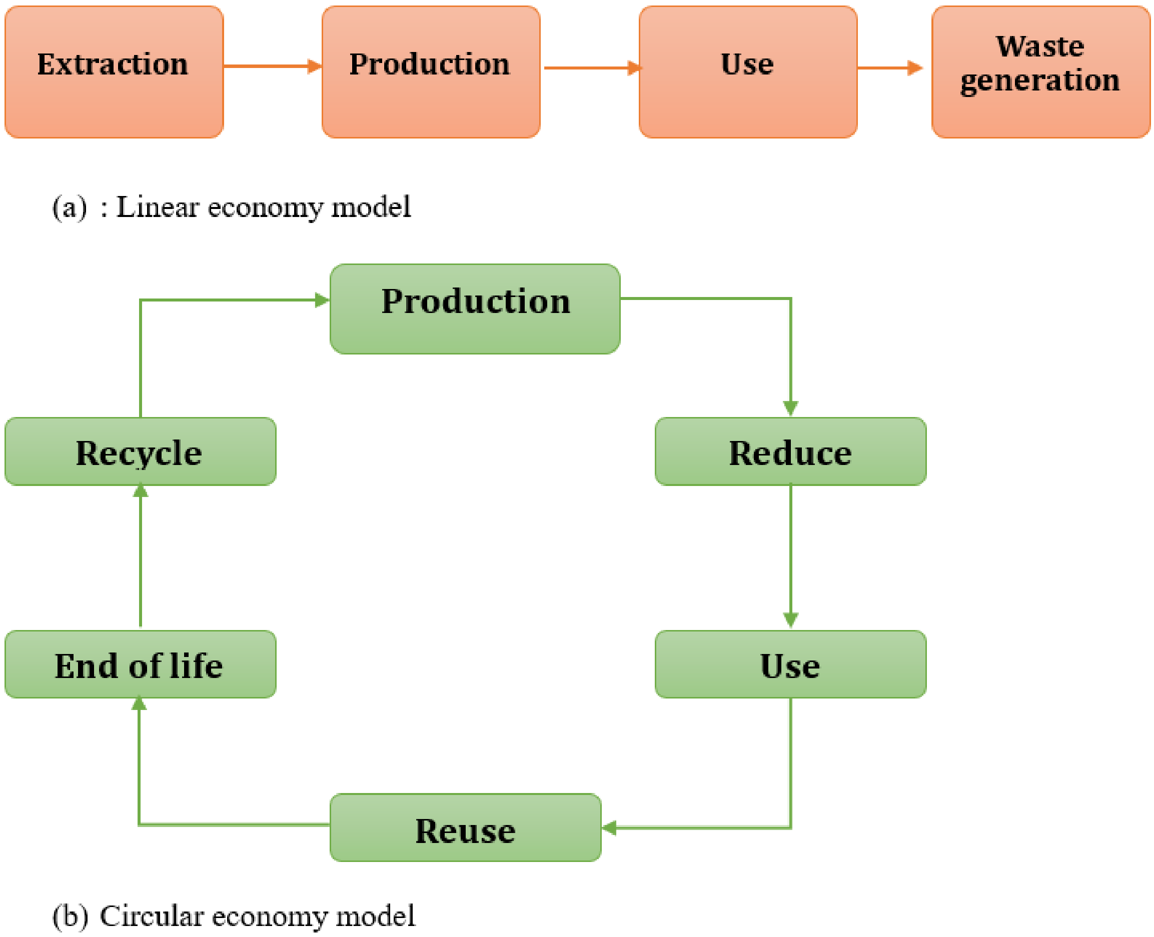

Figure I.9 : Economy models linear and circular.

I.4.2. Advantages of using circular economy models : countries experiences

This section explores various successful circular economy strategies that have been implemented in different countries and their effects on the economy, society, and the environment.

Nigeria has implemented an innovative solution called ColdHubs, which is a solar-powered storage device that preserves fresh food for up to 21 days, reducing food waste and emissions. Since its establishment in 2015, 54 units of ColdHubs have saved approximately 42,000 tons of food, resulting in more than 1 million kilograms of CO_2 reduction by 2020 [51].

Japan is known for its extensive experience with circular economy models. It has established a circular economy society by integrating its people, economy, and social system through optimal usage of non-renewable resources, and strategic reforms for renewable resources. The results have been impressive, with 98% of Japan's metals being recycled in 2007 and a material recovery rate of 74%-89% due to a method that forces consumers to take responsibility for returning electrical equipment [52].

Finland was one of the first countries that approved a circular economy roadmap in 2016, to transition from a "take-make-waste" paradigm to a "carbon-neutral circular economy society" by 2035. The initiative intends to maintain primary raw material consumption at 2015 levels while increasing material circularity and resource productivity. Betolar, a Finnish company, has developed a technology to reduce carbon emissions from cement manufacturing by up to 80% [53,54].

I.5. Algeria current Status : Waste management and Energy resources

Algeria, the largest African country, is known for its diverse population and abundant natural resources, particularly in energy. With over 40 million people and over 2 million km^2 of land, Algeria is the 10th largest producer of natural gas globally. The country is exploring renewable energy sources, particularly solar, to diversify its energy mix and promote sustainability. Balancing fossil fuel use with renewable energy infrastructure is crucial for Algeria's long-term energy security and environmental responsibility.

I.5.1. Waste situation in Algeria

The National Waste Agency launched two campaigns in 2014 and 2018 to determine Algerian waste composition. The program, launched in April 2018, aimed to measure composition differences quarterly until March 2019, aiming to identify the best waste treatment methods or technologies [55]. Results of the evaluation of waste composition in years 2014 – 2018 are indicated in Fig I.10 and Fig I.11

In general, Algeria's waste production in 2020 was 13.5 million tons, with an average of 0.8 kg/habitant/day; the capital has a high generated quantity of 0.9 kg/habitant/day. 90% of this waste is household waste, whereas 10% is other waste [56]. And as indicated in figures below the majority of the generated wastes were organic waste with more than 54% of total waste generated in Algeria, there are many types of waste were found like plastic, textile, metals ...etc.

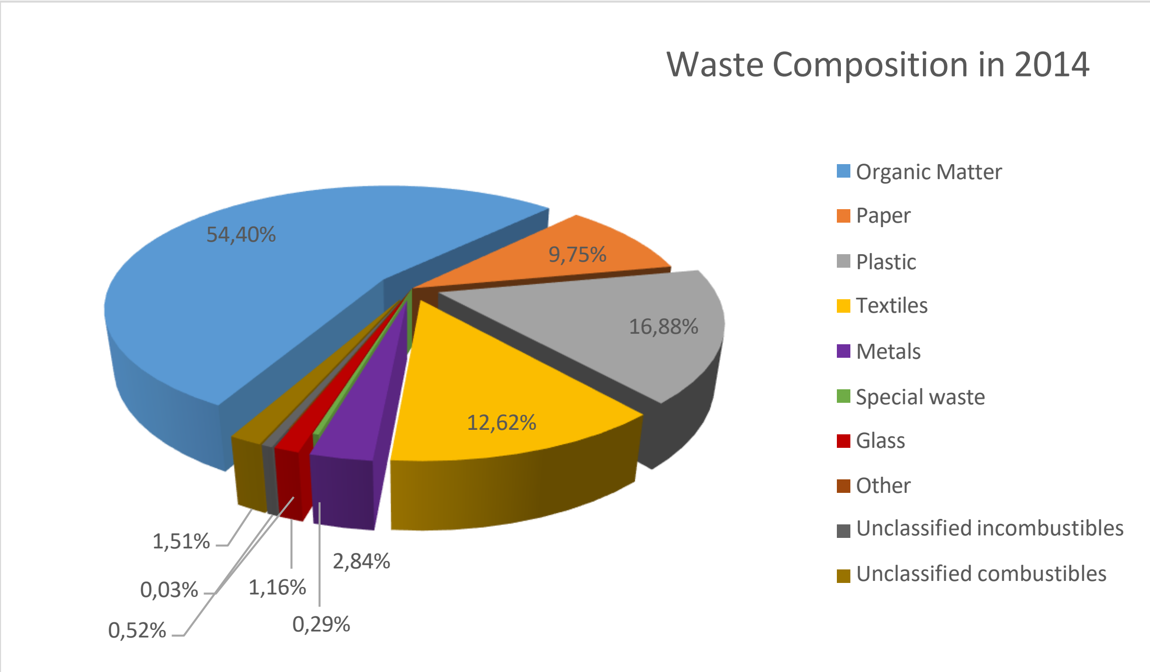

Figure I.10 : Waste composition in Algeria in 2014 [56].

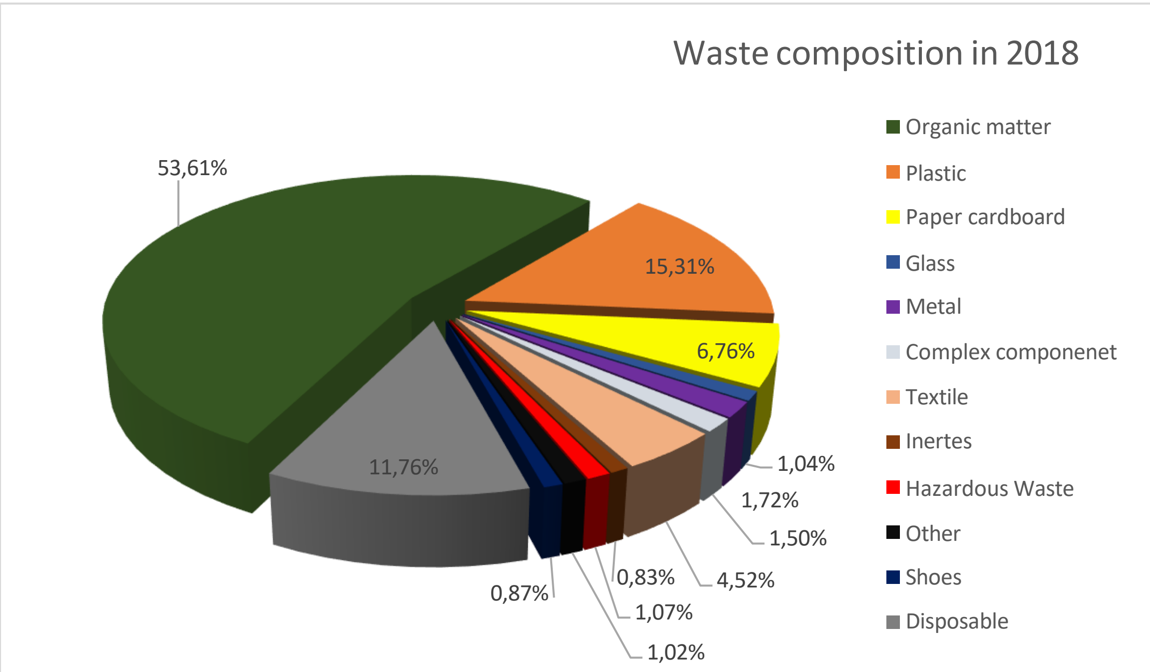

Figure I.11 : Waste composition in Algeria in 2018 [56].

I.5.2. Energetic situation in Algeria

Algeria, an OPEC member with the tenth-largest proven natural gas reserves and the sixth-largest gas exporter, has 12.2 billion barrels of proven oil reserves. The country exports

540,000 barrels of its total production, with 105,043.071 m^3 in December 2021 [57]. Algeria has significant solar, wind, hydro, geothermal, and bio-energy potential [58].

As highlighted in Fig I.12, the majority of energy produced in Algeria comes from fossil fuels, especially natural gas followed by oil, coal utilization has decreased in the last decades due to its harmful consequences. However, the application of renewable resources as energy sources is still limited despite the efforts made by the government. A big part of the energy produced in Algeria is used in two sectors, transportation and residential as indicated in Fig I.13

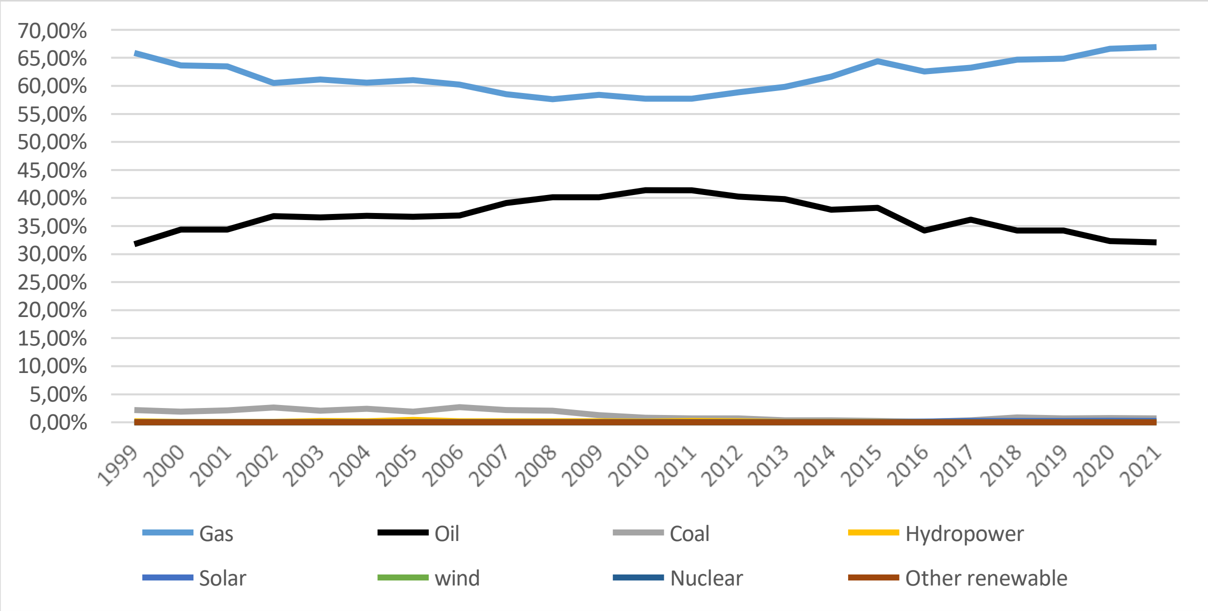

Figure I.12 : Energy consumption by source of energy [16].

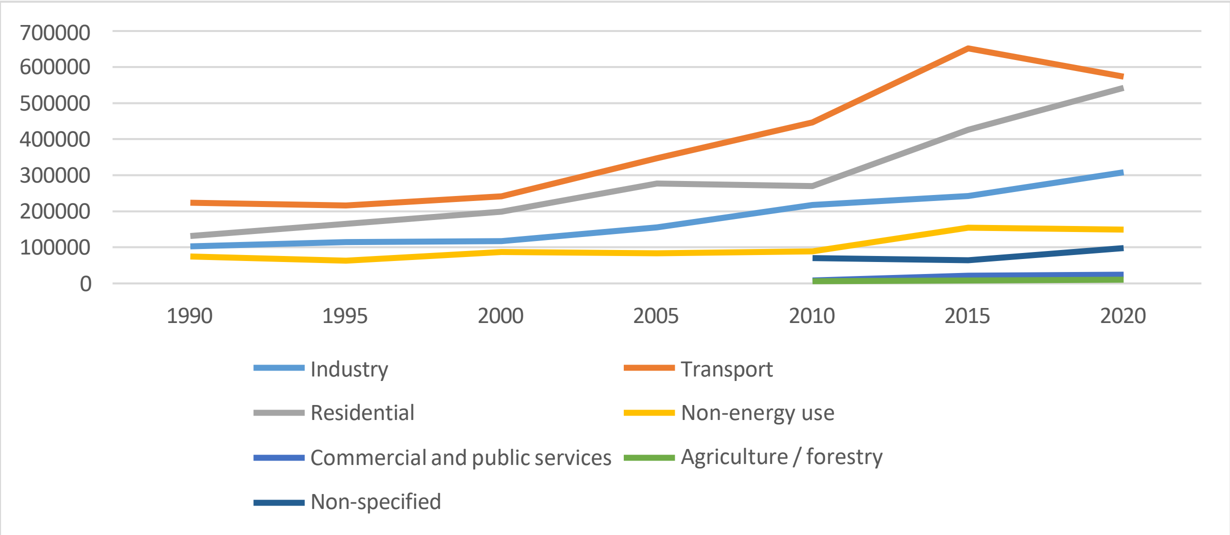

Figure I.13 : Energy consumption by sectors in Algeria [59].

I.6. Conclusion

As discussed in this chapter, waste management and the use of fossil fuels are global problems that have harmful consequences and require effective strategies to limit the generation of large amounts of waste. Algeria is a developing country that has experienced an increase in its economy and population, leading to the problem of waste generation and pollution caused by the extensive use of fossil fuels. Various strategies could be successful in addressing these issues. However, as demonstrated in the previous sections, the circular economy has been successful in numerous countries in limiting waste production and extending the life cycle of waste by recycling and reusing it in other forms.

In conclusion, the findings of this chapter reveal that the circular economy model could be a viable solution for Algeria to address the consequences of both waste generation and pollution caused by fossil fuels. A proposed model focuses on using waste cooking oil and microalgae to produce high-value-added products, specifically high-quality biodiesel. The protocol and mechanism of biodiesel synthesis will be presented and discussed in Chapter II.

References

[1] ‘Climate Change: Global Temperature | NOAA Climate.gov’. Accessed: Apr. 15, 2024. [Online]. Available: http://www.climate.gov/news-features/understanding-climate/climate-change-global-temperature

[2] J. G. Speight, ‘12 - Waste gasification for synthetic liquid fuel production’, in *Gasification for Synthetic Fuel Production*, R. Luque and J. G. Speight, Eds., in Woodhead Publishing Series in Energy. , Woodhead Publishing, 2015, pp. 277–301. doi: 10.1016/B978-0-85709-802-3.00012-6.

[3] D. Vij, ‘Urbanization and Solid Waste Management in India: Present Practices and Future Challenges’, *Procedia - Social and Behavioral Sciences*, vol. 37, pp. 437–447, Jan. 2012, doi: 10.1016/j.sbspro.2012.03.309.

[4] S. Yu *et al.*, ‘Development of an extended STIRPAT model to assess the driving factors of household carbon dioxide emissions in China’, *Journal of Environmental Management*, vol. 325, p. 116502, Jan. 2023, doi: 10.1016/j.jenvman.2022.116502.

[5] L. A. López Ruiz, X. Roca Ramón, and S. Gassó Domingo, ‘The circular economy in the construction and demolition waste sector – A review and an integrative model approach’, *Journal of Cleaner Production*, vol. 248, p. 119238, Mar. 2020, doi: 10.1016/j.jclepro.2019.119238.

[6] *1.1. Definition and classification of waste*. Accessed: Apr. 15, 2024. [Online]. Available: https://sisu.ut.ee/waste/book/11-definition-and-classification-waste

[7] Y. Yao, C. Ramu, A. Procher, J. Littlejohns, J. M. Hill, and J. W. Butler, ‘Potential for Thermo-Chemical Conversion of Solid Waste in Canada to Fuel, Heat, and Electricity’, *Waste*, vol. 1, no. 3, Art. no. 3, Sep. 2023, doi: 10.3390/waste1030041.

[8] Kaza, Silpa, Yao, Lisa C, Bhada-Tata, Perinaz, and Van Woerden, Frank, ‘What a Waste 2.0: A Global Snapshot of Solid Waste Management to 2050’. Accessed: Apr. 15, 2024. [Online]. Available: https://datatopics.worldbank.org/what-a-waste/

[9] Katharina Buchholz, ‘Infographic: The Global State of Waste Management’, Statista Daily Data. Accessed: Apr. 15, 2024. [Online]. Available: https://www.statista.com/chart/31449/waste-management-score-on-the-yale-environmental-performance-index-by-country

[10] C. I. Idumah and I. C. Nwuzor, ‘Novel trends in plastic waste management’, *SN Appl. Sci.*, vol. 1, no. 11, p. 1402, Oct. 2019, doi: 10.1007/s42452-019-1468-2.

[11] M. Vezér and D. Morrow, *Blue investing: searching for solutions to ocean plastics*. 2018. doi: 10.13140/RG.2.2.24098.27842.

[12] H. Ritchie and M. Roser, ‘How much plastic waste ends up in the ocean?’, *Our World in Data*, Dec. 2023, Accessed: Apr. 16, 2024. [Online]. Available: https://ourworldindata.org/how-much-plastic-waste-ends-up-in-the-ocean

[13] M. Lauria, ‘Plastic pollution, by country’, one5c. Accessed: Apr. 16, 2024. [Online]. Available: https://one5c.com/plastic-pollution-by-country-136931514/

[14] FAO, ‘STATISTICAL YEARBOOK WORLD FOOD AND AGRICULTURE 2020’. Accessed: Apr. 17, 2024. [Online]. Available: https://www.fao.org/3/cb1329en/online/cb1329en.html

[15] F. O. Obi, B. O. Ugwuishiwu, and J. N. Nwakaire, ‘Agricultural waste concept, generation, utilization and management’, *Nigerian Journal of Technology*, vol. 35, no. 4, Art. no. 4, Oct. 2016.

[16] H. Ritchie, P. Rosado, and M. Roser, ‘Energy Production and Consumption’, *Our World in Data*, Feb. 2024, Accessed: Apr. 17, 2024. [Online]. Available: https://ourworldindata.org/energy-production-consumption

[17] C. Groth, ‘A New-Growth Perspective on Non-Renewable Resources’, in *Sustainable Resource Use and Economic Dynamics*, L. Bretschger and S. Smulders, Eds., Dordrecht: Springer Netherlands, 2007, pp. 127–163. doi: 10.1007/978-1-4020-6293-3_7.

[18] EIA, ‘Coal explained - U.S. Energy Information Administration (EIA)’. Accessed: Apr. 18, 2024. [Online]. Available: https://www.eia.gov/energyexplained/coal/

[19] GlobalData, ‘Top Five Coal Producing Countries (Million Tonnes, 2021)’. Accessed: Apr. 18, 2024. [Online]. Available: https://www.linkedin.com/company/globaldataplc/

[20] J. Gasparotto and K. Da Boit Martinello, ‘Coal as an energy source and its impacts on human health’, *Energy Geoscience*, vol. 2, no. 2, pp. 113–120, Apr. 2021, doi: 10.1016/j.engeos.2020.07.003.

[21] EIA, ‘Oil and petroleum products explained - U.S. Energy Information Administration (EIA)’. Accessed: Apr. 18, 2024. [Online]. Available: https://www.eia.gov/energyexplained/oil-and-petroleum-products/

[22] H. Sinha and P. Panda, ‘Is Non-Renewable Energy Still the Driver of Economic Growth?’, 2022, pp. 10–17.

[23] M. Aggarwal, ‘US Ranked World’s Biggest Oil Producer - IBT Graphics’, International Business Times. Accessed: Apr. 18, 2024. [Online]. Available: https://www.ibtimes.com/us-ranked-worlds-biggest-oil-producer-ibt-graphics-3702083

[24] S. Othumpangat and V. Castranova, 'Oil Spills', in *Encyclopedia of Toxicology (Third Edition)*, P. Wexler, Ed., Oxford: Academic Press, 2014, pp. 677–681. doi: 10.1016/B978-0-12-386454-3.00359-6.

[25] 'Industrial Uses of Natural Gas – NGSA'. Accessed: Apr. 18, 2024. [Online]. Available: https://www.ngsa.org/industrial-uses-of-natural-gas/

[26] E. Institute, 'Statistical Review of World Energy', Statistical review of world energy. Accessed: Apr. 18, 2024. [Online]. Available: https://www.energyinst.org/statistical-review/home

[27] Alexander Donovan, 'Natural Gas Production'. Accessed: Apr. 18, 2024. [Online]. Available: http://large.stanford.edu/courses/2021/ph240/donovan2/

[28] E. Akyüz, 'Advantages and Disadvantages of Nuclear Energy in Turkey: Public Perception', *EJERE*, vol. 1, no. 1, Art. no. 1, Aug. 2017.

[29] S. Sadekin, S. Zaman, M. Mahfuz, and R. Sarkar, 'Nuclear power as foundation of a clean energy future: A review', *Energy Procedia*, vol. 160, pp. 513–518, Feb. 2019, doi: 10.1016/j.egypro.2019.02.200.

[30] M. Igini, 'The Advantages and Disadvantages of Nuclear Energy', Earth.Org. Accessed: Apr. 19, 2024. [Online]. Available: https://earth.org/the-advantages-and-disadvantages-of-nuclear-energy/

[31] EIA, 'Renewable energy explained - U.S. Energy Information Administration (EIA)'. Accessed: Apr. 19, 2024. [Online]. Available: https://www.eia.gov/energyexplained/renewable-sources/

[32] B. Zohuri, F. Mossavar-Rahmani, and F. Behgounia, 'Chapter 14 - Renewable energy', in *Knowledge is Power in Four Dimensions: Models to Forecast Future Paradigm*, B. Zohuri, F. Mossavar-Rahmani, and F. Behgounia, Eds., Academic Press, 2022, pp. 423–463. doi: 10.1016/B978-0-323-95112-8.00014-3.

[33] Ashok Kumar L., Indragandhi V., and Uma Maheswari Y., 'Chapter 9 - PVSYST', in *Software Tools for the Simulation of Electrical Systems*, Ashok Kumar L., Indragandhi V., and Uma Maheswari Y., Eds., Academic Press, 2020, pp. 349–392. doi: 10.1016/B978-0-12-819416-4.00009-0.

[34] A. Haque, '3 - Solar energy', in *Electric Renewable Energy Systems*, M. H. Rashid, Ed., Boston: Academic Press, 2016, pp. 40–59. doi: 10.1016/B978-0-12-804448-3.00003-7.

[35] L. Phillips, '9 - Solar energy', in *Managing Global Warming*, T. M. Letcher, Ed., Academic Press, 2019, pp. 317–332. doi: 10.1016/B978-0-12-814104-5.00009-0.

[36] N. Sharma, ‘The Top 5 Solar Countries in the World (2024)’, Ornate Solar. Accessed: Apr. 19, 2024. [Online]. Available: https://ornatesolar.com/blog/the-top-5-solar-countries-in-the-world

[37] G. Nikitas, S. Bhattacharya, and N. Vimalan, ‘16 - Wind Energy’, in *Future Energy (Third Edition)*, T. M. Letcher, Ed., Elsevier, 2020, pp. 331–355. doi: 10.1016/B978-0-08-102886-5.00016-5.

[38] IRENA, ‘Wind energy’, International Renewable Energy Agenc. Accessed: Apr. 19, 2024. [Online]. Available: https://www.irena.org/Energy-Transition/Technology/Wind-energy

[39] reve, ‘Countries That Produce the Most Wind Energy | REVE News of the wind sector in Spain and in the world’. Accessed: Apr. 19, 2024. [Online]. Available: https://www.evwind.es/2023/01/14/countries-that-produce-the-most-wind-energy/89725

[40] A. R. Beig and S. M. Muyeen, ‘4 - Wind energy’, in *Electric Renewable Energy Systems*, M. H. Rashid, Ed., Boston: Academic Press, 2016, pp. 60–77. doi: 10.1016/B978-0-12-804448-3.00004-9.

[41] E. Blume-Werry and M. Everts, ‘Hydropower’, in *The Palgrave Handbook of International Energy Economics*, M. Hafner and G. Luciani, Eds., Cham: Springer International Publishing, 2022, pp. 145–156. doi: 10.1007/978-3-030-86884-0_8.

[42] F. Zeren and A. E. Hizarci, ‘Hydropower Energy Consumption, Financial Development, Foreign Direct Investment, and Economic Growth: Further Evidence from Newly Industrialized Countries’, *J Knowl Econ*, Mar. 2023, doi: 10.1007/s13132-023-01135-w.

[43] Madhumitha Jaganmohan, ‘Hydropower generation by country 2022’, Statista. Accessed: Apr. 19, 2024. [Online]. Available: https://www.statista.com/statistics/474799/global-hydropower-generation-by-major-country/

[44] M. Askari, V. Mirzaei Mahmoud Abadi, M. Mirhabibi, and P. Dehghani, ‘Hydroelectric Energy Advantages and Disadvantages’, *American Journal of Energy Science*, vol. 2, pp. 17–20, Apr. 2015.

[45] S. Naranjo Silva and J. Castillo, ‘An Approach of the Hydropower: Advantages and Impacts. A Review’, *Journal of Energy Research and Reviews*, pp. 10–20, Jun. 2021, doi: 10.9734/jenrr/2021/v8i130201.

[46] EIA, ‘Biomass explained - U.S. Energy Information Administration (EIA)’. Accessed: Apr. 19, 2024. [Online]. Available: https://www.eia.gov/energyexplained/biomass/

[47] World Population Review, ‘Biomass Energy by Country 2024’. Accessed: Apr. 19, 2024. [Online]. Available: https://worldpopulationreview.com/country-rankings/biomass-energy-by-country

[48] Chris Woodford, ‘Biofuels - What are they and why are they controversial?’, Explain that Stuff. Accessed: Apr. 19, 2024. [Online]. Available: http://www.explainthatstuff.com/biofuels.html

[49] European Parliament, ‘Circular economy: definition, importance and benefits’, Topics | European Parliament. Accessed: Apr. 19, 2024. [Online]. Available: https://www.europarl.europa.eu/topics/en/article/20151201STO05603/circular-economy-definition-importance-and-benefits

[50] O. US EPA, ‘What is a Circular Economy?’ Accessed: Apr. 19, 2024. [Online]. Available: https://www.epa.gov/circulareconomy/what-circular-economy

[51] Megan Murdie, ‘Circular economy in action: 9 examples of businesses and policy-makers accelerating the transition’, World Economic Forum. Accessed: Apr. 20, 2024. [Online]. Available: https://www.weforum.org/agenda/2023/03/9-examples-circular-economy-accelerating-transition/

[52] O. E. Ogunmakinde, ‘A Review of Circular Economy Development Models in China, Germany and Japan’, *Recycling*, vol. 4, no. 3, Art. no. 3, Sep. 2019, doi: 10.3390/recycling4030027.

[53] J. C. Thomas, ‘This Country has the Best Circular Economy…’, Carom. Accessed: Apr. 20, 2024. [Online]. Available: https://medium.com/carom-consulting/this-country-has-the-best-circular-economy-132ceaddb784

[54] Sean Mowbray, ‘Lessons from Finland’s attempt to transition to a circular economy’, Mongabay Environmental News. Accessed: Apr. 20, 2024. [Online]. Available: https://news.mongabay.com/2024/01/lessons-from-finlands-attempt-to-transition-to-a-circular-economy/

[55] S. Hemidat *et al.*, ‘Solid Waste Management in the Context of a Circular Economy in the MENA Region’, *Sustainability*, vol. 14, no. 1, Art. no. 1, Jan. 2022, doi: 10.3390/su14010480.

[56] Agence Nationale des Déchets, ‘Rapports’, Agence Nationale des Déchets. Accessed: Apr. 21, 2024. [Online]. Available: https://and.dz/rapports/

[57] The International Trade Administration (ITA), ‘Algeria - Oil and Gas - Hydrocarbons | Privacy Shield’. Accessed: Apr. 21, 2024. [Online]. Available: https://www.privacyshield.gov/ps/article?id=Algeria-Oil-and-Gas-Hydrocarbons

[58] Y. Zahraoui, M. R. B. Khan, I. AlHamrouni, S. Mekhilef, and M. Ahmed, ‘Current Status, Scenario, and Prospective of Renewable Energy in Algeria: A Review’, *Energies*, vol. 14, no. 9, Art. no. 9, Jan. 2021, doi: 10.3390/en14092354.
[59] IEA, ‘Algeria - Countries & Regions’, IEA. Accessed: Apr. 21, 2024. [Online]. Available: https://www.iea.org/countries/algeria

Chapter II

Biodiesel feedstock and production processes and catalysts

Chapter II Biodiesel feedstock and production processes and catalysts

II.1. Introduction

In Chapter I, we examined the current state of waste generation and energy resources in Algeria, highlighting the urgent need for new strategies to manage waste and reduce reliance on fossil fuels. To address these issues, applying circular economy principles is proposed as a viable solution. This model focuses on repurposing waste through reuse and recycling, creating products with extended life cycles for use in multiple sectors.

Developing sustainable methods within the circular economy framework is essential, particularly using waste as feedstock to meet waste reduction goals. Generating renewable energy, especially biodiesel, is advocated as a viable strategy due to its environmentally friendly properties and lower emissions compared to traditional fossil fuels.

This chapter will explore biodiesel production in detail, including the methods of its acquisition, primary feedstocks, and the necessary chemical processes. We will also define biodiesel, highlight its diverse resources, and explain the reaction mechanisms and catalysts involved in its synthesis. This comprehensive understanding will facilitate informed choices and promote sustainable energy practices aligned with circular economy objectives.

II.2. Biodiesel

II.2.1. Definition

Biodiesel is a renewable fuel derived from vegetable oils, animal fats, or other organic waste materials, comprising long-chain alkyl esters (methyl, propyl, or ethyl). Produced through a chemical process called transesterification, involves reacting lipids from these sources with alcohol [1].

Biodiesel offers numerous advantages, including biodegradability, renewability, good lubricity, and safety, and exhibiting a superior cetane number and enhanced combustion efficiency in comparison to diesel derived from petroleum [2], making it suitable for various diesel engines without requiring modifications [3]. These qualities position biodiesel as a promising renewable energy source, capable of reducing reliance on fossil fuels, particularly in the transportation sector.

II.2.2. Advantages of Biodiesel

Biodiesel has various advantages as a renewable fuel alternative that is derived from easily available and inexpensive materials such as oils [4], making it a cost-effective solution for energy requirements.

Beyond its economic benefits, biodiesel has a substantially lower environmental effect than standard petroleum-based diesel, generating less hazardous pollutants such as carbon monoxide, hydrocarbons, sulfur, and particulate matter [5]. Furthermore, biodiesel's low toxicity and simplicity of storage improve safety precautions, making it the ideal option for handling and transportation[6]. Notably, its compatibility with fossil diesel enables smooth integration, providing flexibility in blending ratios to meet variable fuel requirements [7]. Overall, biodiesel is a flexible and ecologically friendly option that addresses both economic and ecological issues in the search for long-term energy solutions[8].

As a result, due to its numerous advantages and the high demand for alternative energy sources worldwide, the International Energy Agency has predicted that by 2050, biofuels will meet more than one-quarter of the world's transportation fuel requirements. This will decrease reliance on coal and petroleum products [9].

II.3. Biodiesel synthesis

II.3.1. Feedstocks of biodiesel

Biodiesel production utilizes a wide range of feedstocks derived from renewable biomass resources, including non-edible oils, edible oils, waste edible oils, animal fats, and algae [10]. These feedstocks previously mentioned are used in biodiesel production and can be categorized into three generations, as illustrated in Figure II.1.

The classification attempts to encourage the collection of detailed information about diverse raw materials, with feedstock diversity serving as a method of supporting good environmental practices. Feedstock variety may help protect natural resources and biodiversity while reducing waste by making the most use of existing resources and managing them responsibly [11].

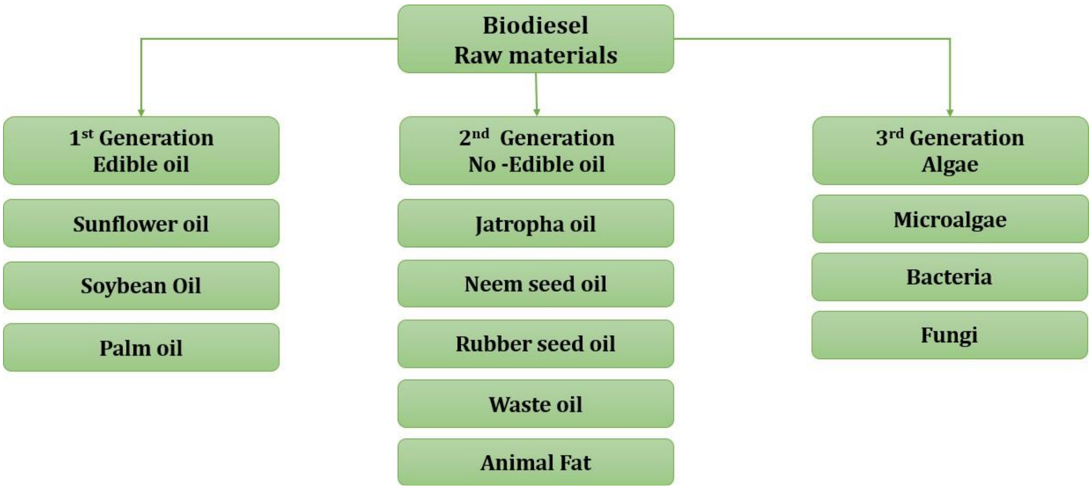

Figure II.14 : Various feedstocks used for biodiesel production [12].

II.3.1.1. 1st Generation : Edible oils

Biodiesel is produced primarily from edible vegetable oils which considered first generation that are widely available in the agricultural sector [13]. Stats show that soybean oil (30%), rapeseed oil (25%), palm oil (18%), and oils from other vegetable seeds (11%), make up the majority of the global feedstock used for biodiesel production [14], highlighting the importance of this generation. Edible oils provide various benefits in biodiesel synthesis, including broad availability, high lipid content, and established processing infrastructure [15]. However, the application of edible vegetable oils or first-generation feedstocks has raised concerns about food versus fuel debates because it competed with food supply, the potential for starvation in developing countries, and environmental issues due to the use of arable land [16].

Different edible oils have been applied as feedstock for biodiesel production, Coconut oil has applied as a feedstock for the production of biodiesel which resulting 90% a biodiesel yield, a relatively high and very accepted [17]. Sunflower Oil has also used as raw materials for biodiesel production yielding 95.3 ± 1.2% of biodiesel [18], soybean oil also proved that it could generate high yield of biodiesel 95 % [19], these several examples confirmed the previous advantages of using edible oils as feedstock for biodiesel synthesis.

Figure II.15 : Edible oils used in transesterification.

II.3.1.2. 2nd Generation : Non-edible oils

Non-edible oils are produced by non-food plants such as jatropha, rubber seed, jojoba, tobacco seed, neem, Karanja, waste cooking oils, and yellow oleander. Furthermore, animal fats such as poultry fat and calf tallow might be considered second-generation biodiesel producers [12] ; they have emerged as valuable alternatives to biodiesel production. Because these feedstocks provide numerous advantages for environmentally friendly fuel generation.

Non-edible oils have several advantages, including availability, renewability, cheaper cost resources, higher heat content, reduced sulfur content, lower aromatic content, and biodegradability. They may be cultivated on marginal ground and in non-agricultural locations with low fertility and moisture needs, reducing competition for food and feed. They are more efficient and ecologically benign than first-generation feedstocks, and their biodiesel yield is equivalent to food oils. Furthermore, non-edible feedstock might yield valuable byproducts for other chemical processes [16]. However, these materials have significant drawbacks. Non-edible oils contain hazardous chemicals that make them unsuitable for human consumption, and biodiesel manufacturing costs are expensive due to the high percentage of free fatty acids (FFAs) [20].

Non-edible oils applied as feedstocks for biodiesel production leading to biodiesel yields of bitter almond oil BAO (91.22 wt.%) and waste fish oil WFO (93.30 wt.%) [21], However, employing waste animal fat produce a moderate biodiesel yield with 65.7% [22].

Figure II.16 : Used cooking oil employed in biodiesel production.

II.3.1.3. 3rd Generation : Algae

Microalgae are microorganisms that can be either monocellular or multicellular and consist of eukaryotic protists and prokaryotic cyanobacteria. They can be found in soils, glaciers, lakes, rivers, hot springs, and seas where sunshine and water are present [23].

Algae have recently shown tremendous potential for biodiesel generation due to their high lipid content (the primary component utilized in biodiesel synthesis) and quick growth rates. Algae may be grown in a variety of habitats, including ponds, bioreactors, and open water systems, making them a flexible and adaptable feedstock source. Their capacity to grow in a variety of environments reduces the demand for arable land and freshwater resources, alleviating worries about competing with food crops and land use issues. Apart from that [24], microalgae have the ability to adsorb organic contaminants such as ammonia, nitrate, and nitrite in wastewater, so they can be used to combine biodiesel generation and wastewater treatment, where they can be grown in wastewater and then used for biodiesel generation, lowering production costs as indicated in various studies [25-27].

Many algae have used for biodiesel production, Spirulina maxima has used and obtained a maximum biodiesel yield of 86.1% [28], Spirulina platensis produced a maximum biodiesel yield 75% [29], Chlorella vulgaris also applied for biodiesel synthesis leads to a high yield of 96% [30], and many more studies which proven that despite the promise findings, more efforts to explore the algae comprise high lipid percentage to enhance the biodiesel yield.

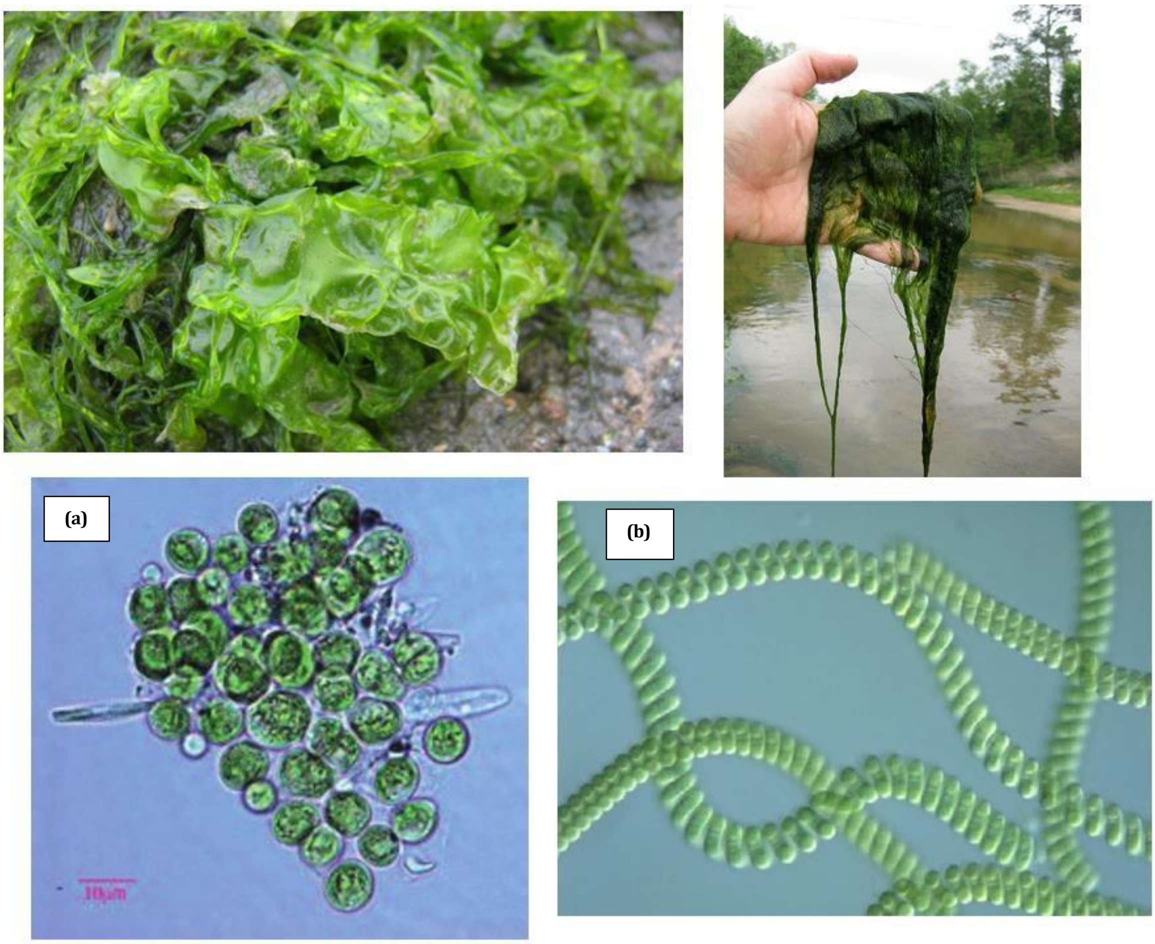

Figure II.17 : Some algae used in biodiesel production : (a) Chlorella [31] and (b) Spirulina [32].

II.3.2. Biodiesel synthesis reaction : Transesterification

As previously stated, there are several techniques for producing biodiesel from feedstock such as direct use and blending, pyrolysis, micro-emulsion [33]. However, transesterification is the most often used process for producing biodiesel with a high yield and outstanding characteristics. This process was developed as early as 1853, when scientists E. Duffy and J. Patrick performed the first transesterification of vegetable oil, many years before the first diesel engine became functional [34]. In general, transesterification is a chemical process that occurs when one molecule of oil or triglycerides found in microalgae oils or lipids reacts with three molecules of alcohol, often methanol or ethanol. This process results in an immiscible mixture containing three molecules of biodiesel known as Free Fatty Acid Methyl Ester (FAME) and glycerol as a byproduct [35], as indicated in Figures II.5 and II.6 which displayed the general equation of the transesterification.

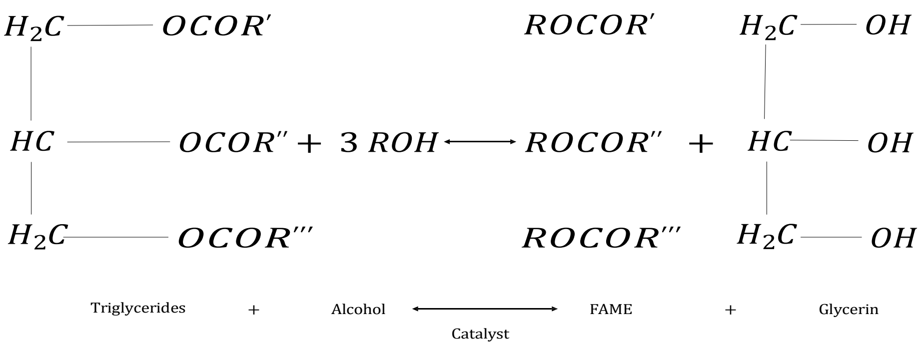

Figure II.18 : Transesterification General Equation.

To fully understand the mechanism of this reaction, Fig II.6 represent the steps of transesterification,

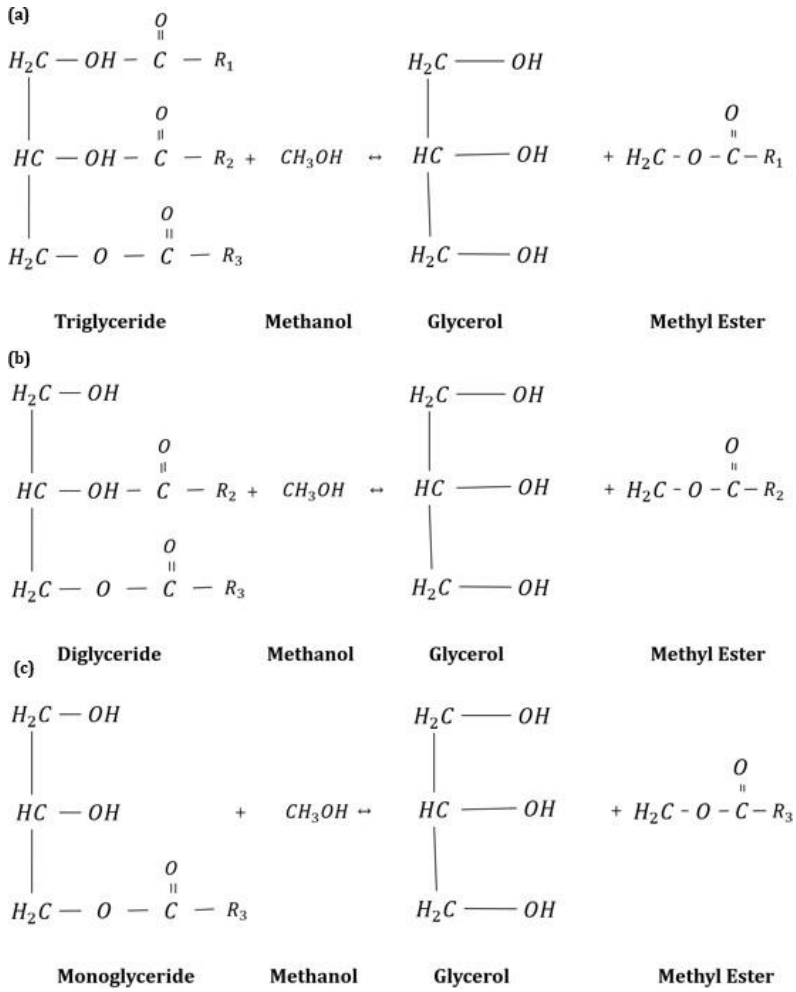

Figure II.19 : Transesterification reaction steps.

In the first step, triglycerides react with an alcohol molecule to form diglycerides and methyl ester molecules, with glycerol as a byproduct. Then, the diglycerides produced further react with alcohol to create monoglycerides and more methyl ester molecules. Finally, the methyl ester reacts with alcohol once again to yield glycerol and the third methyl ester molecule.

All three reactions together are represented by the general equation in Fig II.5, wherein three molecules of alcohol react with triglycerides to produce three molecules of methyl ester, which constitute the produced biodiesel.

However, in some cases and due to some complexation in feedstocks such as high acid value…etc., using a catalyst can surpass these obstacles and improve reaction rate, efficiency, selectivity, and also yield of biodiesel [33]. This catalytic activity optimizes biodiesel production, ensuring economic feasibility and sustainability in the renewable energy industry. The transesterification reaction set-up employed in laboratory is demonstrated Figure II.7.

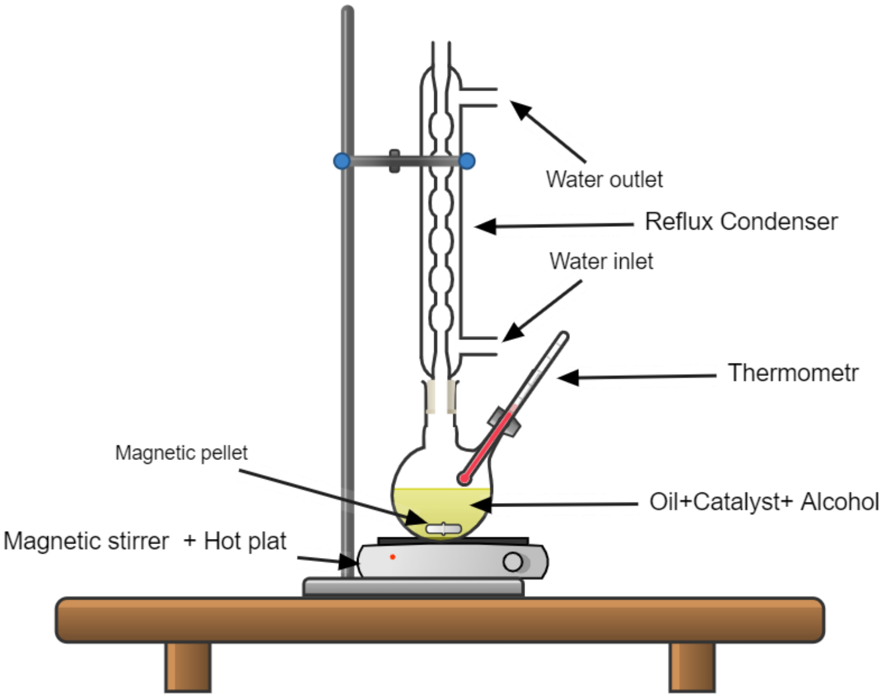

Figure II.20 : Biodiesel production laboratory set-up.

II.4. Catalysts used in biodiesel production

II.4.1. Catalyst role in biodiesel synthesis

A catalyst is an element that accelerates a chemical reaction or reduces the temperature or pressure required to initiate a chemical reaction without being consumed during the process

[36]. These substances are important in biodiesel synthesis because they facilitate the transesterification process, which is required to convert triglycerides into biodiesel and glycerin. These catalysts speed up the reaction, improve selectivity, boost overall process efficiency, and lower production costs by reducing the amount of energy required to reach specified products [37]. According to many previous studies, there are major 3 classes of catalysts used for biodiesel production Homogenous, Heterogenous and Enzymatic catalysts, these types and some examples of each one is summarized in Fig II.8.

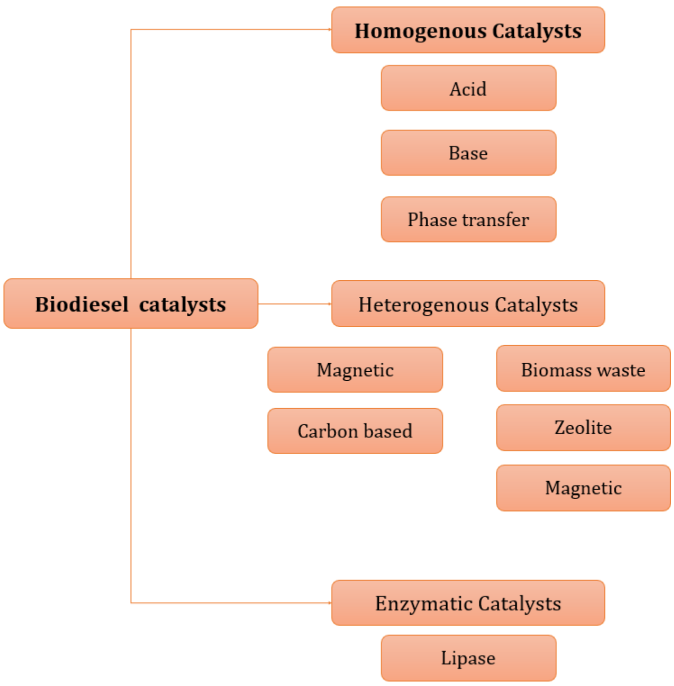

Figure II.21 : Different types of catalysts used for biodiesel production.

II.4.2. Homogenous Catalysts

Homogeneous catalysts are compounds that have been used in the same phase as the reaction system. This kind of catalyst is an effective technique to accomplish chemical transformations under moderate conditions [38].

This type of catalyst is commonly used in biodiesel production because of its simplicity and quick reaction kinetics [39]. Homogenous Catalysts, including hydrochloric acid (HCl), sulfuric acid (H_2SO_4), phosphoric acid (H_3PO_4), organic sulfonic acid (HSO_3R), sodium hydroxide (NaOH), sodium methoxide ($NaOCH_3$), sodium ethoxide ($NaOCH_2CH_3$), sodium butoxide ($NaOC_4H_9$), potassium hydroxide (KOH), and potassium methoxide ($KOCH_3$), fall under these two categories acid and basic catalysts [40], and they are often dissolved in the same solvent as the reactants to facilitate the reaction.

Furthermore, homogeneous catalysts have significant catalytic activity in a short timeframe and may work efficiently at relatively low temperatures, generally ranging from 40°C to 65°C and at an atmospheric pressure condition [41].

As mentioned previously we can classify homogenous catalysts into acid, basic catalysts, in addition there are phase transfer.

- **Homogenous acid catalysts :** The major problem, especially in waste oils, is the high percentage of free fatty acids (FFAs), which influence and reduce the quality of biodiesel produced and increase its synthesis cost [20] . Here come the advantages of acid catalysts like hydrochloric acid (HCl), and sulfuric acid (H_2SO_4)…etc [40], where despite the high levels of free fatty acids (FFAs) in the feedstock, they do not notably impact the efficacy of acid catalysts, which accelerate the reaction, giving a high biodiesel yield. As a result, acid catalysts are used to demonstrate effectiveness in both esterification and transesterification reactions and direct conversion with the low cost feedstocks such as oils waste and fat [42].

  However, these acid catalysts have significant drawbacks as well such as a slow pace reaction rate when compared to other catalysts [43], and the usage of particular acid catalysts might cause corrosive problems in the reactor and pipeline[44].
- **Homogenous Base Catalysts :** These catalysts are more cost-efficient since they produce a high yield of biodiesel with a shorter reaction time at ambient temperature [45]. resulting in a reaction speed 4,000 times quicker than acid-based catalysts [46]. Furthermore, they function at atmospheric pressure. Furthermore, their high conversion rates are related to the lack of intermediary procedures. There are many base catalysts used, according to studies the most used are sodium hydroxide (NaOH), potassium hydroxide (KOH), sodium methoxide (CH_3ONa), and sodium bicarbonate ($NaHCO_3$) [47]. However, homogenous base catalysts have some limitations: they are non-reusable catalysts that must be used with low FFA feedstocks because of the risk of saponification, unlike acid catalysts, and they produce low biodiesel yield owing to emulsion formation [33].
- **Phase transfer catalysts :** Several studies have emphasized the benefits of phase transfer catalysts in terms of improving anion transfer between the polar methanol/glycerol phase and the non-polar oil phase. This type of catalyst accelerates transesterification, removes the need for expensive aprotic solvents, simplifies scaling

up, and increases activity and conductivity to achieve optimal yield in a short period of time[48].

Tab II.1 summarizes the most used homogenous catalysts for biodiesel production mentioned in previous studies.

Table II.1 : Several Homogenous catalysts used in Biodiesel production.

Feedstock	Catalyst	Parameters	Biodiesel yield	Ref
Waste coconut oil	KOH	Molar ration : 6:1 Time : 60 min Catalyst concentration : 1.0wt%	83.32 wt.%	[49]
Karanja oil	H_2SO_4	Molar ration 1:9 Time : 60 min Temperature : 60°C Catalyst concentration : 5wt%	70%	[50]
Sunflower oil	NaOH	Molar ration 6:1 Time : 120 min Temperature : 60°C Catalyst concentration : 1wt%	97.1%	[51]
Rice bran	$NaOCH_3$	Molar ration 7.5:1 Time : 60 min Temperature : 55°C Catalyst concentration : 0.75wt%	83.3%	[52]

II.4.3. Enzymatic catalysts

Enzyme catalysts in transesterification provide several benefits. Enzymes allow for easy recovery and reuse while also demonstrating thermal stability under mild reaction conditions such as pH, temperature, and pressure. Enzyme-catalyzed procedures also allow for efficient downstream product recovery, and can be reused for many cycles [53]. Furthermore, enzymes are unaffected by water concentration in the feedstock [54], resulting in consistently high yields of the desired output [44]. These qualities make enzyme-catalyzed transesterification an appealing alternative for biodiesel generation, with high efficiency and dependability throughout the process. The following Tab II.2 summarized some enzymatic catalysts used in biodiesel production

Table II.2 : Various enzymatic catalysts applied for biodiesel production.

Feedstock	Catalyst	Parameters	Biodiesel yield	Ref
Palm oil	Crude Lipase	Molar ration : 6:1 Time : 36 h Temperature : 35°C	92.07±1.04%	[55]
Canola oil	Rhizomucor miehei lipase	Molar ration 3:1 Time : 96 h Temperature : 50°C Catalyst concentration : 13wt%	45%	[56]
Jatropha curcas oil	Lipase-PDA-TiO_2 NPs	Molar ration 6:1 Time : 30 h Temperature : 37°C Catalyst concentration : 10wt%	92%	[57]
Sunflower oil	Lipase@Bio-MOFs	Molar ration 8:1 Time : 4 h Temperature : 50°C Catalyst concentration : 100mg	>60%	[58]

II.4.4. Heterogenous catalysts

A heterogeneous catalyst is a solid component that reacts in a phase distinct from the liquid reaction mixture [59]. These catalysts function by adsorbing reactant components onto their surfaces. In biodiesel reactions, heterogeneous catalysts typically appear in the solid phase, whereas alcohol and triglycerides occur in the liquid phase [60].

Heterogeneous catalysts have benefits over homogeneous and enzymatic catalysts in recent advanced biodiesel research. It has various benefits, including faster reaction rates, milder reaction conditions, lower energy consumption, simple separation from the reaction mixture, a high potential for catalyst reuse and regeneration, and decreased corrosivity [61]. Also, this type of catalyst is considered a low-cost green compound that could be obtained from cheap sources at low prices, which helps reduce overall biodiesel production costs [62].

Previous research has shown that many different types of heterogeneous catalysts may be employed for biodiesel synthesis, including those formed from biomass waste, zeolite, metal-based, metal oxide, and many more. The qualities, advantages, and disadvantages of the major types of heterogenous will be discussed in the parts that follow.

- **Zeolites :** Zeolites are low-density, crystalline microporous aluminosilicates with structured cavities and molecular-sized channels [63]. These compounds have varied catalytic properties and shape selectivity. Zeolites are gaining popularity as catalysts and support materials in biodiesel synthesis because of their changeable acidity/basicity, large specific surface, adjustable hydrophobicity/hydrophilicity, and outstanding durability [64]. However, they have downsides in biodiesel synthesis, including greater reaction temperatures, longer reaction times, more costly preparation techniques, and lower conversion efficiencies [65].

- **Magnetic catalysts :** Magnetic solid catalysts, such as Fe_3O_4 and γ-Fe_2O_3, are gaining popularity in biodiesel production due to their magnetic response qualities. These catalysts may be easily separated with minimum mass loss by applying an external magnetic field to high-viscosity reaction mixtures, making them suitable for reuse [66]. However, this sort of catalyst has limits in terms of active site leaching-induced deactivation and catalytic reusability, both of which are unresolved challenges [67]. and supported magnetic catalysts feature weak interactions between active components and magnetic supports, necessitating simpler manufacturing techniques for some magnetic catalysts [68].
- **Catalysts derived from Biomass waste :** Catalysts produced from waste biomass sources provide a viable alternative to the constraints of synthetic heterogeneous catalysts in biodiesel synthesis. Compared to their synthetic equivalents, which can involve high prices and the use of potentially hazardous chemical reagents, catalysts generated from organic waste materials offer various benefits [69].
  These catalysts are nontoxic, safe to handle and store, plentiful, and cost-effective since they are derived from renewable sources such as waste eggshells, bones, sea shells, etc. [70], which are regarded as the main sources of calcium oxide (CaO) based catalyst . This catalyst feature great basic strength and has a lesser environmental effect due to its limited solubility in methanol and simplicity of handling [71]. Using waste biomass for catalyst manufacture reduces dependency on nonrenewable resources and hazardous chemicals while also contributing to waste reduction and sustainability in biodiesel synthesis.

Tab II.3 summarize the latest studies where the heterogenous catalysts have been used in biodiesel production.

Table II.3 : Various heterogenous catalysts applied for biodiesel production.

Feedstock	Catalyst	Parameters	Biodiesel yield	Ref
Rubber seed oil	Eggshells	Calcination T° : 900°C Calcination time : 4h Molar ration : 9:1 Time : 4 h Temperature : 65°C Catalyst concentration: 5 wt.%	97.84%	[72]
Waste cooking oil	Waste ostrich bone	Calcination T° : 600-1000°C Molar ration : 15 :1 Time : 4 h Temperature : 60°C Catalyst concentration: 5 wt.%	90.56%	[73]
Recycled cooking oil	$NaOH/CoFe_2O_4$	Calcination T° : 350°C Calcination time : 2h Molar ration : 12 :1 Time : 2 h Temperature : 65°C Catalyst concentration: 3 wt.%	98.71 %	[74]
Waste cooking oil	xMn-yZr/CaO	Calcination T° : 650°C Calcination time : 5h Molar ration : 15 :1 Time : 3 h Temperature : 80°C Catalyst concentration: 3 wt.%	92.1%	[75]
Waste cooking oil	IGO@SrTi	Molar ration : 1 :1 Time : 3 h Temperature : 120°C Catalyst concentration: 0.3g	96%	[76]
Used cooking oil	zeolite supported CaO	Calcination T° : 800 °C Molar ration : 9.7:1 Time : 238.8 min Temperature : 69.1°C Catalyst concentration: 2.1 wt%	93.7%	[77]
Waste frying oil	Ba-based zeolite	Calcination T° : 700 °C Molar ration : 12 :1 Time : 2 h Temperature : 65.38°C Catalyst concentration: 3 wt.%	93.17 ± 0.02%	[78]

II.5. Conclusion

In conclusion, this chapter discussed and emphasized the various feedstocks and catalysts used to make biodiesel. The selection of feedstock and catalysts is crucial in biodiesel production to achieve a high yield with excellent attributes at low cost and in a short period.

The literature indicates that diverse feedstocks were employed for this matter, including edible and non-edible oils, algae, and waste biomass such as waste oils and fat. Every type of feedstock has specific benefits that allow for higher-quality biodiesel and issues that may limit its usage, which require careful assessment of aspects such as availability, cost, and environmental effects. The type of catalyst used (e.g., homogeneous, heterogeneous, enzymatic, chemical, or waste) has a considerable impact on reaction efficiency, speed, product quality, and sustainability.

Each type of catalyst provides unique advantages and limitations, as highlighted in this chapter, and the presentation of the characteristics of each type is important in the step of selecting the most suitable catalyst for transesterification based on specific production requirements and the type of feedstocks used, as well as to limit the cost.

In the end, continued research and innovation in feedstock utilization and catalyst development are essential to further improving the efficiency, sustainability, and economic viability of biodiesel production processes. and this needs the use of advanced and new methods to facilitate the research and investigation.

The use of artificial intelligence methods has been considered the most interesting topic in recent years because it allows for the rapid acquisition of data and high-accuracy results. The application of AI methods in biodiesel production and how they can be useful in the choice of feedstocks, analyzing the results, etc. will be discussed in Chapter III.

References

[1] S. C. Bhatia, '22 - Biodiesel', in *Advanced Renewable Energy Systems*, S. C. Bhatia, Ed., Woodhead Publishing India, 2014, pp. 573–626. doi: 10.1016/B978-1-78242-269-3.50022-X.

[2] S. Parida, M. Singh, and S. Pradhan, 'Biomass wastes: A potential catalyst source for biodiesel production', *Bioresource Technology Reports*, vol. 18, p. 101081, Jun. 2022, doi: 10.1016/j.biteb.2022.101081.

[3] X. Sun, S. Liu, S. Manickam, Y. Tao, J. Y. Yoon, and X. Xuan, 'Intensification of biodiesel production by hydrodynamic cavitation: A critical review', *Renewable and Sustainable Energy Reviews*, vol. 179, p. 113277, Jun. 2023, doi: 10.1016/j.rser.2023.113277.

[4] J. V. L. Ruatpuia *et al.*, 'Green biodiesel production from Jatropha curcas oil using a carbon-based solid acid catalyst: A process optimization study', *Renewable Energy*, vol. 206, pp. 597–608, Apr. 2023, doi: 10.1016/j.renene.2023.02.041.

[5] F. Binhweel, Md. S. Hossain, and M. I. Ahmad, 'Recent Trends, Potentials, and Challenges of Biodiesel Production from Discarded Animal Fats: a Comprehensive Review', *Bioenerg. Res.*, vol. 16, no. 2, pp. 778–800, Jun. 2023, doi: 10.1007/s12155-022-10527-w.

[6] S. Firoz, 'A review: Advantages and Disadvantages of Biodiesel', *International Research Journal of Engineering and Technology*, pp. 530–535, 2017.

[7] B. Wang, B. Wang, S. K. Shukla, and R. Wang, 'Enabling Catalysts for Biodiesel Production via Transesterification', *Catalysts*, vol. 13, no. 4, Art. no. 4, Apr. 2023, doi: 10.3390/catal13040740.

[8] R. C. Rial, 'Biofuels versus climate change: Exploring potentials and challenges in the energy transition', *Renewable and Sustainable Energy Reviews*, vol. 196, p. 114369, May 2024, doi: 10.1016/j.rser.2024.114369.

[9] C. Shimasaki, 'Chapter 10 - Understanding Biotechnology Product Sectors', in *Biotechnology Entrepreneurship (Second Edition)*, C. Shimasaki, Ed., Academic Press, 2020, pp. 123–149. doi: 10.1016/B978-0-12-815585-1.00010-3.

[10] H. A. Jan, N. U. Saqib, A. Aamir, and M. A. Haleem, 'Aleurites moluccana as a Potential Non-edible Feedstock for Industrial-Scale Biodiesel Synthesis Using Homemade Zinc Oxide Nanoparticles as a Catalyst', *Waste Biomass Valor*, vol. 15, no. 2, pp. 1081–1095, Feb. 2024, doi: 10.1007/s12649-023-02238-w.

[11] L. Sinead, ‘The hidden benefits of improving biofuels feedstock diversity’, Linkdein. Accessed: Apr. 23, 2024. [Online]. Available: https://www.linkedin.com/pulse/hidden-benefits-improving-biofuels-feedstock-diversity-sinead-lynch

[12] M. A. H. Shaah *et al.*, ‘A review on non-edible oil as a potential feedstock for biodiesel: physicochemical properties and production technologies’, *RSC Adv.*, vol. 11, no. 40, pp. 25018–25037, Jul. 2021, doi: 10.1039/D1RA04311K.

[13] A. c Ahmia, F. Danane, R. Bessah, and I. Boumesbah, ‘Raw material for biodiesel production. Valorization of used edible oil’, *JREEN*, vol. 17, no. 2, pp. 335–343, Jun. 2014.

[14] S. Brahma *et al.*, ‘Biodiesel production from mixed oils: A sustainable approach towards industrial biofuel production’, *Chemical Engineering Journal Advances*, vol. 10, p. 100284, May 2022, doi: 10.1016/j.ceja.2022.100284.

[15] Zulqarnain *et al.*, ‘A Comprehensive Review on Oil Extraction and Biodiesel Production Technologies’, *Sustainability*, vol. 13, no. 2, Art. no. 2, Jan. 2021, doi: 10.3390/su13020788.

[16] A. E. Atabani *et al.*, ‘Non-edible vegetable oils: A critical evaluation of oil extraction, fatty acid compositions, biodiesel production, characteristics, engine performance and emissions production’, *Renewable and Sustainable Energy Reviews*, vol. 18, pp. 211–245, Feb. 2013, doi: 10.1016/j.rser.2012.10.013.

[17] R. Rasyid, Z. Sabara, H. A. Pratiwi, R. Juradin, and R. Malik, ‘The Production Of Biodiesel From A Traditional Coconut Oil Using NaOH/γ-Al2O3 Heterogeneous Catalyst’, *IOP Conf. Ser.: Earth Environ. Sci.*, vol. 175, no. 1, p. 012025, Jul. 2018, doi: 10.1088/1755-1315/175/1/012025.

[18] S. Jalalmanesh, M. Kazemeini, M. H. Rahmani, and M. Zehtab Salmasi, ‘Biodiesel Production from Sunflower Oil Using K2CO3 Impregnated Kaolin Novel Solid Base Catalyst’, *Journal of the American Oil Chemists’ Society*, vol. 98, no. 6, pp. 633–642, Jun. 2021, doi: 10.1002/aocs.12486.

[19] A. L. Silva, A. F. F. Farias, S. M. P. Meneghetti, E. Antonio dos Santos Filho, and A. C. Figueiredo de Melo Costa, ‘Optimization of biodiesel production via transesterification of soybean oil using α-MoO3 catalyst obtained by the combustion method’, *Arabian Journal of Chemistry*, vol. 15, no. 8, p. 104012, Aug. 2022, doi: 10.1016/j.arabjc.2022.104012.

[20] R. N. Vilas Bôas, M. F. Mendes, R. N. Vilas Bôas, and M. F. Mendes, ‘A REVIEW OF BIODIESEL PRODUCTION FROM NON-EDIBLE RAW MATERIALS USING THE

TRANSESTERIFICATION PROCESS WITH A FOCUS ON INFLUENCE OF FEEDSTOCK COMPOSITION AND FREE FATTY ACIDS', *Journal of the Chilean Chemical Society*, vol. 67, no. 1, pp. 5433–5444, Jan. 2022, doi: 10.4067/S0717-97072022000105433.

[21] A. B. Fadhil, E. T. B. Al-Tikrity, and A. M. Khalaf, 'Transesterification of non-edible oils over potassium acetate impregnated CaO solid base catalyst', *Fuel*, vol. 234, pp. 81–93, Dec. 2018, doi: 10.1016/j.fuel.2018.06.121.

[22] N. Hasan and M. V. Ratnam, 'Biodiesel Production from Waste Animal Fat by Transesterification Using H_2SO_4 and KOH Catalysts: A Study of Physiochemical Properties', *International Journal of Chemical Engineering*, vol. 2022, p. e6932320, Mar. 2022, doi: 10.1155/2022/6932320.

[23] W. G. Morais Junior, M. Gorgich, P. S. Corrêa, A. A. Martins, T. M. Mata, and N. S. Caetano, 'Microalgae for biotechnological applications: Cultivation, harvesting and biomass processing', *Aquaculture*, vol. 528, p. 735562, Nov. 2020, doi: 10.1016/j.aquaculture.2020.735562.

[24] M. V. L. Chhandama, K. B. Satyan, B. Changmai, C. Vanlalveni, and S. L. Rokhum, 'Microalgae as a feedstock for the production of biodiesel: A review', *Bioresource Technology Reports*, vol. 15, p. 100771, Sep. 2021, doi: 10.1016/j.biteb.2021.100771.

[25] H. Huang, S. Zhong, S. Wen, C. Luo, and T. Long, 'Improving the efficiency of wastewater treatment and microalgae production for biofuels', *Resources, Conservation and Recycling*, vol. 178, p. 106094, Mar. 2022, doi: 10.1016/j.resconrec.2021.106094.

[26] C. Arutselvan *et al.*, 'Review on wastewater treatment by microalgae in different cultivation systems and its importance in biodiesel production', *Fuel*, vol. 324, p. 124623, Sep. 2022, doi: 10.1016/j.fuel.2022.124623.

[27] W. N. A. Kadir, M. K. Lam, Y. Uemura, J. W. Lim, and K. T. Lee, 'Harvesting and pre-treatment of microalgae cultivated in wastewater for biodiesel production: A review', *Energy Conversion and Management*, vol. 171, pp. 1416–1429, Sep. 2018, doi: 10.1016/j.enconman.2018.06.074.

[28] M. A. Rahman, M. A. Aziz, R. A. Al-khulaidi, N. Sakib, and M. Islam, 'Biodiesel production from microalgae Spirulina maxima by two step process: Optimization of process variable', *Journal of Radiation Research and Applied Sciences*, vol. 10, no. 2, pp. 140–147, Apr. 2017, doi: 10.1016/j.jrras.2017.02.004.

[29] P. Nautiyal, K. A. Subramanian, and M. G. Dastidar, 'Kinetic and thermodynamic studies on biodiesel production from Spirulina platensis algae biomass using single stage

extraction–transesterification process', *Fuel*, vol. 135, pp. 228–234, Nov. 2014, doi: 10.1016/j.fuel.2014.06.063.

[30] S. T. Al-Humairi, J. G. M. Lee, M. Salihu, and A. P. Harvey, 'Biodiesel Production through Acid Catalyst In Situ Reactive Extraction of Chlorella vulgaris Foamate', *Energies*, vol. 15, no. 12, Art. no. 12, Jan. 2022, doi: 10.3390/en15124482.

[31] F. Palla, 'Biotechnology and Cultural Heritage Conservation', 2020. doi: 10.5772/intechopen.90669.

[32] A. Choopani, 'A Review on Antioxidant Properties of Spirulina', *Journal of Applied Biotechnology Reports*, vol. 3, Jan. 2016.

[33] V. Mandari and S. K. Devarai, 'Biodiesel Production Using Homogeneous, Heterogeneous, and Enzyme Catalysts via Transesterification and Esterification Reactions: a Critical Review', *Bioenerg. Res.*, vol. 15, no. 2, pp. 935–961, Jun. 2022, doi: 10.1007/s12155-021-10333-w.

[34] Mybiodiesel, 'History of Biodiesel - How it all started.', History of Biodiesel. Accessed: Apr. 25, 2024. [Online]. Available: https://www.mybiodiesel.com/biodiesel-history.php

[35] M. Tobar and G. A. Núñez, 'Supercritical transesterification of microalgae triglycerides for biodiesel production: Effect of alcohol type and co-solvent', *The Journal of Supercritical Fluids*, vol. 137, pp. 50–56, Jul. 2018, doi: 10.1016/j.supflu.2018.03.008.

[36] U.S. Department of Energy, 'DOE Explains...Catalysts', Energy.gov. Accessed: Apr. 25, 2024. [Online]. Available: https://www.energy.gov/science/doe-explainscatalysts

[37] I. M. Rizwanul Fattah *et al.*, 'State of the Art of Catalysts for Biodiesel Production', *Frontiers in Energy Research*, vol. 8, 2020, Accessed: Apr. 25, 2024. [Online]. Available: https://www.frontiersin.org/articles/10.3389/fenrg.2020.00101

[38] W. M. C. Sameera, Y. Takeda, and Y. Ohki, 'Chapter Two - Transition metal catalyzed cross-coupling and nitrogen reduction reactions: Lessons from computational studies', in *Advances in Organometallic Chemistry*, vol. 78, P. J. Pérez, Ed., Academic Press, 2022, pp. 35–78. doi: 10.1016/bs.adomc.2022.03.002.

[39] N. Rajendran, A. Pandey, E. Gnansounou, B. Gurunathan, and J. Han, 'Chapter 25 - Techno-economic analysis of biodiesel production from nonedible biooil using catalytic transesterification', in *Biofuels and Bioenergy*, B. Gurunathan and R. Sahadevan, Eds., Elsevier, 2022, pp. 601–626. doi: 10.1016/B978-0-323-90040-9.00003-5.

[40] T. C. Aniokete, O. O. Sadare, and M. O. Daramola, 'Chapter 2 - Prospects of biodiesel production from waste animal fats', in *Waste and Biodiesel*, B. Singh and A. Guldhe, Eds., Elsevier, 2022, pp. 17–44. doi: 10.1016/B978-0-12-823958-2.00002-1.

[41] R. Mohandass, K. Ashok, A. Selvaraju, and S. Rajagopan, 'Homogeneous Catalysts used in Biodiesel Production: A Review', *International Journal of Engineering Research & Technology*, vol. 5, no. 5, May 2016, doi: 10.17577/IJERTV5IS050381.

[42] M. Tariq, S. Ali, and N. Khalid, 'Activity of homogeneous and heterogeneous catalysts, spectroscopic and chromatographic characterization of biodiesel: A review', *Renewable and Sustainable Energy Reviews*, vol. 16, no. 8, pp. 6303–6316, Oct. 2012, doi: 10.1016/j.rser.2012.07.005.

[43] R. Ganesan *et al.*, 'A detailed scrutinize on panorama of catalysts in biodiesel synthesis', *Science of The Total Environment*, vol. 777, p. 145683, Jul. 2021, doi: 10.1016/j.scitotenv.2021.145683.

[44] S. Nomanbhay and M. Y. Ong, 'A Review of Microwave-Assisted Reactions for Biodiesel Production', *Bioengineering*, vol. 4, no. 2, Art. no. 2, Jun. 2017, doi: 10.3390/bioengineering4020057.

[45] B. Basumatary, B. Nath, and S. Basumatary, 'Homogeneous Catalysts Used in Biodiesel Production', in *Biodiesel Production*, John Wiley & Sons, Ltd, 2022, pp. 83–101. doi: 10.1002/9781119771364.ch5.

[46] S. Maroa and F. Inambao, 'A review of sustainable biodiesel production using biomass derived heterogeneous catalysts', *Engineering in Life Sciences*, vol. 21, no. 12, pp. 790–824, 2021, doi: 10.1002/elsc.202100025.

[47] P. R. Yaashikaa, P. S. Kumar, and S. Karishma, 'Bio-derived catalysts for production of biodiesel: A review on feedstock, oil extraction methodologies, reactors and lifecycle assessment of biodiesel', *Fuel*, vol. 316, p. 123379, May 2022, doi: 10.1016/j.fuel.2022.123379.

[48] Y. Zhang, M. Stanciulescu, and M. Ikura, 'Rapid transesterification of soybean oil with phase transfer catalysts', *Applied Catalysis A: General*, vol. 366, no. 1, pp. 176–183, Sep. 2009, doi: 10.1016/j.apcata.2009.07.001.

[49] S. Karnnasuta, V. Punsuvon, and R. Nokkaew, 'Biodiesel Production from Waste Coconut Oil in Coconut Milk Manufacturing', *Walailak Journal of Science and Technology (WJST)*, vol. 12, no. 3, Art. no. 3, 2015.

[50] K. Ferdous, M. Uddin, S. Mondal, and M. Khan, *Preparation of Biodiesel Using Sulfuric Acid as a Catalyst*. 2013. doi: 10.13140/2.1.1312.5447.

[51] U. Rashid, F. Anwar, B. R. Moser, and S. Ashraf, 'Production of sunflower oil methyl esters by optimized alkali-catalyzed methanolysis', *Biomass and Bioenergy*, vol. 32, no. 12, pp. 1202–1205, Dec. 2008, doi: 10.1016/j.biombioe.2008.03.001.

[52] U. Rashid, F. Anwar, T. M. Ansari, M. Arif, and M. Ahmad, 'Optimization of alkaline transesterification of rice bran oil for biodiesel production using response surface methodology', *Journal of Chemical Technology & Biotechnology*, vol. 84, no. 9, pp. 1364–1370, 2009, doi: 10.1002/jctb.2191.

[53] P. Kalita, B. Basumatary, P. Saikia, B. Das, and S. Basumatary, 'Biodiesel as renewable biofuel produced via enzyme-based catalyzed transesterification', *Energy Nexus*, vol. 6, p. 100087, Jun. 2022, doi: 10.1016/j.nexus.2022.100087.

[54] P. Adewale, M.-J. Dumont, and M. Ngadi, 'Recent trends of biodiesel production from animal fat wastes and associated production techniques', *Renewable and Sustainable Energy Reviews*, vol. 45, pp. 574–588, May 2015, doi: 10.1016/j.rser.2015.02.039.

[55] S. Suwanno *et al.*, 'The production of biodiesel using residual oil from palm oil mill effluent and crude lipase from oil palm fruit as an alternative substrate and catalyst', *Fuel*, vol. 195, pp. 82–87, May 2017, doi: 10.1016/j.fuel.2017.01.049.

[56] M. Babaki, M. Yousefi, Z. Habibi, J. Brask, and M. Mohammadi, 'Preparation of highly reusable biocatalysts by immobilization of lipases on epoxy-functionalized silica for production of biodiesel from canola oil', *Biochemical Engineering Journal*, vol. 101, pp. 23–31, Sep. 2015, doi: 10.1016/j.bej.2015.04.020.

[57] A. Zulfiqar *et al.*, 'Lipase-PDA-TiO2 NPs: An emphatic nano-biocatalyst for optimized biodiesel production from Jatropha curcas oil', *Renewable Energy*, vol. 169, pp. 1026–1037, May 2021, doi: 10.1016/j.renene.2020.12.135.

[58] Q. Li, Y. Chen, S. Bai, X. Shao, L. Jiang, and Q. Li, 'Immobilized lipase in bio-based metal-organic frameworks constructed by biomimetic mineralization: A sustainable biocatalyst for biodiesel synthesis', *Colloids and Surfaces B: Biointerfaces*, vol. 188, p. 110812, Apr. 2020, doi: 10.1016/j.colsurfb.2020.110812.

[59] M. O. Faruque, S. A. Razzak, and M. M. Hossain, 'Application of Heterogeneous Catalysts for Biodiesel Production from Microalgal Oil—A Review', *Catalysts*, vol. 10, no. 9, Art. no. 9, Sep. 2020, doi: 10.3390/catal10091025.

[60] B. Maleki, S. S. Ashraf Talesh, and M. Mansouri, 'Comparison of catalysts types performance in the generation of sustainable biodiesel via transesterification of various oil sources: a review study', *Materials Today Sustainability*, vol. 18, p. 100157, Jun. 2022, doi: 10.1016/j.mtsust.2022.100157.

[61] O. D. Okechukwu, E. Joseph, U. C. Nonso, and N.-O. Kenechi, 'Improving heterogeneous catalysis for biodiesel production process', *Cleaner Chemical Engineering*, vol. 3, p. 100038, Sep. 2022, doi: 10.1016/j.clce.2022.100038.

[62] W. M. Kedir, ‘Bifunctional Heterogeneous Catalysts for Biodiesel Production Using Low-Cost Feedstocks: A Future Perspective’, in *Advanced Biodiesel - Technological Advances, Challenges, and Sustainability Considerations*, IntechOpen, 2023. doi: 10.5772/intechopen.109482.

[63] B. K. Singh, Y. Kim, S. Kwon, and K. Na, ‘Synthesis of Mesoporous Zeolites and Their Opportunities in Heterogeneous Catalysis’, *Catalysts*, vol. 11, no. 12, Art. no. 12, Dec. 2021, doi: 10.3390/catal11121541.

[64] G. Yang and J. Yu, ‘Advancements in Basic Zeolites for Biodiesel Production via Transesterification’, *Chemistry*, vol. 5, no. 1, Art. no. 1, Mar. 2023, doi: 10.3390/chemistry5010032.

[65] Ł. Szkudlarek, K. Chałupka, W. Maniukiewicz, J. Albińska, M. I. Szynkowska-Jóźwik, and P. Mierczyński, ‘The Influence of Si/Al Ratio on the Physicochemical and Catalytic Properties of MgO/ZSM-5 Catalyst in Transesterification Reaction of Rapeseed Oil’, *Catalysts*, vol. 11, no. 11, Art. no. 11, Nov. 2021, doi: 10.3390/catal11111260.

[66] W. Xie and J. Li, ‘Magnetic solid catalysts for sustainable and cleaner biodiesel production: A comprehensive review’, *Renewable and Sustainable Energy Reviews*, vol. 171, p. 113017, Jan. 2023, doi: 10.1016/j.rser.2022.113017.

[67] S. G. Krishnan, F. Pua, and F. Zhang, ‘A review of magnetic solid catalyst development for sustainable biodiesel production’, *Biomass and Bioenergy*, vol. 149, p. 106099, Jun. 2021, doi: 10.1016/j.biombioe.2021.106099.

[68] Y. Zhang *et al.*, ‘Advancement in utilization of magnetic catalysts for production of sustainable biofuels’, *Front Chem*, vol. 10, p. 1106426, Jan. 2023, doi: 10.3389/fchem.2022.1106426.

[69] J. I. Orege *et al.*, ‘Recent advances in heterogeneous catalysis for green biodiesel production by transesterification’, *Energy Conversion and Management*, vol. 258, p. 115406, Apr. 2022, doi: 10.1016/j.enconman.2022.115406.

[70] G. P. Chutia and K. Phukan, ‘Biomass derived heterogeneous catalysts used for sustainable biodiesel production: a systematic review’, *Braz. J. Chem. Eng.*, vol. 41, no. 1, pp. 23–48, Mar. 2024, doi: 10.1007/s43153-023-00371-6.

[71] S. F. Basumatary *et al.*, ‘Advances in CaO-based catalysts for sustainable biodiesel synthesis’, *Green Energy and Resources*, vol. 1, no. 3, p. 100032, Sep. 2023, doi: 10.1016/j.gerr.2023.100032.

[72] B. A.V.S.L.Sai, N. Subramaniapillai, M. S. B. Khadhar Mohamed, and A. Narayanan, ‘Optimization of continuous biodiesel production from rubber seed oil (RSO) using

calcined eggshells as heterogeneous catalyst', *Journal of Environmental Chemical Engineering*, vol. 8, no. 1, p. 103603, Feb. 2020, doi: 10.1016/j.jece.2019.103603.

[73] H. Mahmood Khan, T. Iqbal, C. Haider Ali, A. Javaid, and I. Iqbal Cheema, 'Sustainable biodiesel production from waste cooking oil utilizing waste ostrich (Struthio camelus) bones derived heterogeneous catalyst', *Fuel*, vol. 277, p. 118091, Oct. 2020, doi: 10.1016/j.fuel.2020.118091.

[74] D. Bousba *et al.*, 'Efficient biodiesel production from recycled cooking oil using a NaOH/CoFe2O4 magnetic nano-catalyst: synthesis, characterization, and process enhancement for sustainability', *Energy Conversion and Management*, vol. 300, p. 118021, Jan. 2024, doi: 10.1016/j.enconman.2023.118021.

[75] N. Mansir, S. H. Teo, I. Rabiu, and Y. H. Taufiq-Yap, 'Effective biodiesel synthesis from waste cooking oil and biomass residue solid green catalyst', *Chemical Engineering Journal*, vol. 347, pp. 137–144, Sep. 2018, doi: 10.1016/j.cej.2018.04.034.

[76] B. Hadi Jume, P. Joolaei Ahranjani, S. Farshineh Saei, F. M. Zeki Mahmood, Y. Vasseghian, and S. Rezania, 'Strontium titanium trioxide doped magnetic graphene oxide as a nanocatalyst for biodiesel production from waste cooking oil', *Sustainable Energy Technologies and Assessments*, vol. 54, p. 102619, Dec. 2022, doi: 10.1016/j.seta.2022.102619.

[77] A. S. Yusuff, A. O. Gbadamosi, and N. Atray, 'Development of a zeolite supported CaO derived from chicken eggshell as active base catalyst for used cooking oil biodiesel production', *Renewable Energy*, vol. 197, pp. 1151–1162, Sep. 2022, doi: 10.1016/j.renene.2022.08.032.

[78] A. S. Yusuff, A. K. Bhonsle, D. P. Bangwal, and N. Atray, 'Development of a barium-modified zeolite catalyst for biodiesel production from waste frying oil: Process optimization by design of experiment', *Renewable Energy*, vol. 177, pp. 1253–1264, Nov. 2021, doi: 10.1016/j.renene.2021.06.039.

Chapter III

Artificial intelligence in biodiesel production

III.1. Introduction

After reviewing the production of biodiesel under specific conditions and the use of catalysts to enhance reaction rate, selectivity, and durability in the previous chapter, it is essential now to explore methods that simplify and improve the analysis, prediction, and classification of diverse data involved in biodiesel production. The used input includes conditions datasets, analytical data, images... etc.

The primary objective of using automated methods is to enhance the accuracy of results and minimize errors. This chapter will focus on the most innovative and widely used method in recent times: artificial intelligence (AI). We will highlight its major applications in biodiesel production processes and demonstrate how AI can be beneficial in this context.

Additionally, this chapter will discuss other methods such as simulation using the free open-source software DWSIM and Density Functional Theory (DFT). We will examine the advantages of these methods in the biodiesel production process, providing a comprehensive overview of the latest advancements and tools available to researchers and practitioners in the field.

III.2. Artificial Intelligence

III.2.1. Definition

Artificial Intelligence (AI) refers to automated systems, such as computers or machines, that can perform tasks typically done by humans by processing large amounts of data quickly [1]. AI systems are capable of interpreting external data, learning from this data, and using their findings to achieve specific goals and tasks through adaptive methods [2]. AI encompasses various applications, including visual perception, speech recognition, decision-making, and language translation [3].This technology allows automated machines to imitate human thought processes, making them helpful in a variety of industries while dramatically increasing efficiency and effectiveness.

The concept of artificial intelligence (AI) developed in the mid-twentieth century. In 1947, English mathematician Alan Turing discussed the idea during a lecture, suggesting that AI could be best developed through advancements in computer programming. However, the term "Artificial Intelligence" was first coined by John McCarthy in 1956 at the "Dartmouth Summer Research Project on Artificial Intelligence" conference [4].

III.2.2. Different types in Artificial intelligence

III.2.2.1. Machine learning

Machine learning is a branch of artificial intelligence that involves developing algorithms to train machines to do certain tasks [5]. It involved the application of statistics, data mining, probability theory, information theory, algorithmic analysis, and other disciplines [6]. Because of its widespread use in recent years in various disciplines and sectors, such as classification analysis, regression analysis, data clustering, association rule learning, and feature engineering for dimensionality reduction [7], the improvement of machine learning (ML) algorithms over time has been a critical goal which has been investigated from multiple perspectives in recent research.

Machine learning methods are primarily classified into four categories: Supervised, unsupervised, semi-supervised, and reinforcement learning as mentioned in Figure III.1 , which will presented below [8]:

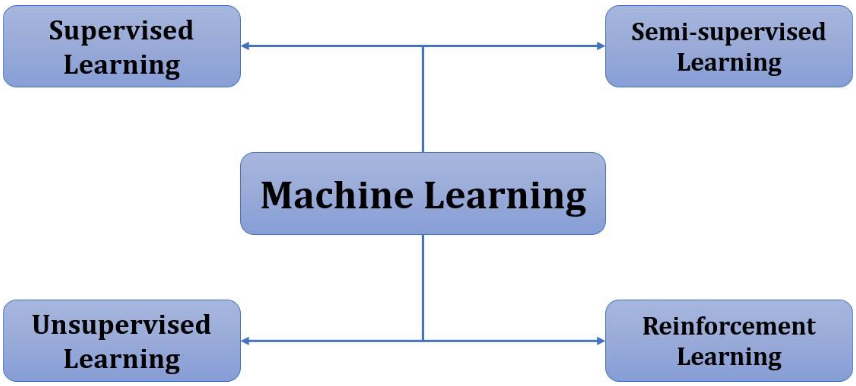

Figure III.22 : Classes of Machine learning.

- **Supervised learning :** it involves training algorithms using labeled data to anticipate outputs for provided inputs [9]. Supervised learning is separated into two types: classification and regression. Classification algorithms organize test results into specified groups, such as discriminating between cats and dogs or deciding whether traffic lights should be red or green. In contrast, regression algorithms forecast numerical values by examining the connection between dependent and independent factors, such as traffic speed. Linear and logistic regression are the two common regression approaches [10]. Different algorithms and methods, including XGBoost, Naïve Bayes, Support Vector Machine, Decision Tree, Random Forest, Logistic

Regression, and K-Nearest Neighbor, are extensively applied in supervised learning, providing a diverse range of tools to create predictive models with high accuracy [11].

- **Unsupervised learning :** Unsupervised learning is task-driven and identifies hidden patterns and structures in unlabeled data. It detects the similarities between unlabeled input data by categorizing sample data based on their commonalities [12] .In the short term, it is a machine learning model that can learn, train, and test itself without supervision, unlike supervised learning [13]. This technique not only gives useful insights into the dataset's basic properties but also serves as a strong tool for data-driven exploration and analysis in different scientific and industrial fields.
- **Semi-supervised learning :** Semi-supervised learning combines supervised and unsupervised learning by using labeled and unlabeled data. This approach is advantageous since labeled data is more difficult to get and unlabeled data is less expensive , an allow to classify unlabeled data from providing small amount of labeled data [14,15].
- **Reinforcement Learning:** Reinforcement Learning, a machine learning approach, allows agents to learn through trial-and-error in an interactive environment [16]. This form of machine learning algorithm constantly trains itself employing a computational approach to learning from actions [17]. Reinforcement learning has been effectively used in a variety of industries, including robotics, gaming, recommendation systems, and finance, demonstrating its adaptability and efficacy in handling difficult issues that older approaches struggle with.

III.2.2.2. Neural Network

Neural Networks, modeled based on the function of the human brain, strive to replicate the brain's pattern recognition skills, these networks consist of linked layers of neurons that interpret incoming data and extract significant characteristics and patterns, similar to how neurons interact in the brain [18]. A Neural Network's fundamental structure consists of input, hidden, and output layers, with connections between nodes reflecting weights that change over the learning process as mentioned in Figure III.2 [19]. These networks are widely used in voice recognition, computer vision, industrial inspection, demonstrating their adaptability and efficacy in addressing difficult issues [20].

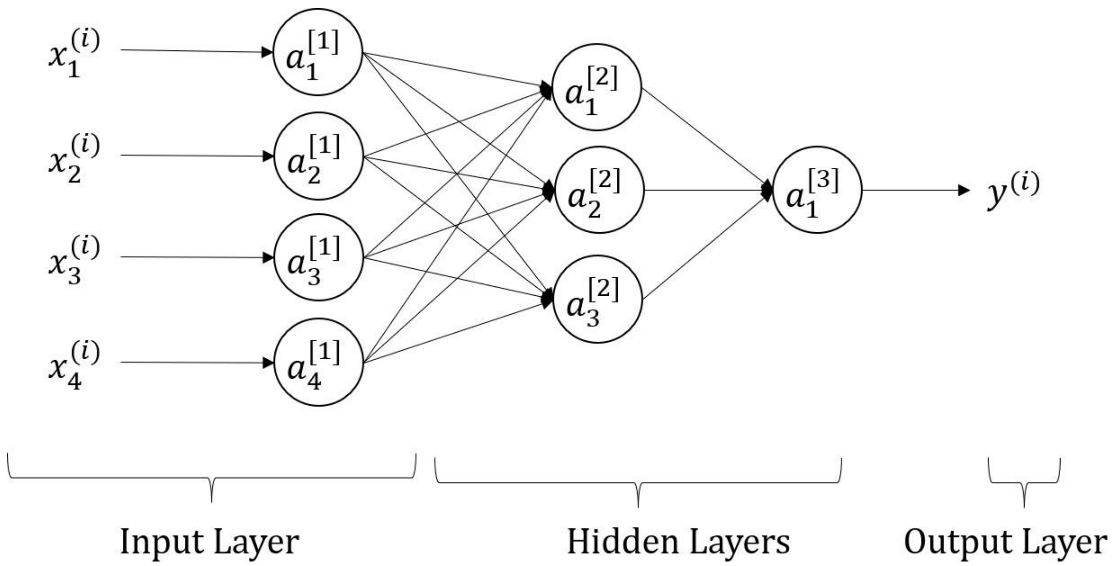

Figure III.23 : Neural Network Structure

III.2.3. Image Segmentation Methods

In recent years and due to limitations of traditional methods of analysis by eye which usually conduct to numerous errors, researchers have employed AI methods in these fields to surpass these drawbacks, Artificial intelligence (AI) has greatly advanced the field of image segmentation and classification analysis, particularly in medical imaging, satellite imagery, and various industrial applications. AI techniques, especially Images segmentation algorithms, classification methods like reinforcement learning ...etc, have shown remarkable success in automating and improving the accuracy of these processes.

III.2.3.1. Image segmentation

Segmentation is a crucial step in image processing that divides a digital image into multiple sections. It is widely used to identify objects, making images more meaningful and easier to analyze. The goal of image segmentation is to divide the image into meaningful connected components and to extract the characteristics of the objects within the image [21].

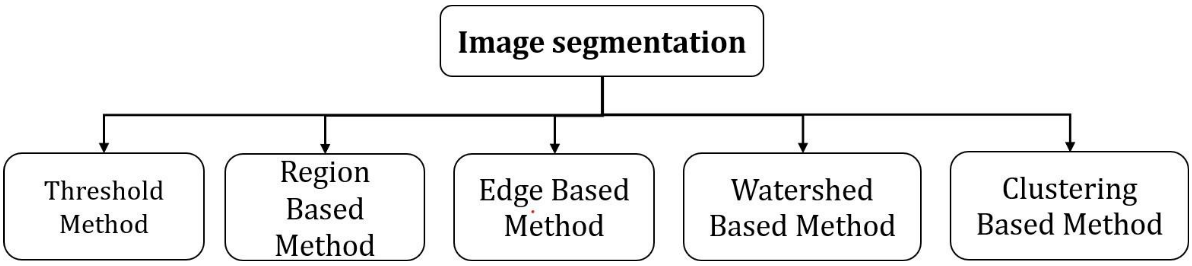

Figure III.24 : Images segmentation different methods.

There are many methods applied for image segmentation as displayed in Figure.3, several ones which been applied in many papers are demonstrated below:

a) **Threshold Segmentation :** This method divides grayscale images based on specific target values. There are two types of threshold segmentation: local and global. The global threshold method uses a single threshold to separate an image into two regions, the target and the background . In contrast, the local threshold method uses multiple thresholds to segment an image into various target regions and backgrounds [22].

b) **Edge Based Segmentation :** This approach detects edges in images by identifying rapid changes in intensity levels. These algorithms find edges where the first derivative of intensity surpasses a threshold or where the second derivative has zero crossings. Common edge-based segmentation techniques include gray histograms and gradient-based algorithms [23].

c) **Region Based Segmentation :** This method segments an image into subregions by identifying clusters of neighboring pixels with similar intensity values. These regions are grouped according to their anatomical or functional roles. Region-based segmentation algorithms are simpler and more resistant to noise than edge detection methods and divide an image into similar regions based on predefined criteria. Techniques in this category include Region Growing, Region Splitting and Merging, and Watershed Transformation [24].

However, image segmentation faces several challenges, necessitating the development of new optimization algorithms inspired by nature, known as Nature-Inspired Optimization Algorithms (NIOAs). These innovative methods are proposed as alternatives to traditional mathematical approaches, which often prove insufficient for complex problems like image segmentation. NIOAs incorporate AI mechanisms where individuals cooperate to solve tasks. Researchers have developed NIOAs based on principles from nature, physics, social behavior, and biology.

These algorithms can be classified into various categories, including Evolutionary Computation Techniques (ECTs), Bio-Inspired Algorithms (BIAs), physics and chemistry-based methods, and other algorithms as indicated in Figure.4 [25].

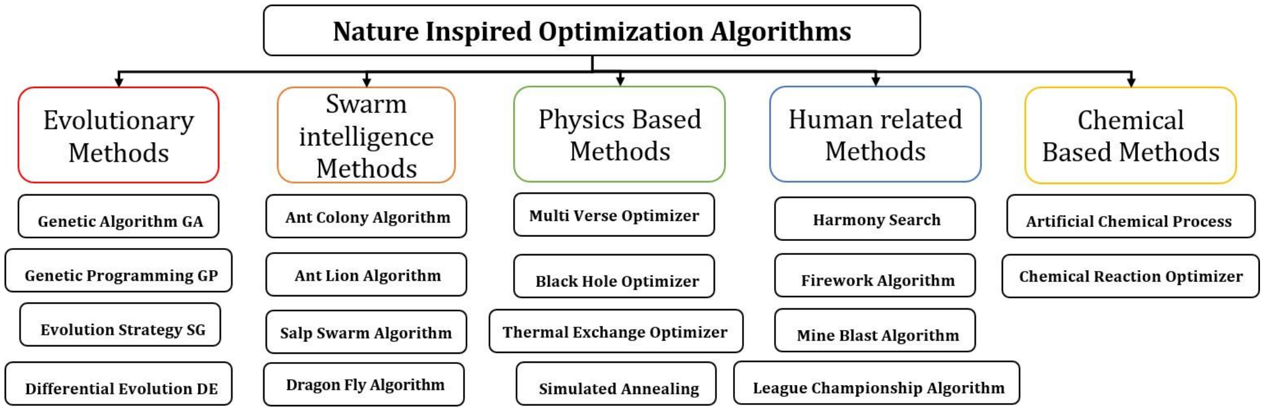

Figure III.25 : Different classes of nature inspired optimizations algorithms.

Each developed nature-inspired optimization method is divided into two phases: exploration and exploitation. Exploration involves a global search or diversification, while exploitation focuses on a local search or intensification to find the optimal solution. These phases with operators used in developing methods allow to enhance the search for better solutions and get good performance especially for images segmentation problems [26]. Several nature-inspired optimization algorithms developed in the recent years as displayed in Table III.1.

Table III.4 : Different nature inspired optimization algorithms developed.

Algorithm Name	Inspiration	Methods of development	Ref
Artificial Bee Colony (ABC)	Honeybee foraging behavior	Investigates and exploits food sources to optimize solutions.	[27]
Firefly Algorithm (FA)	Flashing behavior of fireflies	developed by attracting fireflies based on their brightness to settle on ideal solutions.	[28]
Hunger Games Search (HGS)	Hunger drives behavior in both animals and humans.	Simulates hunger-driven resource seeking behavior. Uses the exploration and exploitation phases to identify optimal solutions	[29]
RIME (Recurrent Icing Memory-based Evolution)	the natural process of ice formation and memory retention.	Recurrent memory processes are employed to preserve valuable information, whereas icing patterns guide search,	[30]
Grey Wolf Optimizer (GWO)	Grey wolves' natural leadership hierarchy and hunting method.	Emulates grey wolves' social hierarchy and hunting habits.	[31]
Whale Optimization Algorithm (WOA)	Bubble-net hunting strategy of whales	Has three operators that replicate humpback whale foraging behavior such as searching for prey, encircling prey, and using a bubble net.	[32]

III.3. Artificial intelligence in Biodiesel production

Our thesis aims to get an efficient biodiesel production mechanism by choosing appropriate catalysts, and suitable feedstocks such as algae, used cooking oil...etc. However, additional methods and approaches are demanded to ensure both results and analysis with high accuracy which allows to minimize the time, effort, and cost put into producing high-quality biodiesel. Employing artificial intelligence (AI) in biodiesel production offers numerous advantages, including improved efficiency, optimization, sustainability, and cost-effectiveness. AI techniques like Artificial Neural Networks (ANN), and Image segmentation can both model, enhance, and optimize production parameters.

These parameters enhanced include Reaction temperature, catalyst Synthesis conditions and their concentration in the reactions, reaction time, reaching to analyze the modification that occurred in catalysts, and choosing the suitable feedstock through classification.

The optimization of these parameters and conditions for sure leads to better control over the transesterification process and higher biodiesel yield and quality. The following points will include several applications of AI in biodiesel production.

III.3.1. Prediction and Optimization of Biodiesel Production Using ANN

The application of Artificial Neural Network (ANN) and other Methods such as ANFIS (Adaptive Neuro-Fuzzy Inference System) and RSM (Response Surface Methodology) in biodiesel production optimization allow to get the optimized parameters and factors affecting in biodiesel synthesis like Temperature, Time, Catalyst concentration, and Alcohol/Oil molar ration, this computational model, is capable of successfully estimate the efficiency of biodiesel production, and to examine the agreement between the experimental and the predicted results. [33,34], These outcomes were proven by several studies as highlighted in Table III.2

Table III.5 : Different ANN methods used for biodiesel predictions.

Paper Title	Methods used	Objective	Ref
Prediction and optimization of biodiesel production by using ANN and RSM	Artificial neural network (ANN) Response Surface Methodology (RSM)	A comparison of the effectiveness of Artificial Neural Networks (ANN) and Response Surface Methodology (RSM) in forecasting and optimizing biodiesel production from pomegranate seed oil.	[35]
Optimization and analysis of bioenergy production using machine learning modeling: Multi-layer perceptron, Gaussian processes regression, K-nearest neighbors, and Artificial neural network models	Multi-layer perceptron (MLP) K-nearest neighbors (KNN) Artificial neural network (ANN) Gaussian processes regression (GPR)	Comparison between four Prediction methods in terms of e the reliability, accuracy, and prediction ability of transesterification of Palm oil to produce biodiesel.	[33]
Biodiesel Production from Jatropha: A Computational Approach by Means of Artificial Intelligence and Genetic Algorithm	ANN Genetic Algorithm	Biodiesel production from jatropha oil optimization using AI and machine learning algorithms, including artificial neural networks (ANN). and genetic algorithms to improve production and quality predictions.	[36]
Biodiesel production from rubber seed oil using calcium oxide derived from eggshell as catalyst – optimization and modeling studies	Artificial neural network (ANN) Response Surface Methodology (RSM)	Using calcium oxide from eggshells as a catalyst, biodiesel was produced from non-edible rubber seed oil. The process parameters were optimized with RSM. Additionally, an ANN was trained to predict biodiesel conversion.	[34]

III.3.2. Classification of feedstocks used for biodiesel production

Selecting suitable raw materials for biodiesel production is crucial for ensuring high yields. Algae, with over 40,000 species, presents a significant challenge for manual identification and classification, which can lead to errors due to some reasons such as boundaries and textures not clear in some images and can be a consuming time process [37]. AI techniques can be employed to classify algae data quickly and accurately, minimizing mistakes in algal categorization. This ensures that the best species are selected for biodiesel production, leading to more consistent and reliable results. Consequently, the use of AI in this field reduces costs associated with trial-and-error methods and manual classification, making the production process more cost-effective and economically viable. The application of this technique in biodiesel production can be summarized as indicated in Figure III.5.

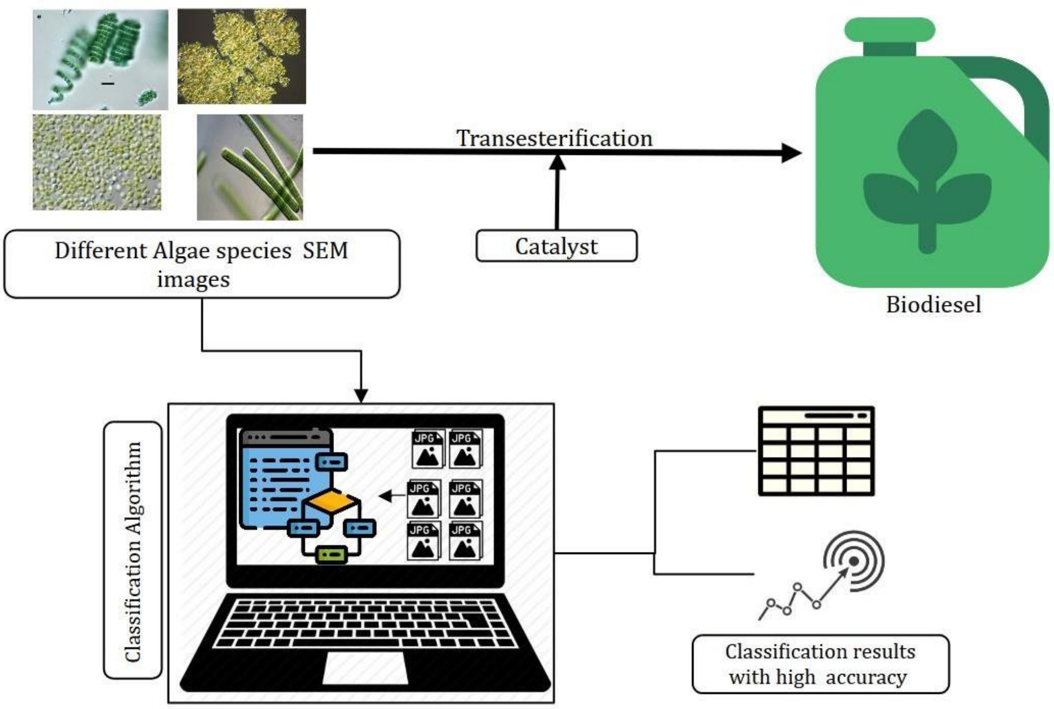

Figure III.26 : Classification method for algae species used in biodiesel production.

Different approaches and methods of AI were employed for this purpose and some of them were displayed in Table III.3.

Table III.6 : Different AI techniques employed for Algae classification and identification.

Paper Title	Methods used	Objective	Ref
Microalgae Classification Using Improved Metaheuristic Algorithm	Improved Metaheuristic Algorithm(A modified Quantum-Based Thermal Exchange Optimization Algorithm)	The objective is to create a more accurate classification technique for microalgae using computer-aided methods.	[38]
Computer Vision Based Deep Learning Approach for the Detection and Classification of Algae Species Using Microscopic Images	Pre-processing with Deep learning technique used to enhance the quantities of data and increase the precision.	Evaluated the utility of three deep learning models for algae detection and compared their performance.	[39]
Automated Microalgae Image Classification	The classification of algal images by four steps: preprocessing, image segmentation using single-resolution edge detection, feature extraction, and classification using an SMO classifier.	Developed an automated microalgae recognition system for algal microscopic pictures.	[37]
Accurate Classification of Algae Using Deep Convolutional Neural Network with a Small Database	Apply a deep convolutional neural network (CNN) algorithm for the accurate identification and classification of algae.	The objective is getting a classification and recognition of algae using CNN method with high accuracy.	[40]

III.3.3. Segmentation for SEM analysis images

SEM image analysis is essential for identifying and understanding surface changes in materials under various conditions such as time, temperature, and preparation methods. This analysis is vital in biodiesel production, particularly when using heterogeneous catalysts prepared under specific protocols. By performing SEM analysis on these catalysts, researchers can observe how different parameters affect catalyst preparation [41].

However, similar to algae classification, SEM image analysis can be time-consuming and challenging due to the difficulty of visual inspection, which can lead to misinterpretations. Additionally, SEM images can be noisy and unclear, complicating their verification.

AI methods can greatly simplify the interpretation of SEM images by applying advanced segmentation techniques. These techniques divide the images into distinct sections and highlight regions of interest, such as specific surface features or defects [42]. By doing so, AI helps to focus on the most relevant parts of the image, reducing noise and unwanted parts in the image. This makes the analysis more efficient and accurate[43], allowing researchers and experts to more easily investigate and understand the material characteristics and the effects of different conditions. Ultimately, AI-enhanced SEM image analysis leads to better insights and more reliable results in research and enhancing production processes to obtain catalysts with high activity and selectivity. As mentioned in Figure.6, the segmentation method applied for Catalyst SEM images can facilitate and make the analysis of SEM images in different conditions (Before and after calcination as example) Different AI methods applied for this matter are presented in Table III.4.

Table III.7 : Various AI techniques employed for SEM images identifications and analysis.

Paper Title	Methods Used	Objective	Ref
Identification of nanocomposites agglomerates in scanning electron microscopy images based on semantic segmentation	Three convolutional neural network models were used to clarify and spot agglomerates in spherical silica-based polyethylene nanocomposites.	The objective is to identify agglomerates in SEM images of spherical silica-based polyethylene nanocomposites by the semantic segmentation technique.	[44]
Scanning electron microscopy (SEM) image segmentation for microstructure analysis of concrete using U-net convolutional neural network	A developed U-Net convolutional neural network was employed for concrete SEM image microstructure analysis.	The objective is to analyze concrete microstructure SEM images using semantic segmentation techniques.	[45]
Automated image segmentation of scanning electron microscopy images of graphene using U-Net Neural Network	the U-Net architecture employed to train on a dataset of images, using moderate image augmentation to enhance the analysis.	Facilitate the analysis of Graphene SEM images by U-Net coupled with images segmentation technique.	[46]
Deep Learning Based Instance Segmentation of Titanium Dioxide Particles in the Form of Agglomerates in Scanning Electron Microscopy	A method for evaluating SEM pictures of titanium dioxide samples that combines Mask-RCNN and transfer learning.	Evaluation of robustness and performance deep learning algorithm Mask R-CNN when applied to SEM images of TiO_2	[47]

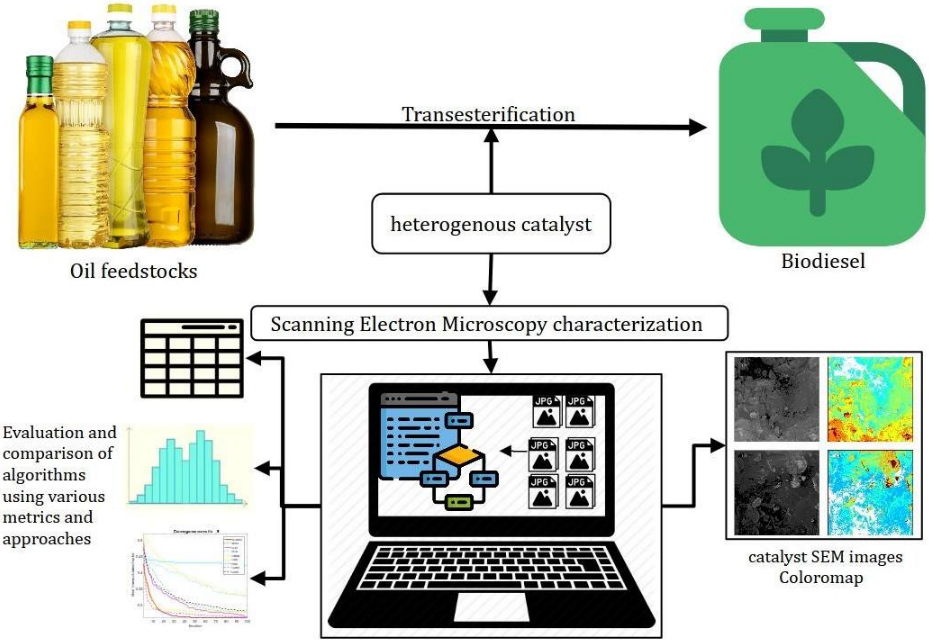

Figure III.27 : Image segmentation methods applied for Catalyst SEM images analysis.

III.4. Other useful methods and software's for biodiesel production

Along with AI approaches, biodiesel production may benefit from a variety of innovative methodologies and software tools meant to increase efficiency, output, and sustainability. The following paragraphs briefly describe several essential methodologies and software programs that are useful in biodiesel production:

III.4.1. JASP

JASP is a user-friendly, open-source statistical software designed for ease of use, available on Windows, Mac OS X, and Linux. It provides tools for performing common statistical tasks and offers descriptive statistics and basic analysis methods, including t-tests for one-sample, paired, and grouped designs, ANOVA for grouped and repeated measures designs, ANCOVA, linear regression, correlation tests, and contingency tables [48]. These tests allow researchers to examine how temperature, catalyst concentration, and reaction time affect biodiesel output and quality. JASP can also assist find connections between raw material qualities and production outputs, allowing for the selection of the optimal raw materials and processing conditions. This results in increased efficiency, cost-effectiveness, and sustainability in biodiesel synthesis.

III.4.2. SPSS

SPSS (Statistical Package for the Social Sciences) is a strong data processing and analysis tool that is particularly useful in biodiesel production research. It may create experiments to discover optimal production settings, such as JASP, do regression analysis to model correlations between variables, and utilize ANOVA to establish the relevance of process parameters. SPSS also uses descriptive statistics to describe data and multivariate analysis to investigate complicated relationships. Furthermore, SPSS may be used to run tests such as Wilcoxon and Friedmann, which are vital in the characterization of distinct novel generated optimization algorithms used for image segmentation and validate their efficiency over the previous ones.

III.4.3. DWSIM

DWSIM was developed by Daniel Medeiros, this software is an open-source chemical process simulation tool. This free software helps users understand the behavior of chemical systems [49]. It is a simulation tool that enables students, researchers, and professionals to simulate biodiesel production, evaluating and optimizing various stages of synthesis. It can simulate the entire production process, optimize reaction conditions, aid in equipment design, and conduct economic and sensitivity assessments for efficient and cost-effective production. DWSIM also provides energy and mass balance calculations and environmental effect evaluations.

DWSIM is a valuable tool for biodiesel production, offering a user-friendly interface, comprehensive thermodynamic models, and customization options. Being an open-source software, its integration capabilities and robust community support [50], these advantages make it even more effective in creating sustainable and cost-efficient biodiesel production processes.

III.4.4. Density Functional Theory

Density Functional Theory (DFT) is a common and effective "ab initio" method for the structure of quantum many-body systems (atoms, molecules, and solids). It analyzes the electronic structure of atoms, molecules, and condensed matter systems [51].

Density Functional Theory (DFT) is essential for designing and optimizing catalysts in chemical reactions, including biofuel synthesis. It has been successfully applied to study the catalytic properties of various catalysts [52]. DFT helps optimize reactions at the molecular level, understand reaction mechanisms, characterize feedstocks, and analyze reactant adsorption on catalyst surfaces [53]. This leads to a deeper understanding of catalyst reactivity and performance in biodiesel synthesis and helps optimize reaction conditions to maximize yield and minimize energy consumption.

DFT also aids in environmental impact evaluations by studying byproduct generation and emissions. It provides molecular-level insights and predictive capacity while also assisting in the development of efficient, environmentally friendly catalysts and processes, resulting in higher-quality biodiesel and more sustainability.

III.5. Conclusion

In this chapter, we looked at numerous AI techniques and their considerable benefits in biodiesel manufacturing. It has been demonstrated that AI technologies like machine learning, neural networks, and adaptive algorithms employed in segmentation can transform the biodiesel business by improving prediction accuracy, characterization analysis, and production process optimization.

These techniques allow for detailed modeling of complicated biodiesel production characteristics, making it easier to pick the best conditions for maximum yield and quality. AI approaches also provide real-time monitoring and quality control, which eliminates the need for trial-and-error testing and reduces production costs. Furthermore, AI's capacity to analyze vast datasets and uncover trends that human researchers may not see helps to drive novel solutions and ongoing progress in biodiesel production. Additionally, we presented various methods and software, explaining their advantages and how they simplify and expedite the simulation and understanding of biodiesel production.

This chapter served as an introduction to the practical aspects of this thesis, where we implemented several AI methods in the biodiesel synthesis process and evaluated their effectiveness. The following chapter will detail the materials like feedstocks, catalysts ...etc., techniques, and AI models employed to streamline the biodiesel production and characterization processes.

References

[1] Thomas Abdallah, *Chapter 13 - Reimagining sustainable mass transit*, Sustainable Mass Transit (Second Edition). Elsevier, 2023, pp. 189–200. doi: 10.1016/B978-0-443-15271-9.00003-0.

[2] A. Kaplan, 'Social Media Powered by Artificial Intelligence, Violence and Nonviolence', 2022.

[3] M. Mamdani and A. S. Slutsky, 'Artificial intelligence in intensive care medicine', *Intensive Care Med*, vol. 47, no. 2, pp. 147–149, Feb. 2021, doi: 10.1007/s00134-020-06203-2.

[4] S. Sharma, 'Benefits or Concerns of AI: A Multistakeholder Responsibility', *Futures*, p. 103328, 2024.

[5] R. P. França, A. C. B. Monteiro, R. Arthur, and Y. Iano, 'An overview of deep learning in big data, image, and signal processing in the modern digital age', *Trends in deep learning methodologies*, pp. 63–87, 2021.

[6] H. Ning, R. Li, and T. Zhou, 'Machine learning for microalgae detection and utilization', *Frontiers in Marine Science*, vol. 9, p. 947394, 2022.

[7] I. H. Sarker, 'Machine Learning: Algorithms, Real-World Applications and Research Directions', *SN COMPUT. SCI.*, vol. 2, no. 3, p. 160, Mar. 2021, doi: 10.1007/s42979-021-00592-x.

[8] M. Mohammed, M. B. Khan, and E. B. M. Bashier, *Machine Learning: Algorithms and Applications*. Boca Raton: CRC Press, 2016. doi: 10.1201/9781315371658.

[9] J. Talukdar, T. P. Singh, and B. Barman, 'Supervised Learning', in *Artificial Intelligence in Healthcare Industry*, J. Talukdar, T. P. Singh, and B. Barman, Eds., Singapore: Springer Nature, 2023, pp. 51–86. doi: 10.1007/978-981-99-3157-6_4.

[10] Y. Wang, Z. Cui, and R. Ke, *Machine learning for transportation research and applications*. Elsevier, 2023. Accessed: Jun. 27, 2024. [Online]. Available: https://books.google.com/books?hl=fr&lr=&id=1aCSEAAAQBAJ&oi=fnd&pg=PP1&dq=Machine+learning+basics++Machine+Learning+for+Transportation+Research+and+Applications,+2023&ots=NxVwJjrgu2&sig=8IyKMC8htBOnhbc_EmvIwbkeNsE

[11] S. Dridi, 'Supervised Learning - A Systematic Literature Review'. OSF, Jun. 13, 2024. doi: 10.31219/osf.io/qtmcs.

[12] İ. Yazici, I. Shayea, and J. Din, 'A survey of applications of artificial intelligence and machine learning in future mobile networks-enabled systems', *Engineering Science and Technology, an International Journal*, vol. 44, p. 101455, 2023.

[13] N. Amor, M. T. Noman, M. Petru, N. Sebastian, and D. Balram, ‘A review on computational intelligence methods for modelling of light weight composite materials’, *Applied Soft Computing*, p. 110812, 2023.

[14] J. E. van Engelen and H. H. Hoos, ‘A survey on semi-supervised learning’, *Mach Learn*, vol. 109, no. 2, pp. 373–440, Feb. 2020, doi: 10.1007/s10994-019-05855-6.

[15] N. Kashyap and A. Mishra, ‘A discourse on metaheuristics techniques for solving clustering and semisupervised learning models’, in *Cognitive Big Data Intelligence with a Metaheuristic Approach*, Elsevier, 2022, pp. 1–19. Accessed: Jun. 27, 2024. [Online]. Available: https://www.sciencedirect.com/science/article/pii/B9780323851176000121

[16] Z. M. Nayeri, T. Ghafarian, and B. Javadi, ‘Application placement in Fog computing with AI approach: Taxonomy and a state of the art survey’, *Journal of Network and Computer Applications*, vol. 185, p. 103078, 2021.

[17] H. Belyadi and A. Haghighat, *Machine learning guide for oil and gas using Python: A step-by-step breakdown with data, algorithms, codes, and applications*. Gulf Professional Publishing, 2021.

[18] L. Vanneschi and S. Silva, ‘Artificial Neural Networks’, in *Lectures on Intelligent Systems*, L. Vanneschi and S. Silva, Eds., Cham: Springer International Publishing, 2023, pp. 161–204. doi: 10.1007/978-3-031-17922-8_7.

[19] E. Antunes *et al.*, ‘Application of biochar for emerging contaminant mitigation’, in *Advances in Chemical Pollution, Environmental Management and Protection*, vol. 7, Elsevier, 2021, pp. 65–91. Accessed: Jun. 27, 2024. [Online]. Available: https://www.sciencedirect.com/science/article/pii/S2468928921000034

[20] ‘Neural Networks’, in *Image Segmentation*, John Wiley & Sons, Ltd, 2022, pp. 63–96. doi: 10.1002/9781119859048.ch4.

[21] H. Zhang and D. Li, ‘Applications of computer vision techniques to cotton foreign matter inspection: A review’, *Computers and electronics in agriculture*, vol. 109, pp. 59–70, 2014.

[22] Y. Song and H. Yan, ‘Image segmentation techniques overview’, in *2017 Asia Modelling Symposium (AMS)*, IEEE, 2017, pp. 103–107. Accessed: Jul. 01, 2024. [Online]. Available: https://ieeexplore.ieee.org/abstract/document/8424314/

[23] D. Kaur and Y. Kaur, ‘Various image segmentation techniques: a review’, *International Journal of Computer Science and Mobile Computing*, vol. 3, no. 5, pp. 809–814, 2014.

[24] S. Saini and K. Arora, ‘A study analysis on the different image segmentation techniques’, *International Journal of Information & Computation Technology*, vol. 4, no. 14, pp. 1445–1452, 2014.

[25] K. G. Dhal, A. Das, S. Ray, J. Gálvez, and S. Das, ‘Nature-Inspired Optimization Algorithms and Their Application in Multi-Thresholding Image Segmentation’, *Arch Computat Methods Eng*, vol. 27, no. 3, pp. 855–888, Jul. 2020, doi: 10.1007/s11831-019-09334-y.

[26] B. Sasmal, A. G. Hussien, A. Das, and K. G. Dhal, ‘A Comprehensive Survey on Aquila Optimizer’, *Arch Computat Methods Eng*, vol. 30, no. 7, pp. 4449–4476, Sep. 2023, doi: 10.1007/s11831-023-09945-6.

[27] D. Karaboga and B. Basturk, ‘Artificial Bee Colony (ABC) Optimization Algorithm for Solving Constrained Optimization Problems’, in *Foundations of Fuzzy Logic and Soft Computing*, Springer, Berlin, Heidelberg, 2007, pp. 789–798. doi: 10.1007/978-3-540-72950-1_77.

[28] X.-S. Yang, ‘Firefly Algorithms for Multimodal Optimization’, in *Stochastic Algorithms: Foundations and Applications*, O. Watanabe and T. Zeugmann, Eds., Berlin, Heidelberg: Springer, 2009, pp. 169–178. doi: 10.1007/978-3-642-04944-6_14.

[29] Y. Yang, H. Chen, A. A. Heidari, and A. H. Gandomi, ‘Hunger games search: Visions, conception, implementation, deep analysis, perspectives, and towards performance shifts’, *Expert Systems with Applications*, vol. 177, p. 114864, 2021.

[30] H. Su *et al.*, ‘RIME: A physics-based optimization’, *Neurocomputing*, vol. 532, pp. 183–214, 2023.

[31] S. Mirjalili, S. M. Mirjalili, and A. Lewis, ‘Grey wolf optimizer’, *Advances in engineering software*, vol. 69, pp. 46–61, 2014.

[32] S. Mirjalili and A. Lewis, ‘The whale optimization algorithm’, *Advances in engineering software*, vol. 95, pp. 51–67, 2016.

[33] H. Jin, Y.-G. Kim, Z. Jin, A. A. Rushchitc, and A. S. Al-Shati, ‘Optimization and analysis of bioenergy production using machine learning modeling: Multi-layer perceptron, Gaussian processes regression, K-nearest neighbors, and Artificial neural network models’, *Energy Reports*, vol. 8, pp. 13979–13996, 2022.

[34] A. V. S. L. S. Bharadwaj, M. Singh, S. Niju, K. M. M. S. Begum, and N. Anantharaman, ‘Biodiesel production from rubber seed oil using calcium oxide derived from eggshell as catalyst – optimization and modeling studies’, *Green Processing and Synthesis*, vol. 8, no. 1, pp. 430–442, Jan. 2019, doi: 10.1515/gps-2019-0011.

[35] C. Özgür, ‘Prediction and optimization of biodiesel production by using ANN and RSM’, *International Journal of Automotive Engineering and Technologies*, vol. 11, no. 2, Art. no. 2, Jul. 2022, doi: 10.18245/ijaet.1057170.

[36] A. Khanna *et al.*, ‘Biodiesel Production from Jatropha: A Computational Approach by Means of Artificial Intelligence and Genetic Algorithm’, *Sustainability*, vol. 15, no. 12, Art. no. 12, Jan. 2023, doi: 10.3390/su15129785.

[37] S. Promdaen, P. Wattuya, and N. Sanevas, ‘Automated microalgae image classification’, *Procedia Computer Science*, vol. 29, pp. 1981–1992, 2014.

[38] L. Wei, S. XiaoPan, and F. Heydari, ‘Microalgae Classification Using Improved Metaheuristic Algorithm’, *Mathematical Problems in Engineering*, vol. 2022, pp. 1–10, May 2022, doi: 10.1155/2022/3783977.

[39] Abdullah, S. Ali, Z. Khan, A. Hussain, A. Athar, and H.-C. Kim, ‘Computer Vision Based Deep Learning Approach for the Detection and Classification of Algae Species Using Microscopic Images’, *Water*, vol. 14, no. 14, Art. no. 14, Jan. 2022, doi: 10.3390/w14142219.

[40] L. Xu, L. Xu, Y. Chen, Y. Zhang, and J. Yang, ‘Accurate Classification of Algae Using Deep Convolutional Neural Network with a Small Database’, *ACS EST Water*, vol. 2, no. 11, pp. 1921–1928, Nov. 2022, doi: 10.1021/acsestwater.1c00466.

[41] A. Abdennouri, E. Zouaoui, H. Ferkous, A. Hamza, M. Grimes, and A. Boukabou, ‘An improved Symmetric Chaotic War strategy optimization algorithm for efficient Scanning electron microscopy image segmentation: Calcium oxide catalyst case’, *Chemometrics and Intelligent Laboratory Systems*, vol. 244, p. 105043, 2024.

[42] X. Muñoz, J. Freixenet, X. Cufı, and J. Martı, ‘Strategies for image segmentation combining region and boundary information’, *Pattern recognition letters*, vol. 24, no. 1–3, pp. 375–392, 2003.

[43] R. S. Thakur, S. Chatterjee, R. N. Yadav, and L. Gupta, ‘Image de-noising with machine learning: A review’, *IEEE Access*, vol. 9, pp. 93338–93363, 2021.

[44] Y. Bai *et al.*, ‘Identification of nanocomposites agglomerates in scanning electron microscopy images based on semantic segmentation’, *IET Nanodielectrics*, vol. 5, no. 2, pp. 93–103, 2022, doi: 10.1049/nde2.12034.

[45] S. S. Bangaru, C. Wang, X. Zhou, and M. Hassan, ‘Scanning electron microscopy (SEM) image segmentation for microstructure analysis of concrete using U-net convolutional neural network’, *Automation in Construction*, vol. 144, p. 104602, 2022.

[46] A. Shah *et al.*, ‘Automated image segmentation of scanning electron microscopy images of graphene using U-Net Neural Network’, *Materials Today Communications*, vol. 35, p. 106127, 2023.

[47] P. Monchot *et al.*, ‘Deep Learning Based Instance Segmentation of Titanium Dioxide Particles in the Form of Agglomerates in Scanning Electron Microscopy’, *Nanomaterials*, vol. 11, no. 4, Art. no. 4, Apr. 2021, doi: 10.3390/nano11040968.

[48] J. Love *et al.*, ‘JASP: Graphical Statistical Software for Common Statistical Designs’, *Journal of Statistical Software*, vol. 88, pp. 1–17, Jan. 2019, doi: 10.18637/jss.v088.i02.

[49] K. Tangsriwong, P. Lapchit, T. Kittijungjit, T. Klamrassamee, Y. Sukjai, and Y. Laoonual, ‘Modeling of chemical processes using commercial and open-source software: A comparison between Aspen Plus and DWSIM’, *IOP Conf. Ser.: Earth Environ. Sci.*, vol. 463, no. 1, p. 012057, Mar. 2020, doi: 10.1088/1755-1315/463/1/012057.

[50] S. Sreemahadevan, K. V. Sivakumar, and M. Palanisamy, ‘Evaluation of the Open Source Process Simulator DWSIM for Bioprocess Simulation’, *Periodica Polytechnica Chemical Engineering*, vol. 68, no. 2, Art. no. 2, May 2024, doi: 10.3311/PPch.23166.

[51] T. Nikšić, D. Vretenar, and P. Ring, ‘Relativistic nuclear energy density functionals: Mean-field and beyond’, *Progress in Particle and Nuclear Physics*, vol. 66, no. 3, pp. 519–548, 2011.

[52] K. Kumar, V. Khatri, F. Parveen, H. K. Kashyap, and S. Upadhyayula, ‘Synthesis of an oxygenated fuel additive from a waste biomass derived aldehyde using a green catalyst: an experimental and DFT study’, *Sustainable Energy Fuels*, vol. 4, no. 6, pp. 2924–2936, Jun. 2020, doi: 10.1039/D0SE00100G.

[53] E. Mohebolkhames, M. Kazemeini, S. Sadjadi, and M. Tamtaji, ‘Synthesis and characterization of K2CO3 over Salmon-fishbone catalyst, kinetics and DFT analyses and biodiesel catalytic production from castor oil’, *Journal of Molecular Structure*, vol. 1302, p. 137426, 2024.

Chapter IV

Materials and methods

IV.1. Introduction

Previous chapters have discussed Algeria's waste and energy concerns and offered solutions for reducing pollution and greenhouse gas emissions driven by the country's high production of waste and heavy reliance on fossil fuels. These include employing catalysts to speed up the process and creating biodiesel from a variety of materials, including algae and waste cooking oil. By using this method, pollution diminishes and a new, environmentally beneficial fuel is produced.

The upcoming chapter will delve into the experimental protocol designed for biodiesel production, detailing each step of the process from resource collection to catalyst application ending in biodiesel synthesis. Additionally, it will highlight the advanced AI techniques implemented to facilitate and optimize the analysis of characterization results, ensuring precise and reliable data interpretation.

IV.2. Experimental Protocol Proposal

Fig IV.1 outlines the proposed framework for biodiesel synthesis in this thesis, which utilizes waste cooking oil and algae as raw materials and cuttlefish bones as a catalyst. The first steps involve breaking down cuttlefish bones to make calcium oxide (CaO), which is a heterogeneous catalyst. Then, the lipid properties, antibacterial activity, and other factors are checked to make sure the feedstock is suitable and the biodiesel is of good quality. In summary, the method includes three main processes: first, prepare the raw materials by assessing the qualities of waste cooking oil and algae; second, convert cuttlefish bones into CaO; and third, use the CaO catalyst to perform the transesterification process, turning oils into biodiesel.

Advanced techniques like SEM (Scanning Electron Microscopy), XRD (X-ray Diffraction), FT-IR (Fourier-Transform Infrared Spectroscopy), and GC-MS (Gas Chromatography-Mass Spectrometry) are used to analyze and characterize the materials used for biodiesel production.

Additionally, an AI method optimizes and facilitates the analysis of CaO SEM image characterization results, ensuring precise and reliable data interpretation.

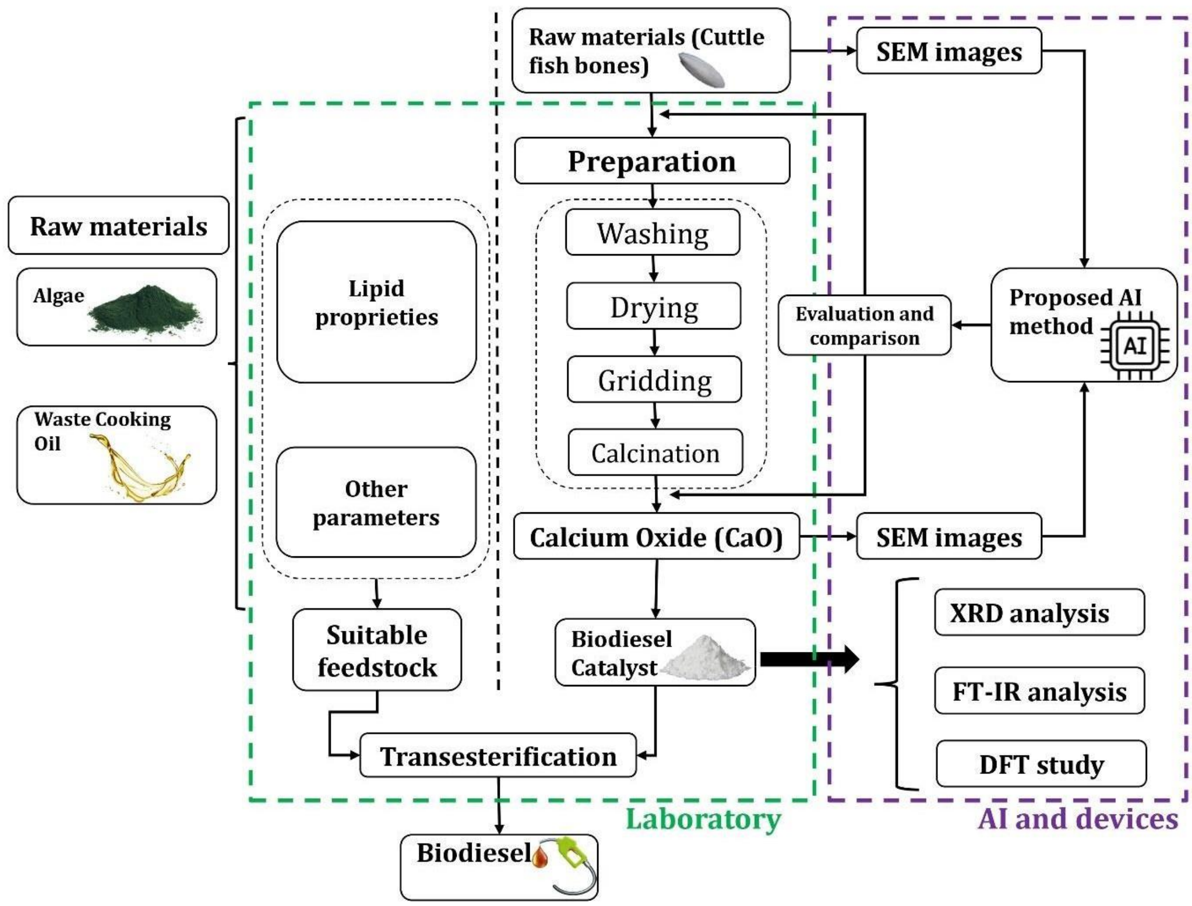

Figure IV.28 : Experimental protocol proposal.

IV.3. Materials and Methods

IV.3.1. Catalyst Preparation

The catalyst selected for biodiesel production is Calcium Oxide (CaO), known for its high stability and excellent performance due to its extremely high basic strength [1]. This catalyst is synthesized by thermally decomposing Calcium Carbonate ($CaCO_3$) as highlighted in Eq.1.

$$CaCO_3 \ni\in CaO + CO_2 \qquad (1)$$

Calcium carbonate ($CaCO_3$) is widely found in natural sources such as eggshells and animal bones. For this study, cuttlefish bones often found along coastlines and recognized for their high calcium content were selected as the primary source of calcium. Cuttlefish bones are also commonly used as dietary supplements for birds, providing essential calcium that strengthens eggshells. Their natural richness in calcium makes them an ideal candidate for examining calcium transformations during catalyst preparation, allowing us to leverage their unique properties in this research.

The Calcium Oxide (CaO) catalyst preparation, as illustrated in Fig IV.2, begins with collecting cuttlefish bones from Oued Bibi Beach during the autumn season. These bones are thoroughly washed to remove impurities and dried overnight at 100 °C. After drying, they are ground into a fine powder using an electric blender. This powder then undergoes calcination at 900°C for 2 hours, resulting in the CaO catalyst, which will be used for transesterification reactions and further analyzed through various characterization techniques.

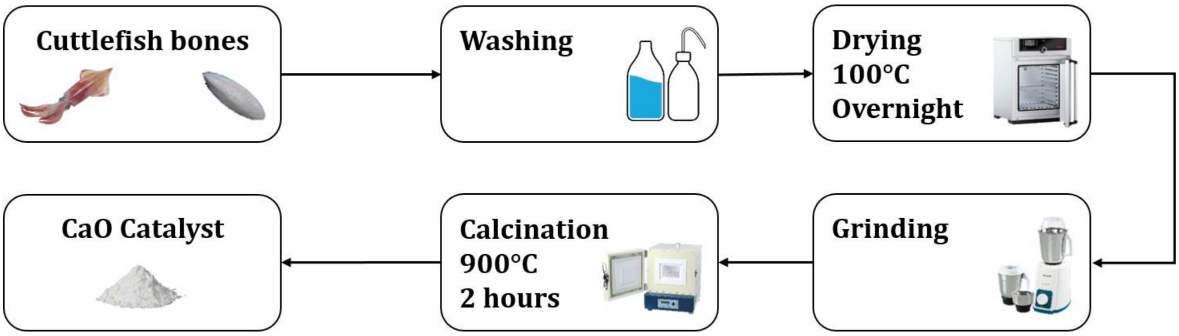

Figure IV.29 : CaO catalyst preparation method.

IV.3.2. Algae and waste cooking oil samples

Algae and waste cooking oil samples were employed for the study. The waste cooking oil was collected from local restaurants in Tamalous, ensuring a sustainable approach by repurposing used oil. The algae samples included Spirulina and Chlorella, sourced from BioHealth DZ, a local startup dedicated to producing biohealth products. These materials were chosen for their availability and potential in biodiesel production.

But before introducing this feedstock's into transesterification reactions, several tests were done to confirm the proprieties of these materials.

IV.3.3. Characterization methods

IV.3.3.1. Catalyst characterization

1) **X-Ray Diffraction:** CaO and $CaCO_3$ identification and highlight their chemical compositions was carried out using X-ray diffraction (XRD) analysis to both before and after calcination. The analysis was performed with a Bruker D8 ADVANCE with

DAVINCI design (Bruker AXS, Germany), operating at 40 mA and 40 kV with Cu Kα radiation (wavelength of 1.54 Å). Data collection spanned a 2θ range of 10–90° with a step size of 0.02° and a time per step of 19.1 s.

2) **Infra-Red Spectroscopy:** The characterization of CaO and $CaCO_3$ was performed using Fourier Transform Infrared (FTIR) spectroscopy to highlight the functional groups found in surfaces. Measurements were done with a Shimadzu QATRTM-S Single-Reflection ATR Accessory equipped with a diamond crystal, covering the wavelength range of 4000–400 cm^{-1}.

3) **Scanning Electron Microscopy:** Scanning Electron Microscopy (SEM) is essential for examining and highlighting surface modifications in materials before and after calcination. This study aims to observe the changes in $CaCO_3$ after thermal treatment to produce CaO catalysts. To achieve this, we used a ThermoScientific Quattro model SEM.

IV.3.3.2. Feedstock characterization

1) **Lipid Proprieties:** This analysis looked on the feedstock's lipid properties and content. For that, 50g of Spirulina and 30g of Chlorella were extracted using methanol as the solvent and following the maceration methods, both spirulina and chlorella were kept overnight under stirring. This characterization helps to determine the lipid content of these algae samples, which is crucial for assessing their potential as a feedstock for biodiesel synthesis.

IV.3.4. AI proposed method for efficient SEM images analysis

Many studies indicate that calcium oxide (CaO) is widely utilized as a catalyst in biodiesel synthesis, largely due to its favorable physical and chemical properties. Physically, CaO boasts a large surface area, structural stability, and strong basic sites, which make it highly effective for catalytic reactions. Chemically, it exhibits notable thermal stability and catalytic activity, making it suitable for high-temperature processes.

The morphology of CaO can vary significantly, influenced by factors such as the choice of raw materials and the calcination temperatures used during preparation. This variability underscores the importance of careful feedstock selection and precise control over calcination conditions to optimize the catalytic efficiency of CaO.

To further understand and optimize the properties of CaO as a catalyst, Scanning Electron Microscopy (SEM) is frequently employed as a key characterization method. SEM analysis provides detailed insights into the catalyst’s surface morphology, which in turn helps elucidate the structural modifications occurring during preparation. This detailed imaging reveals changes that enhance the catalyst's performance, making SEM an invaluable tool for refining feedstock choices and ensuring the highest possible selectivity and activity in biodiesel production.

However, manual examination of SEM images done by researchers can often fall short in providing a thorough understanding, as image noise and other distortions may obscure crucial details. To address this limitation, researchers have developed a range of advanced solutions. Among these, segmentation algorithms stand out as a powerful tool. By breaking down and refining image components, segmentation enhances both the clarity and precision of analysis, transforming complex images into more interpretable representations. This approach not only overcomes the challenges of manual image inspection but also enables more accurate and reliable findings, offering a sharper, more detailed insight into the materials under study

In this context, this practical chapter of our thesis presents a novel Symmetric Chaotic War Strategy Optimization Algorithm (SCWSO), specifically designed to achieve precise segmentation of SEM images of calcium oxide (CaO) catalysts used in the transesterification reaction of biodiesel. Unlike traditional methods that rely on random processes, the whole inspiration of SCWSO came from the hybridization between symmetric chaotic sequences derived from the Henon map and the original optimization algorithm called the War strategy optimization algorithm. This hybridization has been a big advantage in enhancing the segmentation of SEM images. This structured approach not only accelerates the search for optimal solutions but also enhances the clarity and accuracy and eliminates noise present in several images, facilitating interpreting of SEM images of CaO catalysts, making it a powerful tool for detailed catalyst analysis.

A streamlined overview of the SEM image analysis process using SCWSO is illustrated in Fig IV.3.

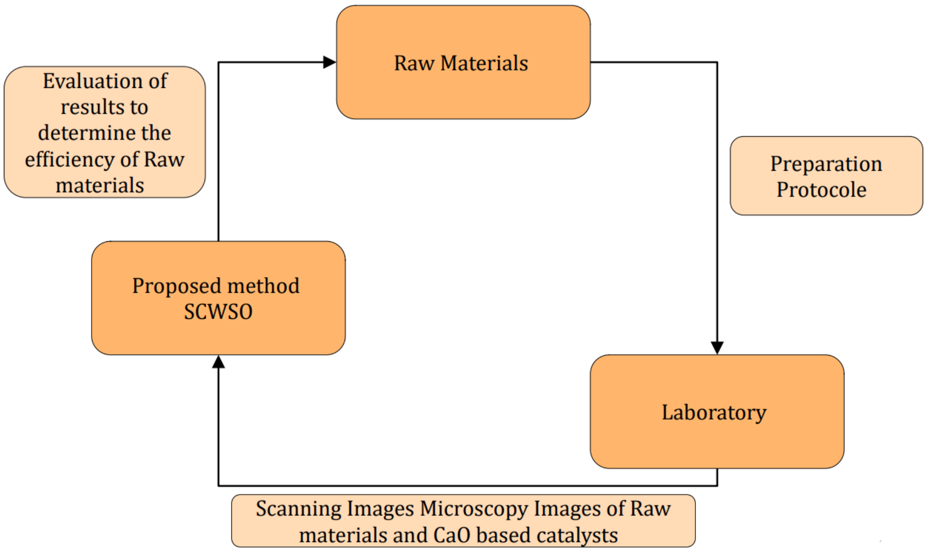

Figure IV.30 : Experimental protocol proposal.

IV.3.4.1. Data used in the method

As with any AI-driven approach, the effectiveness of the SCWSO method in analyzing SEM images of calcium oxide (CaO) catalysts hinges on selecting an appropriate dataset. A well-chosen dataset is essential for evaluating various aspects of the algorithm's performance, ensuring that its capabilities are thoroughly tested and validated. In this study, the images presented in Fig IV.4 and Tab IV.1 were carefully chosen as the dataset for applying the SCWSO method. These images encompass a diverse range of features, providing a robust foundation for testing the method's proficiency in both image segmentation and catalyst characterization, thus offering a comprehensive assessment of SCWSO's analytical potential

Table IV.8 : Dataset employed in AI method.

Image	Title	Reference
SEM-1	Calcined kettle limescale	[2]
SEM-2	Calcined Silver Croaker's stone 4μm	[3]
SEM-3	Calcined chicken egg shell 50kX	[4]
SEM-4	Eggshell-CaO-900-600°C	[5]
SEM- 5	Eggshell-CaO-900°C	[5]
SEM-6	Uncalcined 5X eggshell waste	[6]
SEM-7	Kettle limescale	[2]
SEM-8	Raw chicken egg shell 500X	[4]
SEM-9	Raw chicken egg shell 5kX	[4]
SEM-10	Raw chicken egg shell 50kX	[4]

This dataset was also selected for its relevance in studying the transformation of calcium compounds under calcination, a key process in catalyst preparation. Before calcination, calcium exists as calcium carbonate, which then converts into calcium oxide during the heating process, which present a main objective in our study. By applying the SCWSO method, we can effectively analyze structural changes occurring as calcium carbonate transitions to calcium oxide. This dataset thus enables a comprehensive evaluation of SCWSO's capability to detect and interpret morphological differences across the various calcination stages, offering critical insights into the catalyst's development.

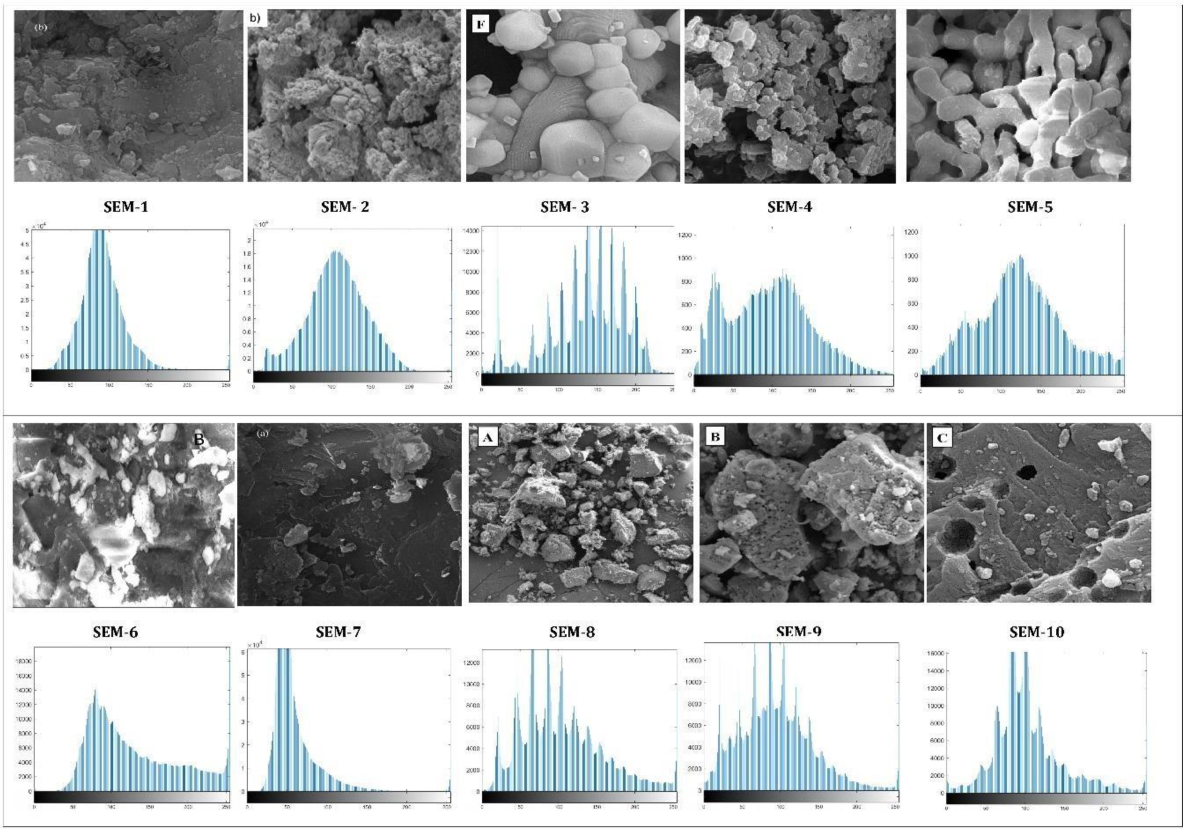

Figure IV.31 : SEM images employed in AI methods

IV.3.4.2. Development of Symmetric Chaotic War Strategy Optimization Algorithm

SCWSO is an enhanced technique of original nature inspired method called War Strategy Optimization WSO incoraopted with different technique such symmetric chaotic and Hennon map

IV.3.4.2.1. War Strategy Optimization algorithm

The WSO method was proposed by Tummala et al.[7], suggesting that each soldier has an equal chance to rise to King or Commander depending on their battle strength. These leaders guide other soldiers, but they may confront formidable local opponents who employ strategic placement and mobility techniques. To summarize, WSO mathematically models the tactics and varied positions used by soldiers and commanders, as follows:

- **Attack position :**

Every soldier adjusts his pose to conform to the King and Commander positions, as stated in Eq. 2:

$$Yi\,(t+1) = Yi\,(t) + 2 \times \rho \times (C - K) + rand \times (Wi \times K - Xi\,(t)) \quad (2)$$

Where $Y_i\,(t + 1)$ is the update position, $Y_i\,(t)$ the former position, C the commander's position, K the king's location, and Wi is the weight

- **Weight and Rank updating :**

Positions get updates by search agents based on interactions among Soldier, Commander, and King grades. If the new location's attack force is less than the previous ones, the soldier returns to his former position. When updates are successful, soldiers' ranks Si rise.

$$Yi(t+1) = (Yi(t+1))(Fn \geq Fp) + (Yi(t))(Fn < Fp) \quad (3)$$

$$Si = (Si+1)(Fn \geq Fp) + (Si)(Fn < Fp) \quad (4)$$

Using the new rank, we can determine the current weight as follows:

$$W_i = W_i\left(\frac{S_i}{Max_{iter}}\right)^{\alpha} \quad (5)$$

- **Defense strategy :**

The king, the commander, and a chosen soldier's placements define the defense strategy for position updates. However, the ranking mechanism and weight changes remain constant following Eq. 6.

$$Y_i(t+1) = Y_i(t) + 2 \times \rho \times (K - Y_{rand}(t)) + rand \times W_i \times (c - Y_i(t)) \quad (6)$$

- **Taking the weak soldiers out and replacing them :**

In every iteration, soldiers with the lowest fitness ratings are picked. Several replacement procedures were investigated, with one of the simplest options being to replace the weakest soldier with a randomly selected soldier, as shown in Eq. 7.

$$Yw\,(t+1) = Lb + rand \times (Ub - Lb) \quad (7)$$

Where L_b and U_b are the lower and upper bounds respectively.

IV.3.4.2.2. Symmetric chaotic

The Henon map, with its multiple distinguishing features, is considered popular chaotic systems. The set of functions H_{ab}: $R^2 \rightarrow R^2$ has the corresponding discrete form, as shown in Eq.8. [8]:

$$H_{ab}\begin{pmatrix} x \\ y \end{pmatrix} = \begin{pmatrix} 1 - ax^2 + y \\ bx \end{pmatrix} \qquad (8)$$

The system variables are (x, y), while the system parameters are (a, b). (H_{ab}) is determined by two parameters (a, b), which for chaotic behavior have canonical values of 1.4 and 0.3. As indicated in Eq. 9, the Henon map can also be expressed iteratively.

$$\begin{cases} x(k+1) = 1 - ax^2(k) + y(k) \\ y(k+1) = bx(k) \end{cases} \qquad (9)$$

With k=1,2…., N

Yet, to fully incorporate WSO with the Henon map, it must be expressed in linear form this way:

$$T_{ab}(z_1, z_2) = H_{ab}\left(\frac{y_1 - \alpha_1}{\beta_1 - \alpha_1}, \frac{y_2 - \alpha_2}{\beta_2 - \alpha_2}\right) \qquad (10)$$

z_1 and z_2 are variables of the system after the linear transformation, The pairings(z_1, z_2) , $(1 - z_1, z_2)$, $(z_1, 1 - z_2)$, and $(1 - z_1, 1 - z_2)$ are used to make the sequence [8].

In our thesis, the Symmetric Chaotic War Strategy Optimization (SCWSO) approach introduces an innovative twist on traditional random sequences by integrating symmetric chaotic patterns generated from the Henon map function. By leveraging chaotic mapping, this approach enhances heuristic algorithms, creating a more diverse and dynamic selection process that improves algorithmic performance. The added variability in SCWSO's search strategy allows for more thorough exploration, enhancing the robustness and precision of the results. The specific performance improvements achieved through this method are detailed in the sections below.

- **Chaotic Defense attack mechanism :**

The modification starts by replacing the random variables in Eqs. 2 and 6 with symmetric chaotic settings, resulting in the following position update Eq .11:

$$DY_I(t+1) = \begin{cases} Y_i(t) + 2 \times (1 - z_1) \times (C - K) + rand \times (W_i \times K - Y_i(t)) & rand < 0.5 \\ Y_i(t) + 2 \times (1 - z_1) \times (K - Y_{rand}(t)) + rand \times W_i \times (c - Y_i(t)) & rand \geq 0.5 \end{cases} \quad (11)$$

- **King-Commanders Based Chaotic Mutation (KCBCM) :**

In order to update a Soldier's best position, the King (K) is chosen as the highest-ranking unit, followed by the Commander (C) and the Lieutenant, depending on the fitness of all N troops. Each i^{th} soldier's new mutation position $X_i(New)$, is then determined.

$$Y_i(New) = Y_i(t+1) + (2 \times (1 - z_1) - 1) \times (K - (C + Lieutenant) + ((1 - z_2) - 1)(K - Y_i(t)) \quad (12)$$

Where, $(1 - z_1)$ and $(1 - z_2)$ are symmetric parameters obtained from the normalized Henon map.

Following these changes, the new position update will be assessed as follows:

$$Y_i(New2) = \begin{cases} Y_i(New1) & if \quad f(Y_i(New1)) < f(Y_i(New)) \\ Y_i(New) & if \quad f(Y_i(New)) < f(Y_i(New1)) \end{cases} \quad (13)$$

With : $Y_i(New) = Y_i + DY_i(t+1)$

- **Search Technique for a Chaotic Multi-Leader Exploring Group (SCMEG) :**

To boost the algorithm's ability to navigate the search area and pick the most suitable candidates. SCMEG (Search strategy for a Chaotic Multi-Leader Exploring Group) strategy, outlined in Eq. 14, is presented; which aim to guide the process toward the best possible finding:

$$Y_{SCMEG}(t+1) = K + W_i \times (X_{ml} - Y_{r1} + Y_{mr} - Y_{r2}) \quad (14)$$

Y_{r1} and Y_{r2} are randomly chosen soldier positions from the entire population, while Y_{ml} and Y_{mr} are randomly selected from the top five best positions in the army. This selection process is explained in Eq.15.

$$Y_i = \{ Y_{SCMEG} \; if \;\; f(Y_{SCMEG}) < f(Y_i) \quad (15)$$

- **Chaotically Weighted Soldier Strategy (CWSS) :**

Chaotically Weighted Soldier Strategy is presented to increase the algorithm's global search efficiency. Eqs. 16 and 17 explain how it utilizes a chaotic search to randomly find new spots inside the present region.

$$Y_{CWSS}(t+1) = Y_i t + 1 + W_i \times (1 - z_1) \times (Y_{r1} - Y_{r2}) \quad (16)$$

$$Y_i = \{Y_{CWSS}\ if\ \ f(Y_{CWSS}) < f(Y_i) \quad (17)$$

To summarize, Algorithm 1 below provides the pseudocode for constructing the SCWSO algorithm, detailing the necessary equations used and its application in analyzing CaO SEM images.

Algorithm 1 : SCWSO pseudo-code

Input: Soldier size (S) = 30, dimension of the war space (dimension of the problem), lb: lower bond, Ub: upper bounds, Max-iteration= 100, Positions of the King (K = zeros (1, dim)), Army Commander (C = zeros (1, dim)), $\rho_r = 0.5$

Output: Best solution

Set the settings; R=zeros (1, soldier size); W = 2*ones* (1, soldier size)

Deploy the soldiers in the conflict zone in an arbitrary and uniform way.

For *1: soldier − size*

Obtain the attack force for each soldier.

end for

Configure the fitness for all of the soldiers (attack force).

Select the highest-fitness soldier as the King and the second-highest as the Commander.

while do $t < T_{max}(Max_{iterations})$

  For *1: soldier − size*

  $\rho = rand$

  if $\rho < \rho_r$ percentage signal given to pursue the strategy

   Upgrade every soldier's location utilizing Eq. 11 (Exploration)

  else

   Upgrade every soldier's location utilizing Eq. 11 (Exploitation)

  end if

   Assess every soldier's attack force.

   Arrange each soldier's fitness.

   Find the optimum locations in the army population employing Eqs. 12, 13, 14, and 15

   Upgrade each soldier's position based on the attack force of their present and former placements via Eq. 3.

   Improve the rank and weight of each soldier located on the territory employing Eq. 4

  end for

Upgrade the Global search with X_{CWSS} based on Eqs. 16 and 17.
Locate the weak soldier with the bad fitness
Relocate the weak soldier picking an appropriate relocation strategy
Upgrade the King and Commander positions
$t = t + 1$
end while
Reveal the King’s attack force and position
Generate coloromap images for the selected pictures

Evaluating time complexity helps to understand the algorithm's efficiency and scalability with increasing problem size. For the SCWSO method, this analysis shows how changes in population size (N), search space (D), and iterations Max_{iter} impact computational resources. Time complexity is evaluated employing big-O notation for the SCWSO algorithm. The initialization, function evaluation, and position update complexities are O(N×D), O(N), and O((N+1) ×D), respectively. Thus, the total time complexity is $O((N+1) \times D \times Max_{iter})$.

IV.3.4.3. SCWSO Evaluation

The SCWSO approach was assessed versus other algorithms to prove its superiority and efficiency in this area, with each SEM image input exposed to up to 100 iterations over 30 independent runs for each technique. All methods have been examined through the same simulation circumstances and their parameters set to default values. Table IV.2 outlines algorithms used, along with their settings.

Table IV.9 : Algorithm used in evaluation and its parameters.

Algorithm Name	Parameter Setting
Common parameters	Population size N = 30 Total number of iterations T = 100 Number of independent runs = 30
Symmetric Chaotic War Strategy Optimization (SCWSO)	a =1.4 , b = 0.3 of Henon map
War Strategy Optimization (WSO) [7]	ρ is a random variable in the range [0, 1]
Sine Cosine Algorithm (SCA) [9]	SCA a = 2 (defaults)
Chimp Optimization Algorithm (Chimp) [10]	Chimp Gauss map the initial condition with x (0) = 0.7. Other parameters set as defaults
Chornobyl Disaster Optimizer (CDO) [11]	Defaults parameters
Golden Jackal Optimization (GJO) [12]	C_1 variable is varied from 1 to 2
Reptile Search Algorithm (RSA) [13]	α = 0.1, β = 0.005 (default)
Grey Wolf Optimizer (GWO) / (IGWO) [14]	C is changed in range [0, 2]

The effectiveness of the developed method is gauged utilizing the following metrics: fitness, peak signal-to-noise ratio (PSNR), structural similarity index (SSIM), and feature similarity index (FSIM). these metrics are summarized as follow:

- **Standard deviation**

To evaluate the algorithm's stability in fitness research, the standard deviation is considered a good test. A high standard deviation indicates increased instability in the algorithm. It can be estimated utilizing Eq. 18 [15].

$$STD = \sqrt{\sum_{i=1}^{T_E} \frac{\sigma_i - \mu}{T_E}} \qquad (18)$$

- **PSNR**

PSNR measures serve to evaluate the similarity between segmented and original images. Higher PSNR values imply higher image quality, which mean less distortion. This value estimated via Eq.19 [16,17]:

$$PSNR = 20 \times log_{10} \times \left(\frac{255^2}{\sqrt{MSE}}\right) \quad (19)$$

MSE indicate the mean square error of image before and after segmentation , determined as follow [16]:

$$MSE = \frac{1}{m \times n} \sum_{i=0}^{m-1} \sum_{j=0}^{n-1} \| I(i,j) - G(i,j) \|^2 \quad (20)$$

$I(i,j)$ and $G(i,j)$ are grayscale values of SEM image before and after segmentation.

- **SSIM**

SSIM results can demonstrate the method's superiority over alternative approaches. Strong finds show robust segmentation of the original images, SSIM determined as follows [17]:

$$SSIM\,(I_{org}, I_{seg}) = \frac{(2\mu_{org}2\mu_{seg} + c_1)(\sigma_{org.seg} + c_2)}{(\mu^2{}_{org} + \mu^2{}_{seg} + c_1)(\mu^2{}_{org} + \mu^2{}_{seg} + c_2)} \quad (21)$$

Where, μ_{org} and μ_{seg} refer to the mean intensities of the original image and the segmented image, while σ_{org} and σ_{seg} are their standard deviations. Covariance between the original and segmented images is denoted as $\sigma_{org \cdot seg}$, and c_1 and c_2 are fixed constants.

- **FSIM**

The high FSIM values imply that the original images were segmented accurately, with the segmented images identical to the original. The process of computing FSIM entails defining phase congruency (PC) and gradient magnitude (GM), which identify visual qualities and compute image gradients. FSIM is calculated using these two expressions as follow [17]:

$$S_{PC} = \frac{2PC_1PC_2 + T_1}{PC_1^2 + PC_2^2 + T_1} \quad (22)$$

Where: S_{PC} measures the similarity between the original and segmented images. PC_1 and PC_2 are phase congruency of the original and segmented images, while T_1 is a positive constant that enhances S_{PC} stability.

$$S_G = \frac{2G_1G_2 + T_2}{G_1^2 + G_2^2 + T_2} \quad (23)$$

S_G computes the similarity between G_1 and G_2, which represent the gradients of the original and segmented pictures. T_2 is a positive constant that varies with the dynamic range of GM values.

Utilizing Eqs. 22 and 23 FSIM can be obtained:

$$S_L(x) = [S_{PC}(x)]^{\alpha}[S_G(x)]^{\beta} \qquad (24)$$

α and β employed to alter the relative findings of PC and GM features.

Also, every evaluation includes the Friedman and Wilcoxon tests, which are good nonparametric techniques for assessing paired and repeated measures data. These tests are useful because of their resilience and applicability, particularly when normalcy assumptions are violated.

- **Analysis of several variant of WSO algorithm and noise images effect**

In this section, three images SEM-1, SEM-2, and SEM-7are used for analysis due to their distinct characteristics. SEM-1 and SEM-7, derived from the same raw materials, enable a comparison to assess the effects of calcination. In contrast, SEM-2 represents CaO obtained from different raw material, allowing an effective comparison of the impact of varying feedstocks in the preparation process.

Different variations were applied to the War Strategy Optimization (WSO) algorithm and tested on SEM images 1, 2, and 7, with multiple thresholds. These variations aimed to evaluate the effectiveness of segmentation using the WSO method and the impact of each variation on performance. The results were then compared with those from the proposed SCWSO approach to assess its overall effectiveness.

In addition, noise studies are required to evaluate SCWSO performance with image degradation. Salt and pepper noise is a typical sort of impulsive noise that causes damaged pixels to display either the highest or lowest gray value. This procedure was used with SEM-1, SEM-2, and SEM-7[18].

IV.4. Biodiesel Production

IV.4.1. Biodiesel from Waste Cooking oil

The waste oil is first filtered to remove impurities and food particles. Then, 50 g of the filtered oil is heated to 100 °C for 10 minutes to evaporate any residual water, and 10 g of methanol is mixed with 1 g of Cuttlefish CaO catalyst and stirred until fully combined. The oil is then heated to 60°C in a reaction vessel, and the methanol-CaO mixture is added, with continuous stirring at 60°C in water bath for 2 hours. After the reaction, the mixture is cooled and allowed to stand overnight, enabling separation into biodiesel and glycerol layers. The biodiesel layer is then separated, washed with water, and dried at 100 °C. Key synthesis conditions include a 5:1 oil-to-methanol (Oi/MeOH) molar ratio, a 2 wt.% Cuttlefish CaO catalyst, a 60°C reaction temperature, and a 2-hour reaction time.

IV.4.2. Biodiesel from Chlorella algae

Chlorella algae was selected as the raw material for biodiesel production. A sample of 25 g of dried, Chlorella biomass was combined with 10 ml of my hexane as a solvent and 75 ml of methanol 75 mL of methanol (12:1 methanol-to-oil molar ratio) and 1.25 g of Cuttlefish CaO catalyst (5 wt% of biomass) in a reaction vessel with a condenser. The mixture was heated to 60°C in water bath and stirred continuously for 4 hours. After cooling, it was filtered to remove solid residues, resulting in a liquid containing biodiesel, unreacted methanol, and glycerol. This liquid was left to settle overnight, allowing the biodiesel to separate from the glycerol layer. The biodiesel was then decanted, washed with warm distilled water until clear, and dried at 100°C. Key conditions included a 12:1 methanol-to-oil ratio, 5 wt.% CaO catalyst, a reaction temperature of 60°C, and a reaction time of 4 hours.

IV.5. Conclusion

Chapter IV outlined the materials and methods required to achieve the objectives set in the previous chapter. It covered the preparation and treatment of waste cooking oil to produce biodiesel, along with a comparison of the yield obtained from this process to that derived from algae. Additionally, the procedure for preparing the catalyst, specifically using cuttlefish bones, was detailed to illustrate its application in biodiesel production. These practical tests were then analyzed through various characterization techniques like XRD, FTIR, and SEM. The chapter also described the development of a novel AI method for segmenting SEM images named

SCWSO, which is a hybridization between a chaotic method and the optimization algorithm WSO, providing a thorough explanation of its implementation and various evaluations applied to confirm its superiority over other approaches. The outcomes of these experiments and their analysis were discussed in detail in the next chapter, which will focus on confirming the effectiveness and efficiency of the proposed materials and methods demonstrated in chapter IV.

References

[1] M. L. Takeno *et al.*, « A novel CaO-based catalyst obtained from silver croaker (Plagioscion squamosissimus) stone for biodiesel synthesis: Waste valorization and process optimization », *Renew. Energy*, vol. 172, p. 1035-1045, 2021.

[2] B. Aghel, M. Mohadesi, A. Ansari, et M. Maleki, « Pilot-scale production of biodiesel from waste cooking oil using kettle limescale as a heterogeneous catalyst », *Renew. Energy*, vol. 142, p. 207-214, 2019.

[3] M. L. Takeno *et al.*, « A novel CaO-based catalyst obtained from silver croaker (Plagioscion squamosissimus) stone for biodiesel synthesis: Waste valorization and process optimization », *Renew. Energy*, vol. 172, p. 1035-1045, 2021.

[4] A. Attari, A. Abbaszadeh-Mayvan, et A. Taghizadeh-Alisaraei, « Process optimization of ultrasonic-assisted biodiesel production from waste cooking oil using waste chicken eggshell-derived CaO as a green heterogeneous catalyst », *Biomass Bioenergy*, vol. 158, p. 106357, 2022.

[5] S. Niju, K. M. Meera, S. Begum, et N. Anantharaman, « Modification of egg shell and its application in biodiesel production », *J. Saudi Chem. Soc.*, vol. 18, nº 5, p. 702-706, 2014.

[6] V. Kavitha, V. Geetha, et P. J. Jacqueline, « Production of biodiesel from dairy waste scum using eggshell waste », *Process Saf. Environ. Prot.*, vol. 125, p. 279-287, 2019.

[7] Tummala. S. L. V. Ayyarao *et al.*, « War Strategy Optimization Algorithm: A New Effective Metaheuristic Algorithm for Global Optimization », *IEEE Access*, vol. 10, p. 25073-25105, 2022, doi: 10.1109/ACCESS.2022.3153493.

[8] M. A. Khelifa, B. Lekouaghet, et A. Boukabou, « Symmetric chaotic gradient-based optimizer algorithm for efficient estimation of PV parameters », *Optik*, vol. 259, p. 168873, 2022.

[9] S. M. Mirjalili, S. Z. Mirjalili, S. Saremi, et S. Mirjalili, « Sine Cosine Algorithm: Theory, Literature Review, and Application in Designing Bend Photonic Crystal Waveguides », in *Nature-Inspired Optimizers*, vol. 811, S. Mirjalili, J. Song Dong, et A. Lewis, Éd., in Studies in Computational Intelligence, vol. 811. , Cham: Springer International Publishing, 2020, p. 201-217. doi: 10.1007/978-3-030-12127-3_12.

[10] M. Khishe et M. R. Mosavi, « Chimp optimization algorithm », *Expert Syst. Appl.*, vol. 149, p. 113338, 2020.

[11] H. A. Shehadeh, « Chernobyl disaster optimizer (CDO): a novel meta-heuristic method for global optimization », *Neural Comput. Appl.*, vol. 35, nº 15, p. 10733-10749, mai 2023, doi: 10.1007/s00521-023-08261-1.

[12] N. Chopra et M. M. Ansari, « Golden jackal optimization: A novel nature-inspired optimizer for engineering applications », *Expert Syst. Appl.*, vol. 198, p. 116924, 2022.

[13] L. Abualigah, M. Abd Elaziz, P. Sumari, Z. W. Geem, et A. H. Gandomi, « Reptile Search Algorithm (RSA): A nature-inspired meta-heuristic optimizer », *Expert Syst. Appl.*, vol. 191, p. 116158, 2022.

[14] S. Mirjalili, S. M. Mirjalili, et A. Lewis, « Grey wolf optimizer », *Adv. Eng. Softw.*, vol. 69, p. 46-61, 2014.

[15] E. Rodríguez-Esparza *et al.*, « An efficient Harris hawks-inspired image segmentation method », *Expert Syst. Appl.*, vol. 155, p. 113428, 2020.

[16] L. Hou *et al.*, « Image segmentation of intracerebral hemorrhage patients based on enhanced hunger games search optimizer », *Biomed. Signal Process. Control*, vol. 82, p. 104511, 2023.

[17] E. H. Houssein, D. A. Abdelkareem, M. M. Emam, M. A. Hameed, et M. Younan, « An efficient image segmentation method for skin cancer imaging using improved golden jackal optimization algorithm », *Comput. Biol. Med.*, vol. 149, p. 106075, 2022.

[18] Q. Zhang, C. Huang, L. Yang, et Z. Yang, « Salt and pepper noise removal method based on graph signal reconstruction », *Digit. Signal Process.*, vol. 135, p. 103941, 2023.

Chapter V

Results and discussion

V.1. Introduction

As outlined in the previous chapter, various methodologies were employed to meet the thesis objectives, which include developing advanced AI techniques for catalyst analysis, designing effective catalysts, and applying them with suitable feedstocks for biodiesel production.

This chapter presents the outcomes of the experimental procedures, highlighting key findings from each approach. The following sections offer a detailed overview of the results, including the performance of the catalysts, the effectiveness of the AI techniques, and the impact of different feedstocks. Additionally, the chapter discusses the materials, protocols, and experimental setups used to ensure the accuracy and reproducibility of the results.

V.2. Improved Symmetric Chaotic War strategy optimization algorithm Outcomes

Findings of various tests applied to the developed SCWSO approach are emphasized and evaluated in the following subsections.

V.2.1. Results of performance metrics evaluation

Tables 1 to 4 in the annex displayed the average outcomes for fitness, PSNR, SSIM, and FSIM evaluation metrics, where the proposed SCWSO algorithm was compared versus various competing algorithms across multiple threshold values (nth = 5, 7, 9, 12, and 15). To provide a more detailed comparison of SCWSO's performance and efficiency, outcomes of the Friedman test conducted on all metrics are included in Tables V.1 to V.4, with visual representations shown in Figures V.1 to V.4, illustrating the average values of each metric for the different methods. A more accurate and efficient algorithm is indicated by higher mean values in PSNR, SSIM, and FSIM, while a lower mean value is preferable for fitness. We highlight the top-performing results in bold for clarity in each table.

V.2.1.1. Fitness results

Table 1 in the annex displays fitness values for previous mentioned algorithms, evaluated across multiple threshold levels. SCWSO consistently achieved the lowest fitness values, excelling in SEM-2, SEM-3, SEM-5, SEM-6, SEM-8, SEM-9, and SEM-10. Additionally, it displayed the lowest standard deviation in 34 out of 50 cases, underscoring its robustness and reliability. While IGWO performed well in 9 instances, notably in SEM-7, and CDO showed competitive results in 7 instances, SCWSO maintained a clear advantage.

Figure V.1 illustrates that SCWSO's average fitness value (0.247711) was consistently lower than those of the competing algorithms, highlighting its superior performance. The Friedman test results in Table V.1 further validate SCWSO’s effectiveness, ranking it first among all algorithms and confirming its leadership in image analysis.

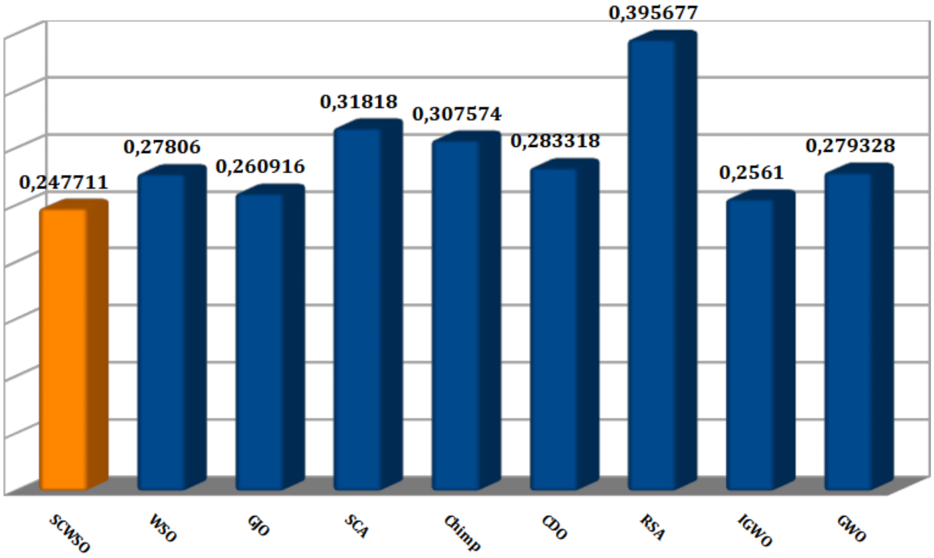

Figure V.32 : Fitness results.

Table V.10 : Friedman test result and ranking of Fitness.

Methods	SCWSO	WSO	GJO	SCA	Chimp	CDO	RSA	IGWO	GWO
FT Results	1.08	4.72	2.82	7.84	7.12	5.28	9.00	2.14	5.00
Rank	1	4	3	8	7	6	9	2	5

V.2.1.2. PSNR results

Findings displayed in Table 2 of the annex indicate that the SCWSO algorithm consistently attained the highest PSNR values across most images and thresholds, performing well in SEM-2, SEM-4, SEM-5, SEM-6, and SEM-10. SCWSO surpassed all other algorithms at each threshold and secured the top three PSNR results in other images. IGWO ranked as the second-best performer, showing strong results in SEM-7 and SEM-9. These findings emphasize SCWSO’s reliability and effectiveness in segmenting distinct CaO-based catalyst SEM images, minimizing distortion, and achieving superior PSNR values.

The Friedman test results, shown in Table V.2, reinforced these findings, placing SCWSO as the top-ranking algorithm for PSNR performance. Figure V.2 illustrates SCWSO's leading average PSNR value of 25.7216, significantly outperforming the second-ranked IGWO with an average of 25.5312. This outcome confirms SCWSO's robust reliability and efficiency in CaO catalyst SEM image segmentation.

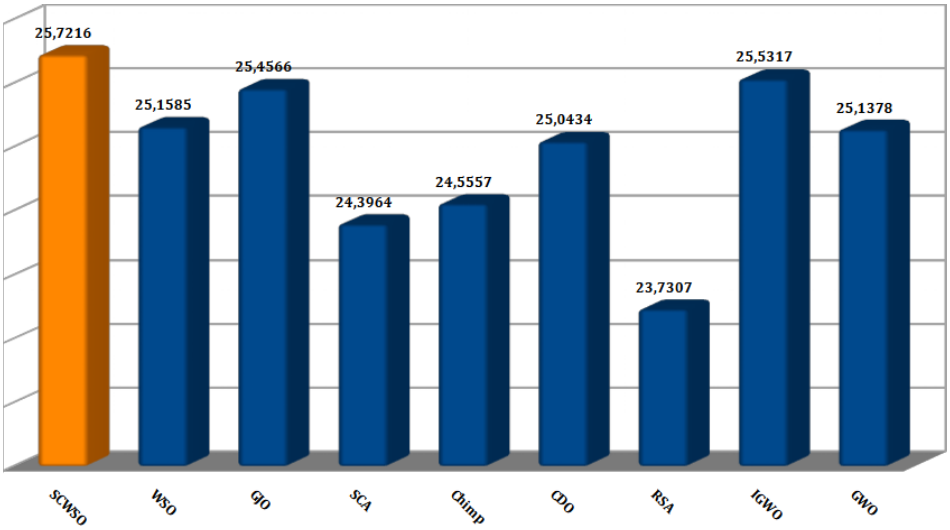

Figure V.33 : PSNR results.

Table V.11 : Friedman test result and ranking of PSNR.

Methods	SCWSO	WSO	GJO	SCA	Chimp	CDO	RSA	IGWO	GWO
FT Results	1.20	4.66	3.20	7.92	7.24	5.42	8.40	2.32	4.64
Rank	1	5	3	8	7	6	9	2	4

V.2.1.3. SSIM results

Table 3, stated in the annex, depicts SSIM results for images segmented using SCWSO and other methods. SCWSO consistently has the highest SSIM ratings, with particular success in SEM-2, SEM-5, SEM-9, and SEM-10. The highest SSIM value was obtained at SEM-9 with a threshold of 15, confirming SCWSO's resilience and efficacy in segmenting CaO-based catalyst SEM images. While IGWO showed strong performance in SEM-3 and SEM-7 at specific thresholds, and CDO and GJO achieved high values in certain cases, SCWSO remained the top performer overall.

Figure V.3 underscores SCWSO's leading average SSIM score of 0.86986, with IGWO and GJO following. The Friedman test results in Table V.3 further validate SCWSO's efficiency, ranking it first among the evaluated methods. These findings affirm SCWSO's superiority in delivering high-quality segmentation for CaO catalyst SEM images.

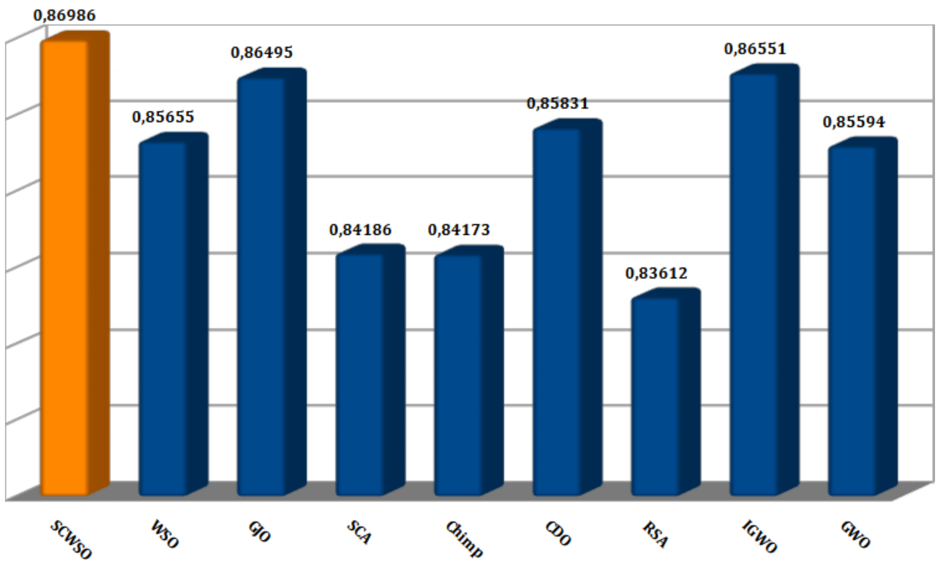

Figure V.34 : SSIM results.

Table V.12 : Friedman test result and ranking of SSIM.

Methods	SCWSO	WSO	GJO	SCA	Chimp	CDO	RSA	IGWO	GWO
FT Results	1.30	5.20	2.80	7.78	7.46	4.66	8.18	2.50	5.12
Rank	1	6	3	8	7	4	9	2	5

V.2.1.4. FSIM results

Table 4 lists in the annex depicts FSIM statistics for CaO-based catalyst segmentation with various approaches. The SCWSO algorithm consistently produced the highest FSIM values, especially in SEM-1, SEM-3, SEM-4, SEM-5, SEM-6, and SEM-10, where it outscored almost all approaches at each threshold. Except for GJO, which performed well in SEM-7 at a threshold of 7, SCWSO outperformed all other algorithms by maintaining great image realism and effectively segmenting SEM images.

Figure V.4 further illustrates SCWSO's superior performance, with an average FSIM value of 0.90809, outperforming IGWO. The Friedman test outcomes highlighted in Table V.4 confirm SCWSO's top rank for FSIM, demonstrating its effectiveness and reliability in SEM image segmentation.

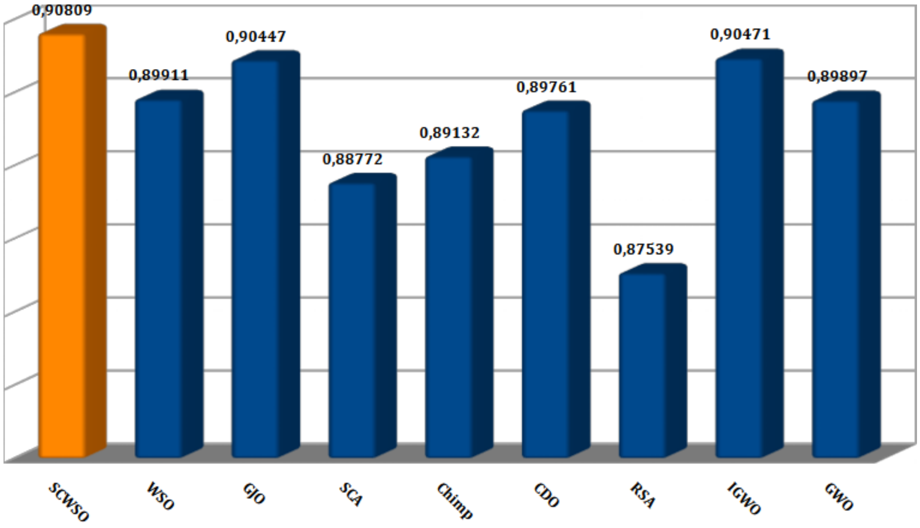

Figure V.35 : FSIM results.

Table V.13 : Friedman test result and ranking of FSIM.

Methods	SCWSO	WSO	GJO	SCA	Chimp	CDO	RSA	IGWO	GWO
FT Results	1.20	4.66	3.20	7.92	7.24	5.42	8.40	2.32	4.64
Rank	1	5	3	8	7	6	9	2	4

V.2.2. Wilcoxon test Results

Wilcoxon test was employed to evaluate SCWSO's performance in PSNR and SSIM to those of other methods. The rank-sum test uses P-values to assess statistical significance, with "++" indicating that SCWSO outperforms the comparison method and "--" indicating that the performance is similar or worse. The symbols "++" and "--" are used to provide clarity.

This test evaluated various algorithms, including SCWSO, WSO, GJO, SCA, Chimp, RSA, IGWO, and GWO, to assess their performance in image segmentation. The findings revealed that SCWSO consistently outperformed the other approaches, with Tables 4 and 5 presented in the annex, showing nearly all comparisons yielding significant results ($p < 0.05$) in 48 to 50 cases. These primary conclusions from Tables 4 and 5 indicate that SCWSO is exceptionally well-suited for segmenting CaO-based catalyst SEM images, providing superior quality over comparable algorithms. The results underscore a significant performance gap between SCWSO and other methods in the field of image segmentation.

V.2.3. Performance Analysis of Various WSO Algorithm Variants

Tables V.5–V.8 showcase the performance of different variants of the War Strategy Optimization (WSO) algorithm applied to SEM-1, SEM-2, and SEM-7 images across various thresholds. Among the tested variants, SCWSO, which leverages a symmetric chaotic approach, consistently delivered superior results across all evaluation metrics, with notable success in SEM-1 and SEM-7. By comparison, CWSO, which integrates certain chaotic techniques, and MWSO1, utilizing only mutation, showed moderate effectiveness. The unmodified WSO algorithm, however, yielded the lowest performance.

These findings are further substantiated by the Friedman test, which ranked SCWSO at the top across all metrics, with MWSO1 and CWSO following in order of effectiveness. This analysis highlights SCWSO's enhanced capability and robustness in optimizing CaO-based catalyst SEM image segmentation relative to its counterparts.

Table V.14 : Fitness results for different variance applied on WSO.

Images	nTh	Metrics	SCWSO	CWSO	MWSO1	WSO
SEM-1	5	Mean	**2.602e-01**	2.658e-01	2.633e-01	2.881e-01
		Std	**1.115e-03**	7.875e-03	1.807e-02	3.922e-02
	7	Mean	**1.465e-01**	1.676e-01	1.488e-01	1.808e-01
		Std	**5.453e-03**	1.615e-02	1.010e-02	2.826e-02
	9	Mean	**9.952e-02**	1.267e-01	1.055e-01	1.294e-01
		Std	**4.940e-03**	1.683e-02	9.086e-03	1.745e-02
	12	Mean	**6.559e-02**	8.906e-02	7.009e-02	8.766e-02
		Std	**4.888e-03**	1.628e-02	7.699e-03	1.063e-02
	15	Mean	**4.945e-02**	6.182e-02	4.963e-02	6.759e-02
		Std	7.164e-03	1.179e-02	**5.227e-03**	1.092e-02
SEM-2	5	Mean	5.007e-01	5.176e-01	**5.006e-01**	5.247e-01
		Std	7.355e-04	1.349e-02	**5.191e-04**	1.491e-02
	7	Mean	**2.796e-01**	3.085e-01	2.800e-01	3.248e-01
		Std	5.961e-03	2.917e-02	**4.377e-03**	3.150e-02
	9	Mean	**1.821e-01**	2.262e-01	1.877e-01	2.161e-01
		Std	**9.779e-03**	2.464e-02	1.622e-02	2.227e-02
	12	Mean	**1.168e-01**	1.488e-01	1.203e-01	1.424e-01
		Std	**7.766e-03**	1.872e-02	1.325e-02	2.069e-02
	15	Mean	**8.501e-02**	1.134e-01	8.661e-02	1.052e-01
		Std	**8.275e-03**	1.575e-02	9.084e-03	1.066e-02
SEM-7	5	Mean	**2.597e-01**	2.780e-01	2.597e-01	2.883e-01
		Std	1.041e-03	3.077e-02	**5.010e-04**	3.104e-02
	7	Mean	**1.524e-01**	1.717e-01	1.546e-01	1.886e-01
		Std	**9.458e-03**	1.764e-02	1.269e-02	2.837e-02
	9	Mean	1.101e-01	1.217e-01	**1.094e-01**	1.395e-01
		Std	1.113e-02	1.462e-02	**1.010e-02**	2.930e-02
	12	Mean	**7.122e-02**	9.691e-02	7.710e-02	1.075e-01
		Std	**6.031e-03**	2.152e-02	8.853e-03	2.050e-02
	15	Mean	**5.514e-02**	7.337e-02	5.674e-02	8.048e-02
		Std	**5.895e-03**	1.557e-02	7.888e-03	1.944e-02
		FT mean	1.13	3.27	1.87	3.73
		Rank	1	3	2	4

Table V.15 : PSNR results for different variances applied on WSO.

Images	nTh	Metrics	SCWSO	CWSO	MWSO1	WSO
SEM-1	5	Mean	**2.282e+01**	2.271e+01	2.278e+01	2.280e+01
		Std	**1.089e-01**	4.934e-01	1.561e-01	7.607e-01
	7	Mean	**2.611e+01**	2.581e+01	2.594e+01	2.528e+01
		Std	**3.807e-01**	9.029e-01	5.116e-01	1.039e+00
	9	Mean	**2.798e+01**	2.704e+01	2.773e+01	2.713e+01
		Std	**6.033e-01**	1.283e+00	6.488e-01	1.009e+00
	12	Mean	**3.029e+01**	2.898e+01	2.988e+01	2.902e+01
		Std	1.075e+00	1.375e+00	**1.013e+00**	1.048e+00
	15	Mean	**3.200e+01**	3.103e+01	3.158e+01	3.048e+01
		Std	**1.012e+00**	1.228e+00	1.203e+00	1.128e+00
SEM-2	5	Mean	2.247e+01	2.222e+01	**2.247e+01**	2.214e+01
		Std	3.132e-02	2.474e-01	**1.973e-02**	2.448e-01
	7	Mean	2.463e+01	2.428e+01	**2.466e+01**	2.408e+01
		Std	1.116e-01	3.757e-01	**9.479e-02**	4.057e-01
	9	Mean	**2.642e+01**	2.559e+01	2.631e+01	2.576e+01
		Std	**2.722e-01**	4.636e-01	4.006e-01	4.803e-01
	12	Mean	**2.821e+01**	2.736e+01	2.818e+01	2.770e+01
		Std	**3.304e-01**	6.145e-01	4.762e-01	6.670e-01
	15	Mean	**2.951e+01**	2.859e+01	2.942e+01	2.882e+01
		Std	5.178e-01	5.298e-01	**4.854e-01**	5.202e-01
SEM-7	5	Mean	2.266e+01	**2.307e+01**	2.268e+01	2.272e+01
		Std	**2.619e-01**	1.280e+00	3.160e-01	1.441e+00
	7	Mean	**2.626e+01**	2.617e+01	2.625e+01	2.541e+01
		Std	**6.292e-01**	1.121e+00	7.583e-01	1.663e+00
	9	Mean	**2.834e+01**	2.807e+01	2.816e+01	2.767e+01
		Std	9.651e-01	1.210e+00	**8.172e-01**	1.234e+00
	12	Mean	**3.053e+01**	2.925e+01	3.023e+01	2.884e+01
		Std	**7.871e-01**	1.747e+00	9.255e-01	1.457e+00
	15	Mean	**3.196e+01**	3.052e+01	3.193e+01	3.043e+01
		Std	**8.560e-01**	1.792e+00	9.867e-01	2.000e+00
		FT mean	1.33	3.27	2.00	3.4
		Rank	1	3	2	4

Table V.16 : SSIM results for different variance applied on WSO.

Images	nTh	Metrics	SCWSO	CWSO	MWSO1	WSO
SEM-1	5	Mean	**7.762e-01**	7.711e-01	7.745e-01	7.676e-01
		Std	**2.510e-03**	1.330e-02	6.024e-03	2.432e-02
	7	Mean	**8.619e-01**	8.498e-01	8.591e-01	8.376e-01
		Std	**6.939e-03**	1.832e-02	9.498e-03	2.596e-02
	9	Mean	**8.996e-01**	8.767e-01	8.938e-01	8.782e-01
		Std	**7.879e-03**	2.104e-02	1.029e-02	1.837e-02
	12	Mean	**9.317e-01**	9.091e-01	9.270e-01	9.110e-01
		Std	1.278e-02	2.025e-02	**1.101e-02**	1.406e-02
	15	Mean	**9.483e-01**	9.357e-01	9.453e-01	9.294e-01
		Std	**1.053e-02**	1.457e-02	1.087e-02	1.447e-02
SEM-2	5	Mean	8.306e-01	8.170e-01	**8.312e-01**	8.120e-01
		Std	1.494e-03	1.574e-02	**1.061e-03**	1.676e-02
	7	Mean	8.756e-01	8.654e-01	**8.760e-01**	8.609e-01
		Std	2.351e-03	1.209e-02	**1.910e-03**	1.292e-02
	9	Mean	**9.108e-01**	8.920e-01	9.087e-01	8.961e-01
		Std	**4.071e-03**	1.256e-02	7.628e-03	9.711e-03
	12	Mean	**9.367e-01**	9.222e-01	9.356e-01	9.263e-01
		Std	**4.849e-03**	1.043e-02	6.919e-03	1.169e-02
	15	Mean	**9.498e-01**	9.366e-01	9.496e-01	9.409e-01
		Std	**5.179e-03**	8.323e-03	6.178e-03	5.958e-03
SEM-7	5	Mean	7.045e-01	**7.216e-01**	7.050e-01	7.038e-01
		Std	**1.285e-02**	6.693e-02	1.559e-02	7.073e-02
	7	Mean	**8.422e-01**	8.391e-01	8.421e-01	8.100e-01
		Std	**1.964e-02**	3.787e-02	2.462e-02	6.528e-02
	9	Mean	**8.940e-01**	8.869e-01	8.911e-01	8.753e-01
		Std	2.379e-02	3.287e-02	**1.963e-02**	3.309e-02
	12	Mean	**9.337e-01**	9.025e-01	9.271e-01	8.975e-01
		Std	**1.155e-02**	4.335e-02	1.547e-02	3.605e-02
	15	Mean	**9.493e-01**	9.246e-01	9.481e-01	9.204e-01
		Std	**9.253e-03**	3.806e-02	1.287e-02	3.969e-02
		FT mean	1.27	3.2	1.87	3.67
		Rank	1	3	2	4

Table V.17 : FSIM results for different variance applied on WSO.

Images	nTh	Metrics	SCWSO	CWSO	MWSO1	WSO
SEM-1	5	Mean	**8.421e-01**	8.385e-01	8.411e-01	8.345e-01
		Std	**2.092e-03**	1.179e-02	5.073e-03	1.798e-02
	7	Mean	**8.959e-01**	8.895e-01	8.924e-01	8.806e-01
		Std	**7.244e-03**	1.657e-02	8.697e-03	1.697e-02
	9	Mean	**9.219e-01**	9.085e-01	9.186e-01	9.099e-01
		Std	**9.112e-03**	1.946e-02	9.944e-03	1.546e-02
	12	Mean	**9.455e-01**	9.312e-01	9.416e-01	9.303e-01
		Std	1.375e-02	1.747e-02	**1.265e-02**	1.421e-02
	15	Mean	**9.601e-01**	9.515e-01	9.558e-01	9.463e-01
		Std	**1.195e-02**	1.365e-02	1.276e-02	1.320e-02
SEM-2	5	Mean	8.774e-01	8.601e-01	**8.774e-01**	8.534e-01
		Std	7.654e-04	1.916e-02	**6.006e-04**	1.936e-02
	7	Mean	**9.032e-01**	8.963e-01	9.022e-01	8.936e-01
		Std	**2.612e-03**	1.184e-02	3.269e-03	1.363e-02
	9	Mean	**9.329e-01**	9.200e-01	9.313e-01	9.218e-01
		Std	5.924e-03	9.323e-03	**5.897e-03**	8.857e-03
	12	Mean	**9.531e-01**	9.401e-01	9.506e-01	9.451e-01
		Std	**5.151e-03**	1.032e-02	6.634e-03	9.461e-03
	15	Mean	**9.616e-01**	9.502e-01	9.611e-01	9.546e-01
		Std	**4.811e-03**	7.407e-03	5.455e-03	4.850e-03
SEM-7	5	Mean	8.130e-01	**8.196e-01**	8.130e-01	8.195e-01
		Std	**5.152e-03**	1.825e-02	6.082e-03	2.326e-02
	7	Mean	8.842e-01	**8.842e-01**	8.827e-01	8.700e-01
		Std	**1.401e-02**	2.427e-02	1.500e-02	3.206e-02
	9	Mean	**9.183e-01**	9.142e-01	9.156e-01	9.091e-01
		Std	1.933e-02	2.358e-02	**1.503e-02**	2.335e-02
	12	Mean	**9.454e-01**	9.265e-01	9.418e-01	9.233e-01
		Std	**1.115e-02**	2.885e-02	1.434e-02	2.344e-02
	15	Mean	**9.580e-01**	9.412e-01	9.580e-01	9.407e-01
		Std	**9.870e-03**	2.669e-02	1.168e-02	2.896e-02
		FT mean	1.27	3.00	2.13	3.6
		Rank	1	3	2	4

V.2.4. Results of Noise Images

Figure V.5 shows outcomes of the integration of salt and pepper noise into SEM-1, SEM-2, and SEM-7 images, which aim to test SCWSO's resistance to image deterioration.

The segmented outputs produced by SCWSO were compared to those of CWSO, WSO, and MWSO1 using MSE and PSNR metrics, as demonstrated in Tables V.9 and V.10. Findings revealed that SCWSO consistently outperformed the other algorithms in terms of MSE and PSNR values. The Friedman test confirmed these findings, rating SCWSO as the best performer, with MWSO1 and CWSO trailing behind in effectiveness.

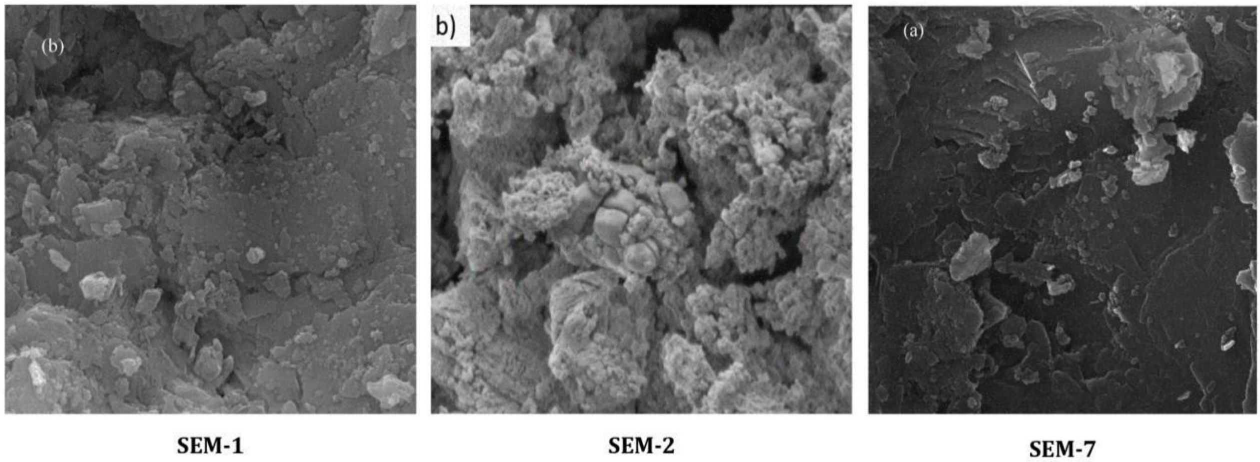

Figure V.36 : Noise effect on various SEM images.

Table V.18 : MSE results for noises images.

Images	nTh	Metrics	SCWSO	CWSO	MWSO1	WSO
SEM-1	5	Mean	3.529e+02	**3.401e+02**	3.484e+02	3.671e+02
		Std	**1.073e+01**	3.564e+01	1.299e+01	7.606e+01
	7	Mean	**1.627e+02**	1.826e+02	1.677e+02	1.926e+02
		Std	1.581e+01	3.793e+01	**1.387e+01**	5.054e+01
	9	Mean	1.129e+02	1.219e+02	**1.128e+02**	1.335e+02
		Std	**1.445e+01**	2.877e+01	1.949e+01	2.921e+01
	12	Mean	**6.578e+01**	8.470e+01	6.589e+01	8.799e+01
		Std	**1.429e+01**	3.539e+01	1.595e+01	3.708e+01
	15	Mean	**4.259e+01**	6.125e+01	4.771e+01	6.207e+01
		Std	**9.346e+00**	2.476e+01	1.263e+01	2.281e+01
SEM-2	5	Mean	**3.580e+02**	3.816e+02	3.588e+02	3.792e+02
		Std	**4.435e+00**	2.524e+01	8.895e+00	2.293e+01
	7	Mean	**2.169e+02**	2.395e+02	2.178e+02	2.394e+02
		Std	4.839e+00	2.612e+01	**3.994e+00**	2.157e+01
	9	Mean	**1.441e+02**	1.649e+02	1.464e+02	1.734e+02
		Std	**9.771e+00**	1.593e+01	1.074e+01	1.743e+01
	12	Mean	**9.120e+01**	1.197e+02	9.853e+01	1.168e+02
		Std	**9.287e+00**	1.609e+01	1.055e+01	1.226e+01
	15	Mean	**6.982e+01**	9.043e+01	7.259e+01	8.235e+01
		Std	**5.939e+00**	1.302e+01	7.520e+00	1.069e+01
SEM-7	5	Mean	3.612e+02	3.628e+02	**3.581e+02**	4.167e+02
		Std	6.777e+01	7.801e+01	**5.867e+01**	1.726e+02
	7	Mean	**1.602e+02**	1.887e+02	1.706e+02	2.083e+02
		Std	**2.563e+01**	5.020e+01	5.067e+01	1.163e+02
	9	Mean	**1.015e+02**	1.160e+02	1.117e+02	1.405e+02
		Std	**2.294e+01**	4.104e+01	2.767e+01	6.246e+01
	12	Mean	6.197e+01	7.120e+01	**6.009e+01**	9.654e+01
		Std	1.987e+01	4.041e+01	**1.859e+01**	5.792e+01
	15	Mean	**4.345e+01**	4.935e+01	5.168e+01	5.327e+01
		Std	**1.208e+01**	1.611e+01	2.558e+01	2.496e+01
		FT mean	1,33	3.07	1,87	3,73
		Rank	1	3	2	4

Table V.19 : PSNR results for noises images.

Images	nTh	Metrics	SCWSO	CWSO	MWSO1	WSO
SEM-1	5	Mean	2.266e+01	**2.284e+01**	2.271e+01	2.256e+01
		Std	**1.310e-01**	4.481e-01	1.631e-01	8.392e-01
	7	Mean	**2.604e+01**	2.560e+01	2.590e+01	2.540e+01
		Std	3.951e-01	8.622e-01	**3.365e-01**	9.892e-01
	9	Mean	2.764e+01	2.739e+01	**2.767e+01**	2.698e+01
		Std	**6.086e-01**	1.020e+00	7.650e-01	9.651e-01
	12	Mean	3.005e+01	2.914e+01	**3.006e+01**	2.896e+01
		Std	**9.564e-01**	1.537e+00	1.015e+00	1.487e+00
	15	Mean	**3.193e+01**	3.052e+01	3.147e+01	3.043e+01
		Std	**8.864e-01**	1.443e+00	1.053e+00	1.376e+00
SEM-2	5	Mean	**2.259e+01**	2.232e+01	2.258e+01	2.235e+01
		Std	**5.254e-02**	2.786e-01	1.016e-01	2.572e-01
	7	Mean	**2.477e+01**	2.436e+01	2.475e+01	2.436e+01
		Std	9.633e-02	4.290e-01	**7.943e-02**	3.777e-01
	9	Mean	**2.655e+01**	2.598e+01	2.649e+01	2.576e+01
		Std	**2.860e-01**	4.086e-01	3.120e-01	4.402e-01
	12	Mean	**2.855e+01**	2.738e+01	2.822e+01	2.748e+01
		Std	**4.217e-01**	5.560e-01	4.662e-01	4.441e-01
	15	Mean	**2.971e+01**	2.861e+01	2.954e+01	2.901e+01
		Std	**3.701e-01**	6.047e-01	4.273e-01	5.777e-01
SEM-7	5	Mean	2.261e+01	**2.264e+01**	2.264e+01	2.226e+01
		Std	6.851e-01	1.018e+00	**6.463e-01**	1.699e+00
	7	Mean	**2.614e+01**	2.551e+01	2.598e+01	2.540e+01
		Std	**7.153e-01**	1.101e+00	1.222e+00	1.880e+00
	9	Mean	**2.817e+01**	2.771e+01	2.778e+01	2.702e+01
		Std	**9.722e-01**	1.370e+00	1.105e+00	1.759e+00
	12	Mean	3.038e+01	3.000e+01	**3.052e+01**	2.876e+01
		Std	**1.195e+00**	1.694e+00	1.223e+00	1.906e+00
	15	Mean	**3.190e+01**	3.140e+01	3.133e+01	3.119e+01
		Std	**1.145e+00**	1.319e+00	1.582e+00	1.589e+00
		FT mean	1,47	2,87	1,87	3,8
		Rank	1	3	2	4

V.2.5. Convergence curves

Figures V.6 and V.7 present convergence curves for SEM-1 and SEM-2 images, providing a detailed comparison of each algorithm's performance over time. SCWSO demonstrated a clear advantage, outperforming other algorithms, including WSO, SCA, Chimp, CDO, GJO, RSA, IGWO, and GWO, not only in achieving the optimal solution but also in the speed of convergence. SCWSO consistently reached the optimal solution in fewer iterations, highlighting its efficiency and effectiveness in solving complex segmentation tasks.

This rapid convergence occurred consistently across all evaluated threshold values, proving SCWSO's versatility and robust performance in a variety of circumstances. SCWSO's fast convergence highlights its ability to provide high accuracy and computational efficiency, making it ideal for real-time and resource-intensive image segmentation applications. These findings highlight SCWSO's ability to provide superior results with faster processing speeds than standard algorithms.

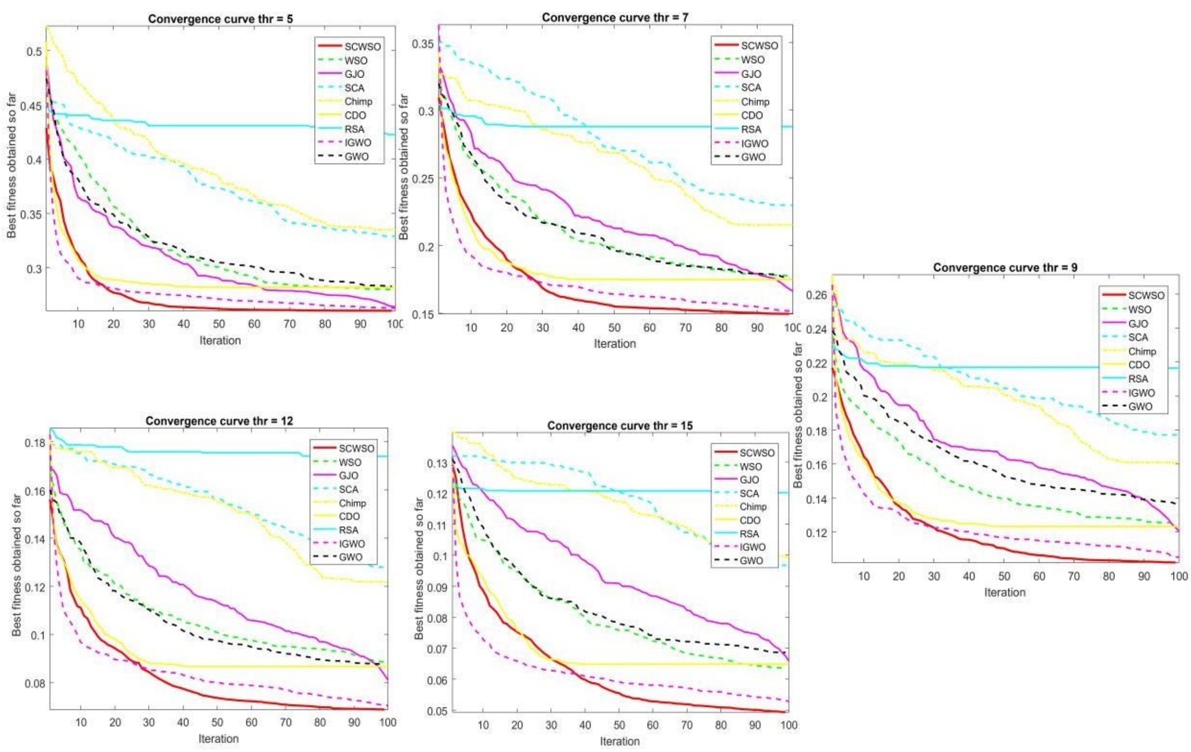

Figure V.37 : Convergence Curves for SEM-1 at all thresholds.

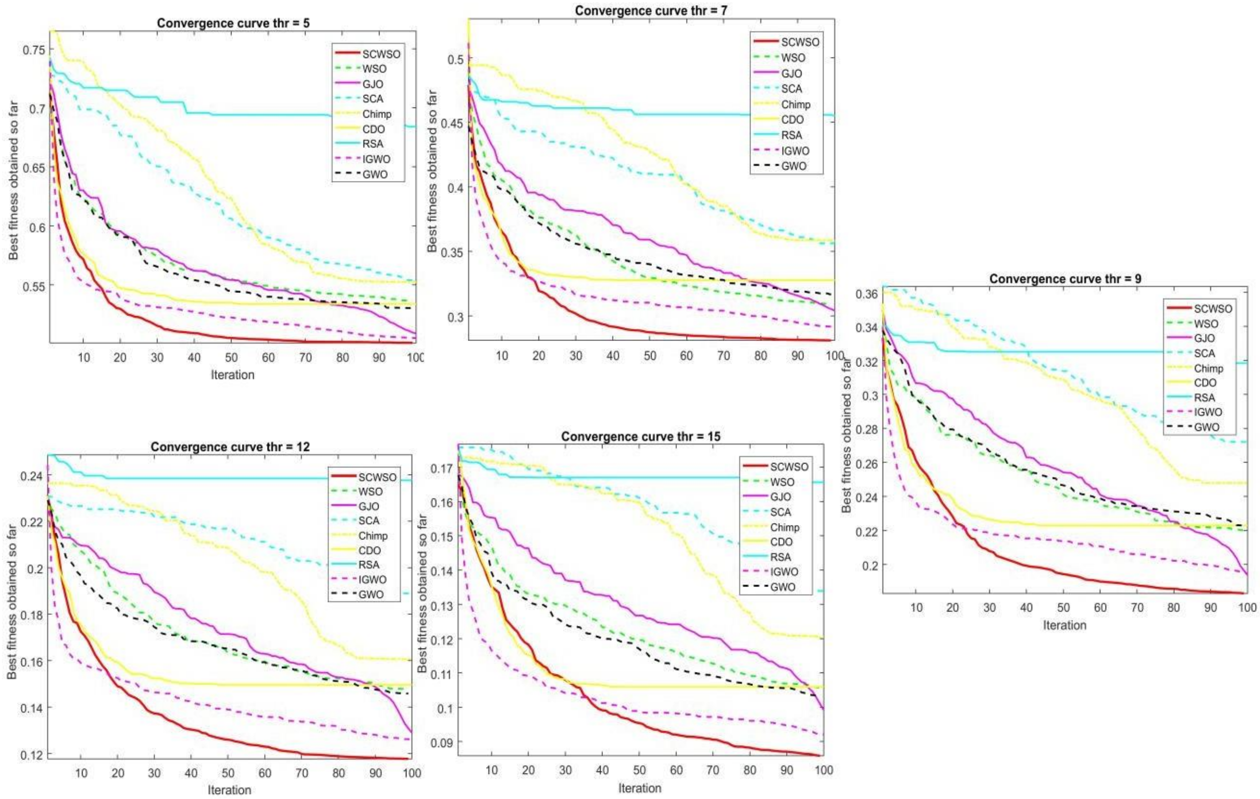

Figure V.38 : Convergence Curves for SEM- 2 at all thresholds.

V.2.6. Images Colormap

Figures V.8–V.10 display colormap images of SEM-7, SEM-1, and SEM-2 segmented at thresholds 5, 7, 9, 12, and 15 employing the SCWSO algorithm. This visualization effectively illustrates SCWSO's capability to improve image quality and accurately delineate various regions, with higher thresholds revealing finer details through distinct color differentiation that emphasizes specific areas and particles. In SEM-7 (pre-calcination), the surface appears smooth and lacks prominent features, particularly at higher thresholds of 12 and 15, where minimal structural variation is observed. Conversely, SEM-1 (post-calcination) displays a notably rough texture due to CO_2 loss, with diverse colors marking varying particle sizes that confirm morphological changes resulting from calcination. On the other hand, SEM-2, dispersed CaO-based catalysts derived from Silver Croaker, showcases unique microparticles with distinct size and structural differences from SEM-1, influencing properties such as surface area and porosity. Lower thresholds, such as 5, reveal more intricate details in this sample. Overall, these results underscore SCWSO's proficiency in segmenting SEM images, enabling the identification of material and surface changes across different raw materials and calcination conditions

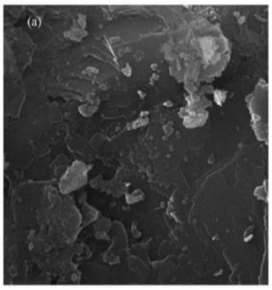	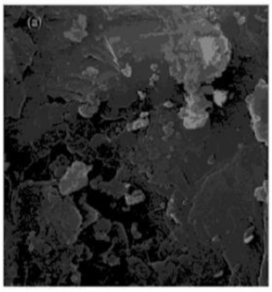	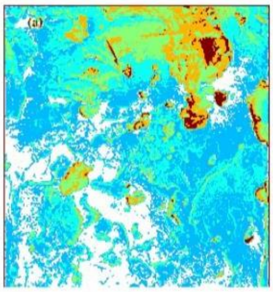	SEM-7 Uncalcined kettle limescale Segmentation and coloromap Number of thresholds : 5
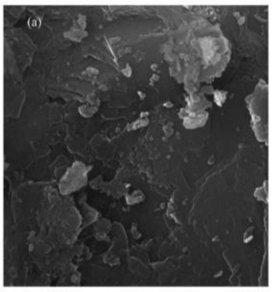	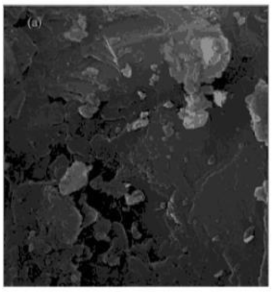	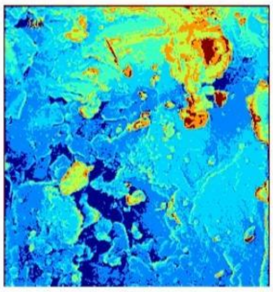	SEM-7 Uncalcined kettle limescale Segmentation and coloromap Number of thresholds : 7
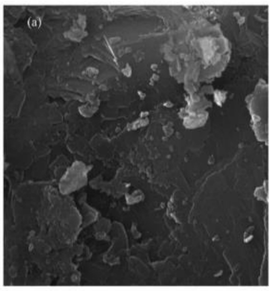	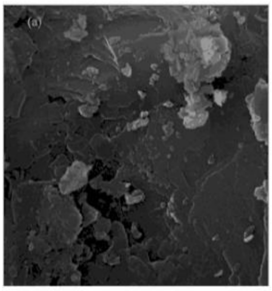	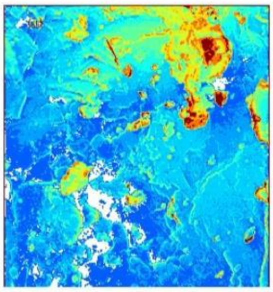	SEM-7 Uncalcined kettle limescale Segmentation and coloromap Number of thresholds : 9
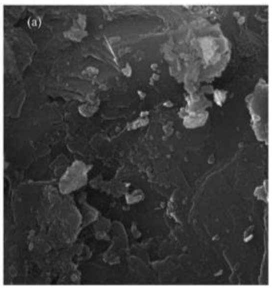	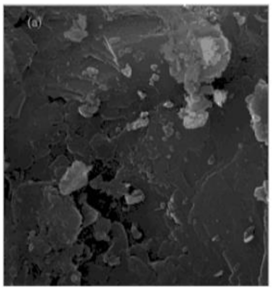	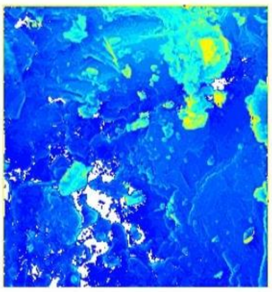	SEM-7 Uncalcined kettle limescale Segmentation and coloromap Number of thresholds : 12
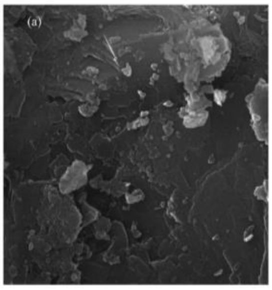	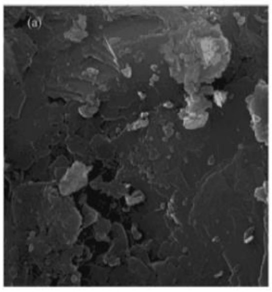	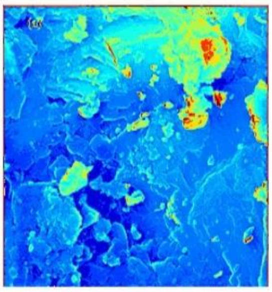	SEM-7 Uncalcined kettle limescale Segmentation and coloromap Number of thresholds : 15

Figure V.39 : Coloromap images for SEM- 7 at all thresholds.

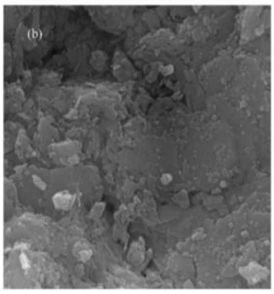	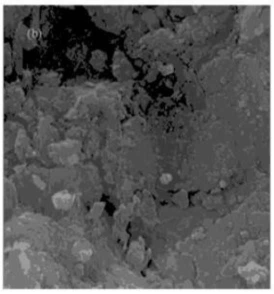	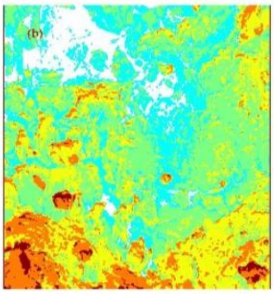	SEM-1 calcined kettle limescale Segmentation and coloromap Number of thresholds : 5
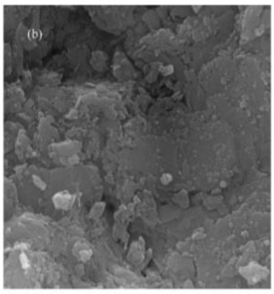	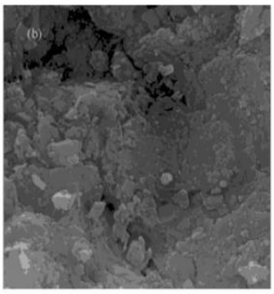	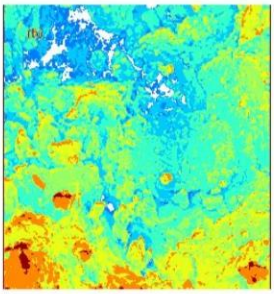	SEM-1 Calcined kettle lime scale Segmentation and coloromap Number of thresholds : 7
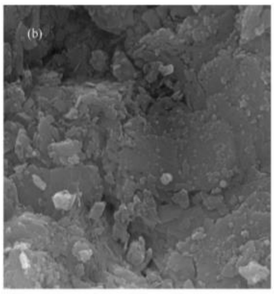	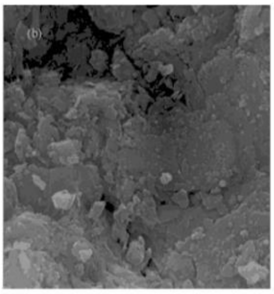	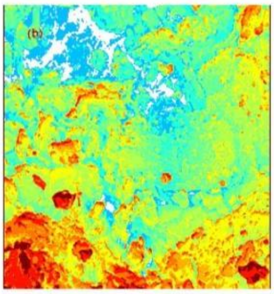	SEM-1 Calcined kettle lime scale Segmentation and coloromap Number of thresholds : 9
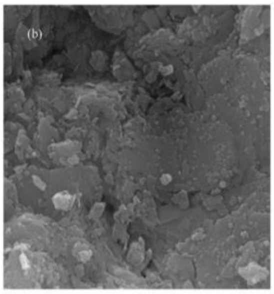	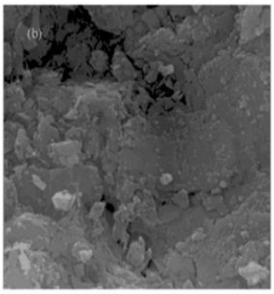	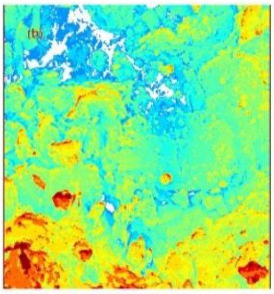	SEM-1 Calcined kettle lime scale Segmentation and coloromap Number of thresholds : 12
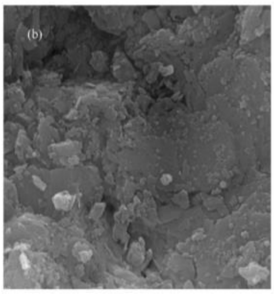	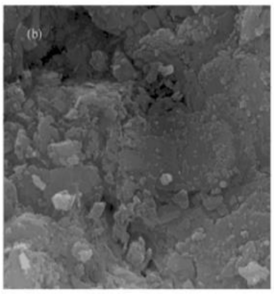	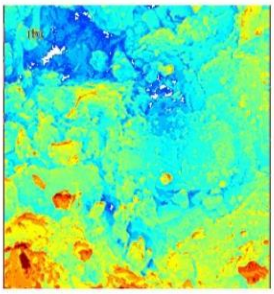	SEM-1 Calcined kettle lime scale Segmentation and coloromap Number of thresholds : 15

Figure V.40 : Coloromap images for SEM- 1 at all thresholds

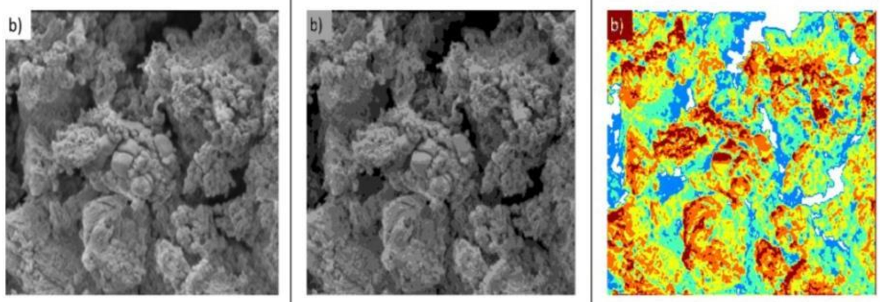

SEM- 2
CaO-based catalyst (silver croaker)
Segmentation and coloromap
Number of thresholds : 5

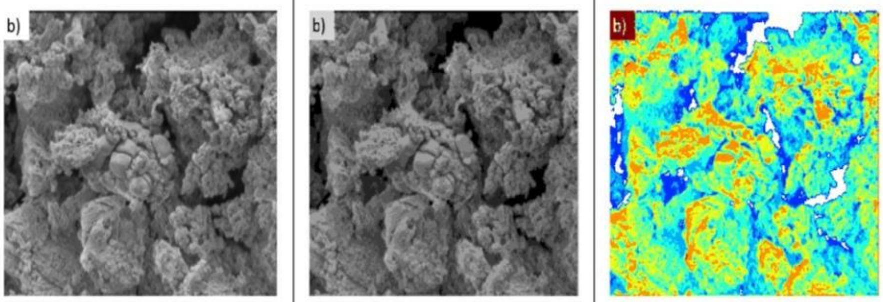

SEM- 2
CaO-based catalyst (silver croaker)
Segmentation and coloromap
Number of thresholds : 7

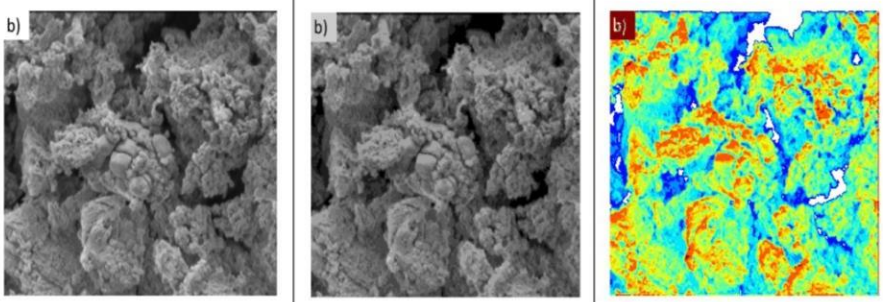

SEM- 2
CaO-based catalyst (silver croaker)
Segmentation and coloromap
Number of thresholds : 9

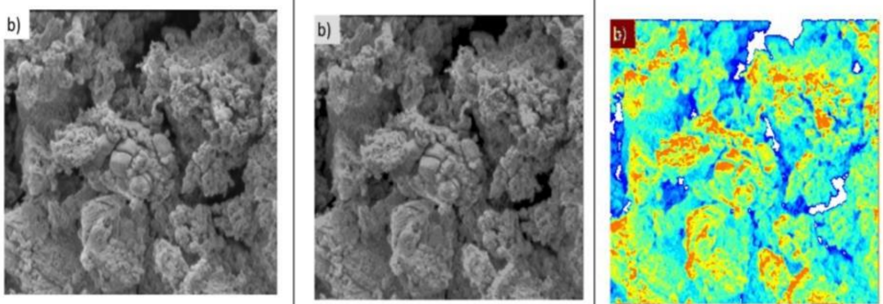

SEM- 2
CaO-based catalyst (silver croaker)
Segmentation and coloromap
Number of thresholds : 12

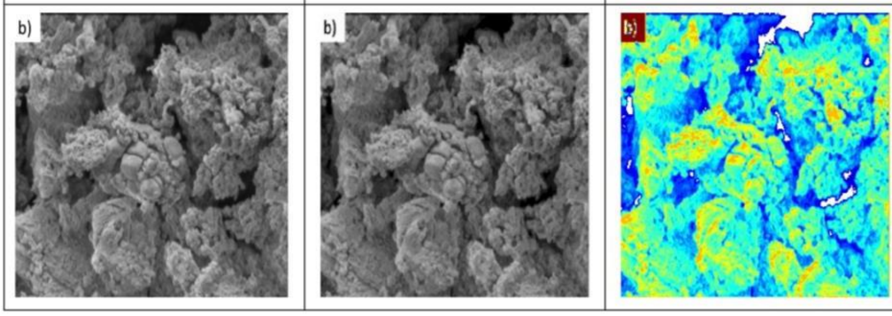

SEM- 2
CaO-based catalyst (silver croaker)
Segmentation and coloromap
Number of thresholds : 15

Figure V.41 : Coloromap images for SEM- 2 at all thresholds.

V.3. Characterization of Calcium Oxide Synthesized from Cuttlefish bones

The characterization of calcium oxide derived from cuttlefish is the main topic of this section. The purpose of the analysis is to assess the synthetic material's structural, chemical, and physical characteristics. As stated in Chapter 4, a number of methods, including Fourier transform infrared spectroscopy (FTIR), scanning electron microscopy (SEM), and X-ray diffraction (XRD), will be used to highlight the material's potential uses across a range of industries by offering in-depth information about its composition, morphology, and functional groups.

V.3.1. Fourier transform infrared spectroscopy (FTIR)

Qualitative FTIR analysis of the uncalcined and calcined waste material was performed to obtain more information about the chemical properties of the catalysts. Figure V.11 shows that the spectra of the dried wastes of cuttlefish bones correspond to $CaCO_3$. The relatively low intensity band at about 3612 cm^{-1} is attributed to the O-H stretching vibration of the physiosorbed moisture on the $CaCO_3$ surface, whereas the peak at 2328 cm^{-1} can be attributed to the carbon dioxide adsorbed from the atmosphere. The rest of the characteristic peaks are due to the different vibration modes of the carbonate group (CO_3^{2-}): the asymmetric C–O stretching vibration at the strong absorption peak at 1422 cm^{-1}, the out-of-plane C-O bending at 876 cm^{-1}, and the in-plane C-O bending vibration at 725 cm^{-1}. Infrared spectroscopy investigations not only provide information about the functional groups in samples but may also be applied to identify the crystal structure of calcium carbonate [1]. The characteristics and positions of the carbonate bands in the spectrum of the wastes match those of calcite, suggesting that the calcium carbonate from the cuttlefish bones is predominantly calcite crystals [2].

On the other hand, the FTIR spectra of the calcined cuttlefish bones displayed somewhat similar types of characteristic peaks as those before calcination, owing to the presence of similar types of functional groups. The sharp absorption peak at 3640 cm^{-1} is associated with the OH bending vibration in $Ca(OH)_2$, which may be produced by the adsorption of water molecules on the surface of Calcium oxide [3]. The stretching vibration bands of (CO_3^{2-}) group at 1422 cm^{-1} and 872 cm^{-1} are due to the chemisorption of CO_2 from the atmosphere, which carbonates CaO [4]. The disappearance of the absorption calcite peak at 724 cm^{-1} suggests successful conversion of $CaCO_3$ presented in cuttlefish waste to CaO by the calcination process under high temperature 900°C.

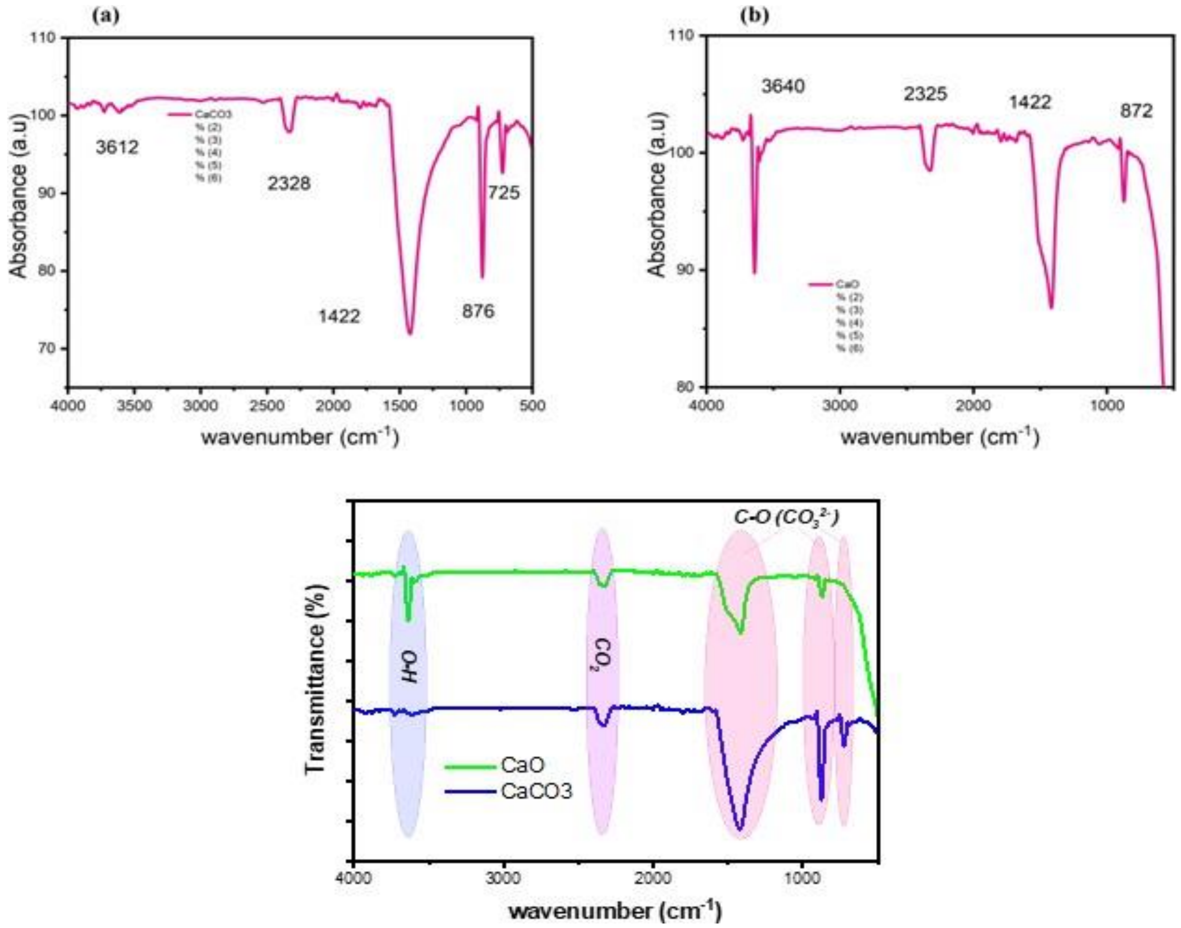

Figure V.42 : FT-IR results of (a) Uncalcined Cuttlefish bones and (b) Calcined Cuttelefish bones.

V.3.2. X-Ray Diffraction analysis

The phase and crystal structure of Cuttlefish bones before and after calcination were determined by X-ray diffraction (XRD) analyses. The XRD patterns mentioned in Figure V.12 support FTIR results, where the calcium wastes are mainly composed of calcium carbonate calcite (CaCO3), which was mineralized to calcium oxide (CaO) under calcination. From Figure V.12(a), the XRD spectra of the uncalcined wastes exhibit diffraction signals at 2θ: 23.06; 29.33; 35.93; 39.4; 43.09; 47.09; 47.46; 48.49; 57.4; 60.61; 64.63; 65.57; 70.17; and 72.97, which corresponds to the crystal plane of hexagonal calcite (JCPDS database No. 98-015-8257); (012), (104), (110), (113), (202), (024), (018), (116), (122),(214),(030), (0012),(0210), and (128) respectively.

Furthermore, no diffraction peaks were identified for other phases, suggesting that nearly pure calcite devoid of contaminants and compounds was obtained [5]. Crystalline calcium oxide was achieved as the predominant phase after calcination (Fig. X(b)). The characteristic diffraction peaks (hkl) at 2θ at 32.42, 37.51, 54.10, and 64.28 correspond to (111), (002), (220), and (311) planes of CaO, respectively (JCPDS card number 98-005-7267) [6]. Low-intensity peaks at 31.4, 39.29, 43.08, and 47.05 correspond to the (006), (113), (202), and (024) planes of calcite (JCPDS reference number: 98-016-4935), which occur as a secondary phase along with portlandite calcium hydroxide at 2θ: 17.98 (001), 50.76 (111), 60.59 (201), and 71.77 (202) (JCPDS 98-020-224) [7, 8].

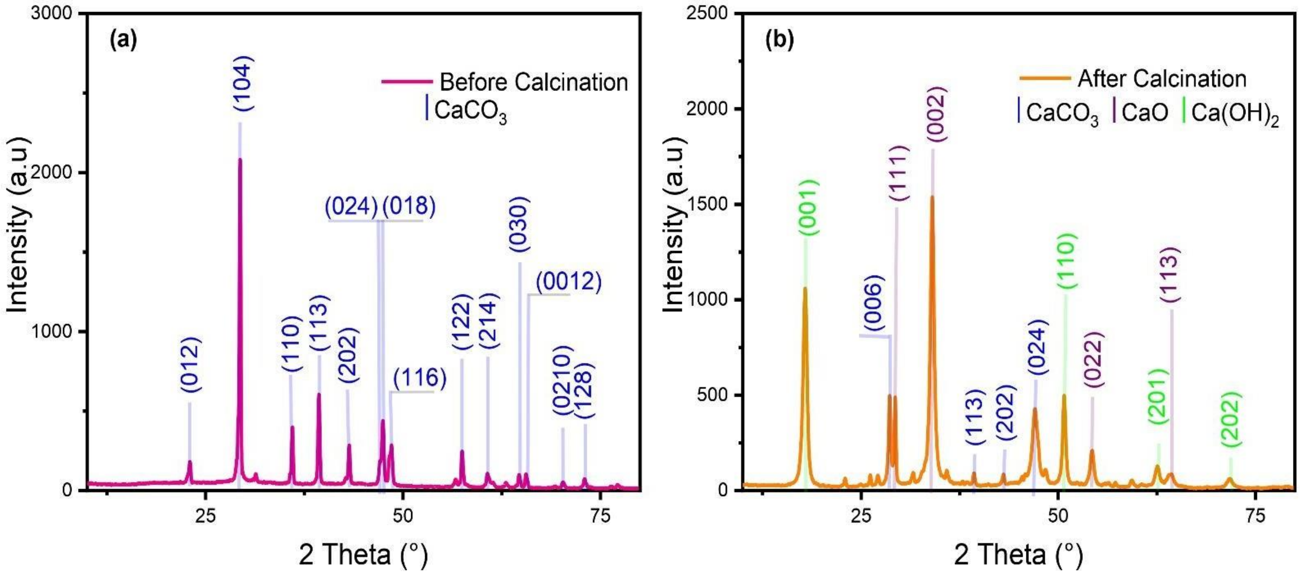

Figure V.43 : XRD findings of (a) Uncalcined Cuttlefish bones and (b) Calcined Cuttelefish bones.

V.3.3. Scanning Electron Microscopy

Scanning Electron Microscopy (SEM) analysis was conducted at various magnifications to investigate morphological changes in cuttlefish samples and to elucidate the structural transformation associated with the calcination step performed under 900 °C temperature.

Figures V.13 (a, b) highlight SEM images of the uncalcined cuttlefish, which revealed bulk morphologies lacking a defined shape, characterized by irregular particles. The surface appeared rough and heterogeneous, indicating the unprocessed state of the material. On the other hand, Figures V.13 (c, d) display SEM images of cuttlefish after calcination at 900°C for 2 hours and demonstrate significant morphological changes. The calcination process resulted in the transformation of irregular particles into smaller, more uniformly shaped particles with a smoother and less rough surface. This structural refinement is indicative of thermal decomposition, leading to the formation of calcium oxide (CaO) from calcium carbonate[9].

The high surface area and regular particle shape observed in the calcined samples suggest an improvement in material properties, potentially enhancing reactivity. These findings highlight the critical role of thermal treatment in altering the transformation of $CaCO_3$ to CaO.

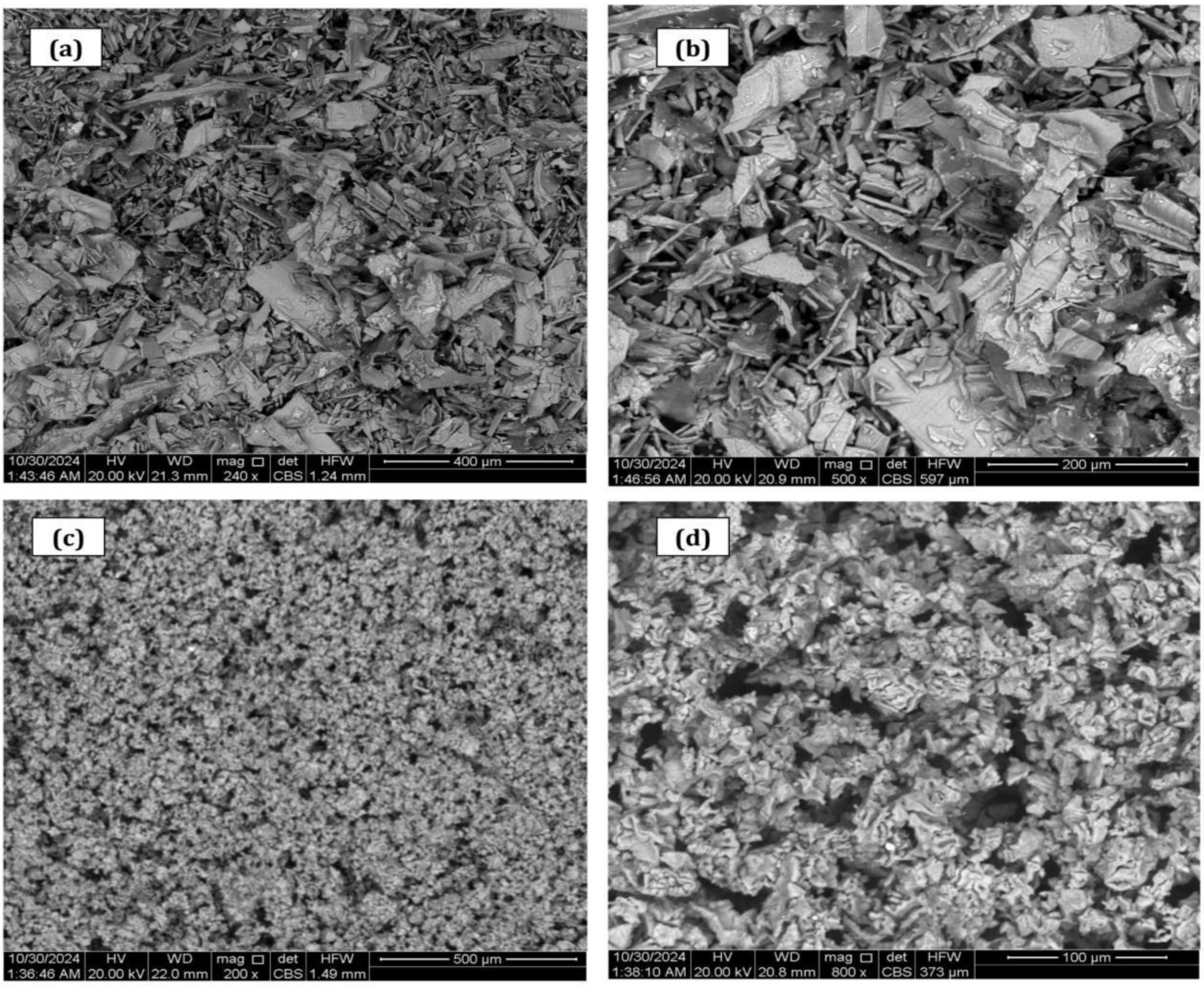

Figure V.44 : SEM images of cuttlefish with different magnifications : (a,b) before calcination (c,d) after calcination.

Energy Dispersive X-ray Spectroscopy (EDX) analysis was performed to complement the SEM findings, providing elemental composition data for cuttlefish samples before and after calcination and were highlighted in Figure.

EDX outcomes of the uncalcined cuttlefish displayed in Figure V.14(e) revealed the presence of calcium carbonate atoms, confirming the material's initial composition as calcium carbonate ($CaCO_3$). These findings align with the unrefined morphology observed in the SEM images, indicating the untreated state of the cuttlefish material.

Post-calcination EDX analysis showed in Figure V.14 (f) demonstrated a complete transformation of calcium carbonate into calcium oxide (CaO). The carbon atoms present in calcium carbonate observed in the uncalcined state were absent in the calcined sample, indicating their consumption during the thermal decomposition process. Results further showed a significant increase in the percentages of calcium and oxygen, confirming the high presence of calcium oxide in the calcined cuttlefish. These EDX results corroborate the SEM observations, providing strong evidence of the structural and chemical transformation of cuttlefish during calcination.

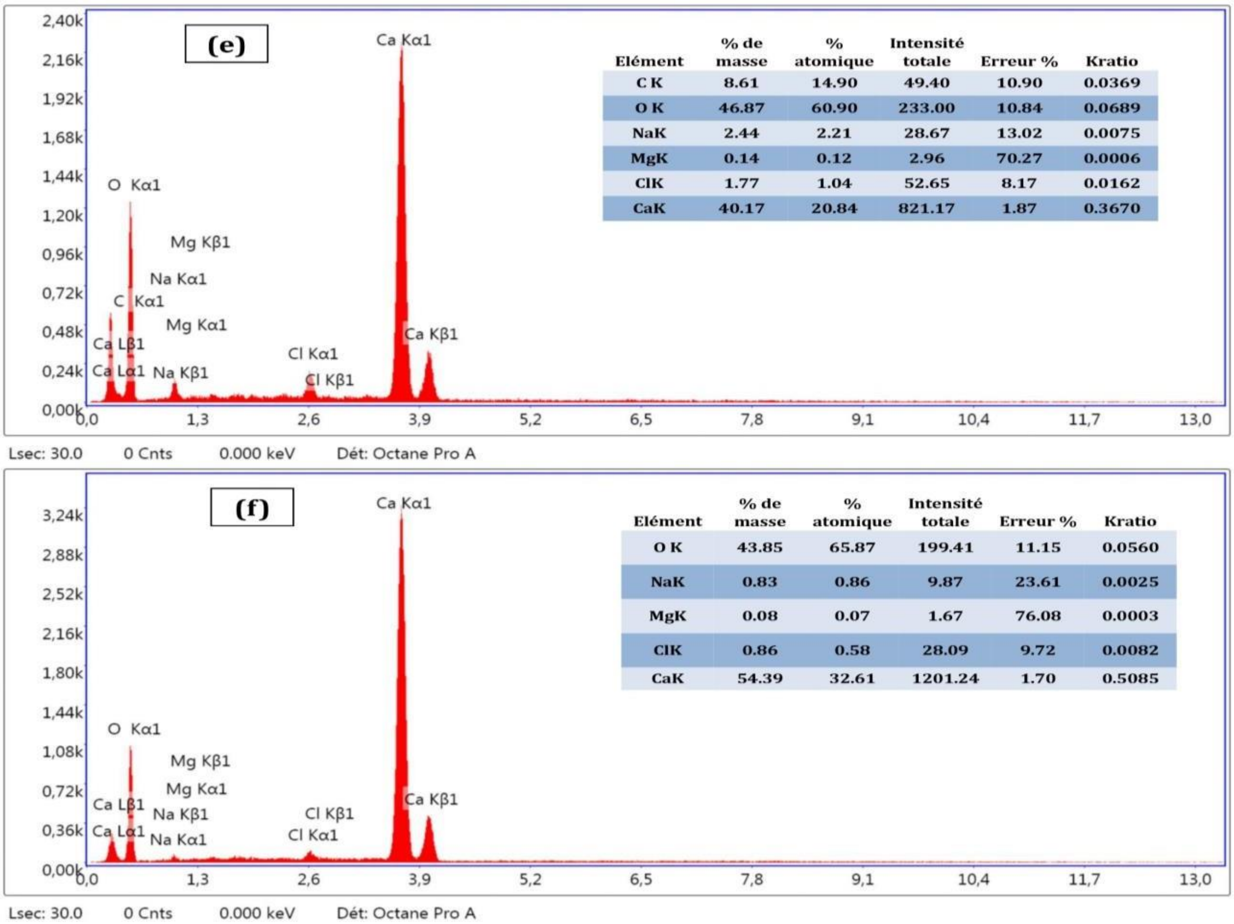

Figure V.45 : EDX spectrum outcomes of : (e) Uncalcined cuttlefish bones, (f) calcined cuttle fish bones.

V.3.3.3. SCWSO application on the SEM images of cuttlefish bones catalyst

Figures V.15-19 illustrate the application of our developed SCWSO algorithm in analyzing scanning electron microscopy (SEM) images of cuttlefish bones, both prior to (Figures V.15-16) and following calcination (Figures V.17-18). These images were captured at various magnifications ranging from X200 to X800, allowing for detailed examination of the structural changes induced by thermal treatment.

In Figures V.15-16, which depict the state of cuttlefish bones before calcination, the colormap images reveal a rough surface characterized by a heterogeneous distribution of particles in diverse shapes and forms. This heterogeneity suggests a smaller surface area. The SCWSO algorithm effectively highlights these parameters, demonstrating its capability to enhance image clarity. By applying various thresholds, the algorithm reveals additional details and more particles of cuttlefish bones, which refer to the presence of calcium carbonate particles.

Conversely, Figures V.17–18 showcase the SEM images after thermal treatment aimed at converting calcium carbonate into calcium oxide. The SCWSO algorithm's results confirm significant changes in the morphology of the cuttlefish bones post-calcination. In Figure V.17, captured at X200 magnification, the surface appears less rough and more homogeneous, with a notable absence of large, irregularly shaped particles. This observation is further supported by Figure V.18, where the SCWSO method successfully elucidates the presence of smaller particles with defined shapes, indicating a smoother and more uniform surface. As additional thresholds are applied, more intricate details emerge, such as organized particle shapes resembling triangles. This transformation confirms that calcium carbonate has been effectively converted into calcium oxide.

Overall, the SCWSO algorithm demonstrates its utility in optimizing SEM image analysis by enhancing detail visibility and providing insights into morphological changes during calcination process.

		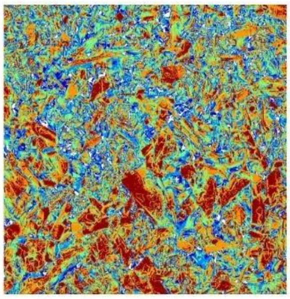	Cuttlefish bones before calcination Segmentation and coloromap Number of thresholds : 5
		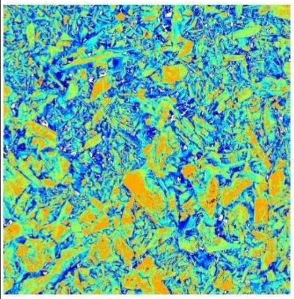	Cuttlefish bones before calcination Segmentation and coloromap Number of thresholds : 7
		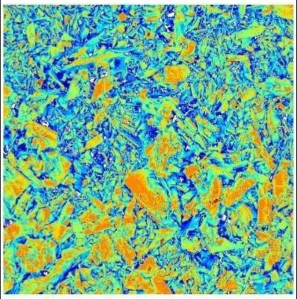	Cuttlefish bones before calcination Segmentation and coloromap Number of thresholds : 9
		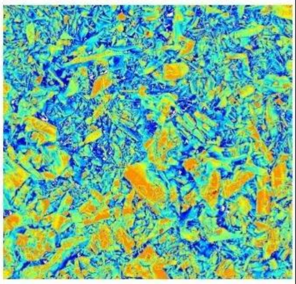	Cuttlefish bones before calcination Segmentation and coloromap Number of thresholds : 12
		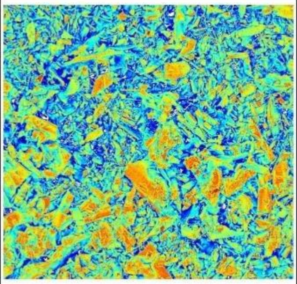	Cuttlefish bones before calcination Segmentation and coloromap Number of thresholds :15

Figure V.46 : Cuttlefish bones before calcination SEM images seegmantation at various thresholds (X240 magnification).

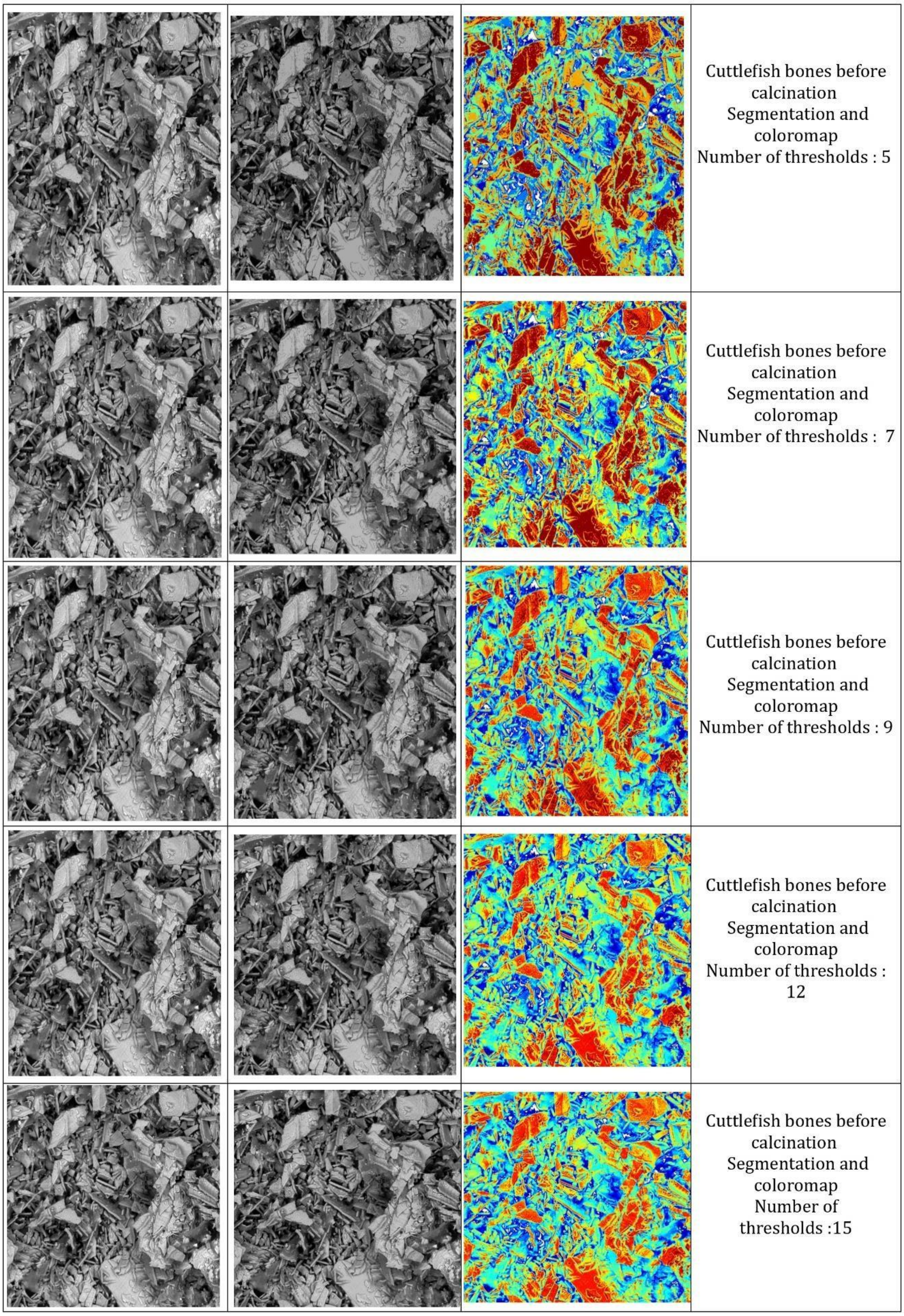

Figure V.47 : Cuttlefish bones before calcination SEM images seegmantation at various thresholds (X500 magnification).

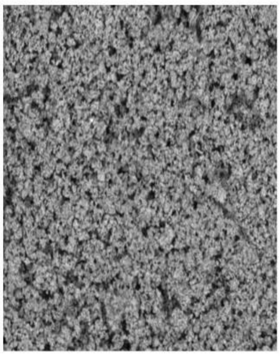	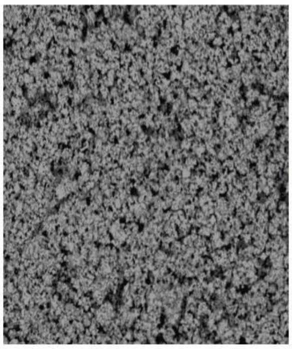	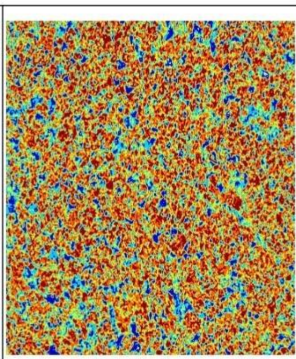	Cuttlefish bones after calcination Segmentation and coloromap Number of thresholds : 5
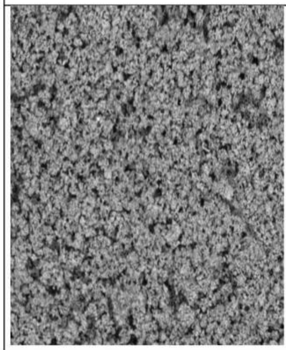	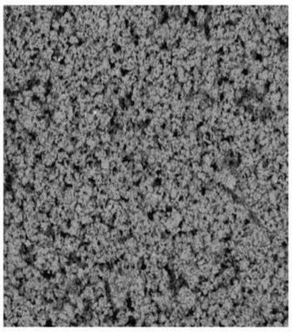	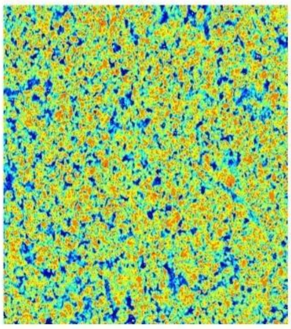	Cuttlefish bones after calcination Segmentation and coloromap Number of thresholds : 7
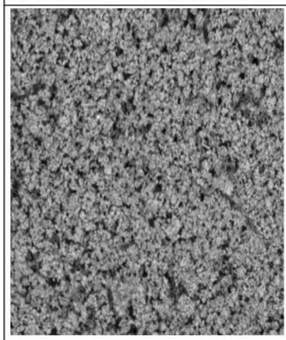	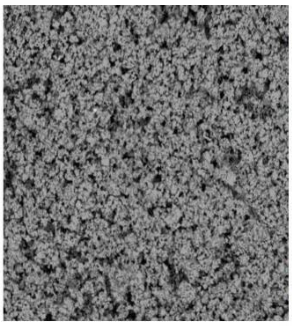	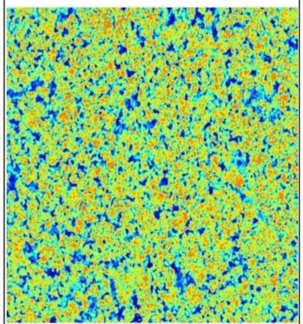	Cuttlefish bones after calcination Segmentation and coloromap Number of thresholds : 9
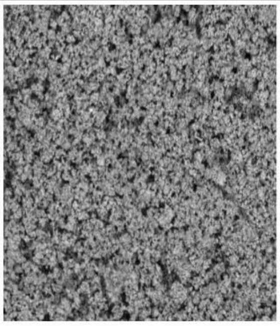	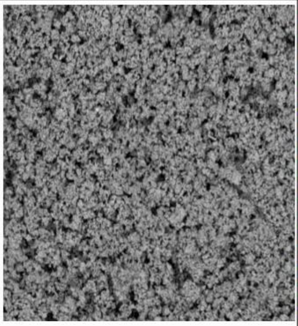	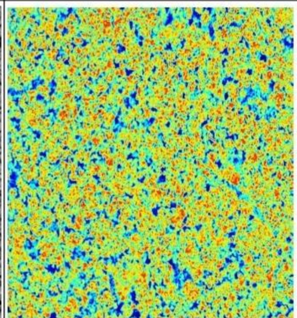	Cuttlefish bones after calcination Segmentation and coloromap Number of thresholds : 12
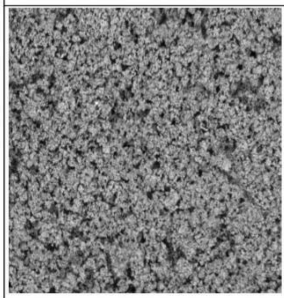	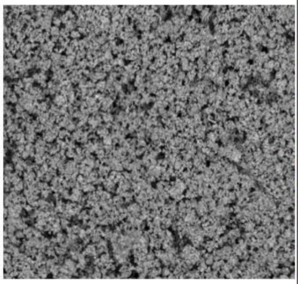	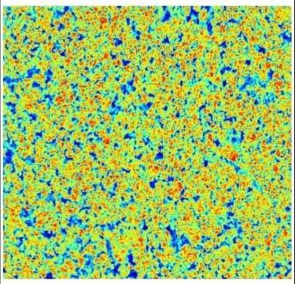	Cuttlefish bones after calcination Segmentation and coloromap Number of thresholds :15

Figure V.48 : Cuttlefish bones after calcination SEM images seegmantation at various thresholds (X200 magnification).

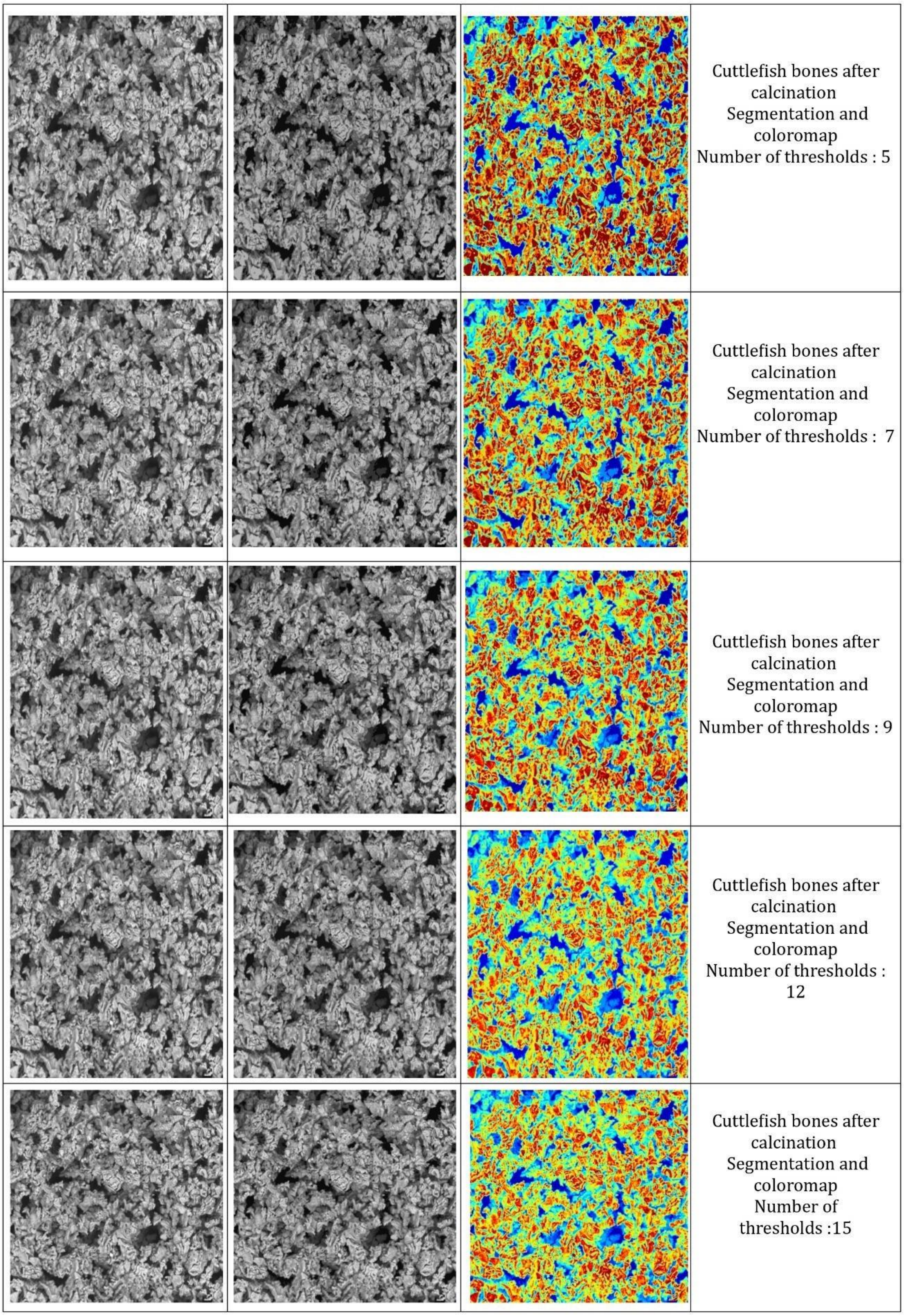

Figure V.49 : Cuttlefish bones after calcination SEM images seegmantation at various thresholds (X800 magnification).

V.4. Biodiesel Feedstocks Analysis

V.4.1. Lipid content

The lipid extraction analysis of Spirulina and Chlorella algae demonstrates significant differences in lipid yields between the two species. From 50 grams of spirulina, 0.41 grams of lipids were extracted, corresponding to a lipid content of 0.82%. In comparison, the extraction from 30 grams of chlorella yielded 1.17 grams of lipids, resulting in a substantially higher lipid content of 3.9% as highlighted in Figure V.19.

These findings emphasize chlorella's superior lipid extraction efficiency compared to spirulina under the tested conditions. The higher lipid yield from chlorella is likely due to its distinct biochemical composition and structural properties. This analysis highlights the importance of selecting an appropriate microalgal species for applications such as biodiesel production. Consequently, chlorella was chosen as the feedstock for subsequent biodiesel production experiments.

Figure V.50 : Lipid extraction resuts of chlorella anad spirulina.

V.4.2. Biodiesel Synthesis

Biodiesel production from waste cooking oil (WCO) and chlorella algae using cuttlefish bone-derived CaO as a catalyst highlights significant differences in yield and process efficiency, as illustrated in Figures V.20 and V.21.

For WCO, a biodiesel yield of 84% fatty acid methyl esters (FAME) was achieved, as shown in the upper section of Figure V.20. The lower section depicts the by-products, including glycerol and residual catalyst. These results were obtained under optimized conditions: a 5:1 oil-to-methanol (Oi/MeOH) molar ratio, a 2 wt.% cuttlefish bone-derived CaO catalyst, a reaction temperature of 60 °C, and a reaction time of 2 hours. This demonstrates the effectiveness of WCO as a low-cost, high-availability feedstock for biodiesel production. Further optimization of parameters including oil-to-methanol ratios, catalyst composition, reaction temperature, and duration could improve yields even further.

In comparison, Chlorella algae, which was chosen based on the lipid content test in the previous section, produced a slightly lower yield of 76% FAME under different conditions: a 12:1 methanol-to-oil ratio, a 5 wt.% CaO catalyst, a reaction temperature of 60 °C, and a reaction time of 4 hours. Despite the lower yield, chlorella algae remains a viable alternative feedstock for biodiesel production. The process integrates lipid extraction and transesterification into a single step, similar to the process used for WCO. Improving lipid extraction methods and further optimizing transesterification conditions could potentially enhance Chlorella's biodiesel yield.

Both feedstocks offer promising routes for biodiesel production, each with unique advantages and challenges. While WCO's high yield and low cost make it an attractive option, Chlorella algae's sustainable nature and potential for higher lipid yields with optimized methods provide long-term promise. Outcomes also underscore the effectiveness of cuttlefish bone-derived CaO as a catalyst. The catalyst not only accelerates the transesterification process but is also easily recoverable, settling with the residue at the bottom of the reaction vessel.

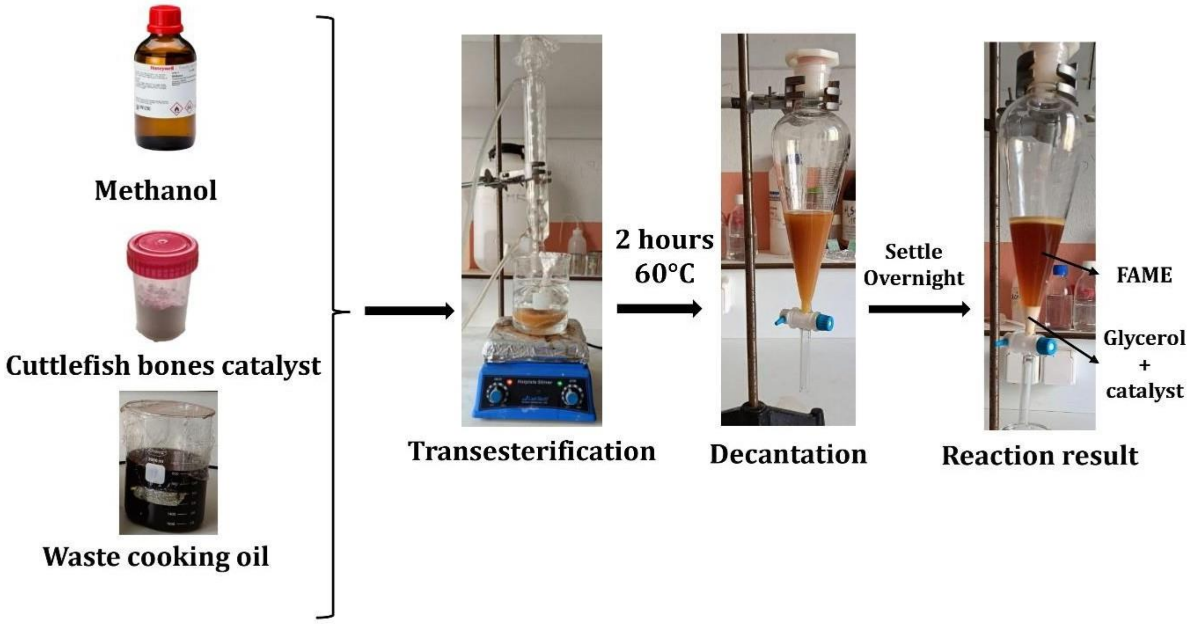

Figure V.51 : Bioidesel production Process from waste cooking oil.

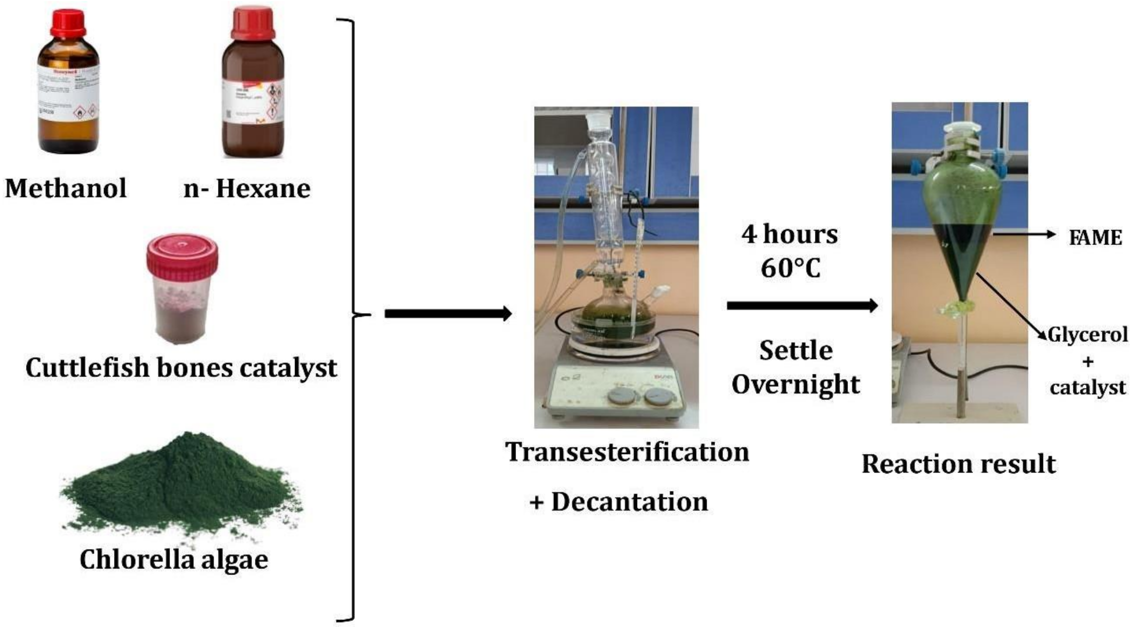

Figure V.52 : Bioidesel production Process from chlorella algae.

V.5. Conclusion

This chapter demonstrated the integration of advanced AI tools and sustainable materials in biodiesel production, which was highlighted in the previous chapter. The SCWSO method proved highly effective in segmenting SEM images over other AI methods, enhancing the analysis of CaO catalysts derived from different sources. Characterization techniques like XRD, FT-IR, and SEM confirmed the suitability of cuttlefish bones as an excellent source of calcium oxide, and the SCWSO method simplified and improved the interpretation of SEM image analyses, confirming its suitability for this kind of issue.

The application of cuttlefish bone-derived CaO in biodiesel production showcased its efficiency and sustainability. Waste cooking oil (WCO) achieved a high yield of 84% FAME, emphasizing its economic and environmental advantages, while Chlorella algae, with a yield of 76% FAME, presented a renewable alternative with potential for further optimization. The catalyst's ease of recovery and cost-effectiveness reinforced its value for biodiesel processes.

This chapter highlights the synergy between AI techniques and sustainable materials, underscoring their potential to advance biodiesel production. Future efforts should focus on refining AI tools, optimizing catalyst preparation, and opening doors for new challenges and applications.

References

[1] M. B. Toffolo, L. Regev, S. Dubernet, Y. Lefrais, and E. Boaretto, 'FTIR-Based Crystallinity Assessment of Aragonite–Calcite Mixtures in Archaeological Lime Binders Altered by Diagenesis', *Minerals*, vol. 9, no. 2, Art. no. 2, Feb. 2019, doi: 10.3390/min9020121.

[2] M. S. Hossain and S. Ahmed, 'Crystallographic characterization of naturally occurring aragonite and calcite phase: Rietveld refinement', *Journal of Saudi Chemical Society*, vol. 27, no. 3, p. 101649, 2023.

[3] T. Witoon, 'Characterization of calcium oxide derived from waste eggshell and its application as CO2 sorbent', *Ceramics International*, vol. 37, no. 8, pp. 3291–3298, 2011.

[4] N. S. Lani, N. Ngadi, N. Y. Yahya, and R. Abd Rahman, 'Synthesis, characterization and performance of silica impregnated calcium oxide as heterogeneous catalyst in biodiesel production', *Journal of Cleaner Production*, vol. 146, pp. 116–124, 2017.

[5] H. Zhai, F. Liu, Y. Huang, Q. Yang, C. Tian, and W. Zhou, 'Preparation of peanut shell-like calcium carbonate from biowaste chicken eggshell and its application for aqueous Victoria Blue B removal', *Microporous and Mesoporous Materials*, vol. 329, p. 111549, 2022.

[6] K. K. Jaiswal, S. Dutta, C. B. Pohrmen, R. Verma, A. Kumar, and A. P. Ramaswamy, 'Bio-waste chicken eggshell-derived calcium oxide for photocatalytic application in methylene blue dye degradation under natural sunlight irradiation', *Inorganic and Nano-Metal Chemistry*, vol. 51, no. 7, pp. 995–1004, Jul. 2021, doi: 10.1080/24701556.2020.1813769.

[7] M. G. Rinaudo, S. E. Collins, and M. R. Morales, 'Eggshell Waste Valorization into CaO/CaCO3 Solid Base Catalysts', *Engineering Proceedings*, vol. 67, no. 1, Art. no. 1, 2024, doi: 10.3390/engproc2024067036.

[8] I. M. Maafa, A. A. S. Alahl, M. O. Abd El-Magied, X. Cui, and A. S. Dhmees, 'Eco-friendly self-terminated process for preparation of CaO catalyst based on chitosan production wastes for biodiesel production', *Journal of Materials Research and Technology*, vol. 30, pp. 1217–1227, 2024.

[9] I. S. Abd Manaf, M. H. A. Rahim, and G. P. Maniam, 'Biodiesel production from catfish (Pangasius) fat via ultrasound-assisted method', *Maejo International Journal of Energy and Environmental Communication*, vol. 1, no. 1, pp. 15–20, 2019.

General conclusion

General Conclusion

Our thesis has delved into one of the most pressing challenges confronting our planet over the past 20–30 years: the dual crises of global warming and environmental pollution. The degradation of air, soil, and water has reached critical levels, demanding urgent and innovative solutions to mitigate the far-reaching risks and threats posed by these issues. By addressing these interconnected problems, this work aims to contribute to the growing body of knowledge dedicated to safeguarding the planet for future generations by applications of multiple recent methods in order to enhance the efficiency of treatment and find new resources that limit reliance on fossil fuels.

Algeria, like many developing countries, has experienced significant growth in economic activities and a rapid rise in population in recent years. While these developments have driven progress, they have also brought adverse consequences for both human health and the environment. The root causes of these challenges were explored in detail in the first chapter, highlighting the nation's heavy reliance on fossil fuels and inefficient waste management practices. These factors have created a critical situation, straining both environmental sustainability and energy security.

To address these pressing issues, this thesis proposes adopting a circular economy model as a viable solution. By emphasizing recycling and reusing waste as feedstock for energy production, this approach aims to reduce the improper handling of waste and decrease dependency on fossil fuels, paving the way for a more sustainable and resilient future.

Chapters II and III outlined the practical implementation of our proposed circular economy model, focusing on sustainable biodiesel production. Our approach emphasized the utilization of two key resources: waste cooking oil, which is generated in significant quantities, particularly by households and restaurants, and algae, which are cultivated in different areas using CO_2, a major byproduct of industrial and transportation sectors. The process employed various types of catalysts to accelerate reactions, improve activity, and enhance selectivity, thereby optimizing biodiesel production.

Furthermore, this thesis explored the integration of advanced technologies, particularly artificial intelligence (AI), in refining biodiesel production processes. AI techniques such as machine learning, neural networks, and adaptive algorithms were highlighted for their ability to model production characteristics with precision, optimize yield and quality, and enable real-time monitoring and quality control. These technologies not only reduce production costs but also drive innovation by simplifying complex simulations. and make the biodiesel production process easier to handle and control.

Chapter IV provided a comprehensive explanation of the protocols employed to achieve the outcomes of the circular economy model described in earlier chapters. The selected raw materials for biodiesel production included waste cooking oil and two types of algae (Spirulina and Chlorella) chosen for their abundance and potential to reduce both fossil fuel dependence and waste accumulation. Additionally, this chapter introduced the biodiesel production from these raw materials using a novel heterogeneous catalyst derived from cuttlefish bones, a readily available resource found along coastlines.

Moreover, this chapter explored the application of advanced artificial intelligence techniques named the Symmetric Chaotic War Strategy Optimization Algorithm (SCWSO) to analyze the cuttlefish bone-derived catalyst SEM images. By employing this AI-driven method, the analysis of the catalyst's results becomes more precise, accessible, and comprehensible.

Finally, Chapter V presented the experimental results, highlighting key findings in biodiesel production from waste cooking oil (WCO) and Chlorella algae. WCO achieved an impressive yield of 84%, demonstrating its high efficiency and practicality for biodiesel production through transesterification. Its low cost and wide availability make it an attractive feedstock for sustainable energy solutions. Chlorella algae, while yielding slightly less at 76%, also showcased considerable potential as a renewable energy source, underscoring the adaptability and promise of these feedstocks in addressing global energy challenges.

In addition, the analysis of the cuttlefish bone-derived calcium oxide (CaO) catalyst using advanced characterization techniques such as XRD, FT-IR, and SEM confirmed its suitability as a cost-effective and abundant source of calcium for catalyst preparation. These findings emphasize the feasibility of leveraging low-cost, readily available materials to advance biodiesel production, supporting the shift towards accessible and sustainable energy technologies.

Moreover, this chapter introduced the application of the improved Symmetric Chaotic War Strategy Optimization algorithm (SCWSO) for segmenting scanning electron microscopy (SEM) images of the CaO catalyst. The SCWSO algorithm demonstrated superior performance across various tests and evaluations, making it suitable for application to SEM images, as detailed in the chapter. Its application to SEM images of the cuttlefish bone-derived catalyst showcased high efficiency, simplifying image analysis and enabling easier comparison of material states before and after calcination. This integration of advanced computational techniques further enhances the precision and practicality of catalyst analysis, driving innovation in the field of biodiesel production.

In conclusion, the experimental findings strongly support the theoretical framework proposed in the earlier chapters. The results validate the suitability of cuttlefish bones as a rich source of calcium, effectively processed into calcium oxide for use as a heterogeneous catalyst in biodiesel production. They also highlight the significant potential of waste cooking oil and algae as suitable feedstocks for biodiesel production, demonstrating their effectiveness in reducing pollution and promoting reliance on eco-friendly sources of energy.

Furthermore, the integration of artificial intelligence approaches, which is image segmentation, into this research has proven to be highly effective. AI applications, such as those utilized for analyzing catalysts in various states, demonstrated exceptional speed, accuracy, and efficiency, significantly streamlining the process. These advancements underscore the transformative role of AI in enhancing research methodologies and optimizing biodiesel production processes, paving the way for sustainable and innovative solutions to environmental and energy challenges.

However, While the experimental results and theoretical models are promising, certain limitations require additional exploration. Key areas for development include optimizing reaction conditions to improve biodiesel yield across various feedstocks and investigating the long-term stability, reusability, and industrial-scale performance of the cuttlefish bone-derived calcium oxide catalyst. Additionally, the SCWSO technique, despite its advantages, showed challenges such as premature convergence, an imbalance between exploration and exploitation, and a tendency to get stuck in local solutions. which revealed an area for development and improvements that will be highlighted in future perspectives sections.

Perspectives

Future Perspectives

Despite the promising findings obtained in the experimental chapter, which support the theoretical proposals outlined in earlier chapters, results demonstrated the suitability of various raw materials for biodiesel synthesis, including cuttlefish bones as a promising, low-cost, and eco-friendly source of calcium, which can be converted to calcium oxide for use as a catalyst. Additionally, AI techniques proved highly effective in streamlining SEM image analysis, making it faster and more efficient.

However, some observations and limitations were identified that require optimization in future studies and led ro areas for further refinement, particularly to enhance the integration of AI with laboratory processes. These insights have led to several recommendations and future perspectives, which are detailed as follows:

Further studies are needed to assess the long-term stability and reusability of the CaO catalyst derived from cuttlefish bones to ensure its effectiveness across different feedstocks and varying operational parameters. This evaluation is crucial for validating its suitability for wider applications.

Additionally, optimizing biodiesel production from waste cooking oil and Chlorella algae is essential to identify the ideal parameters and conditions for achieving higher yields.

Exploring additional feedstocks, such as animal fats and other types of algae, is also recommended to gain deeper insights into the potential of different materials for biodiesel production and expand the range of sustainable raw materials.

Regarding the AI method employed in this thesis (SCWSO), further research is recommended to broaden the range of image datasets analyzed and refine the threshold values to achieve greater accuracy in future applications. To enhance segmentation performance and minimize time-intensive challenges, the innovative SCWSO algorithm should be compared and benchmarked against other meta-heuristic optimization techniques and advanced machine learning methods. This comparative approach will help identify its strengths and areas for improvement in the structure of the SCWSO algorithm, paving the way for more robust and efficient image analysis solutions.

Ultimately, these recommendations aim to provide a clearer direction for future research and contribute to achieving more refined and impactful results in the area of biodiesel production which is directly influence both of waste management situation and energy resources consumption.

Annex

Annex 1 : SCWSO method Evaluation Tables

Table 1: Fitness metrics results for all algorithms.

Images	nTh	Metrics	SCWSO	GWO	WSO	GJO	SCA	Chimp	CDO	RSA	IGWO
SEM-1	5	Mean	**2.603e-01**	2.800e-01	2.638e-01	3.290e-01	3.349e-01	2.820e-01	4.225e-01	2.627e-01	2.829e-01
		Std	**1.460e-03**	2.458e-02	4.386e-03	4.756e-02	5.970e-02	9.410e-03	6.369e-02	2.782e-03	2.909e-02
	7	Mean	**1.496e-01**	1.776e-01	1.664e-01	2.298e-01	2.152e-01	1.749e-01	2.878e-01	1.516e-01	1.766e-01
		Std	1.120e-02	2.120e-02	3.124e-02	4.062e-02	4.512e-02	1.310e-02	5.188e-02	**6.500e-03**	1.891e-02
	9	Mean	**1.020e-01**	1.247e-01	1.205e-01	1.771e-01	1.608e-01	1.232e-01	2.164e-01	1.051e-01	1.366e-01
		Std	8.963e-03	1.908e-02	1.931e-02	3.211e-02	2.817e-02	**7.831e-03**	3.505e-02	7.942e-03	2.617e-02
	12	Mean	**6.871e-02**	8.855e-02	8.100e-02	1.278e-01	1.216e-01	8.659e-02	1.740e-01	7.041e-02	8.750e-02
		Std	**5.866e-03**	1.131e-02	1.437e-02	2.200e-02	2.104e-02	7.392e-03	2.326e-02	6.212e-03	1.271e-02
	15	Mean	**4.936e-02**	6.357e-02	6.585e-02	9.669e-02	9.939e-02	6.487e-02	1.201e-01	5.281e-02	6.863e-02
		Std	**3.213e-03**	1.042e-02	1.156e-02	1.398e-02	1.522e-02	5.613e-03	2.187e-02	4.555e-03	1.042e-02
SEM-2	5	Mean	**5.009e-01**	5.368e-01	5.088e-01	5.539e-01	5.525e-01	5.339e-01	6.841e-01	5.049e-01	5.303e-01
		Std	**1.116e-03**	4.809e-02	1.483e-02	2.210e-02	4.778e-02	1.306e-02	7.936e-02	4.681e-03	1.936e-02
	7	Mean	**2.810e-01**	3.093e-01	3.041e-01	3.563e-01	3.580e-01	3.278e-01	4.549e-01	2.916e-01	3.165e-01
		Std	**6.647e-03**	2.390e-02	3.192e-02	5.050e-02	4.044e-02	1.296e-02	4.853e-02	1.301e-02	2.552e-02
	9	Mean	**1.829e-01**	2.199e-01	1.937e-01	2.720e-01	2.479e-01	2.229e-01	3.183e-01	1.948e-01	2.229e-01
		Std	**9.958e-03**	2.739e-02	2.166e-02	5.276e-02	2.790e-02	1.285e-02	4.970e-02	1.354e-02	2.262e-02
	12	Mean	**1.177e-01**	1.475e-01	1.289e-01	1.889e-01	1.605e-01	1.495e-01	2.376e-01	1.261e-01	1.458e-01
		Std	**9.968e-03**	1.340e-02	1.934e-02	3.037e-02	1.732e-02	1.015e-02	3.342e-02	1.063e-02	1.858e-02
	15	Mean	**8.585e-02**	1.057e-01	9.915e-02	1.339e-01	1.204e-01	1.060e-01	1.656e-01	9.200e-02	1.032e-01
		Std	9.365e-03	1.059e-02	1.600e-02	1.925e-02	1.435e-02	**7.524e-03**	2.650e-02	9.696e-03	1.834e-02
SEM-3	5	Mean	**4.284e-01**	4.446e-01	4.362e-01	5.158e-01	4.823e-01	4.687e-01	6.276e-01	4.335e-01	4.541e-01
		Std	**1.654e-03**	2.212e-02	8.891e-03	6.323e-02	4.534e-02	1.433e-02	8.904e-02	6.207e-03	2.931e-02
	7	Mean	**2.703e-01**	2.924e-01	2.903e-01	3.499e-01	3.447e-01	3.067e-01	4.371e-01	2.801e-01	3.014e-01
		Std	**5.226e-03**	1.576e-02	2.374e-02	3.379e-02	3.276e-02	1.433e-02	9.164e-02	1.201e-02	2.265e-02
	9	Mean	**1.915e-01**	2.210e-01	2.096e-01	2.620e-01	2.465e-01	2.275e-01	3.050e-01	2.046e-01	2.193e-01
		Std	**8.537e-03**	1.353e-02	2.081e-02	3.116e-02	2.268e-02	1.007e-02	2.970e-02	1.111e-02	1.733e-02
	12	Mean	**1.289e-01**	1.475e-01	1.442e-01	1.811e-01	1.702e-01	1.621e-01	2.192e-01	1.385e-01	1.526e-01
		Std	**8.901e-03**	1.506e-02	1.957e-02	2.123e-02	1.806e-02	1.137e-02	2.881e-02	9.535e-03	1.403e-02
	15	Mean	**9.305e-02**	1.096e-01	1.019e-01	1.333e-01	1.293e-01	1.204e-01	1.578e-01	1.055e-01	1.152e-01
		Std	6.783e-03	7.899e-03	1.178e-02	1.332e-02	1.313e-02	7.050e-03	1.875e-02	**5.424e-03**	8.476e-03
SEM-4	5	Mean	**6.727e-01**	6.926e-01	6.814e-01	7.389e-01	7.134e-01	7.085e-01	9.829e-01	6.773e-01	7.143e-01
		Std	**8.778e-04**	2.196e-02	1.330e-02	3.328e-02	1.752e-02	1.503e-02	1.301e-01	7.696e-03	4.248e-02
	7	Mean	**3.970e-01**	4.443e-01	4.203e-01	4.950e-01	4.826e-01	4.513e-01	6.639e-01	4.059e-01	4.338e-01
		Std	**6.217e-03**	4.779e-02	4.513e-02	5.100e-02	5.432e-02	1.803e-02	8.555e-02	1.730e-02	1.975e-02
	9	Mean	**2.681e-01**	3.219e-01	2.875e-01	3.845e-01	3.557e-01	3.186e-01	4.744e-01	2.871e-01	3.064e-01
		Std	**1.164e-02**	3.037e-02	4.184e-02	4.630e-02	3.977e-02	1.954e-02	7.426e-02	1.968e-02	2.252e-02
	12	Mean	**1.772e-01**	2.142e-01	1.905e-01	2.555e-01	2.485e-01	2.159e-01	3.050e-01	1.907e-01	2.214e-01
		Std	1.333e-02	2.252e-02	2.364e-02	2.743e-02	3.688e-02	**1.203e-02**	3.744e-02	1.902e-02	2.445e-02

The best results are in bold

Table 1 – continued

Images	nTh	Metrics	SCWSO	GWO	WSO	GJO	SCA	Chimp	CDO	RSA	IGWO
	15	Mean	1.366e-01	1.674e-01	**1.348e-01**	1.871e-01	1.871e-01	1.582e-01	2.371e-01	1.417e-01	1.666e-01
		Std	1.731e-02	2.234e-02	2.049e-02	2.562e-02	2.462e-02	**1.196e-02**	2.551e-02	1.233e-02	2.507e-02
SEM-5	5	Mean	**7.119e-01**	7.398e-01	7.234e-01	7.796e-01	7.634e-01	7.522e-01	9.722e-01	7.165e-01	7.291e-01
		Std	**9.144e-04**	2.813e-02	1.775e-02	3.936e-02	2.719e-02	1.588e-02	1.035e-01	7.235e-03	2.272e-02
	7	Mean	**4.174e-01**	4.540e-01	4.411e-01	5.041e-01	4.812e-01	4.734e-01	6.080e-01	4.352e-01	4.560e-01
		Std	**3.471e-03**	3.017e-02	2.571e-02	5.443e-02	4.040e-02	2.232e-02	7.470e-02	1.409e-02	2.605e-02
	9	Mean	**2.750e-01**	3.134e-01	2.850e-01	3.567e-01	3.446e-01	3.292e-01	4.410e-01	2.936e-01	3.247e-01
		Std	**1.548e-02**	2.426e-02	3.125e-02	2.548e-02	2.577e-02	2.237e-02	5.427e-02	1.824e-02	3.214e-02
	12	Mean	**1.741e-01**	2.161e-01	1.821e-01	2.412e-01	2.349e-01	2.201e-01	3.024e-01	1.947e-01	2.208e-01
		Std	**1.390e-02**	2.782e-02	2.204e-02	2.042e-02	2.147e-02	1.696e-02	3.620e-02	1.479e-02	3.313e-02
	15	Mean	**1.225e-01**	1.524e-01	1.320e-01	1.771e-01	1.720e-01	1.586e-01	2.129e-01	1.392e-01	1.628e-01
		Std	**1.054e-02**	1.772e-02	1.988e-02	1.882e-02	1.532e-02	1.354e-02	2.335e-02	1.074e-02	2.260e-02
SEM-6	5	Mean	**4.280e-01**	4.432e-01	4.401e-01	4.954e-01	4.838e-01	4.621e-01	6.051e-01	4.344e-01	4.405e-01
		Std	**1.902e-03**	1.997e-02	2.619e-02	2.843e-02	4.438e-02	1.640e-02	7.679e-02	7.675e-03	1.219e-02
	7	Mean	**2.580e-01**	2.847e-01	2.830e-01	3.340e-01	3.265e-01	3.002e-01	4.234e-01	2.711e-01	2.901e-01
		Std	**7.340e-03**	2.058e-02	2.797e-02	3.125e-02	3.338e-02	1.675e-02	5.444e-02	1.028e-02	2.177e-02
	9	Mean	**1.808e-01**	2.051e-01	1.993e-01	2.467e-01	2.494e-01	2.222e-01	3.054e-01	1.956e-01	2.068e-01
		Std	**4.883e-03**	1.612e-02	1.894e-02	2.466e-02	2.070e-02	9.715e-03	3.330e-02	8.272e-03	1.534e-02
	12	Mean	**1.170e-01**	1.439e-01	1.325e-01	1.738e-01	1.597e-01	1.520e-01	2.054e-01	1.335e-01	1.392e-01
		Std	7.561e-03	1.124e-02	1.633e-02	1.422e-02	1.277e-02	9.837e-03	2.998e-02	**5.873e-03**	1.271e-02
	15	Mean	**8.303e-02**	1.017e-01	9.627e-02	1.217e-01	1.192e-01	1.118e-01	1.509e-01	9.468e-02	1.038e-01
		Std	7.164e-03	9.953e-03	1.540e-02	1.789e-02	1.343e-02	7.327e-03	1.813e-02	**6.656e-03**	1.177e-02
SEM-7	5	Mean	**2.609e-01**	3.010e-01	2.713e-01	3.121e-01	3.271e-01	2.774e-01	4.363e-01	2.623e-01	2.980e-01
		Std	3.589e-03	3.623e-02	2.513e-02	3.606e-02	4.474e-02	1.021e-02	8.029e-02	**2.819e-03**	4.936e-02
	7	Mean	**1.524e-01**	1.951e-01	1.597e-01	2.348e-01	2.155e-01	1.804e-01	2.919e-01	1.524e-01	2.012e-01
		Std	9.959e-03	3.046e-02	1.801e-02	3.740e-02	3.478e-02	9.200e-03	4.936e-02	**5.428e-03**	3.474e-02
	9	Mean	1.089e-01	1.415e-01	1.144e-01	1.714e-01	1.780e-01	1.275e-01	2.322e-01	**1.040e-01**	1.483e-01
		Std	1.040e-02	2.217e-02	1.374e-02	3.527e-02	4.150e-02	9.265e-03	3.650e-02	**7.446e-03**	2.850e-02
	12	Mean	7.373e-02	1.035e-01	8.608e-02	1.273e-01	1.344e-01	9.361e-02	1.641e-01	**7.211e-02**	1.026e-01
		Std	6.741e-03	2.227e-02	1.731e-02	2.139e-02	3.011e-02	6.854e-03	2.652e-02	**6.369e-03**	2.044e-02
	15	Mean	5.413e-02	7.793e-02	6.096e-02	1.025e-01	9.738e-02	6.808e-02	1.249e-01	**5.276e-02**	7.702e-02
		Std	5.926e-03	1.787e-02	1.072e-02	1.867e-02	1.545e-02	**5.429e-03**	2.201e-02	5.808e-03	1.767e-02
SEM-8	5	Mean	**5.993e-01**	6.225e-01	6.167e-01	6.617e-01	6.841e-01	6.468e-01	8.577e-01	6.041e-01	6.204e-01
		Std	**7.592e-04**	2.111e-02	4.572e-02	3.069e-02	8.309e-02	1.842e-02	1.128e-01	6.208e-03	2.611e-02
	7	Mean	**3.401e-01**	3.782e-01	3.558e-01	4.630e-01	4.383e-01	3.982e-01	5.585e-01	3.513e-01	3.784e-01
		Std	**1.525e-02**	2.680e-02	3.067e-02	4.451e-02	5.119e-02	2.119e-02	8.315e-02	1.546e-02	2.872e-02
	9	Mean	**2.295e-01**	2.715e-01	2.454e-01	3.202e-01	3.119e-01	2.826e-01	4.089e-01	2.425e-01	2.630e-01
		Std	**1.149e-02**	2.850e-02	3.165e-02	3.252e-02	3.019e-02	1.649e-02	5.878e-02	1.741e-02	2.222e-02
	12	Mean	**1.488e-01**	1.897e-01	1.595e-01	2.243e-01	2.208e-01	1.935e-01	2.800e-01	1.610e-01	1.901e-01
		Std	**1.236e-02**	2.152e-02	1.654e-02	2.819e-02	2.881e-02	1.305e-02	3.858e-02	1.701e-02	1.953e-02
	15	Mean	**1.111e-01**	1.415e-01	1.277e-01	1.718e-01	1.592e-01	1.392e-01	1.967e-01	1.205e-01	1.406e-01
		Std	1.146e-02	1.599e-02	2.174e-02	2.992e-02	2.137e-02	1.100e-02	2.407e-02	**8.789e-03**	1.326e-02
SEM-9	5	Mean	**6.759e-01**	6.939e-01	6.839e-01	7.447e-01	7.232e-01	7.100e-01	9.051e-01	6.818e-01	6.946e-01
		Std	**9.865e-04**	1.785e-02	1.174e-02	4.527e-02	4.453e-02	1.548e-02	8.752e-02	6.503e-03	1.920e-02
	7	Mean	**3.905e-01**	4.299e-01	4.066e-01	4.801e-01	4.686e-01	4.446e-01	6.149e-01	3.955e-01	4.295e-01
		Std	**1.124e-02**	4.151e-02	4.142e-02	2.753e-02	4.111e-02	1.930e-02	9.198e-02	1.726e-02	4.137e-02
	9	Mean	**2.695e-01**	3.105e-01	2.791e-01	3.632e-01	3.495e-01	3.161e-01	4.264e-01	2.735e-01	2.955e-01

Table 1 – continued

	Std	**1.431e-02**	2.708e-02	3.286e-02	3.651e-02	3.706e-02	1.672e-02	5.808e-02	2.227e-02	2.680e-02
12	Mean	**1.728e-01**	2.239e-01	1.818e-01	2.566e-01	2.435e-01	2.143e-01	3.147e-01	1.858e-01	2.107e-01
	Std	1.586e-02	2.279e-02	2.370e-02	3.184e-02	3.639e-02	**1.283e-02**	4.048e-02	1.758e-02	1.995e-02
15	Mean	**1.228e-01**	1.605e-01	1.357e-01	1.899e-01	1.745e-01	1.557e-01	2.327e-01	1.316e-01	1.611e-01
	Std	**1.045e-02**	2.322e-02	2.631e-02	2.842e-02	2.091e-02	1.059e-02	3.049e-02	1.084e-02	2.230e-02

The best results are in bold

Table 1 – continued

Images	nTh	Metrics	SCWSO	WSO	GJO	SCA	Chimp	CDO	RSA	IGWO	GWO
SEM-10	5	Mean	**5.588e-01**	5.799e-01	5.681e-01	6.179e-01	5.926e-01	5.953e-01	7.545e-01	5.631e-01	5.802e-01
		Std	**8.208e-04**	2.126e-02	1.479e-02	3.972e-02	1.927e-02	1.558e-02	1.041e-01	4.915e-03	2.077e-02
	7	Mean	**3.230e-01**	3.602e-01	3.457e-01	4.095e-01	4.037e-01	3.741e-01	4.839e-01	3.318e-01	3.795e-01
		Std	**5.612e-03**	3.140e-02	2.269e-02	3.177e-02	3.698e-02	1.943e-02	5.151e-02	1.080e-02	3.848e-02
	9	Mean	**2.213e-01**	2.538e-01	2.363e-01	3.014e-01	2.925e-01	2.557e-01	3.643e-01	2.302e-01	2.582e-01
		Std	**1.098e-02**	2.435e-02	2.902e-02	3.844e-02	2.951e-02	1.492e-02	4.361e-02	1.255e-02	3.020e-02
	12	Mean	**1.419e-01**	1.782e-01	1.561e-01	2.087e-01	1.853e-01	1.743e-01	2.342e-01	1.529e-01	1.768e-01
		Std	**1.161e-02**	2.164e-02	2.283e-02	2.634e-02	1.482e-02	1.327e-02	3.253e-02	1.335e-02	2.181e-02
	15	Mean	**1.005e-01**	1.264e-01	1.109e-01	1.488e-01	1.395e-01	1.270e-01	1.839e-01	1.105e-01	1.308e-01
		Std	8.977e-03	1.609e-02	1.726e-02	1.835e-02	1.105e-02	**7.102e-03**	2.438e-02	9.184e-03	1.469e-02

Table 2: PSNR metrics results for all algorithms.

Images	nTh	Metrics	SCWSO	WSO	GJO	SCA	Chimp	CDO	RSA	IGWO	GWO
SEM-1	5	Mean	2.281e+01	2.271e+01	2.268e+01	2.216e+01	2.203e+01	**2.317e+01**	2.301e+01	2.284e+01	2.276e+01
		Std	**1.638e-01**	6.982e-01	4.010e-01	1.126e+00	9.006e-01	7.677e-01	8.407e-01	2.541e-01	7.172e-01
	7	Mean	**2.601e+01**	2.573e+01	2.569e+01	2.487e+01	2.446e+01	2.553e+01	2.489e+01	2.590e+01	2.556e+01
		Std	4.556e-01	8.240e-01	6.471e-01	1.089e+00	1.298e+00	9.241e-01	8.818e-01	**4.478e-01**	6.732e-01
	9	Mean	**2.773e+01**	2.730e+01	2.742e+01	2.598e+01	2.628e+01	2.748e+01	2.607e+01	2.739e+01	2.730e+01
		Std	**5.417e-01**	1.042e+00	8.035e-01	1.532e+00	1.423e+00	9.733e-01	9.992e-01	6.435e-01	1.271e+00
	12	Mean	**3.012e+01**	2.902e+01	2.967e+01	2.794e+01	2.855e+01	2.922e+01	2.735e+01	2.960e+01	2.906e+01
		Std	7.967e-01	1.217e+00	1.266e+00	1.427e+00	9.940e-01	9.632e-01	**6.505e-01**	1.042e+00	1.065e+00
	15	Mean	**3.152e+01**	3.095e+01	3.112e+01	2.915e+01	2.940e+01	3.098e+01	2.894e+01	3.126e+01	3.036e+01
		Std	8.879e-01	1.010e+00	1.047e+00	1.066e+00	1.061e+00	9.568e-01	**7.718e-01**	1.161e+00	1.443e+00
SEM-2	5	Mean	**2.246e+01**	2.204e+01	2.237e+01	2.192e+01	2.189e+01	2.209e+01	2.101e+01	2.244e+01	2.210e+01
		Std	**4.243e-02**	4.839e-01	1.930e-01	3.403e-01	3.829e-01	3.040e-01	5.547e-01	7.210e-02	2.642e-01
	7	Mean	**2.463e+01**	2.425e+01	2.428e+01	2.362e+01	2.361e+01	2.399e+01	2.280e+01	2.456e+01	2.416e+01
		Std	**8.618e-02**	3.811e-01	5.607e-01	6.375e-01	5.172e-01	3.988e-01	4.938e-01	1.518e-01	4.339e-01
	9	Mean	**2.643e+01**	2.578e+01	2.627e+01	2.474e+01	2.506e+01	2.564e+01	2.433e+01	2.628e+01	2.563e+01
		Std	**2.904e-01**	5.080e-01	6.057e-01	9.515e-01	6.649e-01	4.112e-01	7.022e-01	2.935e-01	5.172e-01
	12	Mean	**2.822e+01**	2.738e+01	2.807e+01	2.616e+01	2.701e+01	2.697e+01	2.562e+01	2.817e+01	2.751e+01
		Std	**3.807e-01**	4.418e-01	9.204e-01	8.112e-01	7.064e-01	6.918e-01	6.873e-01	4.589e-01	5.866e-01
	15	Mean	**2.947e+01**	2.888e+01	2.933e+01	2.793e+01	2.829e+01	2.854e+01	2.707e+01	2.943e+01	2.889e+01
		Std	**4.430e-01**	5.515e-01	7.519e-01	8.386e-01	8.083e-01	8.293e-01	7.261e-01	5.253e-01	6.682e-01
SEM-3	5	Mean	**2.189e+01**	2.165e+01	2.183e+01	2.093e+01	2.133e+01	2.137e+01	1.995e+01	2.182e+01	2.157e+01
		Std	**5.656e-02**	3.282e-01	1.730e-01	6.495e-01	5.280e-01	3.058e-01	7.615e-01	1.230e-01	3.401e-01
	7	Mean	**2.411e+01**	2.370e+01	2.381e+01	2.284e+01	2.290e+01	2.347e+01	2.180e+01	2.396e+01	2.349e+01
		Std	**1.281e-01**	3.120e-01	4.091e-01	5.638e-01	5.616e-01	3.197e-01	1.061e+00	2.044e-01	4.689e-01
	9	Mean	**2.546e+01**	2.494e+01	2.518e+01	2.403e+01	2.438e+01	2.469e+01	2.342e+01	2.522e+01	2.497e+01
		Std	**2.855e-01**	3.422e-01	4.625e-01	5.815e-01	4.772e-01	3.111e-01	5.717e-01	3.073e-01	4.131e-01
	12	Mean	**2.725e+01**	2.665e+01	2.692e+01	2.569e+01	2.613e+01	2.621e+01	2.502e+01	2.696e+01	2.664e+01
		Std	4.271e-01	4.873e-01	6.520e-01	6.710e-01	5.573e-01	5.060e-01	6.677e-01	4.117e-01	**3.885e-01**
	15	Mean	**2.903e+01**	2.816e+01	2.854e+01	2.708e+01	2.727e+01	2.754e+01	2.656e+01	2.842e+01	2.804e+01

The best results are

Table 1 – continued

		Std	5.305e-01	4.980e-01	7.191e-01	6.014e-01	5.239e-01	4.931e-01	7.652e-01	5.117e-01	**4.829e-01**
SEM-4	5	Mean	**2.179e+01**	2.168e+01	2.171e+01	2.138e+01	2.164e+01	2.149e+01	1.979e+01	2.174e+01	2.147e+01
		Std	**3.693e-02**	1.756e-01	9.761e-02	2.975e-01	1.822e-01	1.872e-01	7.688e-01	7.658e-02	3.241e-01
	7	Mean	**2.412e+01**	2.366e+01	2.397e+01	2.307e+01	2.344e+01	2.350e+01	2.147e+01	2.404e+01	2.375e+01
		Std	**1.893e-01**	3.965e-01	4.969e-01	4.720e-01	5.201e-01	3.207e-01	6.457e-01	2.681e-01	2.882e-01
	9	Mean	**2.580e+01**	2.503e+01	2.551e+01	2.417e+01	2.476e+01	2.494e+01	2.301e+01	2.559e+01	2.521e+01
		Std	**2.323e-01**	4.568e-01	6.724e-01	7.000e-01	5.921e-01	3.844e-01	8.132e-01	4.040e-01	4.361e-01

The best results are

Table 2 – continued

Images	nTh	Metrics	SCWSO	GWO	WSO	GJO	SCA	Chimp	CDO	RSA	IGWO
	12	Mean	**2.763e+01**	2.695e+01	2.739e+01	2.606e+01	2.644e+01	2.676e+01	2.493e+01	2.733e+01	2.691e+01
		Std	**4.329e-01**	4.663e-01	6.923e-01	4.841e-01	6.974e-01	4.965e-01	6.487e-01	5.108e-01	5.239e-01
	15	Mean	**2.895e+01**	2.819e+01	2.887e+01	2.748e+01	2.759e+01	2.804e+01	2.600e+01	2.879e+01	2.829e+01
		Std	**4.774e-01**	5.198e-01	6.353e-01	7.175e-01	7.626e-01	4.925e-01	6.336e-01	5.342e-01	6.155e-01
SEM-5	5	Mean	**2.081e+01**	2.065e+01	2.066e+01	2.031e+01	2.057e+01	2.046e+01	1.894e+01	2.076e+01	2.065e+01
		Std	**5.432e-02**	1.887e-01	2.391e-01	3.541e-01	3.778e-01	2.265e-01	6.267e-01	9.708e-02	3.044e-01
	7	Mean	**2.281e+01**	2.258e+01	2.257e+01	2.206e+01	2.251e+01	2.232e+01	2.083e+01	2.270e+01	2.276e+01
		Std	**2.092e-01**	3.647e-01	3.989e-01	6.662e-01	5.725e-01	4.284e-01	7.197e-01	3.722e-01	4.337e-01
	9	Mean	**2.462e+01**	2.426e+01	2.456e+01	2.341e+01	2.381e+01	2.385e+01	2.233e+01	2.433e+01	2.388e+01
		Std	**2.425e-01**	4.628e-01	4.208e-01	4.533e-01	4.900e-01	5.246e-01	8.172e-01	3.880e-01	5.399e-01
	12	Mean	**2.663e+01**	2.594e+01	2.645e+01	2.516e+01	2.546e+01	2.558e+01	2.402e+01	2.623e+01	2.574e+01
		Std	**2.904e-01**	5.387e-01	6.679e-01	5.693e-01	5.278e-01	5.532e-01	7.922e-01	4.754e-01	7.794e-01
	15	Mean	**2.821e+01**	2.741e+01	2.794e+01	2.665e+01	2.678e+01	2.705e+01	2.555e+01	2.767e+01	2.708e+01
		Std	**4.293e-01**	5.201e-01	8.108e-01	5.890e-01	5.811e-01	5.215e-01	8.848e-01	4.482e-01	4.315e-01
SEM-6	5	Mean	**1.825e+01**	1.819e+01	1.797e+01	1.780e+01	1.740e+01	1.793e+01	1.799e+01	1.819e+01	1.815e+01
		Std	**1.548e-01**	6.508e-01	5.826e-01	1.322e+00	1.066e+00	1.122e+00	1.412e+00	4.641e-01	5.325e-01
	7	Mean	**2.151e+01**	2.107e+01	2.098e+01	2.070e+01	1.993e+01	2.110e+01	2.051e+01	2.126e+01	2.104e+01
		Std	**3.201e-01**	9.697e-01	1.082e+00	1.490e+00	1.365e+00	1.078e+00	1.317e+00	5.049e-01	1.222e+00
	9	Mean	**2.383e+01**	2.319e+01	2.358e+01	2.214e+01	2.193e+01	2.286e+01	2.196e+01	2.378e+01	2.347e+01
		Std	**6.486e-01**	8.242e-01	1.147e+00	1.505e+00	1.468e+00	1.072e+00	1.277e+00	1.109e+00	1.134e+00
	12	Mean	**2.652e+01**	2.553e+01	2.583e+01	2.468e+01	2.441e+01	2.511e+01	2.403e+01	2.587e+01	2.558e+01
		Std	**6.728e-01**	9.936e-01	1.070e+00	1.170e+00	1.263e+00	9.288e-01	1.207e+00	9.814e-01	9.959e-01
	15	Mean	**2.824e+01**	2.731e+01	2.727e+01	2.624e+01	2.625e+01	2.678e+01	2.537e+01	2.766e+01	2.733e+01
		Std	**5.269e-01**	7.289e-01	1.038e+00	1.378e+00	9.074e-01	8.245e-01	1.393e+00	7.405e-01	1.083e+00
SEM-7	5	Mean	2.262e+01	2.279e+01	2.239e+01	2.174e+01	2.104e+01	2.298e+01	**2.306e+01**	2.271e+01	2.237e+01
		Std	**3.350e-01**	1.616e+00	1.015e+00	1.530e+00	1.207e+00	1.158e+00	1.783e+00	7.732e-01	1.452e+00
	7	Mean	2.604e+01	2.531e+01	2.570e+01	2.407e+01	2.444e+01	2.591e+01	2.515e+01	**2.607e+01**	2.565e+01
		Std	7.473e-01	1.383e+00	**6.817e-01**	1.943e+00	1.802e+00	1.569e+00	1.303e+00	6.885e-01	1.643e+00
	9	Mean	**2.834e+01**	2.754e+01	2.783e+01	2.669e+01	2.581e+01	2.798e+01	2.680e+01	2.821e+01	2.725e+01
		Std	9.212e-01	1.393e+00	1.005e+00	1.584e+00	1.941e+00	1.317e+00	9.451e-01	**6.021e-01**	1.850e+00
	12	Mean	**3.027e+01**	2.932e+01	2.955e+01	2.849e+01	2.793e+01	2.987e+01	2.844e+01	2.970e+01	2.943e+01
		Std	8.385e-01	1.593e+00	1.268e+00	1.506e+00	1.749e+00	1.149e+00	**8.296e-01**	1.240e+00	1.960e+00
	15	Mean	**3.173e+01**	3.046e+01	3.162e+01	2.975e+01	3.005e+01	3.145e+01	2.980e+01	3.122e+01	3.051e+01
		Std	1.051e+00	1.989e+00	1.106e+00	1.305e+00	1.229e+00	1.057e+00	1.010e+00	**9.393e-01**	1.502e+00
SEM-8	5	Mean	**2.101e+01**	2.081e+01	2.088e+01	2.068e+01	2.040e+01	2.071e+01	1.967e+01	2.093e+01	2.087e+01
		Std	**2.189e-02**	1.903e-01	2.770e-01	2.172e-01	4.958e-01	1.734e-01	5.338e-01	1.100e-01	1.853e-01
	7	Mean	**2.334e+01**	2.297e+01	2.316e+01	2.232e+01	2.242e+01	2.281e+01	2.146e+01	2.321e+01	2.299e+01
		Std	**1.634e-01**	2.448e-01	3.649e-01	4.571e-01	4.898e-01	2.802e-01	7.214e-01	1.868e-01	2.992e-01
	9	Mean	**2.498e+01**	2.445e+01	2.480e+01	2.380e+01	2.400e+01	2.417e+01	2.299e+01	2.485e+01	2.462e+01
		Std	**2.221e-01**	4.525e-01	5.091e-01	4.004e-01	4.548e-01	3.700e-01	6.569e-01	3.877e-01	3.834e-01
	12	Mean	**2.688e+01**	2.591e+01	2.674e+01	2.521e+01	2.570e+01	2.578e+01	2.448e+01	2.661e+01	2.614e+01
		Std	**3.529e-01**	4.989e-01	5.002e-01	6.423e-01	6.335e-01	5.886e-01	7.145e-01	5.301e-01	4.790e-01
	15	Mean	**2.806e+01**	2.725e+01	2.783e+01	2.661e+01	2.712e+01	2.730e+01	2.614e+01	2.785e+01	2.740e+01
		Std	4.976e-01	**3.893e-01**	6.458e-01	9.317e-01	6.304e-01	5.985e-01	7.573e-01	4.739e-01	4.483e-01

The best results are

Table 2 – continued

SEM-9	5	Mean	**2.147e+01**	2.138e+01	2.144e+01	2.108e+01	2.127e+01	2.125e+01	2.019e+01	2.144e+01	2.135e+01
		Std	**2.487e-02**	1.088e-01	8.802e-02	2.525e-01	2.388e-01	1.277e-01	4.669e-01	7.094e-02	1.379e-01
	7	Mean	2.376e+01	2.341e+01	2.368e+01	2.299e+01	2.322e+01	2.327e+01	2.184e+01	**2.381e+01**	2.346e+01
		Std	**1.723e-01**	3.120e-01	4.128e-01	3.512e-01	4.374e-01	2.411e-01	6.742e-01	1.962e-01	3.803e-01
	9	Mean	2.532e+01	2.486e+01	2.531e+01	2.430e+01	2.461e+01	2.470e+01	2.338e+01	**2.540e+01**	2.504e+01
		Std	**2.975e-01**	3.736e-01	5.068e-01	4.354e-01	4.360e-01	3.154e-01	7.036e-01	3.799e-01	4.205e-01
	12	Mean	**2.729e+01**	2.631e+01	2.713e+01	2.575e+01	2.610e+01	2.638e+01	2.473e+01	2.714e+01	2.661e+01
		Std	**3.190e-01**	5.045e-01	7.134e-01	6.022e-01	6.549e-01	4.221e-01	8.231e-01	4.887e-01	3.435e-01

The best results are

Table 2 – continued

Images	nTh	Metrics	SCWSO	WSO	GJO	SCA	Chimp	CDO	RSA	IGWO	GWO
	15	Mean	**2.877e+01**	2.786e+01	2.849e+01	2.706e+01	2.767e+01	2.762e+01	2.579e+01	2.870e+01	2.787e+01
		Std	**3.866e-01**	6.007e-01	9.316e-01	7.647e-01	5.739e-01	6.010e-01	7.014e-01	4.035e-01	5.968e-01
SEM-10	5	Mean	**2.190e+01**	2.172e+01	2.183e+01	2.141e+01	2.160e+01	2.155e+01	2.024e+01	2.186e+01	2.166e+01
		Std	**4.224e-02**	2.651e-01	1.478e-01	3.768e-01	2.859e-01	2.659e-01	7.731e-01	1.109e-01	2.783e-01
	7	Mean	**2.420e+01**	2.383e+01	2.394e+01	2.325e+01	2.330e+01	2.348e+01	2.229e+01	2.412e+01	2.365e+01
		Std	**1.222e-01**	4.285e-01	3.346e-01	4.552e-01	5.682e-01	3.356e-01	5.458e-01	2.055e-01	4.975e-01
	9	Mean	**2.592e+01**	2.543e+01	2.563e+01	2.453e+01	2.480e+01	2.523e+01	2.346e+01	2.582e+01	2.528e+01
		Std	**3.020e-01**	5.218e-01	5.565e-01	6.940e-01	6.069e-01	4.310e-01	6.662e-01	3.145e-01	5.533e-01
	12	Mean	**2.790e+01**	2.701e+01	2.756e+01	2.610e+01	2.684e+01	2.681e+01	2.540e+01	2.762e+01	2.702e+01
		Std	**3.925e-01**	5.009e-01	7.526e-01	6.036e-01	5.996e-01	5.617e-01	7.495e-01	5.167e-01	6.078e-01
	15	Mean	**2.941e+01**	2.856e+01	2.889e+01	2.763e+01	2.796e+01	2.825e+01	2.665e+01	2.913e+01	2.841e+01
		Std	**3.652e-01**	6.369e-01	8.323e-01	6.932e-01	5.702e-01	4.679e-01	8.960e-01	5.509e-01	4.904e-01

Table 3: SSIM metrics results for all algorithms.

Images	nTh	Metrics	SCWSO	WSO	GJO	SCA	Chimp	CDO	RSA	IGWO	GWO
SEM-1	5	Mean	7.753e-01	7.661e-01	7.711e-01	7.435e-01	7.406e-01	**7.802e-01**	7.655e-01	7.756e-01	7.686e-01
		Std	**4.166e-03**	2.211e-02	1.168e-02	3.732e-02	3.088e-02	1.895e-02	2.923e-02	6.383e-03	2.162e-02
	7	Mean	**8.597e-01**	8.468e-01	8.517e-01	8.220e-01	8.144e-01	8.454e-01	8.217e-01	8.574e-01	8.433e-01
		Std	9.011e-03	1.626e-02	1.654e-02	2.740e-02	3.074e-02	1.741e-02	2.821e-02	**8.990e-03**	1.418e-02
	9	Mean	**8.950e-01**	8.817e-01	8.882e-01	8.504e-01	8.588e-01	8.843e-01	8.517e-01	8.900e-01	8.791e-01
		Std	**8.047e-03**	1.903e-02	1.539e-02	3.324e-02	2.762e-02	1.694e-02	2.246e-02	1.049e-02	2.428e-02
	12	Mean	**9.290e-01**	9.105e-01	9.226e-01	8.884e-01	8.994e-01	9.140e-01	8.777e-01	9.234e-01	9.112e-01
		Std	**7.942e-03**	1.613e-02	1.694e-02	2.667e-02	1.610e-02	1.282e-02	1.307e-02	1.278e-02	1.550e-02
	15	Mean	**9.446e-01**	9.354e-01	9.392e-01	9.090e-01	9.125e-01	9.357e-01	9.057e-01	9.422e-01	9.281e-01
		Std	**7.610e-03**	1.216e-02	1.120e-02	1.584e-02	1.491e-02	1.014e-02	1.232e-02	1.014e-02	1.690e-02
SEM-2	5	Mean	**8.307e-01**	8.077e-01	8.254e-01	8.058e-01	8.033e-01	8.180e-01	7.813e-01	8.297e-01	8.103e-01
		Std	**2.127e-03**	2.059e-02	1.069e-02	1.952e-02	1.523e-02	1.451e-02	2.199e-02	4.497e-03	1.793e-02
	7	Mean	**8.758e-01**	8.648e-01	8.688e-01	8.506e-01	8.504e-01	8.625e-01	8.356e-01	8.727e-01	8.632e-01
		Std	**1.866e-03**	9.553e-03	1.054e-02	1.490e-02	1.099e-02	9.616e-03	2.071e-02	5.352e-03	1.149e-02
	9	Mean	**9.113e-01**	8.942e-01	9.079e-01	8.841e-01	8.875e-01	8.944e-01	8.710e-01	9.056e-01	8.942e-01
		Std	**4.105e-03**	1.136e-02	8.714e-03	1.740e-02	9.437e-03	6.950e-03	2.070e-02	7.073e-03	1.089e-02
	12	Mean	**9.366e-01**	9.221e-01	9.351e-01	9.086e-01	9.208e-01	9.213e-01	8.970e-01	9.317e-01	9.231e-01
		Std	**4.670e-03**	7.181e-03	8.815e-03	1.402e-02	8.563e-03	6.930e-03	1.461e-02	7.204e-03	1.088e-02
	15	Mean	**9.499e-01**	9.404e-01	9.482e-01	9.335e-01	9.391e-01	9.398e-01	9.213e-01	9.472e-01	9.416e-01
		Std	**5.602e-03**	5.976e-03	8.699e-03	9.831e-03	6.877e-03	7.578e-03	1.348e-02	6.944e-03	1.112e-02
SEM-3	5	Mean	**7.073e-01**	7.020e-01	7.042e-01	6.890e-01	6.966e-01	6.961e-01	6.839e-01	7.055e-01	6.994e-01
		Std	**2.411e-03**	1.007e-02	5.796e-03	1.408e-02	1.091e-02	9.832e-03	2.024e-02	6.095e-03	1.161e-02
	7	Mean	**7.648e-01**	7.559e-01	7.577e-01	7.439e-01	7.430e-01	7.510e-01	7.304e-01	7.606e-01	7.491e-01
		Std	6.205e-03	1.060e-02	1.147e-02	1.795e-02	1.519e-02	1.393e-02	2.316e-02	**5.384e-03**	1.465e-02
	9	Mean	**7.953e-01**	7.862e-01	7.934e-01	7.718e-01	7.783e-01	7.813e-01	7.730e-01	7.877e-01	7.863e-01
		Std	9.188e-03	1.379e-02	1.680e-02	2.132e-02	1.638e-02	9.977e-03	2.277e-02	**7.889e-03**	1.339e-02
	12	Mean	**8.457e-01**	8.279e-01	8.450e-01	8.224e-01	8.287e-01	8.233e-01	8.112e-01	8.353e-01	8.285e-01
		Std	1.974e-02	**1.540e-02**	1.996e-02	1.995e-02	1.898e-02	2.050e-02	2.200e-02	1.745e-02	1.672e-02

The best results are

Table 2 – continued

	15	Mean	**8.892e-01**	8.674e-01	8.813e-01	8.511e-01	8.557e-01	8.545e-01	8.425e-01	8.742e-01	8.621e-01
		Std	1.579e-02	1.782e-02	1.584e-02	1.541e-02	1.773e-02	1.766e-02	2.114e-02	**1.239e-02**	1.956e-02
SEM-4	5	Mean	7.519e-01	7.477e-01	7.527e-01	7.427e-01	7.371e-01	**7.534e-01**	7.250e-01	7.497e-01	7.420e-01
		Std	**2.524e-03**	1.165e-02	9.106e-03	1.996e-02	1.279e-02	1.135e-02	2.314e-02	4.055e-03	1.395e-02
	7	Mean	**8.433e-01**	8.228e-01	8.368e-01	8.139e-01	8.171e-01	8.302e-01	7.905e-01	8.392e-01	8.321e-01
		Std	**5.292e-03**	2.200e-02	1.570e-02	1.504e-02	1.924e-02	1.138e-02	1.649e-02	1.143e-02	9.546e-03

The best results are

Table 3 – continued

Images	nTh	Metrics	SCWSO	GWO	WSO	GJO	SCA	Chimp	CDO	RSA	IGWO
	9	Mean	**8.844e-01**	8.644e-01	8.810e-01	8.477e-01	8.584e-01	8.688e-01	8.295e-01	8.790e-01	8.708e-01
		Std	**5.506e-03**	1.390e-02	1.308e-02	1.380e-02	1.493e-02	8.557e-03	2.119e-02	8.744e-03	9.066e-03
	12	Mean	9.147e-01	9.001e-01	**9.150e-01**	8.891e-01	8.952e-01	9.012e-01	8.742e-01	9.096e-01	8.989e-01
		Std	**6.261e-03**	9.992e-03	1.025e-02	1.231e-02	1.217e-02	7.526e-03	1.116e-02	8.642e-03	1.257e-02
	15	Mean	9.305e-01	9.196e-01	**9.375e-01**	9.154e-01	9.179e-01	9.211e-01	8.968e-01	9.306e-01	9.195e-01
		Std	6.190e-03	9.202e-03	7.973e-03	9.911e-03	8.273e-03	**5.184e-03**	1.021e-02	6.109e-03	1.151e-02
SEM-5	5	Mean	**7.427e-01**	7.380e-01	7.402e-01	7.299e-01	7.341e-01	7.337e-01	6.999e-01	7.418e-01	7.395e-01
		Std	**8.966e-04**	5.368e-03	5.895e-03	1.066e-02	1.008e-02	5.072e-03	1.821e-02	1.765e-03	6.563e-03
	7	Mean	**8.032e-01**	7.944e-01	7.959e-01	7.823e-01	7.895e-01	7.920e-01	7.593e-01	8.008e-01	7.991e-01
		Std	**4.186e-03**	1.098e-02	9.068e-03	1.805e-02	1.714e-02	9.146e-03	1.614e-02	6.395e-03	1.004e-02
	9	Mean	**8.457e-01**	8.348e-01	8.429e-01	8.156e-01	8.222e-01	8.298e-01	7.972e-01	8.397e-01	8.297e-01
		Std	**6.444e-03**	9.930e-03	9.941e-03	1.067e-02	1.164e-02	1.029e-02	1.590e-02	8.380e-03	1.313e-02
	12	Mean	**8.849e-01**	8.703e-01	8.818e-01	8.537e-01	8.579e-01	8.681e-01	8.328e-01	8.751e-01	8.641e-01
		Std	**6.824e-03**	1.220e-02	1.273e-02	1.081e-02	1.065e-02	8.157e-03	1.631e-02	1.007e-02	1.700e-02
	15	Mean	**9.087e-01**	8.944e-01	9.056e-01	8.807e-01	8.836e-01	8.920e-01	8.684e-01	8.992e-01	8.891e-01
		Std	**6.854e-03**	1.050e-02	1.342e-02	1.301e-02	1.040e-02	8.439e-03	1.212e-02	8.421e-03	1.088e-02
SEM-6	5	Mean	7.249e-01	7.215e-01	7.141e-01	7.038e-01	6.922e-01	7.134e-01	**7.259e-01**	7.223e-01	7.195e-01
		Std	**5.555e-03**	2.396e-02	2.125e-02	5.064e-02	3.934e-02	4.041e-02	6.015e-02	1.642e-02	1.805e-02
	7	Mean	**8.315e-01**	8.152e-01	8.139e-01	8.031e-01	7.808e-01	8.201e-01	8.030e-01	8.236e-01	8.158e-01
		Std	**8.547e-03**	2.701e-02	3.424e-02	4.640e-02	4.267e-02	3.576e-02	4.208e-02	1.480e-02	3.828e-02
	9	Mean	**8.834e-01**	8.687e-01	8.759e-01	8.360e-01	8.355e-01	8.620e-01	8.437e-01	8.798e-01	8.719e-01
		Std	**1.388e-02**	1.880e-02	2.661e-02	4.054e-02	3.833e-02	2.670e-02	3.351e-02	2.355e-02	2.544e-02
	12	Mean	**9.271e-01**	9.094e-01	9.192e-01	8.941e-01	8.878e-01	9.093e-01	8.832e-01	9.129e-01	9.104e-01
		Std	**1.128e-02**	1.665e-02	1.593e-02	2.416e-02	2.826e-02	1.763e-02	2.671e-02	1.868e-02	1.850e-02
	15	Mean	**9.464e-01**	9.328e-01	9.342e-01	9.182e-01	9.173e-01	9.334e-01	9.018e-01	9.373e-01	9.329e-01
		Std	**7.463e-03**	1.043e-02	1.344e-02	2.202e-02	1.631e-02	8.443e-03	2.786e-02	9.976e-03	1.655e-02
SEM-7	5	Mean	7.023e-01	7.059e-01	6.904e-01	6.547e-01	6.192e-01	7.218e-01	**7.466e-01**	7.061e-01	6.886e-01
		Std	**1.587e-02**	7.831e-02	5.048e-02	7.773e-02	6.564e-02	5.821e-02	1.033e-01	3.642e-02	7.072e-02
	7	Mean	8.351e-01	8.076e-01	8.237e-01	7.593e-01	7.720e-01	8.323e-01	8.276e-01	**8.369e-01**	8.176e-01
		Std	2.621e-02	5.236e-02	2.633e-02	8.385e-02	7.359e-02	5.949e-02	5.939e-02	**2.517e-02**	6.378e-02
	9	Mean	**8.954e-01**	8.723e-01	8.823e-01	8.496e-01	8.153e-01	8.866e-01	8.766e-01	8.929e-01	8.580e-01
		Std	2.061e-02	4.366e-02	2.593e-02	5.326e-02	6.471e-02	3.608e-02	2.965e-02	**1.494e-02**	5.743e-02
	12	Mean	**9.284e-01**	9.075e-01	9.139e-01	8.900e-01	8.745e-01	9.249e-01	9.114e-01	9.162e-01	9.040e-01
		Std	**1.388e-02**	3.552e-02	2.800e-02	3.638e-02	5.086e-02	2.659e-02	1.552e-02	2.464e-02	5.234e-02
	15	Mean	**9.455e-01**	9.218e-01	9.452e-01	9.155e-01	9.207e-01	9.423e-01	9.300e-01	9.384e-01	9.252e-01
		Std	1.307e-02	4.250e-02	1.722e-02	2.730e-02	2.216e-02	1.545e-02	**1.245e-02**	1.439e-02	2.657e-02
SEM-8	5	Mean	**8.457e-01**	8.376e-01	8.401e-01	8.346e-01	8.200e-01	8.399e-01	8.163e-01	8.419e-01	8.416e-01
		Std	**9.492e-04**	1.008e-02	8.032e-03	1.055e-02	1.794e-02	8.597e-03	1.434e-02	5.369e-03	8.481e-03
	7	Mean	**8.973e-01**	8.884e-01	8.929e-01	8.754e-01	8.717e-01	8.844e-01	8.613e-01	8.940e-01	8.887e-01
		Std	**4.167e-03**	7.013e-03	9.003e-03	1.175e-02	1.332e-02	6.303e-03	1.821e-02	5.718e-03	7.220e-03
	9	Mean	**9.205e-01**	9.121e-01	9.178e-01	9.014e-01	9.035e-01	9.091e-01	8.914e-01	9.174e-01	9.135e-01
		Std	**3.915e-03**	8.912e-03	7.007e-03	8.586e-03	8.032e-03	7.303e-03	1.019e-02	6.507e-03	7.188e-03
	12	Mean	9.436e-01	9.310e-01	**9.440e-01**	9.264e-01	9.270e-01	9.341e-01	9.182e-01	9.392e-01	9.325e-01
		Std	**5.011e-03**	7.741e-03	6.370e-03	9.488e-03	9.266e-03	6.451e-03	1.099e-02	5.949e-03	8.131e-03

The best results are

Table 3 – continued

	15	Mean	**9.541e-01**	9.447e-01	9.536e-01	9.409e-01	9.453e-01	9.475e-01	9.362e-01	9.525e-01	9.459e-01
		Std	**5.159e-03**	6.065e-03	7.725e-03	9.867e-03	6.719e-03	7.171e-03	8.195e-03	5.186e-03	7.028e-03
SEM-9	5	Mean	**7.739e-01**	7.680e-01	7.707e-01	7.564e-01	7.553e-01	7.691e-01	7.492e-01	7.723e-01	7.690e-01
		Std	**2.108e-03**	6.324e-03	6.194e-03	1.603e-02	7.519e-03	8.136e-03	1.800e-02	3.571e-03	7.527e-03
	7	Mean	**8.445e-01**	8.331e-01	8.428e-01	8.256e-01	8.229e-01	8.366e-01	8.038e-01	8.430e-01	8.352e-01
		Std	**5.108e-03**	1.401e-02	9.856e-03	1.178e-02	1.464e-02	1.021e-02	2.247e-02	6.962e-03	1.092e-02
	9	Mean	**8.852e-01**	8.712e-01	8.840e-01	8.607e-01	8.593e-01	8.710e-01	8.532e-01	8.849e-01	8.793e-01
		Std	**7.552e-03**	1.154e-02	1.311e-02	1.229e-02	1.123e-02	9.345e-03	1.297e-02	9.254e-03	1.216e-02

The best results are

Table 3 – continued

Images	nTh	Metrics	SCWSO	WSO	GJO	SCA	Chimp	CDO	RSA	IGWO	GWO
	12	Mean	9.224e-01	9.014e-01	**9.228e-01**	8.944e-01	8.972e-01	9.084e-01	8.824e-01	9.170e-01	9.044e-01
		Std	1.133e-02	1.295e-02	1.109e-02	1.152e-02	1.630e-02	9.511e-03	1.261e-02	**9.342e-03**	1.271e-02
	15	Mean	**9.419e-01**	9.226e-01	9.405e-01	9.187e-01	9.219e-01	9.284e-01	9.043e-01	9.386e-01	9.238e-01
		Std	6.256e-03	1.412e-02	1.278e-02	9.411e-03	8.280e-03	6.689e-03	1.192e-02	**5.938e-03**	1.153e-02
SEM-10	5	Mean	**8.232e-01**	8.142e-01	8.186e-01	8.023e-01	8.064e-01	8.090e-01	7.731e-01	8.198e-01	8.153e-01
		Std	**1.822e-03**	1.237e-02	6.762e-03	1.862e-02	1.586e-02	1.492e-02	3.406e-02	5.418e-03	9.778e-03
	7	Mean	**8.870e-01**	8.718e-01	8.779e-01	8.523e-01	8.506e-01	8.631e-01	8.351e-01	8.834e-01	8.665e-01
		Std	**1.823e-03**	1.373e-02	9.913e-03	1.439e-02	1.718e-02	1.233e-02	1.743e-02	6.511e-03	1.679e-02
	9	Mean	**9.155e-01**	9.026e-01	9.086e-01	8.871e-01	8.883e-01	9.042e-01	8.652e-01	9.129e-01	8.996e-01
		Std	**6.314e-03**	1.158e-02	1.173e-02	1.737e-02	1.361e-02	1.110e-02	1.764e-02	7.881e-03	1.764e-02
	12	Mean	**9.418e-01**	9.260e-01	9.379e-01	9.141e-01	9.220e-01	9.276e-01	9.047e-01	9.364e-01	9.238e-01
		Std	**5.973e-03**	9.651e-03	1.035e-02	1.128e-02	1.076e-02	8.050e-03	1.357e-02	8.491e-03	1.160e-02
	15	Mean	**9.560e-01**	9.441e-01	9.532e-01	9.333e-01	9.386e-01	9.449e-01	9.185e-01	9.523e-01	9.412e-01
		Std	**4.296e-03**	8.467e-03	8.742e-03	1.039e-02	7.493e-03	4.314e-03	1.382e-02	5.635e-03	8.223e-03

Table 4: FSIM metrics results for all algorithms.

Images	nTh	Metrics	SCWSO	WSO	GJO	SCA	Chimp	CDO	RSA	IGWO	GWO
SEM-1	5	Mean	**8.423e-01**	8.357e-01	8.391e-01	8.186e-01	8.171e-01	8.402e-01	8.212e-01	8.418e-01	8.348e-01
		Std	**3.241e-03**	1.416e-02	7.065e-03	2.862e-02	2.175e-02	1.348e-02	1.863e-02	4.977e-03	1.806e-02
	7	Mean	**8.946e-01**	8.876e-01	8.909e-01	8.719e-01	8.676e-01	8.848e-01	8.698e-01	8.924e-01	8.863e-01
		Std	8.712e-03	1.351e-02	1.016e-02	2.220e-02	2.498e-02	1.494e-02	2.338e-02	**7.832e-03**	1.367e-02
	9	Mean	**9.186e-01**	9.112e-01	9.150e-01	8.914e-01	8.985e-01	9.133e-01	8.910e-01	9.132e-01	9.119e-01
		Std	**8.122e-03**	1.559e-02	1.229e-02	2.524e-02	2.299e-02	1.605e-02	2.208e-02	8.605e-03	1.862e-02
	12	Mean	**9.437e-01**	9.328e-01	9.398e-01	9.203e-01	9.303e-01	9.338e-01	9.123e-01	9.371e-01	9.319e-01
		Std	**9.658e-03**	1.554e-02	1.623e-02	1.943e-02	1.374e-02	1.352e-02	1.195e-02	1.222e-02	1.460e-02
	15	Mean	9.544e-01	9.517e-01	**9.545e-01**	9.337e-01	9.387e-01	9.524e-01	9.351e-01	9.518e-01	9.464e-01
		Std	**9.546e-03**	1.186e-02	1.122e-02	1.201e-02	1.462e-02	1.166e-02	1.261e-02	1.131e-02	1.672e-02
SEM-2	5	Mean	**8.769e-01**	8.507e-01	8.724e-01	8.476e-01	8.494e-01	8.624e-01	8.232e-01	8.754e-01	8.519e-01
		Std	**1.746e-03**	2.303e-02	1.193e-02	2.251e-02	1.581e-02	1.481e-02	2.230e-02	3.126e-03	2.169e-02
	7	Mean	**9.026e-01**	8.927e-01	8.972e-01	8.847e-01	8.856e-01	8.966e-01	8.685e-01	8.978e-01	8.938e-01
		Std	**4.257e-03**	9.822e-03	1.204e-02	1.677e-02	1.462e-02	1.363e-02	2.228e-02	1.026e-02	1.366e-02
	9	Mean	**9.343e-01**	9.184e-01	9.301e-01	9.065e-01	9.126e-01	9.174e-01	8.924e-01	9.281e-01	9.187e-01
		Std	**5.865e-03**	1.268e-02	8.385e-03	1.623e-02	1.331e-02	9.921e-03	2.392e-02	6.256e-03	1.015e-02
	12	Mean	**9.522e-01**	9.425e-01	9.495e-01	9.277e-01	9.400e-01	9.403e-01	9.190e-01	9.485e-01	9.418e-01
		Std	**4.542e-03**	6.772e-03	7.965e-03	1.388e-02	7.676e-03	8.814e-03	1.371e-02	6.836e-03	7.431e-03
	15	Mean	**9.617e-01**	9.542e-01	9.605e-01	9.473e-01	9.549e-01	9.519e-01	9.389e-01	9.611e-01	9.545e-01
		Std	6.052e-03	6.383e-03	6.239e-03	8.980e-03	8.702e-03	6.490e-03	1.293e-02	**5.342e-03**	9.176e-03
SEM-3	5	Mean	**8.017e-01**	7.990e-01	8.012e-01	7.826e-01	7.931e-01	7.939e-01	7.688e-01	8.010e-01	7.965e-01
		Std	**1.551e-03**	5.898e-03	4.637e-03	1.485e-02	1.165e-02	6.436e-03	1.520e-02	3.383e-03	9.395e-03
	7	Mean	**8.541e-01**	8.439e-01	8.460e-01	8.250e-01	8.289e-01	8.393e-01	8.021e-01	8.505e-01	8.389e-01
		Std	**4.583e-03**	8.915e-03	1.097e-02	1.259e-02	1.103e-02	9.739e-03	2.366e-02	5.334e-03	1.210e-02
	9	Mean	**8.806e-01**	8.691e-01	8.714e-01	8.488e-01	8.560e-01	8.640e-01	8.321e-01	8.742e-01	8.717e-01

The best results are

Table 3 – continued

		Std	7.893e-03	1.091e-02	1.147e-02	1.394e-02	1.170e-02	8.155e-03	1.442e-02	**7.656e-03**	1.068e-02
	12	Mean	**9.103e-01**	8.990e-01	8.990e-01	8.764e-01	8.840e-01	8.927e-01	8.660e-01	9.048e-01	8.990e-01
		Std	**8.741e-03**	1.042e-02	1.096e-02	1.149e-02	1.118e-02	1.152e-02	1.567e-02	1.035e-02	8.904e-03
	15	Mean	**9.318e-01**	9.197e-01	9.220e-01	8.988e-01	9.028e-01	9.082e-01	8.918e-01	9.180e-01	9.172e-01
		Std	**6.768e-03**	8.094e-03	8.878e-03	1.246e-02	9.651e-03	7.586e-03	1.469e-02	8.062e-03	7.339e-03
SEM-4	5	Mean	**8.562e-01**	8.534e-01	8.543e-01	8.473e-01	8.551e-01	8.496e-01	8.114e-01	8.557e-01	8.484e-01
		Std	**6.925e-04**	4.465e-03	3.226e-03	7.617e-03	5.304e-03	4.119e-03	1.771e-02	2.357e-03	7.579e-03

The best results are

Table 4 – continued

Images	nTh	Metrics	SCWSO GWO	WSO	GJO	SCA	Chimp	CDO	RSA	IGWO
	7	Mean	**8.992e-01**	8.908e-01	8.975e-01	8.851e-01	8.908e-01	8.889e-01	8.508e-01	8.981e-01	8.914e-01
		Std	**2.905e-03**	7.251e-03	8.646e-03	1.146e-02	1.222e-02	8.017e-03	1.383e-02	4.565e-03	5.429e-03
	9	Mean	**9.262e-01**	9.132e-01	9.244e-01	9.013e-01	9.153e-01	9.138e-01	8.816e-01	9.233e-01	9.175e-01
		Std	**4.893e-03**	8.647e-03	1.060e-02	1.448e-02	1.070e-02	9.246e-03	1.615e-02	9.059e-03	6.823e-03
	12	Mean	9.478e-01	9.382e-01	**9.483e-01**	9.293e-01	9.379e-01	9.360e-01	9.173e-01	9.455e-01	9.370e-01
		Std	**5.556e-03**	8.186e-03	9.362e-03	9.139e-03	8.400e-03	8.247e-03	1.426e-02	6.160e-03	7.884e-03
	15	Mean	9.582e-01	9.518e-01	**9.613e-01**	9.464e-01	9.520e-01	9.507e-01	9.269e-01	9.588e-01	9.510e-01
		Std	**3.789e-03**	6.456e-03	7.404e-03	9.246e-03	8.091e-03	6.420e-03	1.324e-02	5.411e-03	6.615e-03
SEM-5	5	Mean	**7.945e-01**	7.903e-01	7.911e-01	7.837e-01	7.879e-01	7.862e-01	7.550e-01	7.929e-01	7.914e-01
		Std	**9.031e-04**	4.766e-03	5.083e-03	8.885e-03	8.558e-03	5.136e-03	1.644e-02	2.291e-03	5.450e-03
	7	Mean	**8.448e-01**	8.378e-01	8.389e-01	8.269e-01	8.348e-01	8.344e-01	8.037e-01	8.424e-01	8.414e-01
		Std	**2.651e-03**	7.687e-03	7.517e-03	1.444e-02	1.197e-02	7.422e-03	1.379e-02	5.814e-03	8.066e-03
	9	Mean	**8.818e-01**	8.725e-01	8.806e-01	8.563e-01	8.626e-01	8.659e-01	8.369e-01	8.757e-01	8.665e-01
		Std	**4.829e-03**	9.617e-03	7.449e-03	8.990e-03	9.079e-03	9.099e-03	1.418e-02	7.024e-03	1.044e-02
	12	Mean	**9.143e-01**	9.023e-01	9.128e-01	8.890e-01	8.928e-01	8.984e-01	8.687e-01	9.063e-01	8.972e-01
		Std	**5.414e-03**	8.725e-03	1.028e-02	9.232e-03	9.095e-03	7.452e-03	1.281e-02	7.908e-03	1.303e-02
	15	Mean	**9.352e-01**	9.224e-01	9.324e-01	9.120e-01	9.150e-01	9.184e-01	8.967e-01	9.274e-01	9.169e-01
		Std	5.755e-03	7.359e-03	1.077e-02	8.403e-03	7.536e-03	7.752e-03	1.204e-02	**5.606e-03**	8.222e-03
SEM-6	5	Mean	**8.088e-01**	8.073e-01	8.053e-01	7.969e-01	7.958e-01	8.032e-01	7.850e-01	8.079e-01	8.076e-01
		Std	**1.503e-03**	9.528e-03	7.596e-03	1.716e-02	1.216e-02	1.308e-02	2.317e-02	4.690e-03	7.699e-03
	7	Mean	**8.736e-01**	8.627e-01	8.614e-01	8.504e-01	8.446e-01	8.584e-01	8.361e-01	8.672e-01	8.631e-01
		Std	**4.743e-03**	1.298e-02	1.909e-02	2.209e-02	1.763e-02	1.508e-02	2.704e-02	7.283e-03	1.638e-02
	9	Mean	**9.106e-01**	8.966e-01	9.043e-01	8.772e-01	8.749e-01	8.900e-01	8.688e-01	9.066e-01	9.009e-01
		Std	**8.920e-03**	1.186e-02	1.623e-02	2.085e-02	2.104e-02	1.475e-02	2.119e-02	1.514e-02	1.465e-02
	12	Mean	**9.429e-01**	9.275e-01	9.320e-01	9.132e-01	9.114e-01	9.201e-01	9.029e-01	9.309e-01	9.291e-01
		Std	**8.494e-03**	1.154e-02	1.385e-02	1.581e-02	1.588e-02	1.404e-02	1.605e-02	1.193e-02	1.339e-02
	15	Mean	**9.567e-01**	9.460e-01	9.468e-01	9.324e-01	9.342e-01	9.402e-01	9.179e-01	9.487e-01	9.460e-01
		Std	**6.154e-03**	9.132e-03	1.152e-02	1.597e-02	1.023e-02	9.289e-03	1.644e-02	9.165e-03	1.396e-02
SEM-7	5	Mean	8.123e-01	8.204e-01	8.121e-01	8.068e-01	7.985e-01	8.207e-01	**8.313e-01**	8.149e-01	8.164e-01
		Std	**5.939e-03**	2.736e-02	1.334e-02	1.899e-02	1.637e-02	2.006e-02	4.043e-02	1.282e-02	2.559e-02
	7	Mean	8.790e-01	8.666e-01	8.725e-01	8.498e-01	8.568e-01	8.781e-01	8.777e-01	**8.794e-01**	8.756e-01
		Std	1.711e-02	2.837e-02	**1.402e-02**	3.415e-02	3.264e-02	3.358e-02	2.809e-02	1.558e-02	3.323e-02
	9	Mean	**9.176e-01**	9.067e-01	9.097e-01	8.940e-01	8.794e-01	9.122e-01	9.061e-01	9.155e-01	9.012e-01
		Std	1.684e-02	2.739e-02	1.822e-02	3.350e-02	3.429e-02	2.592e-02	2.059e-02	**1.137e-02**	3.454e-02
	12	Mean	**9.405e-01**	9.319e-01	9.319e-01	9.201e-01	9.130e-01	9.395e-01	9.323e-01	9.304e-01	9.317e-01
		Std	1.263e-02	2.529e-02	2.016e-02	2.782e-02	3.235e-02	1.958e-02	**1.261e-02**	1.874e-02	2.979e-02
	15	Mean	9.548e-01	9.417e-01	**9.557e-01**	9.386e-01	9.415e-01	9.540e-01	9.478e-01	9.473e-01	9.429e-01
		Std	1.230e-02	2.913e-02	1.390e-02	2.085e-02	1.741e-02	1.336e-02	**1.038e-02**	1.216e-02	2.024e-02
SEM-8	5	Mean	**8.895e-01**	8.855e-01	8.866e-01	8.852e-01	8.780e-01	8.836e-01	8.567e-01	8.876e-01	8.871e-01
		Std	**1.228e-03**	5.638e-03	7.413e-03	8.885e-03	1.361e-02	6.368e-03	1.650e-02	3.568e-03	5.462e-03
	7	Mean	**9.275e-01**	9.200e-01	9.242e-01	9.112e-01	9.125e-01	9.166e-01	8.897e-01	9.245e-01	9.219e-01
		Std	**4.290e-03**	6.126e-03	7.885e-03	1.021e-02	9.255e-03	7.809e-03	1.936e-02	5.138e-03	7.526e-03
	9	Mean	**9.453e-01**	9.377e-01	9.419e-01	9.280e-01	9.339e-01	9.325e-01	9.156e-01	9.429e-01	9.394e-01
		Std	**3.520e-03**	7.768e-03	8.153e-03	7.333e-03	6.396e-03	7.574e-03	1.504e-02	6.000e-03	6.480e-03

The best results are

Table 4 – continued

	12	Mean	9.578e-01	9.498e-01	**9.591e-01**	9.424e-01	9.497e-01	9.463e-01	9.332e-01	9.557e-01	9.510e-01
		Std	**3.338e-03**	6.415e-03	5.032e-03	9.885e-03	7.383e-03	6.972e-03	1.152e-02	4.913e-03	5.088e-03
	15	Mean	9.638e-01	9.574e-01	**9.642e-01**	9.552e-01	9.602e-01	9.599e-01	9.506e-01	9.628e-01	9.598e-01
		Std	4.479e-03	**4.179e-03**	5.324e-03	8.698e-03	7.676e-03	5.342e-03	9.335e-03	5.157e-03	5.320e-03
SEM-9	5	Mean	**8.428e-01**	8.387e-01	8.415e-01	8.319e-01	8.347e-01	8.383e-01	8.085e-01	8.419e-01	8.394e-01
		Std	**9.689e-04**	4.959e-03	2.394e-03	7.702e-03	6.763e-03	4.183e-03	1.221e-02	1.971e-03	4.473e-03
	7	Mean	8.899e-01	8.832e-01	8.884e-01	8.748e-01	8.775e-01	8.816e-01	8.499e-01	**8.905e-01**	8.839e-01
		Std	**4.158e-03**	7.422e-03	7.440e-03	7.257e-03	9.052e-03	5.365e-03	1.673e-02	4.801e-03	7.421e-03

The best results are

Images	nTh	Metrics	SCWSO	GWO	WSO	GJO	SCA	Chimp	CDO	RSA	IGWO
	9	Mean	9.175e-01	9.069e-01	9.161e-01	8.975e-01	9.036e-01	9.048e-01	8.829e-01	**9.178e-01**	9.123e-01
		Std	5.891e-03	8.308e-03	9.782e-03	8.090e-03	7.861e-03	**5.285e-03**	1.197e-02	8.427e-03	8.044e-03
	12	Mean	9.437e-01	9.279e-01	**9.442e-01**	9.219e-01	9.253e-01	9.286e-01	9.042e-01	9.406e-01	9.313e-01
		Std	6.933e-03	8.465e-03	9.680e-03	8.030e-03	1.050e-02	6.717e-03	1.231e-02	7.592e-03	**6.404e-03**
	15	Mean	**9.560e-01**	9.429e-01	9.559e-01	9.373e-01	9.462e-01	9.428e-01	9.208e-01	9.542e-01	9.445e-01
		Std	**5.287e-03**	9.106e-03	1.062e-02	9.756e-03	6.681e-03	5.863e-03	1.075e-02	5.363e-03	6.711e-03
SEM-10	5	Mean	**8.720e-01**	8.694e-01	8.709e-01	8.585e-01	8.657e-01	8.631e-01	8.269e-01	8.714e-01	8.672e-01
		Std	**1.490e-03**	7.096e-03	5.746e-03	9.642e-03	8.599e-03	7.498e-03	1.978e-02	3.562e-03	9.479e-03
	7	Mean	**9.162e-01**	9.088e-01	9.115e-01	8.972e-01	8.986e-01	9.005e-01	8.760e-01	9.150e-01	9.053e-01
		Std	**4.355e-03**	1.165e-02	8.131e-03	1.332e-02	1.491e-02	1.110e-02	1.730e-02	6.204e-03	1.207e-02
	9	Mean	**9.397e-01**	9.305e-01	9.371e-01	9.159e-01	9.206e-01	9.286e-01	8.986e-01	9.378e-01	9.289e-01
		Std	**5.626e-03**	1.167e-02	9.670e-03	1.060e-02	9.939e-03	7.524e-03	1.259e-02	6.319e-03	1.078e-02
	12	Mean	**9.589e-01**	9.481e-01	9.548e-01	9.373e-01	9.484e-01	9.447e-01	9.267e-01	9.559e-01	9.486e-01
		Std	**4.984e-03**	8.335e-03	9.204e-03	8.085e-03	6.822e-03	8.711e-03	1.376e-02	5.908e-03	9.102e-03
	15	Mean	**9.690e-01**	9.601e-01	9.652e-01	9.537e-01	9.571e-01	9.583e-01	9.421e-01	9.661e-01	9.592e-01
		Std	**4.329e-03**	8.227e-03	6.866e-03	6.705e-03	4.487e-03	5.394e-03	1.319e-02	6.119e-03	6.376e-03

Table 5. P and H Comparison findings from the Wilcoxon test between the proposed SCWSO vs Different methods.

Images	nTh	WSO		GJO		SCA		Chimp		CDO		RSA		IGWO		GWO	
		P	h	P	h	P	h	P	h	P	h	P	h	P	h	P	h
SEM-1	5	0.673279807 –	0	0.734325291 –	0	0.014795424 ++	1	6.31976e-05 ++	1	0.000570644 ++	1	0.245190309 –	0	0.030009891 ++	1	1.7344e-06 ++	1
	7	1.7344e-06 ++	1	1.7344e-06 ++	1	1.7344e-06 ++	1	1.7344e-06 ++	1	1.7344e-06 ++	1	1.7344e-06 ++	1	1.7344e-06 ++	1	1.7344e-06 ++	1
	9	1.7344e-06 ++	1	1.7344e-06 ++	1	1.7344e-06 ++	1	1.7344e-06 ++	1	1.7344e-06 ++	1	1.7344e-06 ++	1	1.7344e-06 ++	1	1.7344e-06 ++	1
	12	1.7344e-06 ++	1	1.7344e-06 ++	1	1.7344e-06 ++	1	1.7344e-06 ++	1	1.7344e-06 ++	1	1.7344e-06 ++	1	1.7344e-06 ++	1	1.7344e-06 ++	1
	15	1.7344e-06 ++	1	1.7344e-06 ++	1	1.7344e-06 ++	1	1.7344e-06 ++	1	1.7344e-06 ++	1	1.7344e-06 ++	1	1.7344e-06 ++	1	1.7344e-06 ++	1
SEM-2	5	1.7344e-06 ++	1	0.001035681 ++	1	1.7344e-06 ++	1	1.7344e-06 ++	1	1.7344e-06 ++	1	1.7344e-06 ++	1	0.000175692 ++	1	1.7344e-06 ++	1
	7	1.7344e-06 ++	1	1.7344e-06 ++	1	1.7344e-06 ++	1	1.7344e-06 ++	1	1.7344e-06 ++	1	1.7344e-06 ++	1	1.7344e-06 ++	1	1.7344e-06 ++	1
	9	1.7344e-06 ++	1	1.7344e-06 ++	1	1.7344e-06 ++	1	1.7344e-06 ++	1	1.7344e-06 ++	1	1.7344e-06 ++	1	1.7344e-06 ++	1	1.7344e-06 ++	1
	12	1.7344e-06 ++	1	1.7344e-06 ++	1	1.7344e-06 ++	1	1.7344e-06 ++	1	1.7344e-06 ++	1	1.7344e-06 ++	1	1.7344e-06 ++	1	1.7344e-06 ++	1
	15	1.7344e-06 ++	1	1.7344e-06 ++	1	1.7344e-06 ++	1	1.7344e-06 ++	1	1.7344e-06 ++	1	1.7344e-06 ++	1	1.7344e-06 ++	1	1.7344e-06 ++	1
SEM-3	5	6.33914e-06 ++	1	0.000160464 ++	1	1.92092e-06 ++	1	1.7344e-06 ++	1	1.7344e-06 ++	1	1.7344e-06 ++	1	0.015788387 ++	1	1.7344e-06 ++	1
	7	1.7344e-06 ++	1	1.7344e-06 ++	1	1.7344e-06 ++	1	1.7344e-06 ++	1	1.7344e-06 ++	1	1.7344e-06 ++	1	1.7344e-06 ++	1	1.7344e-06 ++	1
	9	1.7344e-06 ++	1	1.7344e-06 ++	1	1.7344e-06 ++	1	1.7344e-06 ++	1	1.7344e-06 ++	1	1.7344e-06 ++	1	1.7344e-06 ++	1	1.7344e-06 ++	1
	12	1.7344e-06 ++	1	1.7344e-06 ++	1	1.7344e-06 ++	1	1.7344e-06 ++	1	1.7344e-06 ++	1	1.7344e-06 ++	1	1.7344e-06 ++	1	1.7344e-06 ++	1
	15	1.7344e-06 ++	1	1.7344e-06 ++	1	1.7344e-06 ++	1	1.7344e-06 ++	1	1.7344e-06 ++	1	1.7344e-06 ++	1	1.7344e-06 ++	1	1.7344e-06 ++	1
SEM-4	5	2.16302e-05 ++	1	5.79245e-05 ++	1	1.92092e-06 ++	1	2.60333e-06 ++	1	2.8786e-06 ++	1	1.92092e-06 ++	1	2.59671e-05 ++	1	1.7344e-06 ++	1
	7	1.7344e-06 ++	1	1.7344e-06 ++	1	1.7344e-06 ++	1	1.7344e-06 ++	1	1.7344e-06 ++	1	1.7344e-06 ++	1	1.7344e-06 ++	1	1.7344e-06 ++	1
	9	1.7344e-06 ++	1	1.7344e-06 ++	1	1.7344e-06 ++	1	1.7344e-06 ++	1	1.7344e-06 ++	1	1.7344e-06 ++	1	1.7344e-06 ++	1	1.7344e-06 ++	1
	12	1.7344e-06 ++	1	1.7344e-06 ++	1	1.7344e-06 ++	1	1.7344e-06 ++	1	1.7344e-06 ++	1	1.7344e-06 ++	1	1.7344e-06 ++	1	1.7344e-06 ++	1
	15	1.7344e-06 ++	1	1.7344e-06 ++	1	1.7344e-06 ++	1	1.7344e-06 ++	1	1.7344e-06 ++	1	1.7344e-06 ++	1	1.7344e-06 ++	1	1.7344e-06 ++	1
SEM-5	5	2.60333e-06 ++	1	0.000135948 ++	1	2.60333e-06 ++	1	4.44934e-05 ++	1	5.21649e-06 ++	1	1.7344e-06 ++	1	0.000306387 ++	1	1.7344e-06 ++	1
	7	1.7344e-06 ++	1	1.7344e-06 ++	1	1.7344e-06 ++	1	1.7344e-06 ++	1	1.7344e-06 ++	1	1.7344e-06 ++	1	1.7344e-06 ++	1	1.7344e-06 ++	1
	9	1.7344e-06 ++	1	1.7344e-06 ++	1	1.7344e-06 ++	1	1.7344e-06 ++	1	1.7344e-06 ++	1	1.7344e-06 ++	1	1.7344e-06 ++	1	1.7344e-06 ++	1
	12	1.7344e-06 ++	1	1.7344e-06 ++	1	1.7344e-06 ++	1	1.7344e-06 ++	1	1.7344e-06 ++	1	1.7344e-06 ++	1	1.7344e-06 ++	1	1.7344e-06 ++	1
	15	1.7344e-06 ++	1	1.7344e-06 ++	1	1.7344e-06 ++	1	1.7344e-06 ++	1	1.7344e-06 ++	1	1.7344e-06 ++	1	1.7344e-06 ++	1	1.7344e-06 ++	1
SEM-6	5	0.125438239 –	0	1.7344e-06 ++	1	0.028485956 ++	1	0.00183258 ++	1	0.958990172 –	0	0.585711569 –	0	0.803618522 –	0	1.7344e-06 ++	1
	7	1.7344e-06 ++	1	1.7344e-06 ++	1	1.7344e-06 ++	1	1.7344e-06 ++	1	1.7344e-06 ++	1	1.7344e-06 ++	1	1.7344e-06 ++	1	1.7344e-06 ++	1
	9	1.7344e-06 ++	1	1.7344e-06 ++	1	1.7344e-06 ++	1	1.7344e-06 ++	1	1.7344e-06 ++	1	1.7344e-06 ++	1	1.7344e-06 ++	1	1.7344e-06 ++	1
	12	1.7344e-06 ++	1	1.7344e-06 ++	1	1.7344e-06 ++	1	1.7344e-06 ++	1	1.7344e-06 ++	1	1.7344e-06 ++	1	1.7344e-06 ++	1	1.7344e-06 ++	1
	15	1.7344e-06 ++	1	1.7344e-06 ++	1	1.7344e-06 ++	1	1.7344e-06 ++	1	1.7344e-06 ++	1	1.7344e-06 ++	1	1.7344e-06 ++	1	1.7344e-06 ++	1
SEM-7	5	0.038723026 ++	1	1.7344e-06 ++	1	0.001708773 ++	1	7.69086e-06 ++	1	0.765519292 –	0	0.005667173 ++	1	0.308614851 –	0	1.7344e-06 ++	1
	7	1.7344e-06 ++	1	1.7344e-06 ++	1	1.7344e-06 ++	1	1.7344e-06 ++	1	1.7344e-06 ++	1	1.7344e-06 ++	1	1.7344e-06 ++	1	1.7344e-06 ++	1
	9	1.7344e-06 ++	1	1.7344e-06 ++	1	1.7344e-06 ++	1	1.7344e-06 ++	1	1.7344e-06 ++	1	1.7344e-06 ++	1	1.7344e-06 ++	1	1.7344e-06 ++	1

	12	1.7344e-06 ++	1	1.7344e-06 ++	1	1.7344e-06 ++	1	1.7344e-06 ++	1	1.7344e-06 ++	1	1.7344e-06 ++	1	1.7344e-06 ++	1	1.7344e-06 ++	1
	15	1.7344e-06 ++	1	1.7344e-06 ++	1	1.7344e-06 ++	1	1.7344e-06 ++	1	1.7344e-06 ++	1	1.7344e-06 ++	1	1.7344e-06 ++	1	1.7344e-06 ++	1
SEM-8	5	2.8786e-06 ++	1	2.35342e-06 ++	1	1.7344e-06 ++	1	1.7344e-06 ++	1	1.7344e-06 ++	1	1.7344e-06 ++	1	1.02463e-05 ++	1	1.7344e-06 ++	1
	7	1.7344e-06 ++	1	1.7344e-06 ++	1	1.7344e-06 ++	1	1.7344e-06 ++	1	1.7344e-06 ++	1	1.7344e-06 ++	1	1.7344e-06 ++	1	1.7344e-06 ++	1
	9	1.7344e-06 ++	1	1.7344e-06 ++	1	1.7344e-06 ++	1	1.7344e-06 ++	1	1.7344e-06 ++	1	1.7344e-06 ++	1	1.7344e-06 ++	1	1.7344e-06 ++	1
	12	1.7344e-06 ++	1	1.7344e-06 ++	1	1.7344e-06 ++	1	1.7344e-06 ++	1	1.7344e-06 ++	1	1.7344e-06 ++	1	1.7344e-06 ++	1	1.7344e-06 ++	1
	15	1.7344e-06 ++	1	1.7344e-06 ++	1	1.7344e-06 ++	1	1.7344e-06 ++	1	1.7344e-06 ++	1	1.7344e-06 ++	1	1.7344e-06 ++	1	1.7344e-06 ++	1
SEM-9	5	1.02463e-05 ++	1	0.346905139 –	0	1.7344e-06 ++	1	3.18168e-06 ++	1	1.7344e-06 ++	1	1.7344e-06 ++	1	3.16517e-06 ++	1	1.7344e-06 ++	1
	7	1.7344e-06 ++	1	1.7344e-06 ++	1	1.7344e-06 ++	1	1.7344e-06 ++	1	1.7344e-06 ++	1	1.7344e-06 ++	1	1.7344e-06 ++	1	1.7344e-06 ++	1
	9	1.7344e-06 ++	1	1.7344e-06 ++	1	1.7344e-06 ++	1	1.7344e-06 ++	1	1.7344e-06 ++	1	1.7344e-06 ++	1	1.7344e-06 ++	1	1.7344e-06 ++	1
	12	1.7344e-06 ++	1	1.7344e-06 ++	1	1.7344e-06 ++	1	1.7344e-06 ++	1	1.7344e-06 ++	1	1.7344e-06 ++	1	1.7344e-06 ++	1	1.7344e-06 ++	1
	15	1.7344e-06 ++	1	1.7344e-06 ++	1	1.7344e-06 ++	1	1.7344e-06 ++	1	1.7344e-06 ++	1	1.7344e-06 ++	1	1.7344e-06 ++	1	1.7344e-06 ++	1
SEM-10	5	2.60333e-06 ++	1	0.031603382 ++	1	1.7344e-06 ++	1	3.88218e-06 ++	1	1.7344e-06 ++	1	1.7344e-06 ++	1	1.02463e-05 ++	1	1.7344e-06 ++	1
	7	1.7344e-06 ++	1	1.7344e-06 ++	1	1.7344e-06 ++	1	1.7344e-06 ++	1	1.7344e-06 ++	1	1.7344e-06 ++	1	1.7344e-06 ++	1	1.7344e-06 ++	1
	9	1.7344e-06 ++	1	1.7344e-06 ++	1	1.7344e-06 ++	1	1.7344e-06 ++	1	1.7344e-06 ++	1	1.7344e-06 ++	1	1.7344e-06 ++	1	1.7344e-06 ++	1
	12	1.7344e-06 ++	1	1.7344e-06 ++	1	1.7344e-06 ++	1	1.7344e-06 ++	1	1.7344e-06 ++	1	1.7344e-06 ++	1	1.7344e-06 ++	1	1.7344e-06 ++	1
	15	1.7344e-06 ++	1	1.7344e-06 ++	1	1.7344e-06 ++	1	1.7344e-06 ++	1	1.7344e-06 ++	1	1.7344e-06 ++	1	1.7344e-06 ++	1	1.7344e-06 ++	1

Table 6. P and H Comparison findings from the Wilcoxon test between the proposed SCWSO vs. WSO, SCWSO vs. Different methods.

Images	nTh	WSO		GJO		SCA		Chimp		CDO		RSA		IGWO		GWO	
		P	h	P	h	P	h	P	h	P	h	P	h	P	h	P	h
SEM-1	5	0.298943752 –	0	0.893644387 –	0	0.000771217 ++	1	1.64e-05 ++	1	0.020671114 ++	1	0.005319684 ++	1	0.01319417 ++	1	1.73e-06 ++	1
	7	1.73e-06 ++	1	1.73e-06 ++	1	1.73e-06 ++	1	1.73e-06 ++	1	1.73e-06 ++	1	1.73e-06 ++	1	1.73e-06 ++	1	1.73e-06 ++	1
	9	1.73e-06 ++	1	1.73e-06 ++	1	1.73e-06 ++	1	1.73e-06 ++	1	1.73e-06 ++	1	1.73e-06 ++	1	1.73e-06 ++	1	1.73e-06 ++	1
	12	1.73e-06 ++	1	1.73e-06 ++	1	1.73e-06 ++	1	1.73e-06 ++	1	1.73e-06 ++	1	1.73e-06 ++	1	1.73e-06 ++	1	1.73e-06 ++	1
	15	1.73e-06 ++	1	1.73e-06 ++	1	1.73e-06 ++	1	1.73e-06 ++	1	1.73e-06 ++	1	1.73e-06 ++	1	1.73e-06 ++	1	1.73e-06 ++	1
SEM-2	5	1.73e-06 ++	1	4.07e-05 ++	1	1.73e-06 ++	1	2.35e-06 ++	1	0.0003065 ++	1	1.73e-06 ++	1	0.085895826 –	0	1.73e-06 ++	1
	7	1.73e-06 ++	1	1.73e-06 ++	1	1.73e-06 ++	1	1.73e-06 ++	1	1.73e-06 ++	1	1.73e-06 ++	1	1.73e-06 ++	1	1.73e-06 ++	1
	9	1.73e-06 ++	1	1.73e-06 ++	1	1.73e-06 ++	1	1.73e-06 ++	1	1.73e-06 ++	1	1.73e-06 ++	1	1.73e-06 ++	1	1.73e-06 ++	1
	12	1.73e-06 ++	1	1.73e-06 ++	1	1.73e-06 ++	1	1.73e-06 ++	1	1.73e-06 ++	1	1.73e-06 ++	1	1.73e-06 ++	1	1.73e-06 ++	1
	15	1.73e-06 ++	1	1.73e-06 ++	1	1.73e-06 ++	1	1.73e-06 ++	1	1.73e-06 ++	1	1.73e-06 ++	1	1.73e-06 ++	1	1.73e-06 ++	1
SEM-3	5	3.11e-05 ++	1	4.86e-05 ++	1	2.84e-05 ++	1	1.92e-06 ++	1	9.32e-06 ++	1	0.000261343 ++	1	0.089607669 –	0	1.73e-06 ++	1
	7	1.73e-06 ++	1	1.73e-06 ++	1	1.73e-06 ++	1	1.73e-06 ++	1	1.73e-06 ++	1	1.73e-06 ++	1	1.73e-06 ++	1	1.73e-06 ++	1
	9	1.73e-06 ++	1	1.73e-06 ++	1	1.73e-06 ++	1	1.73e-06 ++	1	1.73e-06 ++	1	1.73e-06 ++	1	1.73e-06 ++	1	1.73e-06 ++	1
	12	1.73e-06 ++	1	1.73e-06 ++	1	1.73e-06 ++	1	1.73e-06 ++	1	1.73e-06 ++	1	1.73e-06 ++	1	1.73e-06 ++	1	1.73e-06 ++	1
	15	1.73e-06 ++	1	1.73e-06 ++	1	1.73e-06 ++	1	1.73e-06 ++	1	1.73e-06 ++	1	1.73e-06 ++	1	1.73e-06 ++	1	1.73e-06 ++	1
SEM-4	5	0.005319684 ++	1	0.00183258 ++	1	0.00727105 ++	1	5.31e-05 ++	1	0.942610512 –	0	2.84e-05 ++	1	0.552073834 –	0	1.73e-06 ++	1
	7	1.73e-06 ++	1	1.73e-06 ++	1	1.73e-06 ++	1	1.73e-06 ++	1	1.73e-06 ++	1	1.73e-06 ++	1	1.73e-06 ++	1	1.73e-06 ++	1
	9	1.73e-06 ++	1	1.73e-06 ++	1	1.73e-06 ++	1	1.73e-06 ++	1	1.73e-06 ++	1	1.73e-06 ++	1	1.73e-06 ++	1	1.73e-06 ++	1
	12	1.73e-06 ++	1	1.73e-06 ++	1	1.73e-06 ++	1	1.73e-06 ++	1	1.73e-06 ++	1	1.73e-06 ++	1	1.73e-06 ++	1	1.73e-06 ++	1
	15	1.73e-06 ++	1	1.73e-06 ++	1	1.73e-06 ++	1	1.73e-06 ++	1	1.73e-06 ++	1	1.73e-06 ++	1	1.73e-06 ++	1	1.73e-06 ++	1
SEM-5	5	0.004681835 ++	1	0.001035681 ++	1	2.13e-06 ++	1	4.73e-06 ++	1	4.73e-06 ++	1	1.73e-06 ++	1	0.503832969 –	0	1.73e-06 ++	1
	7	1.73e-06 ++	1	1.73e-06 ++	1	1.73e-06 ++	1	1.73e-06 ++	1	1.73e-06 ++	1	1.73e-06 ++	1	1.73e-06 ++	1	1.73e-06 ++	1
	9	1.73e-06 ++	1	1.73e-06 ++	1	1.73e-06 ++	1	1.73e-06 ++	1	1.73e-06 ++	1	1.73e-06 ++	1	1.73e-06 ++	1	1.73e-06 ++	1
	12	1.73e-06 ++	1	1.73e-06 ++	1	1.73e-06 ++	1	1.73e-06 ++	1	1.73e-06 ++	1	1.73e-06 ++	1	1.73e-06 ++	1	1.73e-06 ++	1
	15	1.73e-06 ++	1	1.73e-06 ++	1	1.73e-06 ++	1	1.73e-06 ++	1	1.73e-06 ++	1	1.73e-06 ++	1	1.73e-06 ++	1	1.73e-06 ++	1
SEM-6	5	0.062682812 –	0	1.73e-06 ++	1	0.004991554 ++	1	0.000189097 ++	1	0.926255087 –	0	0.628843002 –	0	0.845080424 –	0	1.73e-06 ++	1
	7	1.73e-06 ++	1	1.73e-06 ++	1	1.73e-06 ++	1	1.73e-06 ++	1	1.73e-06 ++	1	1.73e-06 ++	1	1.73e-06 ++	1	1.73e-06 ++	1
	9	1.73e-06 ++	1	1.73e-06 ++	1	1.73e-06 ++	1	1.73e-06 ++	1	1.73e-06 ++	1	1.73e-06 ++	1	1.73e-06 ++	1	1.73e-06 ++	1
	12	1.73e-06 ++	1	1.73e-06 ++	1	1.73e-06 ++	1	1.73e-06 ++	1	1.73e-06 ++	1	1.73e-06 ++	1	1.73e-06 ++	1	1.73e-06 ++	1
	15	1.73e-06 ++	1	1.73e-06 ++	1	1.73e-06 ++	1	1.73e-06 ++	1	1.73e-06 ++	1	1.73e-06 ++	1	1.73e-06 ++	1	1.73e-06 ++	1
SEM-7	5	0.035008957 ++	1	1.73e-06 ++	1	0.002957462 ++	1	8.47e-06 ++	1	0.628843002 –	0	0.000663921 ++	1	0.205864241 –	0	1.73e-06 ++	1
	7	1.73e-06 ++	1	1.73e-06 ++	1	1.73e-06 ++	1	1.73e-06 ++	1	1.73e-06 ++	1	1.73e-06 ++	1	1.73e-06 ++	1	1.73e-06 ++	1
	9	1.73e-06 ++	1	1.73e-06 ++	1	1.73e-06 ++	1	1.73e-06 ++	1	1.73e-06 ++	1	1.73e-06 ++	1	1.73e-06 ++	1	1.73e-06 ++	1
	12	1.73e-06 ++	1	1.73e-06 ++	1	1.73e-06 ++	1	1.73e-06 ++	1	1.73e-06 ++	1	1.73e-06 ++	1	1.73e-06 ++	1	1.73e-06 ++	1
	15	1.73e-06 ++	1	1.73e-06 ++	1	1.73e-06 ++	1	1.73e-06 ++	1	1.73e-06 ++	1	1.73e-06 ++	1	1.73e-06 ++	1	1.73e-06 ++	1
SEM-8	5	8.92e-05 ++	1	1.73e-06 ++	1	1.73e-06 ++	1	1.73e-06 ++	1	9.32e-06 ++	1	1.73e-06 ++	1	0.000268946 ++	1	1.73e-06 ++	1
	7	1.73e-06 ++	1	1.73e-06 ++	1	1.73e-06 ++	1	1.73e-06 ++	1	1.73e-06 ++	1	1.73e-06 ++	1	1.73e-06 ++	1	1.73e-06 ++	1
	9	1.73e-06 ++	1	1.73e-06 ++	1	1.73e-06 ++	1	1.73e-06 ++	1	1.73e-06 ++	1	1.73e-06 ++	1	1.73e-06 ++	1	1.73e-06 ++	1

	12	1.73e-06 ++	1	1.73e-06 ++	1	1.73e-06 ++	1	1.73e-06 ++	1	1.73e-06 ++	1	1.73e-06 ++	1	1.73e-06 ++	1	1.73e-06 ++	1
	15	1.73e-06 ++	1	1.73e-06 ++	1	1.73e-06 ++	1	1.73e-06 ++	1	1.73e-06 ++	1	1.73e-06 ++	1	1.73e-06 ++	1	1.73e-06 ++	1
SEM-9	5	9.71e-05 ++	1	7.69e-06 ++	1	5.22e-06 ++	1	3.88e-06 ++	1	5.79e-05 ++	1	9.32e-06 ++	1	0.016877584 ++	1	1.73e-06 ++	1
	7	1.73e-06 ++	1	1.73e-06 ++	1	1.73e-06 ++	1	1.73e-06 ++	1	1.73e-06 ++	1	1.73e-06 ++	1	1.73e-06 ++	1	1.73e-06 ++	1
	9	1.73e-06 ++	1	1.73e-06 ++	1	1.73e-06 ++	1	1.73e-06 ++	1	1.73e-06 ++	1	1.73e-06 ++	1	1.73e-06 ++	1	1.73e-06 ++	1
	12	1.73e-06 ++	1	1.73e-06 ++	1	1.73e-06 ++	1	1.73e-06 ++	1	1.73e-06 ++	1	1.73e-06 ++	1	1.73e-06 ++	1	1.73e-06 ++	1
	15	1.73e-06 ++	1	1.73e-06 ++	1	1.73e-06 ++	1	1.73e-06 ++	1	1.73e-06 ++	1	1.73e-06 ++	1	1.73e-06 ++	1	1.73e-06 ++	1
SEM-10	5	6.34e-06 ++	1	1.73e-06 ++	1	2.88e-06 ++	1	1.92e-06 ++	1	3.88e-06 ++	1	1.73e-06 ++	1	2.13e-06 ++	1	1.73e-06 ++	1
	7	1.73e-06 ++	1	1.73e-06 ++	1	1.73e-06 ++	1	1.73e-06 ++	1	1.73e-06 ++	1	1.73e-06 ++	1	1.73e-06 ++	1	1.73e-06 ++	1
	9	1.73e-06 ++	1	1.73e-06 ++	1	1.73e-06 ++	1	1.73e-06 ++	1	1.73e-06 ++	1	1.73e-06 ++	1	1.73e-06 ++	1	1.73e-06 ++	1
	12	1.73e-06 ++	1	1.73e-06 ++	1	1.73e-06 ++	1	1.73e-06 ++	1	1.73e-06 ++	1	1.73e-06 ++	1	1.73e-06 ++	1	1.73e-06 ++	1
	15	1.73e-06 ++	1	1.73e-06 ++	1	1.73e-06 ++	1	1.73e-06 ++	1	1.73e-06 ++	1	1.73e-06 ++	1	1.73e-06 ++	1	1.73e-06 ++	1